

ADSORPTIVE SEPARATIONS IN THE PRODUCTION OF NEUTRAL WINE ALCOHOL

by

Elroy Mario Goliath

Dissertation presented for the Degree



DOCTOR OF PHILOSOPHY IN ENGINEERING
(Chemical Engineering)

in the Department of Chemical Engineering
at the University of Stellenbosch

Promoter

PROFESSOR F L D CLOETE

STELLENBOSCH

DATE: March 2002

DECLARATION

I, the undersigned, hereby declare that the work contained in this dissertation is my own original work and that I have not previously in its entirety or in parts, submitted it at any university for a degree.

SUMMARY

This study describes the design, construction, complete industrialisation and operation of a dual bed vacuum swing adsorption (VSA) demonstration plant, which operates at atmospheric and sub-atmospheric conditions. All design objectives as set out initially were met. The plant removes contaminants such as methanol and water from neutral wine spirit. Neutral wine spirit is a key component of various local and international spirituous products which include liqueurs, gin, vodka, fortified wines and brandy.

Neutral wine spirit can chemically be described as the azeotropic mixture of ethanol and water, which occurs at an ethanol content of 96.4 vol. %. Methanol is naturally present in all products from the vine. Fermentation and distillation concentrate methanol even more, and due to physical and chemical characteristics, its separation consumes as much as 45 % of total production costs. Neutral wine spirit is produced by the proven technology of continuous atmospheric distillation. Continuous improvement of the distillation process is limited due to the physical constraints of an old facility, but also due to previous design philosophies and approaches.

The VSA plant consists of two adsorbers, packed to a total height of 1.71 m and a diameter of 0.4 m. Adsorption took place at 100 °C and regeneration at the same bed temperature with purified nitrogen gas at 170 °C and a vacuum of 17 kPa (abs). Experiments were divided into Group I and Group II experiments. Group I investigated the ability to separate methanol and water from the azeotrope and to which efficiency it occurred. It consisted of 120 adsorption cycles of 5 minutes each and 60 samples were drawn for analyses. Breakthrough was not allowed to occur. The azeotropic feed was consistently dehydrated to a water content < 0.05 wt %, while methanol was reduced to < 4 mg/100mLAA. The type of 3A molecular sieve (MS 564 CS) was specifically selected to ensure analytic as well as organoleptic compliance with the product specification. Molecular sieve 4A was removed due to organoleptic problems with the product.

Group II experiments were performed in the format of a sensitivity analysis. The effects of various process parameters on the methanol breakthrough curves were individually assessed. Eighteen experiments were performed over a period of 8 days, with 86 samples drawn. The duration of an adsorption cycle was 30 minutes, allowing methanol breakthrough to occur. Water was preferentially adsorbed. Negative methanol bed loadings during high water loadings confirmed that water was able to displace methanol molecules. In the presence of water, molecular sieve 3A was capable of adsorbing 0.6 mg methanol/100mLAA, while in the absence of water with synthetically dosed methanol, molecular sieve 3A achieved a maximum loading of 12.3 mg methanol/100mLAA. The latter corresponded with a maximum methanol feed content of 1118 mg/100mLAA.

In general, quicker breakthrough occurred at higher flow rates and feed concentrations. Continuous breakthrough caused bed contamination and a 24-hour thermal regeneration was performed following experiment 12. The feed flow rate was increased from the theoretical 50 ℓ/hr to 70 ℓ/hr without any additional capital layout. Selected process conditions were found to be effective in continuously separating methanol from ethanol. Depending on the strategy of integration, profitability studies shows a Return on Investment of between 110.1% - 220.8% for the adsorption project.

Adsorption is superior to distillation in the separation of methanol. Due to the level of innovation involved, it is recommended that the contents of this study remain confidential and patent protection is to be extended. This dissertation speaks to both the wine making as well as the chemical engineering fraternity. It seeks to provide credibility to both parties, by clarifying the unknown issues fundamental to the respective disciplines.

OPSOMMING

Hierdie studie definieer die ontwerp, vervaardiging en volledige industrialisasie van 'n dubbelbed vakuüm adsorpsie demonstrasie aanleg (VSA) wat by atmosferiese en sub-atmosferiese kondisies bedryf word. Alle ontwerpdoelwitte is bereik. Die aanleg verwyder selektief metanol en water vanuit neutrale wynspiritus. Neutrale wynspiritus is 'n sleutelkomponent van verskeie spiritualieë in die plaaslike en internasionale wyn en spiritus bedryf. Hierdie produkte sluit in likeurs, jenever, vodka, gefortifiseerde wyne en brandewyn.

Chemies, kan neutrale wynspiritus beskryf word as die azeotropiese mengsel van etanol en water teen 96.4 vol. %. Metanol het 'n natuurlike teenwoordigheid in alle produkte vanaf die wynstok. Gisting en distillasie konsentreer metanol tot 'n hoër mate en weens fisiese en chemiese eienskappe word metanol teen hoër koste vanaf die etanol stroom geskei. Die metanol verwyderingskomponent beloop soveel as 45 % van die produksiekoste van die totale proses. Neutrale wynspiritus word deur die gevestigde tegnologie van kontinue atmosferiese distillasie geproduseer. Kontinue verbetering van die proses word beperk deur die fisiese ouderdom en toestand van die fasiliteite, maar is ongelukkig ook die resultaat van vorige ontwerpfilosofieë en benaderings.

Die adsorbeërs is gepak tot 'n hoogte van 1.71 m met 'n deursnit van 0.4 m. Adsorpsie het by 100 °C plaasgevind en regenerasie by dieselfde bedtemperatuur met stikstofgas by 170 °C en 'n vakuüm van 17 kPa (abs). Eksperimentele werk is in Groep I en Groep II eksperimente verdeel. Groep I het die effektiewe prosesvermoë om metanol en water vanuit die azeotroop te verwyder ondersoek. Dit het bestaan uit 120 adsorpsie siklusse van 5 minute elk. Sestig monsters is getrek vir analise. Deurbreek van metanol was nie toe gelaat om plaas te vind nie. Die azeotropiese toevoer is konsekwent tot 'n water inhoud < 0.05 massa % gedehidrateer is.

'n Metanol inhoud < 4 mg/100 mLAA is bereik. Die tipe 3A molekulêre sif (MS 564 CS) was spesifiek vir die toepassing geselekteer om sodoende 'n analities sowel as organolepties aanvaarbare produk te lewer. Molekulêre sif 4A was verwyder weens die vorming van produk wangeure.

Groep II eksperimente is in die vorm van 'n sensitiviteits analise uitgevoer. Die effek van verskeie veranderlikes is individueel op die metanol deurbreekkurve getoets. Agtien eksperimente is oor 'n tydperk van 8 dae gedoen, met 'n totaal van 86 monsters wat getrek is. 'n Adsorpsie siklus het 30 minute geduur en het deurbreek van metanol toegelaat. Water is by voorkeur geadsorbeer. Negatiewe metanol bedladings tydens hoë water-teenwoordigheid toon dat water wel metanolmolekule op 'n adsorpsie-posisie kan verplaas. In die teenwoordigheid van water is 'n bedlading van 0.6 mg metanol/100mLAA verkry, met 'n maksimum van 12.3 mg metanol/100mLAA in die afwesigheid van water. Laasgenoemde verteenwoordig 'n toevoer met 'n metanol inhoud van 1118 mg/100mLAA.

In die algemeen is gevind dat 'n toename in toevoer vloeitempo en konsentrasie die tyd vir deurbreek verkort. Kontinue deurbreek het kontaminasie van die bed teweeg gebring en 'n termiese regenerasie is vir 24 ure na eksperiment 12 gedoen. Die teoretiese ontwerp vloeitempo was 50 l/hr, maar resultate het getoon dat die aanleg tot 70 l/hr kan verwerk sonder addisionele koste. Die geselekteerde prosesondisies was effektief in die versekering van die kontinue skeiding van metanol en etanol. Die lewensvatbaarheidstudie toon, afhangende van die strategie van integrasie, 'n Opbrengs op Belegging van tussen 110.1% - 220.8%.

Adsorpsie het 'n beter skeidingsvermoë as konvensionele distillasie vir die verwydering van metanol vanuit etanol. Weens die vlak van innovasie betrokke, word dit voorgestel dat die inhoud van hierdie studie vertroulik gehou word en dat patent beskerming verleng sal word. Hierdie verhandeling spreek tot beide die wynmaak sowel as chemiese ingenieurs dissiplines. Daar is gepoog om geloofwaardigheid vir beide partye te skep deur die onbekende aspekte van albei dissiplines aan te spreek.

VACUUM SWING ADSORPTION PLANT - KVV PAARL



DEDICATION

In memory of my mother, Doreen Goliath. She gave me life, supported me in all my endeavors, and provided me with strength, wisdom and inspiration. She guided me through all the challenges of life and showed me that no boundaries exist in the quest for success. I love her dearly. She passed away peacefully during the writing of this dissertation.

ACKNOWLEDGEMENTS

The author wishes to acknowledge the following parties for their contribution to this study:

1. My supervisor, Prof. Cloete for his guidance and direction.
2. The management of KVV for allowing me the opportunity to bring to life this technical innovation.
3. The KVV Research Fund for funding this project.
4. Xpro-Solutions and Logichem for their assistance in managing the multi-disciplined contractors who manufactured the plant components.
5. Quality Applications Development for programming the control system based on my design and requirements.
6. The electrical and mechanical workshops at KVV for their assistance.
7. The laboratory at the Department of Chemical Engineering, in particular Dr. Denise Venter and Saybolt Laboratories – Durban for performing the gas chromatographic analyses.
8. The Department of Chemical Engineering at the University of Stellenbosch under the direction of Prof. Lorenzen, for indirectly planting the seed that led to the realization of this concept.
9. Last but not least, to my wife Sandy for her assistance, love and understanding during the very many hours spent on this thesis instead of with her.

TABLE OF CONTENTS

<u>CHAPTER</u>		<u>PAGE</u>
	DECLARATION	
	SUMMARY	
	OPSOMMING	
	ACKNOWLEDGEMENTS	v
	TABLE OF CONTENTS	vi
	LIST OF TABLES	x
	LIST OF FIGURES	xii
	LIST OF EQUATIONS	xv
	LIST OF SYMBOLS	xvi
1	INTRODUCTION	1
1.1	Extent of the South African Wine Industry	1
1.2	The Importance of Process Innovation	4
2	LITERATURE SURVEY	8
2.1	Distillation	8
2.2	The Production of Neutral Wine Alcohol	15
2.2.1	The wine column and first rectifier	15
2.2.2	The hydro selection column	16
2.2.3	The second rectifier (spirits column)	17
2.2.4	The impurities column	17
2.2.5	The final column	17
2.3	Optimisation of the Existing Process	18
2.3.1	Modelling of distillation columns through simulation	18
2.3.2	Application of pinch analysis	19
2.3.3	Energy recovery with steam jet ejectors	19
2.3.4	Heat loss through natural convection	19
2.3.5	Alternatives to distillation	20
2.4	Adsorption vs. Distillation	20

2.5	THE NATURAL PRESENCE OF METHANOL IN WINE	22
2.5.1	The toxicological effects of methanol	24
2.6	Fundamental Principles of Adsorption	25
2.6.1	Forces of adsorption	26
2.6.2	Selectivity	29
2.6.3	Hydrophilic and hydrophobic behaviour	32
2.6.4	Pore size distribution	32
2.6.5	Physical strength	33
2.6.6	Practical adsorbents	34
2.7	Zeolites / Molecular Sieves	36
2.7.1	Type X molecular sieves	37
2.7.2	Type A molecular sieves	37
2.7.3	Manufacturing procedure	40
2.7.4	Applications for gas separation	42
2.7.5	Adsorption isotherms	43
2.7.6	Theories of adsorption equilibria	45
2.7.7	Water adsorption	52
2.8	The Adsorption of Methanol	58
2.8.1	Benefits of methanol removal through adsorption	58
2.8.2	Mechanisms for the adsorption of methanol onto zeolites	59
2.9	Adsorber Design Considerations	64
2.9.1	Design parameters for a basic PSA process	66
2.9.2	Major improvements on the basic PSA process	70
2.9.3	Desorption and regeneration of adsorbents	73
2.9.4	Increasing the energy efficiency of adsorption	78
2.9.5	Performance of adsorbers	78
2.9.6	Azeotrope dehydration	80
3	ADSORPTION IN A SINGLE SMALL COLUMN	84
3.1	Experimental Conditions	84
3.2	Experimental Results and Discussion	87

4	DESIGN OF A VACUUM SWING ADSORPTION SYSTEM	90
4.1	Design Objectives	90
4.2	Design Considerations for the Adsorption Plant	90
4.2.1	Selection of molecular sieve	91
I	Basic Adsorbent Properties	93
II	Application Considerations	95
III	Equipment	101
IV	Process Flowsheet	102
4.2.2	Final Process Flow	107
5	EXPERIMENTAL PROCEDURES AND RESULTS	114
5.1	Experimental Methods	115
5.1.1	Group I experimental runs	115
5.1.2	Group II experimental runs	121
5.2	Methods of Analyses	123
5.3	Results and Discussion	124
5.3.1	Group I experimental runs	124
5.3.2	Group II experimental runs	132
5.4	Energy Analysis	140
5.5	Financial Analysis and Feasibility	142
5.5.1	Profitability due to additional product	144
5.5.2	Profitability due to reduced wine purchasing	145
5.5.3	Issues of capital layout	146
6	FUTURE WORK AND PROPOSALS FOR INTEGRATION	148
6.1	Additional Runs	148
6.2	Improvements to Plant	149
6.3	Integration with Existing Processes	150
6.4	Application to Other Separation Problems	152
7	CONCLUSIONS AND RECOMMENDATIONS	153
	REFERENCES	159

APPENDICES		166
APPENDIX A	KWV DISTILLATION PROCESS AND INSTRUMENTATION DIAGRAM	167
APPENDIX B	ADSORBENT PROPERTIES AND APPLICATIONS	170
APPENDIX C	W.R. GRACE MOLECULAR SIEVE CHARACTERISTICS	174
APPENDIX D	ADSORBER DESIGN	184
APPENDIX E	ENGINEERING SPECIFICATION	192
APPENDIX F	PLANT DESIGN INFORMATION	205
APPENDIX G	COMMISSIONING SCHEDULE	223
APPENDIX H	EXPERIMENTAL RESULTS	227
APPENDIX I	METHANOL-ETHANOL V/L DATA	240

LIST OF TABLES

<u>TABLE</u>		<u>PAGE</u>
1.1	Production and utilisation of crop	1
1.2	Producer sales and income	2
1.3	State revenue from wine products	2
1.4	Excise clearance and market share	3
2.1	Parameters of physical adsorption and chemisorption	27
2.2	Selectivity classification of some adsorbents	31
2.3	Polarity and pore classification	34
2.4	Characteristics of major zeolite sorbents	41
2.5	Molecules admitted to zeolites according to molecular dimensions	43
2.6	Adsorption experimental conditions and results	55
2.7	Adsorber design considerations	65
2.8	Methods of regeneration with process examples	74
2.9	Values of crossover ratio	79
3.1	Experimental conditions for adsorption in a single small column	85
3.2	Variation in methanol feed concentration	87
3.3	Methanol adsorption results	87
4.1	Cycle sequence chart	104
4.2	Development of design configurations	104
4.3	Process sequence chart	111
5.1	Schedule of experimental runs(Group I)	120
5.2	Schedule of experimental runs(Group II)	121
5.3	Experimental conditions and results(Group I)	126
5.4	Desorption conditions and efficiency(Group I)	130
5.5	Sensitivity analysis(Group II)	139

5.6	Energy analysis	141
5.7	Production quantities (additional product)	144
5.8	Profitability (additional product)	145
5.9	Production quantities (reduced wine purchasing)	145
5.10	Profitability (reduced wine purchasing)	146

LIST OF FIGURES

<u>FIGURE</u>		<u>PAGE</u>
1.1	Study layout	7
2.1	Typical tray-type distillation column with major accessories	8
2.2(a)	Vapour/liquid equilibrium diagram for the ethanol/water system	10
2.2(b)	Minimum and maximum boiling point azeotropes	12
2.2(c)	Composition profile for azeotropic distillation	13
2.3	Variation of thermal efficiency, theoretical stages and reflux ratio with relative volatility	20
2.4	Hydrolysis of pectin materials	22
2.5	Growth of patents relating to PSA	26
2.6	Potential energy diagram for adsorption	28
2.7	Pore size distribution for various adsorbents	33
2.8	Comparison of relative humidity effects on various desiccants	36
2.9	Structure of molecular sieves A and X	37
2.10	Correlation between effective pore size and Lennard-Jones kinetic diameter	39
2.11(a)	Grace molecular sieve production process	40
2.11(b)	Scanning electron micrograph of 3A and 4A	42
2.12	Types of adsorption isotherms	44
2.13	Schematic of experimental apparatus for drying the ethanol/water azeotrope	54
2.14	Effect of bed temp. on breakthrough for 3A and 4A	56
2.15	Effect of concentration on breakthrough for 3A and 4A	57
2.16	Different adsorption states of methanol (Si/Al ratio)	61
2.17	Methanol molecule in zeolite cage	62
2.18	Adsorption complexes of methanol at an acid site	63

2.19	Charge densities of adsorbed complex	63
2.20	Use of multiple beds in a basic PSA process	72
2.21	The effect of process variables on adsorption equilibrium	75
2.22	Temperature during non-isothermal adsorption	81
2.23	Regeneration temperature with heat of adsorption	82
2.24	Regeneration temperature without heat of adsorption	83
3.1	Experimental apparatus during previous study	84
3.2	Typical temperature profile for adsorption onto molecular sieve 3A	86
3.3	Breakthrough curves for experiments 5 and 6	88
3.4	Breakthrough curve for experiment 8	89
4.1	Flow distribution effect of ceramic bead bed support	102
4.2	Process control flowchart	103
4.3	Relationship between gas combustion and concentration	106
5.1	Typical vacuum depletion curve	116
5.2	Typical oil heating curve	117
5.3	Typical bed heating curve	117
5.4	Radial temperature effect before gas distribution plate	118
5.5	Radial temperature effect after gas distribution plate	118
5.6	Synchronised pressure curves for both adsorbers	119
5.7	Ethanol adsorption curve for cycles 30 and 40	124
5.8	Methanol adsorption curve for cycles 50 and 60	127
5.9	Efficiency of adsorption over 120 adsorption cycles	127
5.10	Ethanol adsorption curve for cycles 70 and 80	128
5.11	Methanol adsorption curve for cycles 70 and 80	128
5.12	Bed loading curves for water and methanol(Group I)	129
5.13	Changes in adsorption efficiency	131
5.14	Typical temperature profile as function of axial position (Group I)	132
5.15	Effect of feed concentration on methanol breakthrough curve	133

5.16	Effect of feed flow rate on methanol breakthrough Curve	134
5.17	Effect of regeneration pressure on methanol breakthrough	135
5.18	Effect of purge flow rate on methanol breakthrough curve	135
5.19	Effect of synthetic methanol feed concentration on methanol breakthrough	136
5.20	Effect of bed temperature on methanol breakthrough curve	137
5.21	Methanol bed loadings (batches 1 – 12)	138
5.22	Methanol bed loadings (batches 13 – 18)	140
5.23(a)	Standard spirits production routing	143
5.23(b)	Proposed routing	143
5.24	Capital cost distribution for VSA on a larger scale	147
5.25	Projected capital/capacity layout	147

LIST OF EQUATIONS

<u>EQUATION</u>		<u>PAGE</u>
2.1	Lennard-Jones potential function	22
2.2	Separation factor	24
2.3	Crystalline aluminosilicates stoichiometry	30
2.4	Chemical representation of crystal structure	31
2.5 - 2.7	Derivation for Langmuir isotherm	46
2.8 – 2.10	Derivation for Henry's Law Isotherm	46-47
2.11 – 2.12	Derivation for the Freundlich Isotherm	47
2.13 – 2.16	Derivation for the BET Equation	48 – 49
2.17 – 2.18	Derivation for Polanyi's Potential Theory	50
2.19 – 2.25	Derivation for the Gibbs Isotherm	50 – 51
2.26	Derivation for the Statistical thermodynamic model	51
2.27	Sabri Ergun	67
2.28	Sabri Ergun factor E_1	67
2.29	Sabri Ergun factor E_2	67
2.30	Superficial fluid velocity	67
2.31	Maximum superficial velocity	67
2.32	Differential pressure ratio	68
2.33	Minimum purge flow rate	68
2.34	Minimum purge flow rate for industrial use	68
2.35	Temperature elevation in heat front	68
2.36	Bed length to prevent heat transfer front exit	68
2.37	Axial dispersion factor (heat transfer)	68
2.38	Bed length to prevent mass transfer front exit	69
2.39	Axial dispersion factor (mass transfer)	69
2.40	Laminar layer conductance ($N_{RE} > 50$)	69
2.41	Laminar layer conductance ($N_{RE} < 50$)	69
2.42	Reynolds number	69
2.43	Adsorbent granular conductance	69
2.44	Overall heat transfer coefficient	69
2.45	Design pressure ratio for Skarstrom cycle	72
2.46	Crossover ratio	78

LIST OF SYMBOLS

a,	external surface area per unit volume (m^{-1})
A,	total cross section area of packed vessel (m^2)
b,	mass transfer rate combining factor (dimensionless)
c,	specific heat ($\text{J.kg}^{-1}.\text{K}^{-1}$)
C,	axial dispersion factor (dimensionless)
D,	diameter
g,	gravitational acceleration (ms^{-2})
h,	individual heat transfer coefficient ($\text{W.m}^2.\text{K}^{-1}$)
H,	heat of adsorption (J.kg^{-1} adsorbate)
H_R ,	relative saturation
k,	individual mass transfer coefficient (m.s^{-1})
k_h ,	adsorbent granular conductance ($\text{W.m}^{-1}.\text{K}^{-1}$)
K,	overall mass transfer coefficient (ms^{-1})
L,	length (m)
ℓ_{AA} / L_{AA}	litres of absolute alcohol
n,	polytropic compression exponent
N,	number of compression stages (dimensionless)
N_{Pr} ,	Prandtl number
N_{Re} ,	Reynolds number
N_{Sc} ,	Schmidt number
p,	pressure (Pa)
p^* ,	vapour pressure (Pa)
q,	heat loss rate (J.s^{-1})
R,	purge ratio ; crossover ratio
t,	time (s)
T,	temperature (K)
U,	over all heat transfer coefficient ($\text{W.m}^{-2}.\text{K}^{-1}$)
v,	axial velocity (m.s^{-1})
w,	mass flow rate (kg.s^{-1})
X^* ,	equilibrium concentration in fluid (kg.kg^{-1})
X,	concentration in fluid (kg.kg^{-1})

X_0 ,	adsorbent residual loading ahead of MTZ (g adsorbate/g adsorbent)
X_i	adsorbent loading in equilibrium (concentration behind MTZ) (g adsorbate/g adsorbent)
Y^* ,	equilibrium adsorbent capacity (kg.kg^{-1})
Y ,	equivalent adsorbent capacity (kg.kg^{-1})

GREEK LETTERS

α	relative volatility
δ	diffusivity ($\text{m}^2.\text{s}^{-1}$)
Δ	finite difference
ε	effective interstitial void fraction ; Lennard-Jones potential well
η	adsorption efficiency
ρ	density (kg.m^3)
λ	thermal efficiency
σ	force constant
ϕ	Potential energy (kJ/mole)
ψ	granule shape factor

CHAPTER ONE

INTRODUCTION

The production of fermented products, especially those that undergo the process of distillation is technically sophisticated. It is however not always appreciated which advances have been made in the last 20 years. There are various reasons for this, the most important one probably being the way advertisement has emphasized the traditional image of these products for promotional purposes. This at the expense of the technological skills required to make a success of them and also due to a lack of available information on the production processes.

1.1 EXTENT OF THE SOUTH AFRICAN WINE INDUSTRY

The areas in South Africa currently under vines are approximated at 104 179 hectares^[77]. These vines are grown and managed by 4 515 primary wine producers with an investment of R8 367 million (replacement value) and 337 wine cellars, which is equivalent to an investment of R3 904 million. The industry provides employment to 3 300 wine cellar personnel and approximately 345 000 farm workers including their dependants.

Wine for brandy and wine spirits production, forms a significant portion of the total wine crop in South Africa. Table 1.1 shows the production and utilisation of crop over various years in South Africa.

Table 1.1. Production and Utilisation of Crop^[77]

Year	Grapes (tons)	Good wine (litre)	Rebate wine (litre @ 10%)	Distilling wine (litre @ 10%)	Non alcoholic (litre @ 10%)	Total crop (litre @ 10%)
1993	1,023,506	395,039,213	45,857,111	187,162,544	183,031,719	811,090,587
1994	1,020,337	420,720,723	74,429,354	224,778,655	84,454,121	804,382,853
1995	1,063,915	497,584,351	79,633,856	175,449,865	91,960,391	844,628,463
1996	1,148,114	576,663,976	126,060,326	142,347,061	54,261,522	899,332,885
1997	1,120,602	546,688,605	142,354,553	122,413,493	69,458,508	880,915,159
1998	1,041,004	544,387,811	107,515,284	118,348,265	45,324,129	815,575,489
1999	1,173,596	595,907,559	47,972,702	152,961,143	117,254,086	914,095,490

The producer's and sales and income from rebate wine and distilling wine remains a significant portion of their income, as depicted in Table 1.2.

Table 1.2. Producers Sales and Income (RM)^[77]

Year	Wholesalers	Good wine	Rebate wine	Distilling wine	Total income
1993	35.4	417.5	35.6	203.7	692.2
1994	36.3	539.9	71.5	218.8	866.5
1995	55.5	599.7	85.5	222.5	963.2
1996	71.4	809.2	155.3	197.3	1,233.2
1997	97.9	990.9	199.9	173.9	1,462.6
1998	102.8	980.3	165.6	163.9	1,412.6
1999	123.5	1,004.2	70.4	237.8	1,435.9

Perhaps the biggest contribution of brandy and spirituous products is towards the state, in terms of Customs and Excise revenue as depicted in the following Table 1.3.

Table 1.3. State Revenue from Wine Products (RM)^[77]

Year	Excise duty			VAT			Total income
	Wine	Brandy & wine spirit	Sub-total	Wine	Brandy & wine spirit	Sub-total	
1993	96.4	264.3	360.7	251.7	152.1	403.8	764.5
1994	125.0	359.6	484.6	401.6	198.7	600.3	1084.9
1995	162.1	417.8	579.9	474.7	227.6	702.3	1282.2
1996	197.2	506.1	703.3	636.2	273.8	910.0	1613.3
1997	243.9	542.5	786.4	588.1	279.7	867.8	1654.2
1998	269.0	522.7	791.7	621.6	263.1	884.7	1676.4
1999	287.6	494.3	781.9	639.4	241.1	880.5	1662.4

Clearly in terms of Excise duty, state revenue from brandy and wine spirits far exceeds that of wine. This higher income from brandy is also evident at primary and secondary producer's level. Brandy remains the top selling spirit in South Africa as can be seen in the following table.

This positive market share for brandy continuously stimulates the demand for neutral wine spirit, as brandy by law in South Africa contains up to 70 vol. % spirits. Wine spirits is also used for the production of products such as vodka, gin, liqueurs and also for fortification purposes.

Table 1.4. Excise Clearance and Market Share^[77]

Year	Excise clearance (MLAA)					% Market share		
	Brandy	Wine spirit	Cane spirit	Grain spirit	Total	Brandy	Whisky	Other
1993	17.77	0.43	11.73	0.37	30.3			
1994	20.86	0.2	15.76	0.79	37.6			
1995	21.87	0.27	14.95	0.4	37.5	46.2	18.5	35.3
1996	23.88	0.38	15.41	0.23	39.9	48.1	16	35.9
1997	23.52	0.25	15.58	0.34	39.7	49.6	13.8	36.6
1998	19.78	0.29	14.79	0.71	35.6	50.3	10.4	39.3
1999	17.5	0.29	14.84	0.75	33.4	45.6	11.6	42.8

Competition for wine spirits market share in South Africa is fierce, where quality and costs are the determining factors. Reduction of the latter calls for innovative thinking with regards to process technology and practical process adaptations. As the largest producer of brandy and spirits in South Africa, KVV supplies up to 60 % of all brandy products on the local market.

The company was founded in 1918 to represent the interests of South African wine farmers. KVV was transformed on 2 December 1997, from a cooperative into a group of companies, which are further divided into divisions. KVV Group Ltd. has three subsidiaries which operate as independent units; KVV South Africa, KVV International and KVV Investments. KVV South Africa is a subsidiary of KVV Group Ltd. and established a production centre of excellence in the activity areas of wine, brandy, grape juice concentrate, wine grape planting material and packaging. KVV International, the global trading company of KVV Group, began operating commercially in 1995. It is the leading South African exporter of fine wines and brandies in the global market. KVV is operative in 28 focus markets abroad. These markets are divided into 7 divisions, i.e. UK, Europe, The Americas, Germany, The Far East, Middle East and South East Asia and Africa.

1.2 THE IMPORTANCE OF PROCESS INNOVATION

With the vision of being a “production centre of excellence”, KVV South Africa continuously strives to improve its processes. These process improvements and accompanying capital expenditure were however focussed predominantly on the wine cellars and grape juice concentrate plants. This had a negative effect on the development of the processes of brandy and spirits production. It was especially the process for spirit distillation, which takes place in continuous atmospheric distillation columns that received little attention at all in terms of future development. Spirits distillation at KVV and in the rest of the South African Wine Industry in general, is therefore lacking behind the modern distillation facilities of the international competitors. A detailed study of the spirits distillation process at KVV was performed by the author^[18] and the following problem areas surrounding these processes were evident:

- very little capital expenditure was aimed at the spirits distillation process over decades;
- various design inconsistencies exist in the process;
- plant maintenance appeared to be unstructured and a break-first-repair-afterwards approach was followed;
- unsubstantiated process modifications by the experts of the time was performed on the distillation plants on a continuous basis. These modifications however could be seen as production experiments and were not based on sound engineering principles.

Due to this latter issue, chemical engineering principles and the structured application of optimisation to the distillation processes are required to improve product quality and reduce the operating costs of distillation. The old design philosophies which were used in this case, as well as the experimental ways in which the process modifications were undertaken, left KVV with production facilities which deviates in certain instances considerably from classical distillation processes. Therefore, the improvement of this process calls for an unconventional way of thinking, taking into consideration the inherent process

dynamics such as thermodynamics, heat transfer, mass transfer and distillation principles. There should be no reason why the standard of industrial research and chemical engineering applicability in the wine industry, should differ from any other highly technological production orientated industry.

This level of thinking and application of technology will have the following benefits for the company:

- a competitive edge over its rivals in the brandy and spirits production industry;
- a reduction in product unit cost;
- a gain in product marketability;
- KVV could play a leading role in innovative process developments.

Therefore, if the above issues were to be seen as the objectives for a research project and correlated with the detail evaluation which the author performed previously,^[18] the issue of the ease of component separation continuously surfaces in the analysis of the process. Of all components to be separated in the distilling wine, the analysis clearly showed that the primary alcohol methanol, appeared to be separated with great difficulty and high expense from the ethanol molecules. During the study it therefore became clear that it would be beneficial to KVV, if engineering time and costs were focussed on removing methanol from wine spirits in a manner more cost effective and less energy demanding than the existing distillation process.

As a natural component of wine, methanol will always be present during distillation and will always increase the separation costs involved. This study therefore focuses on the innovative separation of methanol from intermediate products during the distillation of wine spirits.

The **objectives of this thesis and study** are the following:

- To quantify the problem of methanol removal from neutral wine spirits and other grades of ethanol.
- To demonstrate the importance and the added benefits of methanol removal through adsorption onto molecular sieves to KWV.
- To quantify financially the feasibility of the suggested process.
- To build and demonstrate a sound knowledge and understanding of the above-mentioned separation.
- To demonstrate that methanol and water are selectively adsorbed from the ethanol stream onto specific molecular sieves
- To demonstrate the principle that methanol adsorption is not dependant on the presence of water
- To design, manufacture, assemble, commission and successfully operate a continuous, robust adsorption demonstration plant of value to KWV and the rest of the industry.
- To determine the boundaries of operating conditions for the mentioned plant.
- To demonstrate process stability running the experiments over a long period of time (days)
- To understand the risks involved and how they are to be reduced.

This study reflects the author's logical path of thinking which leads to the design, construction and operation of a full-scale production plant in order to prove the principles involved. To define more clearly the structure of this thesis, Figure 1.1 shows the study layout around which this work was performed. The process, which is suggested and substantiated by the study, is completely new to the local as well as international wine industry. Due to the significance of this innovation, patent protection is to be extended following completion of the study.

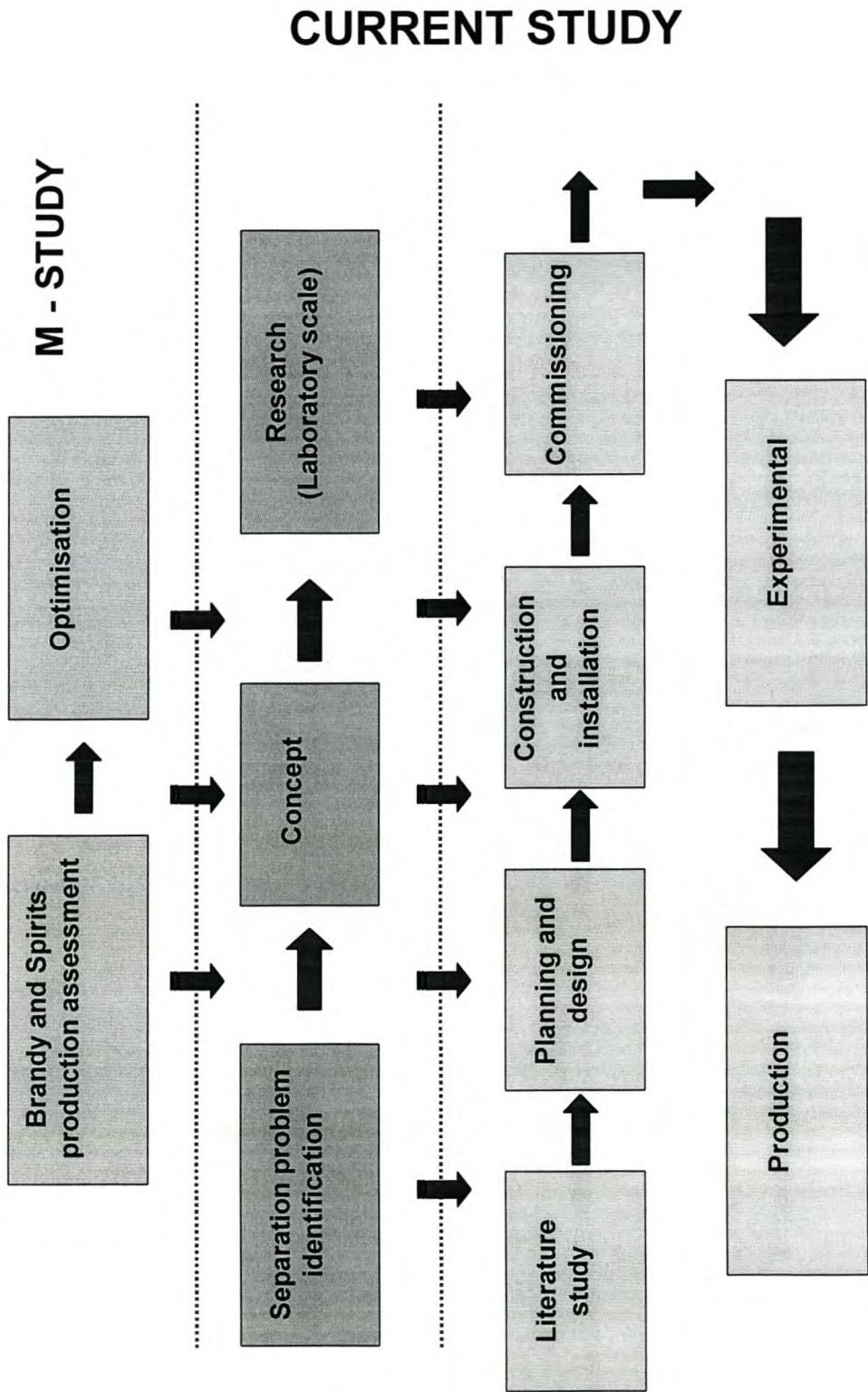


Figure 1.1 Study layout

CHAPTER TWO

LITERATURE SURVEY

2.1 Distillation

The separation of liquid mixtures into their several components is one of the major operations in the chemical and petroleum industry today. Of all the separation processes, distillation has proven itself to be the most preferred. Throughout the chemical industry, the demand for purer products coupled with the relentless pursuit of greater efficiency has necessitated continuous research into the techniques of distillation. Distillation is also the preferred process in the spirits industry. A typical tray-type distillation column with major external accessories is shown schematically in Figure 2.1.

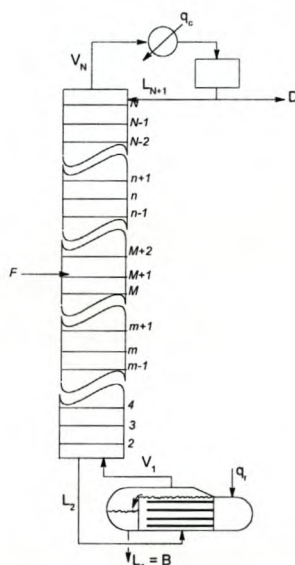


Figure 2.1. Typical tray-type distillation column with accessories.^[50]

Such a system would contain the following elements:

- a feed composed of the various components to be separated;
- A source of energy to drive the process (in most cases this energy source is steam, either directly entering the base of the tower or transferring its energy to the tower contents through an indirect heat exchanger called a reboiler);

- an overhead purified product, consisting primarily of the feed component with a lower boiling point;
- a bottoms product containing the component of the feed possessing the higher boiling point;
- an overhead heat exchanger (condenser) normally water cooled to condense the vapour resulting from the boiling which was created by the energy input.

Following condensation, the overhead vapour is split into two streams. One stream is the overhead product and the other the reflux, which is returned to the top of the tower to supply the liquid down-flow required in the upper portion of the tower. Separation operations achieve its objective by the creation of two or more co-existing zones, which differ in temperature, pressure, composition and phase state^[50]. Distillation utilises vapour and liquid phases at essentially the same temperature and pressure for the co-existing zones. Various kinds of devices such as dumped or ordered packings and plates or trays are used to bring the two phases into intimate contact. The vertical cylindrical column provides in a compact form with the minimum of ground requirement, a large number of separate stages of evaporation and condensation.

The separation of liquid mixtures by distillation depends on differences in component volatilities. The greater the relative volatilities, the easier the separation. In Figure 2.1, vapour flows up the column, while liquid flows countercurrent down the column. The vapour and liquid are contacted on plates or packing material. Part of the condensate from the condenser is returned to the top of the column to provide liquid-flow above the reflux, while part of the liquid from the base of the column is vapourised in the reboiler and returned to provide the vapour flow.

Figure 2.2(a) shows a vapour/liquid equilibrium diagram for the ethanol/ water system at atmospheric pressure.

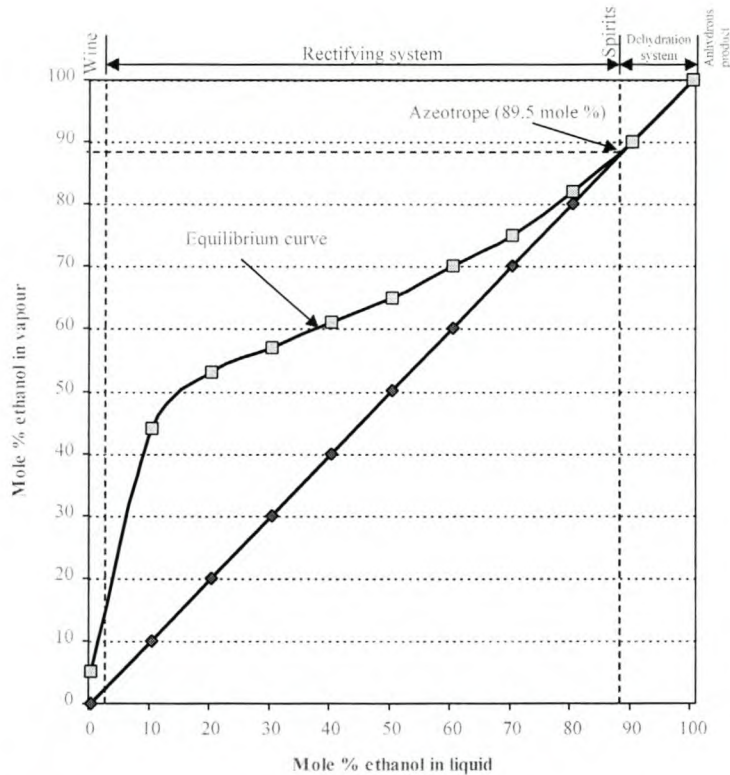


Figure 2.2(a). Vapour/liquid equilibrium for the ethanol/water system at atmospheric pressure.^[38] (see also appendix I for calculations)

The equations for the top and bottom operating lines are derived from material balances respectively done across the top and bottom section of the distillation column. For a binary system these equations represent straight lines. The operating lines contain elements which take into consideration the reflux ratio to the column and condition of the feed stream. Once drawn into the V/L equilibrium diagram such as depicted in Figure 2.2(a), a method such as McCabe and Thiele or Lewis-Sorel can be used to determine the theoretical number of plates required to effect a certain separation. Also the minimum amount of theoretical plates can be determined through expressions such as that of Fenske, which are readily available from literature.

If also available, the enthalpy (h) / concentration(x,y) curves of a particular distillation system can be used to determine the amount of theoretical plates. From this information, by also considering the actual tray efficiency that is

exhibited in a distillation system, the actual amount of trays required can be calculated. Tray efficiencies for various C/H systems as drawn up by the familiar O'Connell or Murphree, are also readily available. If a packed distillation column is used for a particular separation, it is assumed that the packed portion of the column can be divided into a number of segments of equal height. Each segment then acts as an equilibrium stage, and liquid and vapour leaving the segment are in equilibrium.

The HETP (height equivalent to a theoretical plate) which is measured experimentally, is the height of packing needed to obtain the change in composition obtained with one theoretical equilibrium contact. In normal industrial equipment the HETP varies between 0.3 m and 1.2 m.^[74] The smaller the HETP, the shorter the column and the more efficient the packing. HETP varies with the packing type and size, components being separated and gas / vapour flow rates.

An azeotrope is a mixture of liquids that reflects a maximum or minimum boiling point relative to the boiling points of surrounding mixture compositions. Azeotrope formation takes place when boiling points of the pure components are sufficiently close. Generally, wide-boiling point mixtures ($\Delta T > 30^\circ \text{C}$), does not have a tendency to form azeotropes^[50]. From Figure 2.2 (a), it is clear that the azeotropic composition is reached at approximately 89 mole % or 96.4 vol. %.

At this point, the liquid and vapour have exactly the same composition. An azeotrope is homogeneous if only one liquid phase is present. When the activity coefficient is greater than unity, giving a positive deviation from Raoult's Law, the molecules of the components in the system repel each other and exert a higher partial pressure than if their behaviour were ideal.^[11]

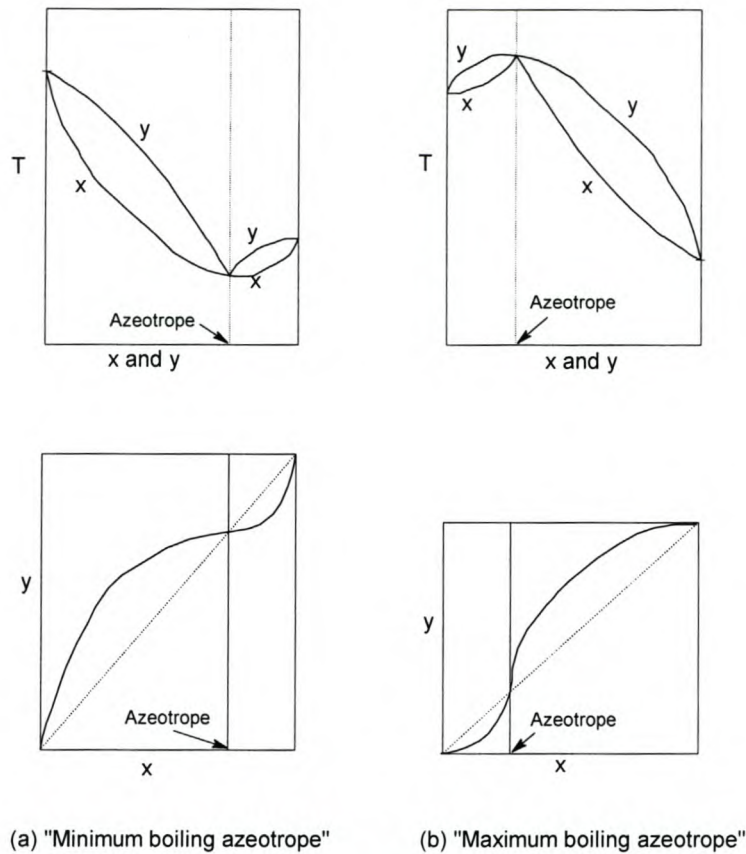


Figure 2.2 (b). Types of azeotropic behaviour.^[11]

This leads to the formation of a minimum boiling azeotrope as indicated in Figure 2.2(b). For values of the activity coefficient < 1 , negative deviation from Raoult's Law results in lower partial pressure and the formation of a maximum boiling azeotrope. Below the azeotrope composition, ethanol is the more volatile component and above the azeotrope composition it is the less volatile^[74].

Although atmospheric distillation can only produce a product just below the azeotropical position, this study will clearly show how an alternative process can be used to break the azeotrope as well as separate other unwanted components. This alternate process is however not the only means of producing absolute alcohol.

Low pressure simple distillation (< 11.5 kPa abs), azeotropic and extractive distillation are distillation techniques that are extensively used to dehydrate the azeotrope. Low pressure distillation applied to existing distillation facilities

at KVV is impractical and capital intensive due to the physical age of the equipment. The principles of extractive and azeotropic distillation are based on the addition of foreign substances to the mixture, to increase the relative volatility of the key components and thus making separation easier. Due to this principle of separation, these techniques cannot be used in the potable alcohol industry, as these chemicals are of industrial grade and in some instances toxic to human consumption. Although not applicable to this study, these two processes are discussed in brief below.

In azeotropic distillation, the substance added forms a low boiling azeotrope with one or more of the two components in the mixture. If benzene is added to the ethanol water azeotrope, then a ternary azeotrope is formed with a boiling point of 64.85 °C, which is less than that of the binary azeotrope (78.15 °C)^[50]. The addition of the relatively non-polar benzene entrainer serves to volatilise water (highly polar) to a greater extent than ethanol (moderately polar). In some instances pentane or diethyl ether are also used as entrainers. Figure 2.2 (c) is a composition profile of the azeotropic distillation column in the dehydration process with benzene as entrainer.

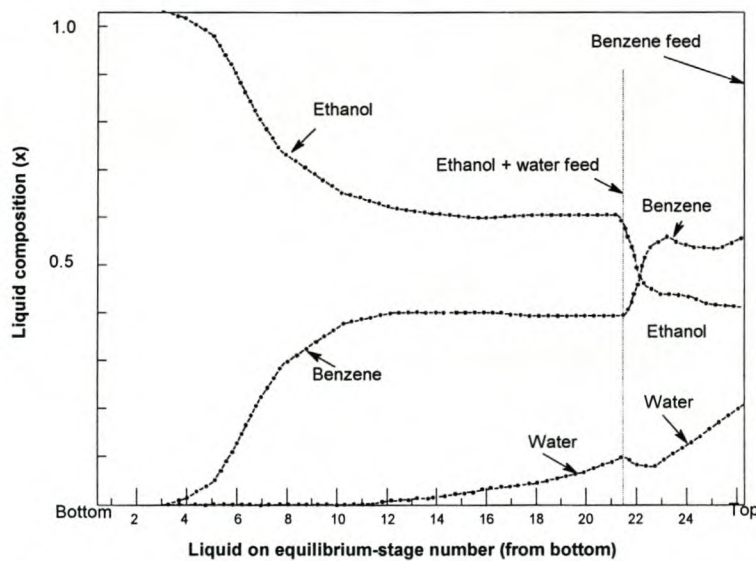


Figure 2.2(c). Composition profile for azeotropic distillation of ethanol and water, with benzene as entrainer.^[11]

Extractive distillation is a method of rectification similar in purpose to azeotropic distillation. To a binary mixture which is difficult to separate by ordinary means, a third component (a solvent of low volatility) is added which increases the relative volatility of the original constituents, thus permitting separation. The solvent added to the mixture differentially affects the activities of the two components and hence the relative volatility. The boiling point of the solvent is usually so much higher than the feed, that the formation of new azeotropes is impossible.

A further characteristic is that any troublesome azeotrope present in the untreated feed disappears in the presence of the solvent. The absence of azeotropes and the fact that the solvent can be recovered by simple distillation, makes extractive distillation a less complex and more widely used process than azeotropic distillation.^[50] Extractive distillation is also a more desirable process than azeotropic distillation since no large quantities of solvent need to be vapourised. The solvent to be used is selected on the basis of selectivity, volatility, ease of separation from the top and bottom products and the cost.

Both azeotropic and extractive distillation are used for the production of industrial grade absolute alcohol, particularly for use as fuel for motor vehicles. However, the purity required for potable alcohol is such that the inevitable traces of organic solvents make these processes unacceptable and unfeasible. Therefore, in order to break the azeotrope for potable alcohol production, innovative techniques unknown to the wine industry need to be investigated and implemented.

2.2 THE PRODUCTION OF NEUTRAL WINE ALCOHOL

The process for the production of a fine neutral spirit has been described in great detail by the author^[18]. Since this process forms the basis of the existing as well as the previous study, a short process description is given below (refer to appendix A1).

Fine neutral spirits can in chemical terms be described as the azeotropic blend of ethanol and water which occurs at 96.4 vol. % ethanol. It is distilled from a distilling wine, which was produced by the dry fermentation of juice, extracted from grapes during the winemaking process. The composition of this wine is commonly very complex and consists of various components, including ethanol, water, methanol, acetaldehyde, ethyl acetate, n-propanol, n-butanol, iso butanol and iso amyl alcohol. Higher carboxylic acids are also present.

The distillation of fermented ethanol differ from synthetic ethanol, in that it contains impurities such as fusel oils (a mixture composed of higher boiling alcohols and lower boiling esters). A complicated, costly and energy intensive distillation system is required to remove these impurities, which include a 2-phase liquid decantation^[18]. For fuel ethanol these impurities need not to be separated. The distillation system at KVV for spirits production is similar to that used throughout the world. The distillation train consists of the following major columns.

2.2.1 The wine column and first rectifier

The distilling wine discussed above, is fed onto the top plate of the wine column. The wine column and first rectifier are operated in series. The heads from the wine column is directly fed into the bottom of the first rectifier. The overhead vapours from the first rectifier are cooled in a series of three shell and tube heat exchangers:

- a preheater for preheating the wine feed;
- a partial condenser;
- a final condenser.

The copper wine column contains 13 bubble-cap trays with a column diameter of 1.6 m and a total height of 6.1 m. The first rectifier with a height of 11 m and a diameter of 1.1 m contains 16 bubble-cap trays. Crude ethanol at 96 vol. % is removed as a side stream on the tenth plate, creating a maximum concentration of esters, aldehydes, SO₂, methanol and methyl esters in the column heads. Small quantities of SO₂ present in the wine are vented to atmosphere after the final condenser. Fusel oil and lighter oil fractions are fed into the impurities column for further column concentration and separation.

2.2.2 The hydro selection column

This column has a diameter of 1.4 m with a height of 7.8 m. The crude ethanol from the first rectifier which is fed onto the middle plate of this 42 bubble-cap tray column, still contains impurities which are detectable through sensory evaluation. Dilution water at ± 90 °C is fed onto the first plate of the column, diluting the crude ethanol to about 15 vol. %. In the diluted state, only iso amyl alcohol is more volatile than n-propanol. If n-propanol is therefore distilled over several plates while flowing down in the column, the n-propanol will volatilise and will be dragged upwards with the vapour streams. There is a considerable increase in alcohol concentration when one moves from the water feed plate to the following plate below. On the water feed plate, a concentration of less than 20 vol. % can be expected with 80 – 90 vol. % just above.

The net effect of this would be that the volatile components lower down in the column would volatilise and move upward with the vapour stream, until it moves through the zone with the sharp alcohol gradient. This causes all volatile components on the first plate to condense and move downwards onto the dilution plate to volatilise again. The accumulated components are then extracted from the zone by removal of a fraction. The diluted alcohol at the bottom of the column is therefore stripped from all volatiles except methanol, before it is fed into the second rectifier or spirits column.

2.2.3 The second rectifier (spirits column)

This column with its 68 bubble-cap trays has a rectification function and produces a spirit at 96.4 vol. %. The column has a diameter of 1.45 m and a height of 11.5 m. Methanol is the primary impure component. Spirits are removed from this column as a side product on the tenth plate from the top. A further side stream of higher boiling point components is also drawn off the eighteenth plate from the bottom and fed into the impurities column.

2.2.4 The impurities column

All fractions removed in the previous columns contain fractions in excess of 80 vol. % ethanol that need to be recycled. This takes place in the impurities column consisting of 60 plates with a diameter of approximately ± 0.55 m and an overall height of 11.3 m. Surplus alcohol is withdrawn from the column heads and fed back into the wine column. This rate of withdrawal regulates the temperature in the column in such a way that the ethanol gradient is formed above the feed plate. High concentrations of fusel oil accumulate in this zone and is fed to the fusel oil separator.

2.2.5 The final column

This column with a height of 11.6 m and a diameter of 0.9 m has 60 plates. The column is commonly known as the methanol column. The column lowers the methanol content to ± 50 mg/100 mL AA. Due to the similarities in the vapour pressures and other characteristics of ethanol and methanol, this separation is done with thermodynamic difficulty. Due to the methanol presence, the process for the production of neutral wine spirits becomes significantly energy intensive. This energy factor, methanol's toxicological character as a component in a potable product, as well as its usage in product adulteration, make the economical separation of this chemical component an engineering challenge.

The author^[18] concluded that the removal of methanol, makes an extensive contribution of up to 45 % to the overall energy consumption of this

conventional distillation process. All these factors justify the investigation into the reasons for the natural presence of methanol in wine and subsequently its distillate, as well as searching for an innovative way of removing this component at a reduced operating cost. These issues pertaining to methanol is discussed in detail later. The high concentration methanol fraction is removed from the final condenser as overheads. The purified product is pumped from the base of the column through a final cooler to the product tank. This spirit is now ready for use in various products including vodka, gin, liqueurs and most important of all, brandy.

2.3 OPTIMISATION OF THE EXISTING PROCESS

A detailed study was completed by the author^[18] on the optimisation of the existing wine spirits production process in the South African Wine Industry. Various mechanisms and techniques were used to make optimization suggestions into the existing process. The more prominent methods and approaches that were used includes the following:

2.3.1 Modelling of distillation columns through simulation

Dynamic equation-based process simulation was used to simulate the production process under discussion with the two simulators Aspen and Chemcad. The primary objective was to obtain valuable tray-by-tray chemical compositions and enthalpies, which could be used to apply the principles of other techniques on the individual columns. The process of modelling the distillation columns can be summarised as follows:

- supplying the simulator with an interactive process flow diagram;
- selecting proper simulation units equivalent to the actual process;
- feeding data of stream characteristics into the interactive simulator;
- supplying physical data of distillation columns;
- choosing the correct thermodynamic model.

Simulation is discussed and used later to determine the thermodynamic condition and properties in the feed stream and inside the adsorber columns.

2.3.2 Application of Pinch Analysis (distillation column targeting)

Pinch Analysis is a systematic thermodynamic method, which is used to optimise the flow of heat and mass in a system. The most common application of pinch analysis is in the optimisation of heat exchanger networks. A different application of pinch analysis is distillation column targeting. This technique relates to the design of distillation columns and in particular to the optimisation of columns. The process involves options such as different reflux ratios, pressures, side-condensing/side-reboiling and feed preheating and cooling. Alongside heat load and temperature targets, the methodology clarifies the effect of design modifications on column capital cost, even prior to the actual design. The technique is applicable to non-ideal, multi-component systems and complex distillation configurations. Various proposals regarding column design and energy efficiency were made.

2.3.3 Energy recovery with steam jet ejectors

Since the primary objective of the study was to maximise energy savings, an attempt was made to recover the energy content of the effluent stream from the wine column. This energy would be recovered by making use of steam jet ejectors. The proposed system consisted of a flash cooler with the vacuum being created by a steam jet ejector. The ejector used motive steam at 1 MPa, which is the design pressure of most boilers utilised at KWW. This motive steam, together with the steam recovered from the flash cooling, was injected into the base of the column. Different ejector configurations were investigated and a proposal was made.

2.3.4 Column heat loss through natural convection

Heat losses from distillation columns to the surrounding atmosphere were evaluated by modelling a column as an annular fin system from which natural convection was drawing energy. The proposal made some suggestions into the efficiency and feasibility of insulating distillation columns to prevent excessive convection losses to atmosphere.

2.3.5 Investigation into alternatives to distillation

Distillation is still the preferred technique for ethanol/water separation because of its long history of use. However, non-conventional processes were also investigated to evaluate their efficiency in ethanol/water separations. Investigated alternatives included:

- ethanol/water fractionation by means of a carrier gas method;
- membrane pervaporation;
- adsorption.

Of all the processes investigated, adsorption seemed to be the more practical as well as applicable process to use in this case.

2.4 ADSORPTION vs. DISTILLATION

Because of its simplicity and mere universal applicability, distillation has assumed a dominant role in separations technology and is the standard against which other potential processes are generally measured. However, distillation is not an energy efficient process and with the ever increasing cost of energy, alternative separation processes are increasingly drawing attention.

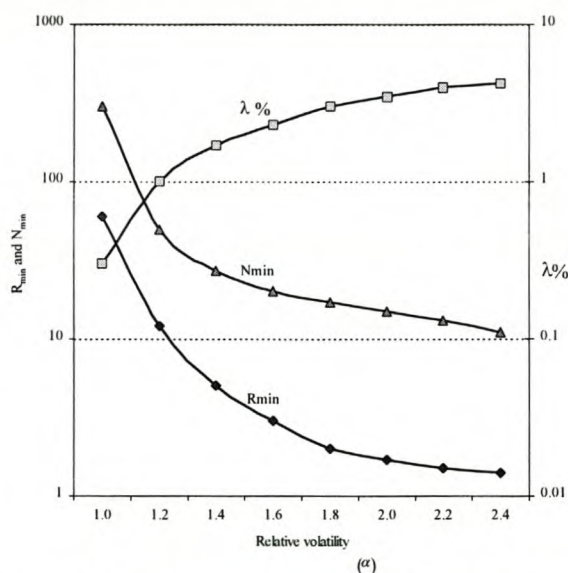


Figure 2.3. Variation of thermal efficiency (λ), minimum number of theoretical stages (N), and minimum reflux ratio (R) with relative volatility (α) for separation of a 50-50 molar mixture into top and bottom products each of 99% purity.^[54]

Figure 2.3 shows a plot of the thermal efficiency and minimum reflux requirement vs. relative volatility for the separation by distillation of a hypothetical 50/50 mixture of two aromatic hydrocarbons (A and B) into two streams, one containing (99% A + 1% B) and the other containing (99% B + 1% A). Thermal efficiency is calculated as the ratio of the free energy of mixing, to the reboiler heat load at minimum reflux. The heat of evaporation has been taken as 8070 cal/mole, corresponding to toluene. For separation of the mixture of benzene and toluene ($\alpha = 2.4$) the thermal efficiency is about 4.2 %.^[54]

As the relative volatility is decreased, the thermal efficiency falls rapidly due to the increasing reflux requirement. Also shown in Figure 2.3 is a plot of the minimum number of theoretical stages required to effect the specified separation at total reflux. This number increases rapidly with decreasing α and it is evident that for systems in which $\alpha < 1.2$, distillation is very inefficient. Although the cost of adsorption separation processes can sometimes be higher than that of a distillation unit with an equivalent number of theoretical stages, much higher separation factors are commonly attainable in an adsorption system. As the relative volatility decreases, an adsorption process eventually becomes the more economic option. The breakeven point depends to a considerable extent on the particular system as well as on the cost of energy, but as a rough guide, adsorption becomes competitive with distillation separations when the relative volatility is less than about 1.25. In this case $\alpha = 1.69$ (see appendix I), showing that the distillation is approaching inefficiency and impractical separation.

For purification processes involving light gases where the alternative is cryogenic distillation, the cost comparison is generally more favourable to adsorption so that adsorption is commonly a preferred route, even when the volatility is high. Whether adsorption can become a competitive low energy alternative to a more traditional separation process such as distillation, depends on many technical and economic factors.

Separations which are often difficult or even impossible to achieve by distillation, perhaps because of low relative volatilities or the formation of azeotropes, are often technically straightforward by adsorption, given the availability of an absorbent material with the appropriate selectivity for the components to be separated.

2.5 THE NATURAL PRESENCE OF METHANOL IN WINE

Pectic substances are present in all grapes. These polyoxides are homogalacturonanes and rhamnogalacturonanes.^[49] The main characteristic of homogalacturonanes is the presence of a skeleton of galacturonic acid molecules, in which carboxylic functions can be more esterified by means of methanol. Rhamnogalacturonanes are made up of an alternate succession of rhamnose and galacturonic acid as well as lateral chains of neutral sugars. Both types of pectants are normally found associated in the same structure, which therefore contains homogalacturonic and rhamnogalaturonic areas.

The pectic substances participate with the other constituents of the cellular wall to the creation of a tri-dimensional meshwork made more solid by the contribution of covalent, ionic and mechanic links. The presence of pectins in all fruits, including grapes, is accompanied by an equally extensive spread of enzymes, capable of breaking them down. The pectolitic enzymes which are produced by the micro organisms, can be classified into two groups namely hydrolases and lyases. Amongst the first ones, the pectinmethylesterase breaks down the methoxylic group of the galacturonic acid, thus freeing methanol.^[49,2] The pectin materials hydrolyse as follows:

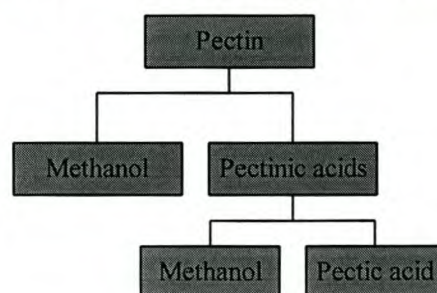


Figure 2.4. Hydrolysis of pectin materials.^[2]

Normally one finds that with the liberation of methanol, an increase in free amino acids also occurs.

The fact that methanol is formed by the hydrolysis of naturally occurring pectants, is substantiated by the fact that methanol content is higher:

- when pectolitic enzymes are added to the must;
- in wines made by fermentation on the skins;
- in wines made from macerated grapes compared to those from non-macerated grapes.

Flanzy and Bouzigues (1995) found more methanol in wines made from must stored on the skins at 0 °C for 13 – 22 days, compared to those not stored in this way. This seems reasonable since the pectinmethylesterase is present mostly on the skin. When methanol-containing wines are distilled to wine spirits, it was found that the methanol content increased at least five-fold ^[35]. Also of interest is the fact that grain and molasses alcohol have much lower methanol concentrations than alcohol produced from grapes. Adulteration of alcohol containing products appears all over the world, including in South Africa. In these cases methanol is normally used to replace a part of the potable ethanol, with the benefit to the perpetrator not having to pay the Customs and Excise Duty of approximately R30/ℓAA.^[77] Recent adulteration of wines in Italy has caused international scandals. Methanol is also the main component of stone and pome fruit brandies, excluding Calvados.

As a rule, plum Mirabel and Williams distillates, contain more than 1000 mg/100 ml AA, whereas Cherry distillates range lower, from 400 - 800 mg/100 ml AA^[51]. Since during fermentation of the fruit mash, a certain minimum amount of methanol is formed by enzymatic cleavage of pectin as was mentioned earlier. Up to now the methanol content of fruit brandies has been used for the evaluation of authenticity and possible adulterations such as addition of neutral alcohol or of distillates from cheap materials or addition of sugar to the mash. Cherry distillates for example are expected to contain a methanol concentration of at least 400 mg/100 ml AA and similar rules exist for the other brandies.

2.5.1 The toxicological effects of methanol

Methanol is absorbed in the stomach and more quickly when it is in its free form. The absorbed methanol is then slowly converted to formaldehyde by alcohol dehydrogenase in the liver (Liesivuori 1991). If methanol is co-ingested with a significant amount of ethanol, the methanol conversion is temporarily blocked since ethanol has nine times the affinity for alcohol dehydrogenase as does methanol^[39]. This then allows the body to eliminate methanol via the lungs and urine before it gets converted to formaldehyde. Formaldehyde is converted to formic acid by aldehyde dehydrogenase in the liver, by formaldehyde dehydrogenase in the blood or through the tetrahydrofolic acid dependent one-carbon pool.

Methanol is a deadly poison in small amounts. The toxic effect of methanol vary widely from person to person but while around 30 ml or 24 g of methanol is considered lethal, as little as 6 ml of methanol has killed an adult person (Bennett 1953). The most well known effect caused by acute or chronic poisoning of methanol, is damage to the optic nerve fibers. It has been reported that as little as 10 ml (approximately 10 g) of methanol can cause blindness^[15]. Many of the signs and symptoms of intoxication due to methanol ingestion, are not specific to methanol, e.g. headaches, ear buzzing, dizziness, nausea, gastro-intestinal disturbances, weakness, memory lapses, numbness and shooting pains in the hands and forearms, behavioral disturbances and neuritis. The most characteristic signs and symptoms of methanol poisoning in humans are the various visual disturbances, which can occur without acidosis, although they unfortunately do not always appear. Some of these symptoms can be misty vision, progressive contraction of visual fields (visual tunneling), mist before the eyes, blurring of vision and obscuration of vision.

Cook (1991) found in a study that after only a 75 minute exposure to 192 ppm of methanol (below the exposure time and level that would lead to a significant change in urinary or plasmaformic measures), the overall results

showed no changes in some categories but did show statistically significant changes in other important measurements. The subjects showed:

- slightly greater fatigue from work load
- slight impairment of concentration and memory
- a slight change in brain wave patterns in response to light and sound

Methanol also oxidises ten times slower than ethanol. Therefore several ways to decrease the methanol content of brandies have been discussed (Tanner 1982). These methods include heat treatment of the mash to inactivate the pectolitic enzymes or fruit juice fermentation instead of mash fermentation. There were however still technological and sensory problems. The removal of methanol from the brandy by a special distillation procedure or from the enzyme treated mash before fermentation is also possible (Tanner 1982), but results in the loss of flavour volatiles. All these factors considered, it becomes justified to investigate the process which can reduce or eliminate methanol from neutral wine spirits completely. This study confirms the successful use (on production scale) of adsorption to achieve this objective.

2.6 FUNDAMENTAL PRINCIPLES OF ADSORPTION

Adsorption separation processes are in widespread industrial use. Particularly in the petroleum refining and petro-chemical industries the underlying physical and chemical principles on which such processes are based, are reasonably well understood. In the last few years, adsorption technology has become increasingly important in terms of market development and market share. This increased commercialisation of the technology stimulates further research into both the adsorbents and their applications. The rapid growth in the number of patents for pressure swing adsorption processes (which will be discussed in more detail later) is shown in Figure 2.5.

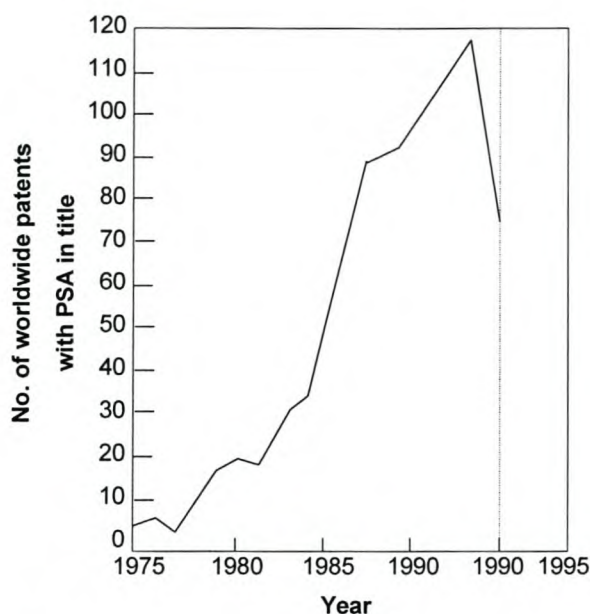


Figure 2.5. Growth of patents relating to PSA^[13].

Indeed the subject is continually advancing as new and improved applications occur in competition with other well-established process technologies, such as distillation and absorption. In adsorption, molecules distribute themselves between two phases, one of which is a solid while the other can be liquid or gas. Adsorption is the result of interactive forces of physical attraction between the surface of a porous solid and component molecules being removed from the bulk phase. Thus, adsorption is the accumulation of concentration at a surface, as opposed to absorption which is the accumulation of concentration within the bulk of a solid or liquid.

2.6.1 Forces of adsorption

In discussing the fundamentals of adsorption, it is useful to distinguish between physical adsorption involving only relatively weak intermolecular forces and chemisorption, which involves essentially a formation of a chemical bond between the sorbate molecule and the surface of the adsorbent^[54].

Adsorption may be classified as chemical adsorption or physical adsorption, depending on the nature of the surface forces. It will be shown later that understanding the nature and type of adsorption forces becomes important in the interpretation of results from a designed adsorber.

During physical adsorption, the forces are relatively weak, involving mainly Van der Waals interactions, supplemented in many cases by electrostatic contributions from field gradient-dipole or quadrupole interactions ^[28]. By contrast in chemisorption there is significant electron transfer equivalent to the formation of a chemical bond between the sorbate and the solid surface.

Table 2.1. Parameters of physical and chemical adsorption^[28]

Parameter	Physical adsorption	Chemisorption
Heat of adsorption	low, < 1-5 times latent heat of evaporation	high, > 1-5 times latent heat of evaporation
Specificity	Nonspecific	Highly specific
Nature of adsorbed phase	Monolayer or multilayer, no dissociation of adsorbed species	Monolayer only
Temperature range	Only significant at relatively low temperatures	Possible over a wide range of temperatures
Forces of adsorption	No electron transfer - polarization of sorbate may occur	Electron transfer leading to bond formation between sorbate and surface
Reversibility	Rapid, nonactivated, reversible	Activated, may be slow and reversible

Such interactions are both stronger and more specific than the forces of physical adsorption and are obviously limited to monolayer coverage. In the discussion of adsorption theories later, it is shown that an approach such that suggested by Langmuir can easily be used to model a monolayer system for chemical adsorption. The adsorption mechanisms for methanol adsorption discussed in chapter 2.8.2 shed some light on the forces involved in methanol adsorption. It typically shows that a model such as the Brunauer-Emmett-Teller approach would be more suitable since both physical and chemical forces are involved. If however the assumption is for a multi-component adsorption, other models or theories need to be used.

The differences in the general features of physical and chemisorption systems can be understood on the basis of this difference in the nature of the surface forces (refer to Table 2.1). Almost all adsorptive separation processes depend on physical adsorption rather than chemisorption.^[54] When a molecule having three degrees of freedom of translation approaches an

unsaturated surface, at least one degree of freedom of translation is lost as a consequence of its attraction to the surface where it is constrained to movement across the adsorbent surface.

The force fields associated with the gas phase molecules as they approach one another can be calculated by means of the Lennard-Jones potential energy equation. The following figure shows how the potential energy curves of an adsorbate / adsorbent system relates to experimental heats of adsorption.

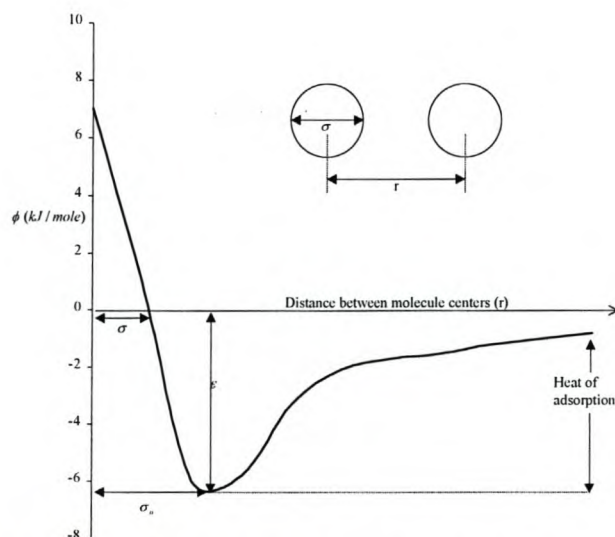


Figure 2.6. Lennard-Jones potential energy function for adsorption.^[54]

The dispersion and repulsion energies involved lead to the following potential function^[54].

$$\phi = 4\varepsilon \left[\left(\frac{\sigma}{r} \right)^{12} - \left(\frac{\sigma}{r} \right)^6 \right] \quad (2.1)$$

The potential energy function is the sum of all interactions between an adsorbate molecule and the molecules in lattice of the adsorbent. Understanding the role of the potential well and how it affects an actual adsorption system is crucial. Since the potential well translates into the heat of adsorption (discussed later for energy conservation purposes), Equation 2.1 plays a valuable role in situations where heat of adsorption for a system is unknown. Benefits of retaining heat of adsorption are discussed later.

The function passes through a minimum known as the potential well, the depth (ϵ) which is the energy of adsorption at a temperature of absolute zero. For a given adsorbate / adsorbent system, ϵ equates closely with measured heats of adsorption. Physical adsorption is an exothermic process and heat is always released when adsorption occurs. The strength of the surface forces depend on the nature of both the solid and the sorbate. If the forces are relatively weak involving only van der Waals interactions supplemented in the case of polar or quodropolar species by electrostatic forces, we have what is called physical adsorption or physisorption. In contrast, if the interaction forces are strong, involving a significant degree of electron transfer, we have chemisorption ^[55]. These interaction forces finally determines the ease (or difficulty) with which regeneration is to be performed and also which methods are to be used.

Most practical adsorption separation processes depend on physisorption rather than on chemisorption since, except for a few rather specialised applications, the capacities achievable in chemisorption systems are too small for an economic process. It is shown later that a combination of forces play a role in the adsorption of methanol from the ethanol stream. The role of the adsorbent is to provide the surface area required for selective sorption of the preferentially adsorbed species. A high selectivity is a primary requirement, but a high capacity is also desirable since the capacity determines the size and therefore the cost of the bed. To achieve a high capacity, commercial adsorbents are made from microporous materials. As a result, the rate of adsorption or desorption is generally controlled by diffusion through the pore network and such factors must be considered in the selection of an adsorbent and the choice of operating conditions.

2.6.2 Selectivity

Selectivity may depend on a difference in either adsorption kinetics or adsorption equilibrium^[54]. The extent of the ability of an adsorbent to separate molecule A from molecule B is known as its selectivity. The separation factor provides a numerical value for selectivity and is defined as follows^[54]:

$$\alpha_{AB} = \frac{X_A / X_B}{Y_A / Y_B} \quad (2.2)$$

X_A and Y_A are respectively the mole fractions of component A in adsorbed and fluid phases at equilibrium. The separation factor is analogous to relative volatility. Selectivity may manifest itself in one or a number of ways in any particular separation process^[13]:

- differences may exist in the thermodynamic equilibrium for each adsorbate / adsorbent action; this is often known as the equilibrium effect;
- differences may exist in the rates at which different adsorbates travel into the internal structure of the adsorbent; this is often known as the kinetic effect;
- pore openings may be too small to allow penetration by one or more of the adsorbates; this is known as the molecular sieving effect and can be considered to be an extreme case of the kinetic effect;
- differences may exist in the rate at which different adsorbates can be desorbed from the adsorbate; this is generally known as the desorption effect.

Kinetic separations are in general possible only with molecular sieve adsorbents such as zeolites or carbon sieves. The kinetic selectivity is measured by the ratio of the micropore or inter-crystalline diffusivities for the components considered^[54]. Differences in diffusion rates between molecules of comparable molecular weight become large enough to provide a useful separation only when diffusion is hindered by steric effects.

This requires that the diameter of the micropore be comparable with the dimensions of the diffusing molecule. Molecular sieve separations which depend on the virtually complete exclusion of the larger molecules from the micropores, have in the separation of linear from branched and cyclic hydrocarbons onto 5A zeolites may be regarded as the extreme limit of a kinetic separation, in which the rate of adsorption of one component is

essentially zero^[28]. Because the geometric requirements for a molecular sieve separation are stringent, such separations are less common than separations based on differences in the adsorption equilibrium or on moderate differences in intra-crystalline diffusivity.

While most adsorbents have a relatively wide distribution of pore size, kinetic selectivity depend on steric hindrance and therefore requires a very narrow distribution of pore size. This is a characteristic feature of zeolitic adsorbents, since these materials are crystalline and the dimensions of the micropores are determined by the crystal structure. By contrast the carbon molecular sieves are amorphous materials similar to high area activated carbons, but with a much lower, much narrower distribution of pore size. This uniformity of pore size is achieved by careful control of the conditions during the activation step and by controlled deposition of easily crackable or polymerisable hydrocarbons such as acetylene. Table 2.2 provides a classification of commercial adsorbents based on equilibrium and kinetic selectivity.

Table 2.2. Selectivity classification of commercial adsorbents^[55]

Equilibrium selective		Kinetically selective	
Hydrophilic	Hydrophobic	Amorphous	Crystalline
Activated alumina	Activated carbon	Carbon molecular sieve (CMS)	Small-pore zeolites and zeolite analogs
Silica gel	Microporous silica		
Al-rich zeolites	Silicalite, dealuminated mordenite and other silica-rich zeolites		
Polymeric resins containing -OH groups or cations	Other polymeric resins		

In kinetic selective adsorbents the primary parameters determining the selectivity are the pore size and pore size distribution. The nature of the material is generally of secondary importance.

2.6.3 Hydrophilic and hydrophobic behaviour

For equilibrium controlled adsorbents, the primary classification is between hydrophilic and hydrophobic surfaces. If the surface is polar, generally as a result of the presence of ions in the structure, but also as a result of the presence of ions or polar molecules strongly bound to the solid surface, it will preferentially attract polar molecules and in particular water. Thus, on highly polar adsorbents such as zeolites or activated alumina, water (a small polar molecule) is strongly adsorbed while methane (a small non-polar molecule of similar molecular weight and therefore with comparable van der Waals interaction energy) is only weakly adsorbed. Ionic adsorbents such as zeolites owe their hydrophilic nature to the polarity of the heterogeneous surface.^[55]

However, when the surface contains hydroxyl groups, molecules such as water can also interact strongly by hydrogen bond formation. As with polar adsorbents, water is therefore preferentially adsorbed but in this case the hydrophilic selectivity is attributable mainly to the hydro bond energy rather than to surface polarity.^[11] It is this characteristic that affects also the separation of methanol from ethanol in the presence of water. A quantity of water is naturally present in the wine spirits (azeotrope). The ability of water to displace methanol due to its strong H-bonding is also investigated later. Where the hydrophilic selectivity comes from hydrogen bonding, polar molecules with no active hydrogens, will be held only with an affinity comparable to non-polar sorbates.

2.6.4 Pore size distribution

According to the IUPAC classification, pores are divided into three categories by size: micropores $< 20 \text{ \AA}$; mesopores $20 - 500 \text{ \AA}$; macropores $> 500 \text{ \AA}$.^[55] In a micropore, the guest molecule never escapes from the force-field of the solid surface, even at the centre of the pore. It is therefore reasonable to consider all molecules within a micropore, to be in the adsorbed phase. By contrast, in mesopores and macropores, the molecules in the central region of the pore are essentially free from the force field of the surface. It becomes

physically reasonable to consider the pore as a two-phase system, containing both adsorbed molecules at the surfaces and free gases molecules in the central region ^[78]. Micropores contain very little surface area relative to the pore volume and contribute little to the adsorptive capacity. Representative pore size distributions for several different adsorbents are shown in Figure 2.7.

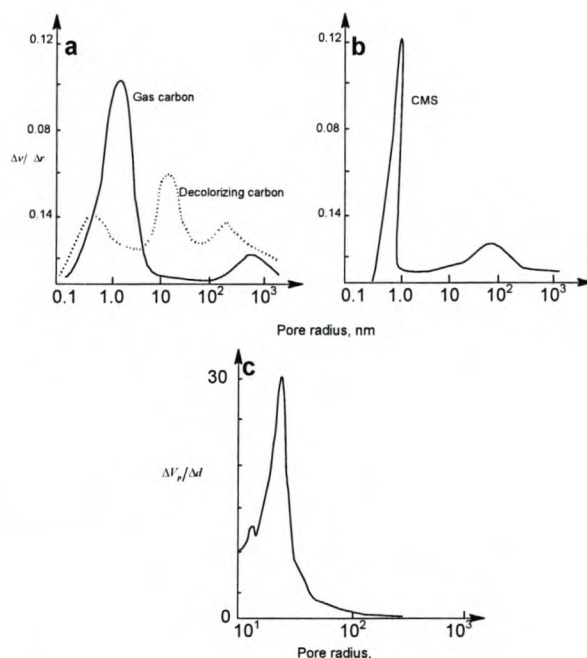


Figure 2.7. Pore size distributions for (a) typical activated carbons; (b) carbon molecular sieves; (c) typical activated alumina.^[55]

2.6.5 Physical strength

Repeated pressurisation and depressurisation of an adsorbent bed, tends to cause a attrition of the adsorbent particles. Physical strength is therefore a prime consideration in the choice of an adsorbent for a PSA process. Such considerations may indeed prelude the use of an otherwise desirable adsorbent in favour of a material that, from kinetic and equilibrium considerations alone, may appear to have inferior properties. Both the crush strength and the abrasion resistance, are strongly dependent upon the way in which the adsorbent particles are manufactured, including such factors as nature of the binder and the pre-treatment conditions.

The importance of the binder is discussed later under the manufacturing process for zeolites. It is also shown later that in order to reduce abrasion and possible attrition, certain adsorption techniques are used and built into the design.

2.6.6 Practical adsorbents

The requirement for adequate adsorptive capacity restricts the choice of adsorbents for practical separation processes to microporous adsorbents with pore diameters ranging from a few Angstroms to a few tenths of Angstroms. To be technically effective in a commercial separation process, whether this be a bulk separation or a purification, an adsorbent material must have a high internal volume which is accessible to the components being removed from the fluid. The adsorbent must also have good mechanical properties such as strength and resistance to attrition and it must have good kinetic properties, i.e. it must be capable of transferring adsorbing molecules rapidly to the adsorption sites. It is this quick transport ability that gives a molecular sieve bed the flexibility to treat more adsorbate per unit time than other adsorbents and is more likely to tolerate higher feed flow rates and concentrations than the design projections. This aspect needs also to be evaluated.

In most applications, the adsorbent must be regenerated after use and therefore it is desirable that regeneration can be carried out efficiently and without damage to mechanical and adsorptive properties. The raw materials and methods for producing adsorbents need to be inexpensive for adsorption to compete successfully on economic grounds with alternative separation processes^[13]. The adsorptive properties depend on the pore size and the pore size distribution as well as the nature of the solid surface. A simple classification of some of the common adsorbents according to pore size distribution and polarity is shown in the following table.

Table 2.3. Polarity and pore classifications of some adsorbents^[28]

Surface polarity	Pore size distribution	
	Narrow	Broad
Polar	Zeolites (Al rich)	Activated alumina Silica gel
Nonpolar	Carbon molecular sieves	Activated carbon

The physical properties as well as typical applications of various commercial adsorbents are given in appendix B. The high internal surface area of an adsorbent creates the high capacity needed for a successful separation or purification process. As can be seen from appendix B1, the most important adsorbents used today are silica gel, activated alumina, carbons, zeolites, polymers, resins as well as clays. There is however a fundamental difference between these materials.

In the traditional adsorbents, there is a distribution of micropore size and both the mean micropore diameter and the width of the distribution about this mean are controlled by the manufacturing process. These adsorbent materials contain complex networks of interconnected micropores, mesopores and macropores.

In contrast, in zeolitic adsorbents the pores or channels have precise dimensions although a macroporous structure is created when pellets are manufactured from zeolite crystals by the addition of a binder. The micropore size of a zeolitic adsorbent is controlled by the crystal structure and there is virtually no distribution of pore size.^[54] This leads to significant differences in the adsorptive properties and it is therefore convenient to consider the zeolites and other crystalline adsorbents such as the aluminum phosphate molecular sieves as a separate class of adsorbents.

Molecular sieves also differ from all other types of adsorbents in that they have an extremely high equilibrium adsorption capacity for water and polar compounds at very low concentrations of these compounds in the fluid phase. This characteristic is illustrated in Figure 2.8.

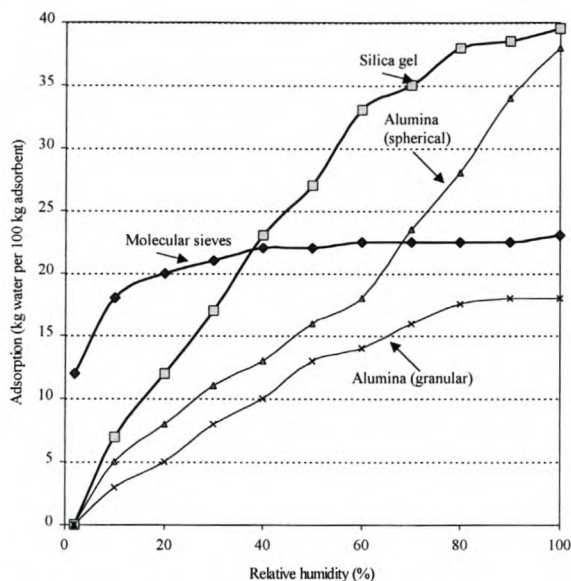


Figure 2.8. Comparison of relative humidity effect on various desiccants.^[20]

Due to this obvious superiority of molecular sieves, they became the preferred adsorbent for this study.

2.7 ZEOLITES / MOLECULAR SIEVES

Zeolites are porous crystalline aluminosilicates, which comprise assemblies of SiO_4 and AlO_4 tetrahedra joined together through the sharing of oxygen atoms. More than 150 synthetic zeolite types are known, the most important commercially being the synthetic types A and X, synthetic mordenite and the ion exchange varieties^[13]. Since the micropore structure is determined by the crystal lattice, it is precisely uniform with no distribution of pore size^[54]. It is this feature which distinguishes the zeolites from the traditional microporous adsorbents. The zeolites are therefore crystalline rather than amorphous and the micropores are actually intra-crystalline channels with dimensions precisely determined by the crystal structure. The crystalline aluminosilicates of alkali, or alkali-earth elements, such as sodium, potassium and calcium are represented by the following stoichiometry^[20]:



The channel size in zeolites is determined by the number of atoms, which form the apertures (windows) leading to the cages. Apertures may be constructed from rings of 6,8,10 or 12 oxygen items together with the same number of aluminum and/or silicon atoms.^[78] The following graphic is a representation of the framework structure of zeolites A and X .

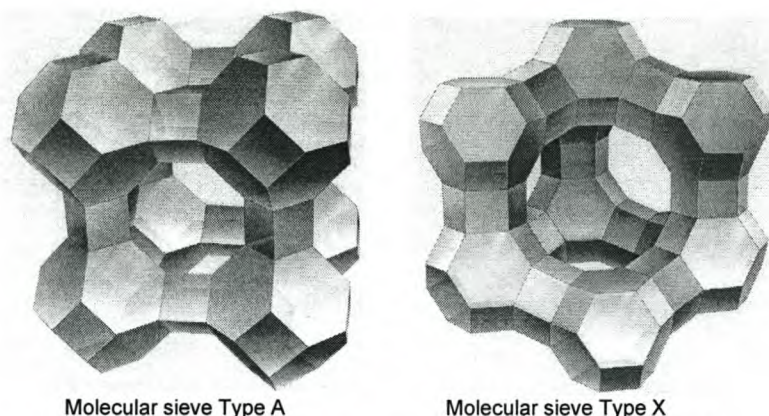


Figure 2.9. Structure of commercial molecular sieves Type A and X

2.7.1 Type X molecular sieves

The crystal structure of the type X zeolite is built up by arranging the basic sodalite cages in a tetrahedral stacking (diamond structure) with bridging across the six membered oxygen atom ring.^[40] These rings provide opening windows 9 – 10 Å in diameter into the interior of the structure. The overall electrical charge is balanced by positively charged cations as in the type A structure^[20]. The value of X can be as great as 276, making the water in this type of molecular sieve 35 wt. % of the anhydrous zeolite.

2.7.2 Type A molecular sieves

In the most common commercial zeolite, type A, the tetrahedra are grouped to form a truncated octahedron with a silica or alumina tetrahedron at each point. This structure is known as a sodalite cage. It contains a small cavity, which is of no practical significance since the largest openings through the six-sided faces of the octahedron are not large enough to permit the entrance of even small molecules. When sodalite cages are stacked in simple cubical forms, the result is a network of cavities approximately 11.5 Å in diameter, accessible through openings on all six sides.^[54] These openings are surrounded by 8 oxygen ions.

One or more changeable cations also partially block the face area. In the sodium form, this ring of oxygen ions provides an opening of 4.2 Å in diameter into the interior of the structure. This crystalline structure is represented chemically by the following formula^[78].



The water of hydration, which fills the cavities during crystallisation, is loosely bound and can be removed by moderate heating. This type of removal of the water of hydration is called thermal regeneration. Pressure effects can also be used to remove the water of hydration. The voids formally occupied by this water can be refilled by adsorbing a variety of gases and liquids (methanol in this case). The number of water molecules in this structure (the value of X) can be as great as 27, making the water in the saturated formula 28.5 wt. % of the anhydrous zeolite.^[78] The sodium ions which are associated with the aluminum tetrahedra, tend to block the openings or conversely may assist the passage of slightly oversized molecules by their electrical charge. As a result, the sodium form of the molecular sieve, which is commercially called 4A, can be regarded as having uniform openings of approximately 4 Å in diameter. By replacing a large fraction of the sodium with potassium ions, the 3A molecular sieve is formed with openings of about 3 Å. Similarly when calcium ions are used for exchange, the 5A molecular sieve is formed with approximately 5 Å opening. In zeolite A, there are 12 negative charges to be balanced by cations in each unit cell. The most probable locations for the cations are:

- Type I, which is at the centre of the six-member ring, thus at one of the eight corners of the cavity;
- Type II which is at the eight-member aperture directly obstructing the entrance;
- Type III is near the four-member ring inside the cavity.

Type A zeolites are synthesized in the sodium form with 12 sodium cations occupying all eight sites in I and three sites in II plus one site in III. This is the

commercial type 4A zeolite with an effective aperture size of 3.8 Å. The sodium form can be replaced by various other cations or by a hydrogen ion. The commercial type 3A zeolite is formed by exchanging Na^+ with K^+ resulting in a smaller effective aperture size due to the larger K^+ . The reduction in the free diameter of the windows by blocking cations, causes a dramatic reduction in the diffusivity of the guest molecules.

The extent to which the windows are obstructed depends on the number and nature of the cations, since different cations show different affinities for the window sites. By appropriate choice of cationic form, it is sometimes possible to develop kinetic selectivity and even in certain cases, to obtain a molecular sieve separation between species which can both diffuse easily in an obstructed sieve.

The following schematic representation shows the effective apertures for some cationic forms of A and X zeolites as well as in some other sieves.

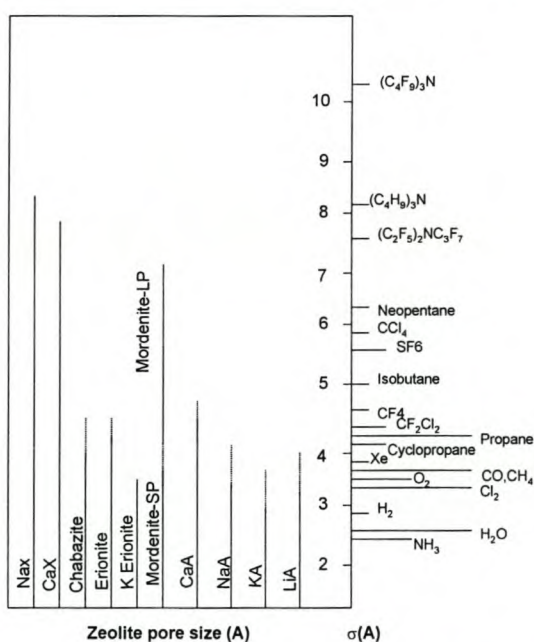


Figure 2.10 Chart showing correlation between effective pore size of various zeolites and Lennard-Jones kinetic diameter. The dotted portions indicate the range over which the cut-off occurs between low and high temperatures (77-420 K).^[54]

Figure 2.10, together with the classification from Yang (Table 2.5), could be used as basis to solve a potential separation problem.

2.7.3 Zeolite manufacture procedure

Commercial zeolite pellets are manufactured in the following process sequence: synthesis, pelletising and calcination. Many alkaline metal hydroxides and raw materials containing silica and alumina can be used in low temperature synthesis. The steps involving the $\text{Na}_2\text{O}-\text{Al}_2\text{O}_3-\text{SiO}_2-\text{H}_2\text{O}$ system, which is used in synthesising zeolites of types A, X and Y are depicted in Figure 2.11(a).

The first step involves gel formation between sodium hydroxide, sodium silicate and sodium aluminate in aqueous solution at room temperature. The gel is formed by co-polymerisation of the silicate and aluminate species by a condensation polymerisation mechanism [78]. The gels are crystallised in a closed hydrothermal system at temperatures of 25 °C and 175°C. Higher temperatures up to 300°C are used in some cases. The time for crystallisation ranges from a few hours to several days.

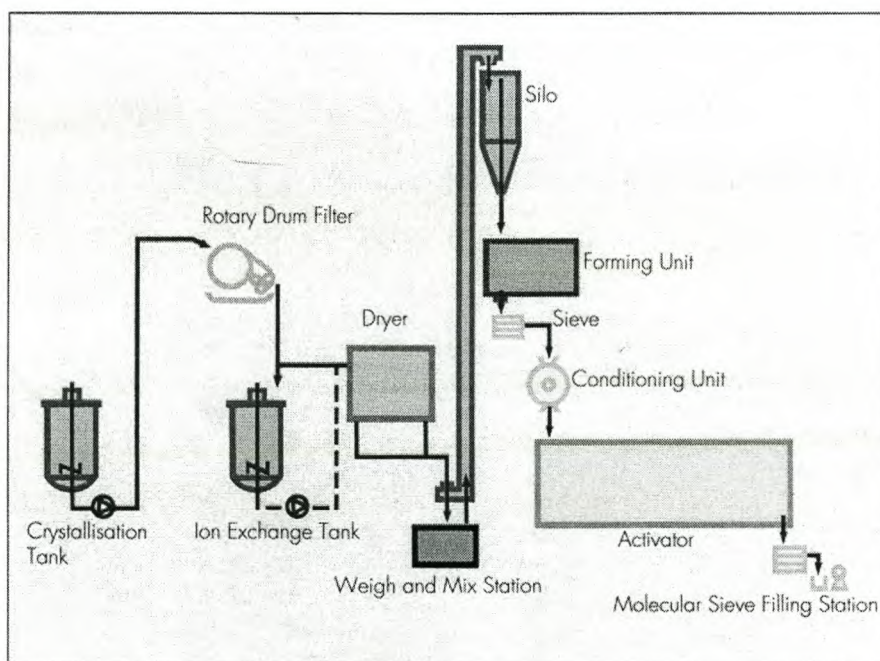


Figure 2.11(a). Grace molecular sieve production.^[22]

The crystals formed are cubic, single crystals with sizes ranging from 1 – 10 microns. The crystals, after calcination at about 600°C are further agglomerated and pelletised with or without a binder amounting to less than 20 % of the pellets. The binder has a negligibly small capacity for the adsorption gases. The importance of the type of binder used should not be underestimated, as is shown later in the design approach in chapter 4. The characteristics of the major commercial zeolite sorbents in the pelletised forms, are given in Table 2.4.

Table 2.4. Characteristics of major zeolite sorbents

Zeolite Type	Major Cation	Aperture Size (Å)	Bulk Density	Water Capacity, wt%
3A (Linde)	K	3	40	20
3A (Davidson)	K	3	46	21
4A (Linde)	Na	4	41	22
4A (Davidson)	Na	4	44	23
5A (Linde)	Ca	5	45	21.5
5A (Davidson)	Ca	5	44	21.7
10X (Linde)	Ca	8	40	31.6
13X (Linde)	Na	10	38	28.5
13X (Davidson)	Na	10	43	29.5

At least three different pellet forming processes are in common use: extrusion to form cylindrical pellets, granulation to form spherical particles and combined processes involving extrusion followed by rolling to form spheres.^[54] Commonly used binders consists of mixtures in various proportions of sepiolite, kaolinite, attapulgite and montmorillonite, often with added silica or alumina. A scanning electron micrograph of zeolite 3A is shown in Figure 2.11(b).

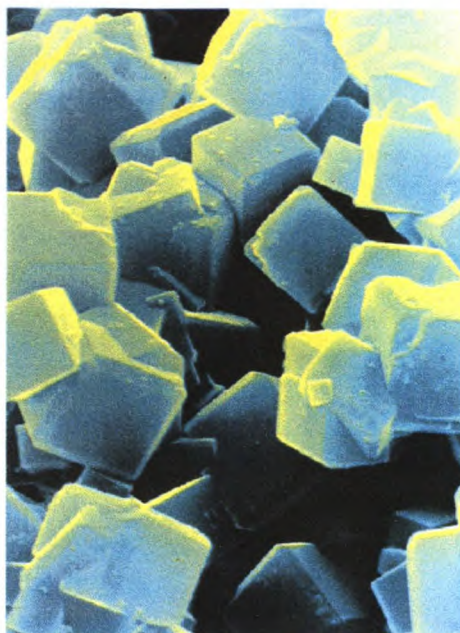


Figure 2.11(b). Scanning electron micrograph of molecular sieve 3A.^[22]

2.7.4 Applications for gas separation

In Table 2.5, important industrial gases are grouped according to their molecular sizes which are smaller than the apertures of zeolite types and hence can be sorbed.

In principle, any mixture containing gases from different groups, can be separated by molecular sieving. Many of the important zeolite based gas separation processes currently practiced in the industry, however, are not based on molecular sieving action. They are based on the different strengths or different equilibrium amounts adsorbed of the constituents in the mixture ^[78].

The different molecule positions of water, ethanol and methanol (marked) clearly shows that zeolites offer separation capability between these molecules.

Table 2.5. Molecules admitted to zeolites according to molecular dimensions and zeolite aperture sizes^[78]

Molecular size increasing \longrightarrow			
Type 5	He, Ne, Ar, Co	Kr, Xe	C ₃ H ₈
	H ₂ , O ₂ , H ₂ O	CH ₄	<i>n</i> -C ₄ H ₁₀ C ₂ F ₆
	Size limit for Ca- and Ba- mordenites (3.8 Å)	C ₂ H ₆	<i>n</i> -C ₇ H ₁₆ CF ₂ Cl ₂
		CH ₃ OH	<i>n</i> -C ₁₄ H ₃₀ CF ₃ Cl
		CH ₃ CN	etc. CHFCl ₂
		CH ₃ NH ₂	C ₂ H ₅ Cl
		CH ₃ Cl	C ₂ H ₅ Br
		CH ₃ Br	C ₂ H ₅ OH
		CO ₂	C ₂ H ₅ NH ₂
		C ₂ H ₂	CH ₂ Cl ₂
	CS ₂	CH ₂ Br ₂	
Type 4	Size limit for Na-mordenite and Linde sieve 4A (4.0 Å)		CHF ₂ Cl
			CHF ₃
			(CH ₃) ₂ NH
			CH ₃ I
			B ₂ H ₆
Type 3	Size limit for Ca-rich chabazite Linde sieve, 5A, Ba zeolite and gmelinite (4.9 Å)		

2.7.5 Adsorption isotherms

If a quantity q of a gas or vapour is adsorbed by a porous solid at constant temperature and the steady state equilibrium partial pressure is P (or concentration C) then the function $q(P)$ is the adsorption isotherm. Isotherms can take one of several forms known as types I – V, illustrated by Figure 2.12.

Each of these types is observed in practice, but by far the most common types are I, II and IV.

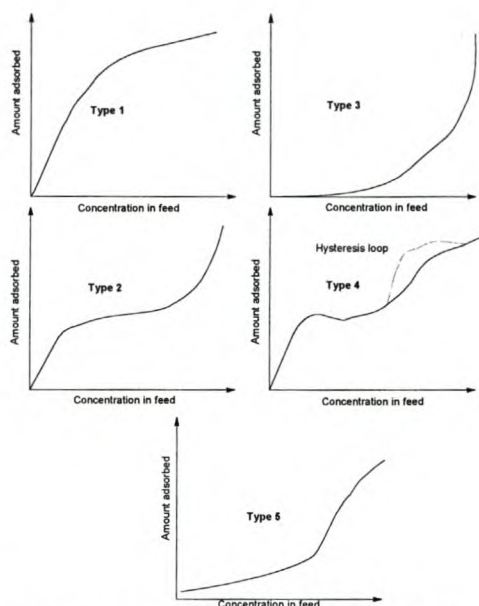


Figure 2.12. Types of adsorption isotherms showing adsorbent capacity as a function of feed composition^[29]

An inherent property of type I isotherms is that adsorption is limited to the completion of a single monolayer of adsorbate at the adsorbent surface. Type I isotherms are observed for the adsorption of gases on microporous solids, whose pore sizes are not much larger than the molecule diameter of the adsorbate; complete filling of these narrow pores then corresponds to the completion of a molecular monolayer. Type II isotherms do not exhibit a saturation limit. Near to the first point of inflexion of such isotherms, a monolayer is completed, following which adsorption occurs in successive layers. Adsorption, which has a wide distribution of pore sizes, form type II isotherms. Condensation of the adsorbent vapour occurs within the larger pores. The adsorbent displays a higher capacity for adsorption as the adsorbate saturated vapour pressure is approached.

Similarly, type III isotherms, which are continuously convex, with respect to the partial pressure axis, show a steady increase in adsorption capacity with increasing relative pressure. Type IV isotherms are similar to type II isotherms except that adsorption terminates near to a relative pressure of unity. Type V isotherms are similar to type III isotherms at low relative pressure but then a point of inflection is reached and a saturation limit is approached as the relative pressure is further increased.

It is not uncommon for isotherms of types II and IV to have a hysteresis loop as shown in Figure 2.12. Above a relative pressure of about 0.2, many porous adsorbents desorb a larger quantity of vapour at a given relative pressure and the amount corresponding to adsorption^[13]. Such hysteresis can provide useful information concerning the geometric shapes of pores in which vapour condensation occurs.

When a liquid surface is concave to its own vapour in equilibrium with the liquid, Thompson (1871), showed that the vapour pressure is lower than it would be if the liquid surface were planar. This becomes a significant point when considering condensation of a vapour within narrow pores and capillaries.^[13] In a porous adsorbent there is a continuous progression from multilayer adsorption to capillary condensation in which the smaller pores become completely filled with liquid sorbate. This occurs because the saturation vapour pressure in a small pore is reduced in accordance with the Kelvin equation, by the effect of surface tension^[54]. The presence of capillary condensation generally coincides with an inflection in the equilibrium isotherm.

2.7.6 Theories of adsorption equilibria

A variety of different isotherm equations have been proposed, some of which have a theoretical foundation and some being of a more empirical nature. Many of these equations are valid over small relative pressure ranges, but do not fit experimental data when tested over the full range of relative pressures. Only those which are commonly used for the description of physical adsorption of gases or vapours onto the surface of porous adsorbents will be outlined.

2.7.6.1 The Langmuir isotherm^[13]

This isotherm describes adsorbate-adsorbent systems in which the extent of adsorbate coverage is limited to one molecular layer at or before a relative pressure of unity is reached.

The basic assumptions on which the model is based are:

- Molecules are adsorbed at a fixed number of well-defined localized sites;
- Each site can hold one adsorbate molecule;
- All sites are energetically equivalent;
- There is no interaction between molecules adsorbed on neighboring sites.

Langmuir supposed that the rate of desorption from the surface is directly proportional to the fractional surface coverage θ and that the rates of adsorption and desorption are equal at equilibrium. Thus

$$k_a p(1 - \theta) = k_d \theta \quad (2.5)$$

where k_a and k_d are rate constants for adsorption and desorption. The more usual form of Equation 2.5 is

$$\theta = \frac{q}{q_m} = \frac{bp}{1 + bp} \quad (2.6)$$

where $b = q/q_m$ and q_m is the quantity q of adsorbate in a single monolayer. By application of the kinetic theory, the constant b can be identified as

$$\frac{1}{b} = \frac{v}{\sigma} (2\pi mkT)^{1/2} \exp\left(-\frac{Q}{R_g T}\right) \quad (2.7)$$

where v is the pre-exponential factor of the desorption rate coefficient, σ is the condensation coefficient, m is the mass of the adsorbate molecule, k is the Boltzmann constant and Q is the heat of adsorption.

2.7.6.2 Henry's law^[54,13]

At low pressures, Equation 2.6 reduces to the linear form

$$\theta = \frac{q}{q_m} = bp \quad (2.8)$$

If one assumes that the adsorbate obeys the perfect gas laws and substitute $R_g T c$ in Equation 2.8 for p , a more frequent form of the equation is obtained. Thus

$$q = q_m b R_g T c = K(T) c \quad (2.9)$$

where $K(T)$, which incorporates b and q_m is known as Henry's constant and is temperature dependent. Thus a linear relationship between pressure and adsorbed gas phase concentration is equivalent to an ideal gas type of equation of state for the adsorbed layer in terms of spreading pressure. At constant low coverage the constant b in Equation 2.7 is proportional to $T^{-1/2} \exp(Q/R_g T)$. It follows that $K(T)$ is proportional to $T^{1/2} \exp(Q/R_g T)$. If one neglects the weak component $T^{1/2}$ of the variable, one obtains

$$\ln K = \frac{Q}{R_g T} \quad (2.10)$$

Evaluation of the heat of adsorption (Q) may thus be obtained from the slope of a plot of $\ln K$ against $1/T$ for low coverages.

2.7.6.3 The Freundlich isotherm^[55]

Theory shows that the heat of adsorption decreases with in magnitude with increasing extent of adsorption. If this decline is logarithmic, it implies that adsorption sites are distributed exponentially with respect to an adsorption energy which differs between groups of adsorption sites. The well known Freundlich isotherm, is represented by

$$\ln \theta = \frac{R_g T}{Q_0} \ln p + \text{constant} \quad (2.11)$$

for small values of θ . Q_0 is a constant in a term which Zeldowitch (1935) introduced to account for the way in which the energy of adsorption sites was distributed. Equation 2.11 can be written in the familiar Freundlich form

$$\theta = k p^{1/n} \quad (2.12)$$

valid for $n > 1$. If compared to the Langmuir isotherm one finds that it does not indicate an adsorption limit when coverage is sufficient to fill a monolayer ($\theta = 1$). Application of the Freundlich isotherm to the adsorption of organic chemicals onto carbons is common and the hybrid Langmuir-Freundlich theory has proved useful in correlating data for gas mixtures.

2.7.6.4 The Brunauer-Emmett-Teller (BET)^[13]

Except for type I (Langmuir) isotherms, all other types referred to imply that the extent of adsorption does not reach a limit corresponding to completion of a monolayer. The main difficulty is that in chemisorption the sites are usually widely spaced so that the saturation limit bears no obvious relationship to specific surface area, while physical adsorption normally involves multi layer adsorption. The formation of the second and subsequent molecular layers commences at pressures well below that required for completion of the monolayer so it is not immediately obvious how to extract the monolayer capacity from the experimental isotherm.

Brunauer, Emmett and Teller argued that the rate of condensation (adsorption) onto the bare surface equals the rate of evaporation from the first layer of adsorbate. If θ denotes the fraction of surface which is bare and $z_m\theta_1$ the number of first layer sites occupied (in which z_m is the number of molecules necessary to complete a monolayer and θ_1 is the corresponding fraction of sites) then, for dynamic equilibrium between the gas phase at pressure p and the first layer of adsorbate,

$$a_1 p \theta_0 = b_1 z_m \theta_1 e^{-E_1/R_g T} \quad (2.13)$$

a_1 is the number of molecules which would successfully condense onto the bare surface per unit time per unit pressure and b_1 is the frequency with which molecules possessing sufficient energy E_1 leave the surface. The exponential term is the probability that molecules have an energy greater than E_1 to escape from the first layer.

For adsorbed molecules between layers (i-1) and i

$$a_i p \theta_{i-1} = b_i z_m e^{-E_i/R_g T} \quad i = 2, 3, \dots, n \quad (2.14)$$

Because the adsorbate vapour totally condenses when the saturated vapour pressure p_s is reached, then $\theta_1 = \theta_2$ when $p = p_s$ and so

$$a_2 p_s = b_2 z_m e^{-E_1/R_g T} \quad (2.15)$$

Following algebraic manipulation, in its most useful form, the BET equation is obtained for Equations 2.13, 2.14 and 2.15

$$\frac{p}{q(p_s - p)} = \frac{1}{q_m c} + \frac{(c-1)}{q_m c} \cdot \frac{p}{p_s} \quad (2.16)$$

The BET equation is extensively used to determine the surface area of porous adsorbents. The inherent assumptions of importance in the BET theory are:

- No interaction between neighbouring adsorbed molecules and;
- The heat evolved during the filling of second and subsequent layers of molecules equals the heat of liquefaction.

The BET equation is seldom used for correlating adsorption data. One reason lies in the complexity involved in its mathematical form. Another reason is that the equation is not applicable to adsorption under supercritical conditions. Under these conditions the model reverts to the Langmuir model.

2.7.6.5 Polanyi's potential theory^[54]

The Potential Theory is well documented in the text by Brunauer (1943). Polanyi considered contours of equipotential energy above solid surfaces and ascribe a volume ϕ_i to the space between the i th equipotential surface of energy ε and the adsorbent surface. The potential ε was assumed to be independent of temperature so that $\varepsilon = f(\phi)$ is essentially an isotherm equation. The adsorption potential is defined as the work of compression of the gas from a pressure p to the saturation pressure p_s .

For one mole of a perfect gas of volume v in an open thermodynamic system the adsorption potential is therefore

$$\varepsilon = \int_p^{p_s} v dp = R_g T \ln\left(\frac{p_s}{p}\right) \quad (2.17)$$

assuming that the work of creating a liquid surface is small in comparison with the magnitude of ε . The volume in the adsorption space is

$$\phi = nV_m \quad (2.18)$$

where n is the number of moles adsorbed per unit mass of adsorbent and V_m is the molar volume. The theory is general in that it encompasses multilayer adsorption on energetically nonuniform surfaces.

2.7.6.6 The Gibbs adsorption isotherm^[13,54]

The Gibbs adsorption isotherm provides a general relation between spreading pressure (or energy) and adsorbed phase concentration. The Gibbs function for a mobile adsorbate may be represented as $G(p, T, A, n)$ where A is the area over which the adsorbate has distributed itself and n is the number of moles of adsorbate on the adsorbent surface. At constant temperature T and pressure p , a change in G can be written

$$dG = \left(\frac{\partial G}{\partial A}\right)_{p,T,n} dA + \left(\frac{\partial G}{\partial n}\right)_{p,T,A} dn \quad (2.19)$$

The integrated form of Equation 2.19 is therefore

$$G = -\pi A + \mu n \quad (2.20)$$

On general differentiation

$$dG = -\pi dA + A d\pi + \mu dn + n d\mu \quad (2.21)$$

which shows how all variables A , π , n and μ contribute to a change in G . Further manipulation of the above equations results in

$$-Ad\pi + nd\mu = 0 \quad (2.22)$$

Substituting the classic thermodynamic relation $\mu(p)$ for the vapour phase at pressure p ,

$$d\mu = R_g T d \ln p \quad (2.23)$$

where p is the partial pressure of the adsorbate, one obtains

$$Ad\pi = nR_g T d \ln P \quad (2.24)$$

which is the differential form of the Gibbs adsorption isotherm. In its integral form it becomes

$$\pi = R_g T \int_0^{p_s} \left(\frac{n}{A} \right) d \ln P = \left(\frac{R_g T}{MS_g} \right) \int_0^{p_s} q(p) d \ln p \quad (2.25)$$

in which $q(p)$ is the mass of gas adsorbed per unit mass of adsorbent, M the molecular mass of adsorbate and S_g the surface area per unit mass of adsorbent. The spreading pressure π may then be calculated.

2.7.6.7 Statistical thermodynamic model^[13]

There has been some success (Ruthven 1984 and Wong 1985) in applying adsorption theory to the adsorption of gases in regular cage-like structures of zeolites. A configurational integral is written which is the integral of the exponential of the negative value of potential energies over the position of each and every molecule within the cage. A Lennard-Jones potential is employed as the potential energy function. The configurational integral was greatly simplified and results in an expression for the number sorbate molecules per cage. The result can be expressed as an isotherm which takes the form

$$\bar{S} = \frac{Kp + A_2(Kp)^2 + \dots A_n(Kp)^n / (n-1)!}{1 + Kp + A_2(Kp)^2 / 2! \dots A_n(Kp)^n / n!} \quad (2.26)$$

where \bar{S} is the average number of molecules per zeolite cage and K is the Henry constant discussed earlier.

The techniques discussed to obtain single-component experimental isotherms may also be employed to gather data for multicomponent isotherms. Correlations based upon the Langmuir, Polanyi and Gibbs theories for the adsorption of gases have emerged and the statistical thermodynamic approach outlined by Ruthven has also been extended to incorporate the adsorption of gas mixtures. These theories include the Extended Langmuir equation, the Lewis correlation, the Grant and Manes model, the Ideal Adsorbed Solution (IAS) model and the Vacancy Solution model. These theories will however not be discussed further and are readily available from text.

The use of adsorption equilibrium theories as part of a model, can be used to predict the adsorption dynamics in a specific system such as the one described in this study. In this particular case, the adsorption theory selected needs to make provisions for a multi-layer approach incorporating mixtures. The latter is important due to the expected influence of water on the adsorption of methanol onto the adsorption site. The model can easily be used to determine the relevant boundary conditions for the system. Another way of determining the boundaries and predicting the process is through the use of a sensitivity analysis. With this technique, the impact of change in a single parameter can be analysed to various degrees. The latter approach is followed in this study.

2.7.7 Water adsorption

In the industrial production of ethanol, whether by chemical or bio-chemical process routes, the raw product is generally a dilute aqueous solution. The recovery of ethanol to a dryness in excess of the azeotropic composition, is normally achieved by azeotropic or extractive distillation processes. As was indicated previously, an adsorption process would be a simple and

economical alternative to distillation. Theo and Ruthven^[71] confirmed experimentally that fuel grade ethanol (99.19 wt. %) could be produced by liquid phase adsorption of water from an aqueous ethanol, using 3A molecular sieves. Although not used in this study, liquid adsorption might be of some use, if for some reason vapour adsorption is found to be impractical when integrated with the distillation process. The rate of adsorption was shown to be controlled primarily by intraparticle pore diffusion resistances with some additional contribution from external film resistances^[17].

Carton^[6] experimentally compared drying the ethanol water azeotrope by vapour phase and liquid phase adsorption of water onto 3A molecular sieves. They concluded that the vapour phase process was more favourable since steeper breakthrough curves and thus greater adsorptive capacities were obtained. They also indicated that an additional disadvantage of liquid phase adsorption, is the retention of a substantial amount of feed in the void volume at the end of the adsorption stage.

Garg^[17] indicated that an energy efficient adsorption cycle could also be developed which is attractive for the removal of large amounts of water (up to 20 % or more) from process streams. This application for the dehydration of ethanol water azeotrope, was indicated to be accomplished with less capital and lower energy cost (560 kJ/ℓ) than conventional azeotropic distillation methods. High water loads to an adsorption system operating with a conventional thermal swing adsorption / desorption cycle however require large adsorbent inventories and frequent regeneration. Garg indicated that technology has been extended and a cycle has been developed which reduces the regeneration energy requirements. Sowerby and Crittenden^[63] presented a study in order to determine the relative merits of various type A molecular sieves for the recovery of dry ethanol (> 99.95 wt. %) from a vapour feed of composition around that of the azeotrope.

Particular attention was paid to the balance between the maintenance of a product with a low water content during the adsorption step i.e. high selectivity, and the ease of regeneration by heating, hydrogen purging and pressure reduction. The following figure indicates the apparatus that was used for their experimental method.

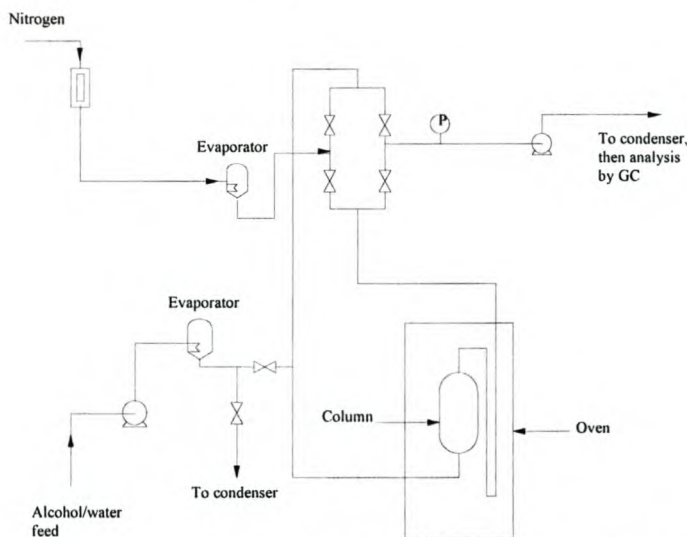


Figure 2.13. Schematic of experimental apparatus for drying the ethanol/water azeotrope.^[63]

The column was packed to a height of 40 cm with a commercially available bead of molecular sieves 3A, 4A, 5A and 10 A, which was manufactured by W.R. Grace & Co. Adsorption experiments were carried out with flow in the upward direction, with the initial column temperature in the range of 88 °C– 136 °C. The experimental conditions used for a selection of typical adsorption experiments, are summarised in Table 2.6. They indicated that it was necessary to minimise radial temperature gradients, channeling and wall effects. They also found however that conflicting criteria was arising when attempting to minimise all of these effects simultaneously.

Table 2.6 shows that, under certain conditions, both 3A and 4A molecular sieves are capable of producing dry alcohol. This was also confirmed by the author in a previous study^[18].

Table 2.6. Adsorption experimental conditions and results^[63]

Sieve	Experimental conditions			Initial bed effluent (wt% H ₂ O)	Av. Bed load (g/g)	Time for T _{max} (s)	T _{max} (°C)	MTZ L (cm)	kJ given to effluent ethanol
	Initial bed temp (°C)	Feed flow (cm ³ /s)	Feed (wt% H ₂ O)						
Variation in initial bed temperature									
3A	88	0.092	3.95	0.02	0.128	2580	134.5	39.82	1263
	108	0.098	3.89	0.03	0.125	2280	146	38.07	823
	123	0.098	5.21	0.12	0.106	1380	172	70.83*	1090
Variation in feed flowrate									
	105	0.061	3.75	0.04	0.121	3660	137	40.48	790
	105	0.088	4.85	0.03	0.12	1680	153	27.66	904
	115	0.098	4.6	0.1	0.112	1680	162	43.67*	1015
Variation in feed concentration									
	105	0.088	4.85	0.03	0.12	1680	153	27.66	904
	105	0.099	9.17	0.09	0.123	810	163	79.79	911
	104	0.085	12.8	0.16	0.145	780	178	123.11*	1156
Variation in initial bed temperature									
4A	92	0.096	4.4	0.02	0.163	2820	138.5	28.72	927
	106	0.096	4.8	0.03	0.148	2580	149	26.11	935
	136	0.085	4.4	0.09	0.087	1800	159	47.39*	791
Variation in feed flowrate									
	106	0.033	4.38	0.03	0.122	6480	135	34.81	355
	107	0.065	5.61	0.04	0.148	3000	147.5	32.92	550
	110	0.095	4.71	0.1	0.114	1800	144	42.51*	810
Variation in feed concentration									
	106	0.096	4.8	0.03	0.148	2580	149	26.11	935
	108	0.0858	9.55	0.08	0.136	1140	171	68.45*	803
	109	0.087	13.5	0.12	0.171	900	187	97.83*	587
5A	91	0.093	3.93	0.02	-	-	-	-	-
	109	0.091	3.93	0.13	-	-	-	-	-
10A	90	0.055	5	3.25	-	-	-	-	-
	109	0.075	4.6	0.5	-	-	-	-	-

Sowerby and Crittenden detected acetaldehyde and diethyl ether in the product during experiments while the column was packed with either 5A or 10A molecular sieves.

It was believed that these two sieves absorbed not only the water, but also some of the ethanol, which was present in the greatest quantity in the vapour feed. The consequential rise in bed temperature, was therefore much more dramatic than with either 3A or 4A molecular sieves, and peak temperatures of up to 210 °C were observed. At relatively high temperatures, molecular sieves are active catalysts for the dehydration of ethanol and therefore 5A and 10A molecular sieves were not considered further here.

They found that dry alcohol was only produced if the initial bed temperature was less than 120°C for 3A and 136°C for 4A molecular sieves. Figure 2.14 shows that for conditions when dry alcohol is produced, i.e. the mass transfer

zone length is less than the bed length, increasing the initial bed temperature decreases the time for breakthrough to occur.

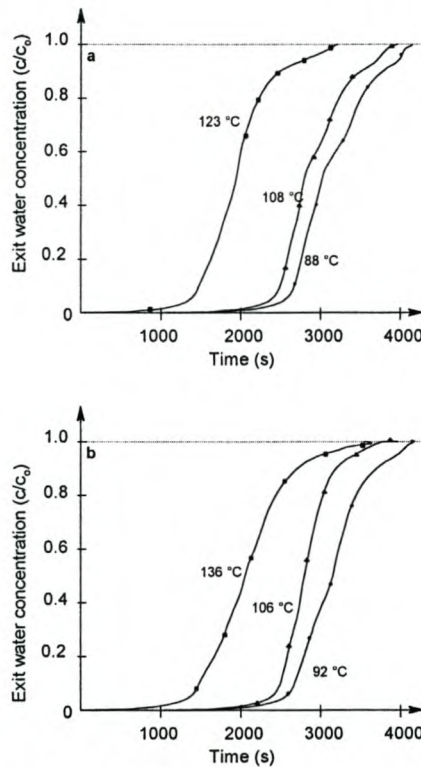


Figure 2.14. Effect of the variation in initial bed temperature on the breakthrough curve for molecular sieve 3A (a) and molecular sieve 4A (b).^[63]

There were two reasons for this. First, the capacity of the molecular sieves for water decreases with increasing temperature. Secondly, increasing the bed temperature causes an increase in the rate of diffusion within the solid, thereby resulting in an increase in the adsorption rate. Figure 2.14 and Table 2.5 also show that for the runs in which dry ethanol is produced, the time for complete breakthrough to occur, and the MTZ length are reduced as the temperature is increased. Figure 2.15 shows that the increase in the water concentration in the feed, decreases the time for breakthrough to occur. This event occurred immediately when the feed water concentration was in excess of 12 – 13 wt. %. The main reason for earlier breakthrough times with increase in water concentration, was that the adsorbent was exposed to more adsorbate per unit time.

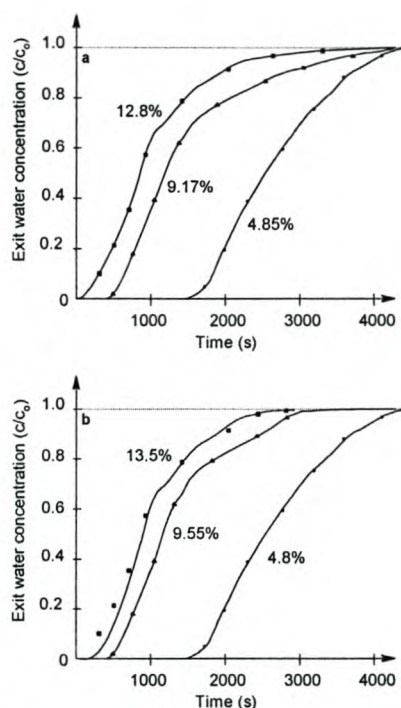


Figure 2.15 Effect of the variation in feed concentration on the breakthrough curve.^[63]

In general, the results that were given, show that for broadly comparable operating conditions, the performance of 4A molecular sieves with respect to the adsorption of water from the ethanol water vapour feed, is superior to that of the 3A molecular sieve. The criteria for this conclusion, are to produce dry ethanol with a short MTZ length and a high bed capacity. Both 3A and 4A molecular sieves were capable of producing dehydrated ethanol less than 0.05 % water under certain conditions.

Confirming the results of Sowerby and Crittenden, the average bed loading proved that zeolite 4A had a higher capacity for water adsorption than zeolite 3A. Although the primary focus of this study is on methanol adsorption from an ethanol stream, the influence of water needs to be understood and quantified. It should therefore form part of a sensitivity analysis.

Although the adsorption of water is not the primary focus of this study, the information in this chapter (2.7.7) plays a valuable role in understanding how water might influence the adsorption. This influence is evaluated during the sensitivity analysis later.

2.8 THE ADSORPTION OF METHANOL

As was indicated earlier, methanol is a natural constituent of grapes and wine and inevitably will end up in the final distillate. The natural presence of methanol in wine therefore has a significant effect on the production cost of ethanol distillation plants throughout the industry. Due to its toxic character and distinctive aroma, the producers of all potable, spirit containing alcoholic consumables, are by law compelled to almost completely separate the methanol fraction from the final product. It has been established that the separation of traced quantities of natural methanol from the spirit by means of atmospheric ethanol distillation, consume up to 45 % of the energy of the total process.

2.8.1 Benefits of methanol removal through adsorption

The following benefits can be derived from methanol separation by adsorption:

- adsorption is a less energy intensive process than distillation;
- almost complete elimination of methanol presence through adsorption where as distillation will always be between 50 and 250 mg / 100 ml AA;
- eliminating the toxicity potential;
- reducing the possibility of product adulteration through methanol;
- marketing benefits;
- financial benefits;
- new approach for the company as well as the rest of the industry;
- KWV will play a leading role in this new development.

It is therefore clear that the importance of the implementation of a production facility of this type, as well as its successful continuous operation, should not be under estimated.

2.8.2 Mechanisms for the adsorption of methanol onto zeolites

Various factors lead to the final conclusion that methanol could commercially be removed from wine spirits by means of adsorption. These factors included steric properties, physical properties as well as some other indications in the literature. The following characteristics of methanol indicated that adsorption could possibly take place on to molecular sieves.

- The critical diameter of methanol (4.4 Å) just slightly exceeds the critical diameter of water (3.2 Å);
- The configuration of methanol molecule indicates that it might compete with a water molecule for an adsorption site;
- Methanol has a polarity of 1.7 D which could possibly allow it to compete with the strongly polarised water molecule;
- Various literature sources also supported this theory. Coulson and Richardson^[11] indicated that methanol has properties that would allow it to be recoverable by adsorptive techniques. Further in his classification of zeolites in fundamentals of chromatography, Heftman^[23] indicates that methanol is a typical substance that might be sorbed onto zeolite Type IV. It was also indicated by Yang^[78], when he classified different molecules admitted to zeolites according to molecular dimension and zeolite aperture sizes (referred to Table 2.4). Yang therefore supported the theory that methanol could be removed by means of a Type IV or similar molecular sieve.

The above mentioned characteristics of the methanol molecule show to some extent that methanol adsorption does not take place as a coincidence due to the presence of water. To confirm this however, methanol adsorption in the absence of water needs to form part of a sensitivity analysis on the process output.

Zeolites are powerful industrial catalysts and combines acidity with shape selectivity for reactants, products and the intervening transition states.

Amongst the wealth of chemical reactions catalysed by these materials, one of the most important is the conversion of methanol initially to dimethyl ether and subsequently to gasoline. All research and literature is focussed on these types of catalytic chemical reactions but not on using zeolite as a means of separating methanol from ethanol. These studies however provide valuable information, in order to understand more clearly the mechanisms for the separation of methanol onto molecular sieves. Two major studies have been done by Shah^[62] and Rep^[52] in order to understand the catalytic behaviour of zeolites during the adsorption of methanol.

2.8.2.1 Interaction of methanol with alkali metal exchanged molecular sieves - IR spectroscopic study

The directed and localised interaction of polar molecules with hydroxy groups and metal cations and the oxygen atoms of the pore walls of a molecular sieve, have been seen to be most important for the nature of the sorbate / sorbent bonding and its activation in catalytic transformations. Consequently the interaction of small polar molecules such as methanol with acidic zeolites, have been thoroughly investigated, leading to a profound understanding of subtle details of the sorbent / sorbate interactions^[52].

It has been observed that methanol molecules tend to form ring-like hydrogen bonded structures. Preliminary experiments so far indicates strong interactions between the oxygens of pore walls and the sorbed polar molecules as well as inter-molecular hydrogen bonding between sorbed molecules. However consensus whether this leads to cleavage of some polar bonds (formation of alcoholate species at ambient temperatures) has not yet been reached.

During this IR spectroscopic study, it was decided to systematically study the non-reactive interaction of methanol with molecular sieves containing various alkaline metal cations and to compare this with theoretical calculations.

The study suggested three different adsorption states or structures of methanol while adsorbing to the zeolites, i.e.

- Structure 1 – freely vibration OH group;
- Structure 2 – hydrogen bonding between the methanol OH group and the lattice oxygen;
- Structure 3 – hydrogen bonding and additional lateral interaction between adsorbed methanol molecules.

These structures are shown schematically in Figure 2.16. They provide a better understanding of how and why methanol adsorbs onto molecular sieves. It also provided valuable information to project the conditions in the proposed adsorption plant.

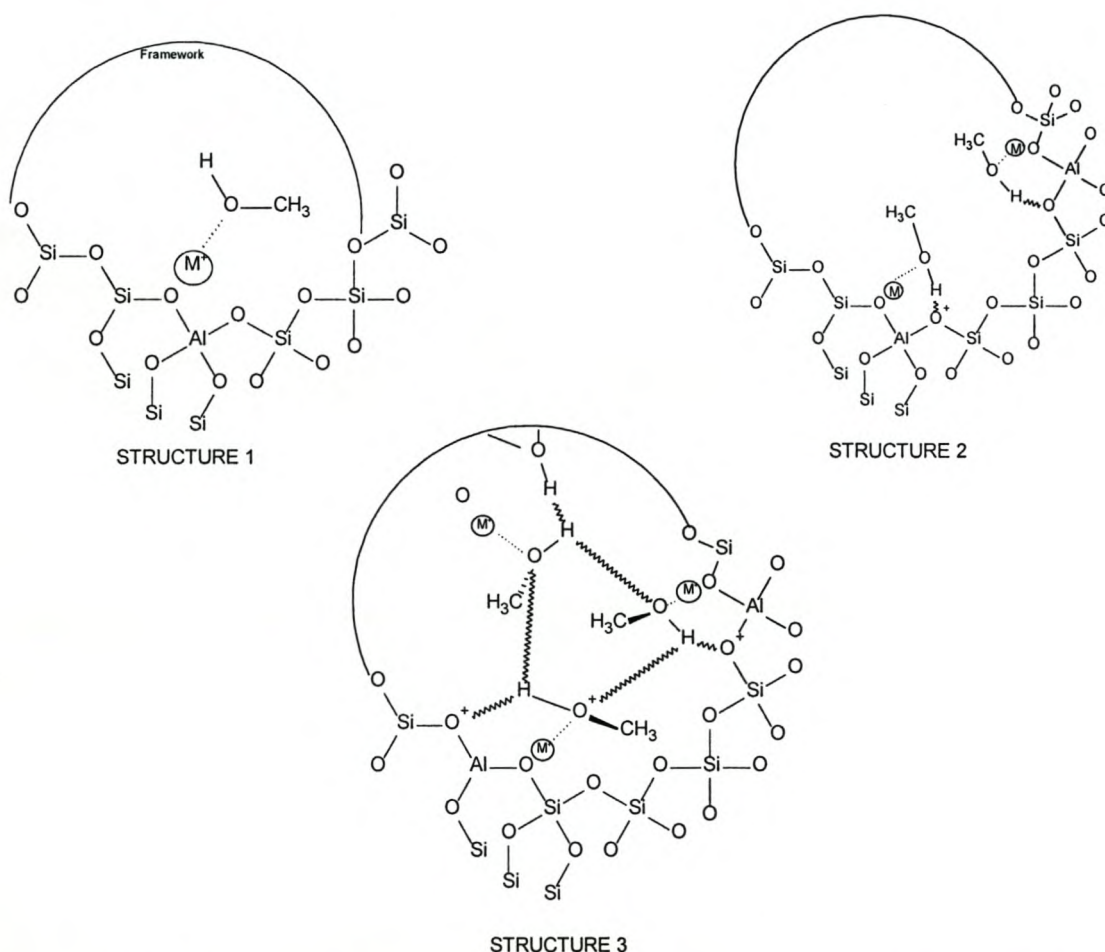


Figure 2.16. The different adsorption states of methanol in zeolites related to Si/Al ratio.^[52]

2.8.2.2 First principle quantum mechanical study of the adsorption of methanol

There has been much interest in the use of quantum mechanical methods to determine the energetics of proton transfer from the zeolite framework to methanol because this is believed to be the first step in the activation of the adsorbate. By using a variety of techniques, it has been shown that methanol is physisorbed and that the methoxonium ion is unstable, representing a transition state for the exchange of hydrogen between the two oxygens. Recent advances in massively parallel computing, coupled with improved algorithms, have greatly increased the scope of first principle quantum mechanical calculations for periodic systems, allowing the investigation of the mechanisms of zeolite catalysis. Such techniques were used by Shah ^[62] to address the question of methanol adsorption to allow us to examine differences in behaviour associated with particular zeolite structures. The following graphic shows a methanol molecule adsorbs in the centre of a zeolite cage.

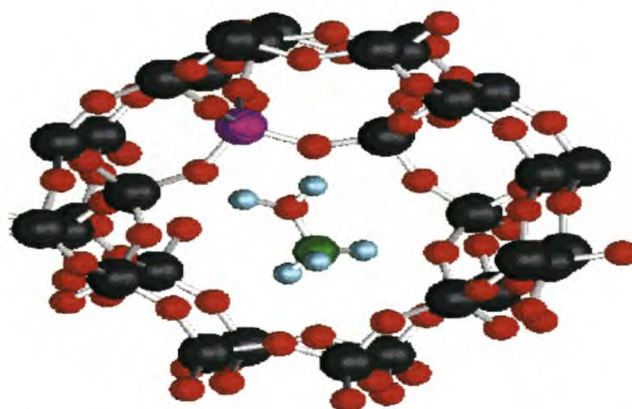


Figure 2.17. Methanol molecule in a zeolite cage.^[61]

This is the stable geometry as calculated by a full ab initio calculation that includes periodic boundary conditions to properly represent the zeolite framework. Two possible adsorption complexes of methanol at an acid site were identified. Complex A indicated that methanol is physisorbed with no proton transfer and complex B shows that methanol is chemisorbed with proton transfer to form a methoxonium cation.

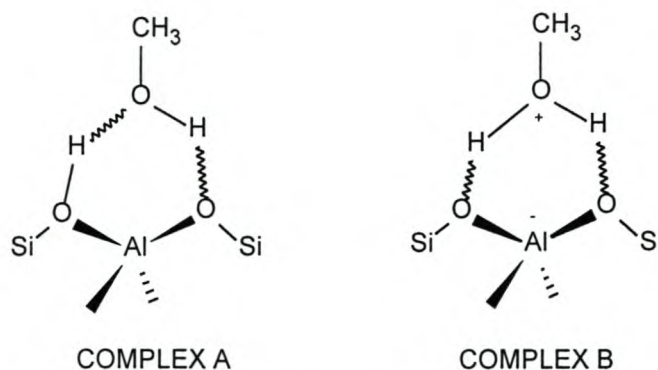


Figure 2.18. Possible adsorption complexes of methanol at an acid site.^[60]

This was the major question of whether proton is transferred from the framework to the methanol. Previous cluster calculations suggested that proton transfer is unstable. A periodic model however shows the protonated methanol is stable with little or no barrier to this transfer. This theory is supported by the following charge density iso-surfaces of the adsorbed complex:

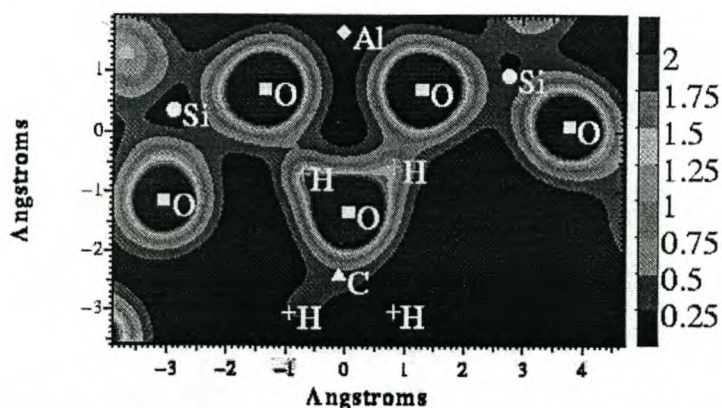


Figure 2.19 Charge densities indicating bonding lengths and types of bonding of the adsorbed complex.^[61]

This shows the framework to be largely ionic with charge density concentrated on the oxygen atoms. Definite covalent bonding between the methanol oxygen and both hydrogens close to it, therefore confirms proton transfer does occur. Nonetheless, noticeable charge overlap between the methoxonium ion formed and the framework also indicates strong hydrogen bonding. The framework - H distance are only about 1.4 Å.^[60]

This therefore also indicates that the proton remains bound to the zeolite framework and the methanol lies in the cage region of the framework. The methanol hydrogen bridges across to the oxygen on the other side of the six rings rather than simply across the aluminum. One methyl hydrogen is 3.0 Å from a framework oxygen. The others are bigger than 3.5 Å from any of the framework oxygens. There is therefore a delicate balance between the chemisorbed and the physisorbed states of the methanol in aluminosilicates. In regions containing medium-sized pores, it appears that methanol is preferentially adsorbed and is activated through protonation^[62].

When methanol is situated in the more open cage regions of zeolites, it appears to be unprotonated and potentially chemically less activated. It was speculated that the medium-sized pores are the most active sites for methanol reaction because these are where methanol appears to be protonated. The presence of both methanol and methoxonium species in regions with different structural characteristics, explains the difficulty in unambiguously assigning experimental IR spectra.

2.9 ADSORBER DESIGN CONSIDERATIONS

Although the separation of gas or liquid components by adsorption is wide spread in the chemical process industries, the principles underlining the process design of adsorption units are not widely known amongst engineers. Some of the design methods and models are semi-empirical and others rely solely on first principles (solutions of differential mass balance equations) with no empirical parameters.

Irrespective of the design method and model utilised, the following adsorber design principles can be considered as a guide. Some of the principles in Table 2.7 are followed in chapter 4 to design the proposed adsorption system.

Table 2.7 Adsorber design considerations (adapted)^[29]

I. Basic adsorbent properties	II. Application considerations	2. Pulsed, fluidised bed
A. Isotherm data	A. Operating conditions	B. Geometry
1. Uptake, release measurements	1. Flowrate	1. Number of beds
2. Hysteresis observed	2. Feed and product concentrations	2. Bed dimensions
3. Pretreatment conditions	3. Pressure, temperature	C. Column internals
4. Aging upon multiple cycles	4. Desired recovery	1. Bed support, ballast
5. Multicomponent effects	5. Cycle time	2. Materials of construction
B. Mass transfer behaviour	6. Contaminants	3. Flow distribution
1. Interface character	B. Regeneration technique	4. Dead volumes
2. Intraparticle diffusion	1. Thermal: steam, hot fluid, kiln	5. Insulation
3. Film diffusion	2. Chemical: acid, base, solvent	IV. Process flowsheet
4. Dispersion	3. Pressure shift	A. Process control
C. Particle characteristics	4. Regenerant, adsorbate recovery or disposal	1. Control sequence
1. Porosity	C. Energy requirements	2. Cycle sequence
2. Pore size distribution	D. Adsorbent life	3. Instrumentation
3. Specific surface area	1. Attrition, swelling	4. SCADA
4. Density	2. Aging, fouling	B. Configuration
5. Particle size distribution	III. Equipment	1. Process configuration progression
6. Particle shape	A. Contactor type	2. Risk issues
7. Abrasion resistance	1. Fixed: axial, radial flow	3. Final process and instrumentation diagram
8. Crush strength		
9. Composition, stability		
10. Hydrophobicity		

Data in 5 categories are also required for the process and equipment design phases of any adsorption process. ^[13]

- **Adsorbate / adsorbent thermodynamic equilibrium relationships, including appropriate interaction data for multi-component systems;** it is necessary initially to identify an adsorbate which is capable of effecting the required separation. It is then necessary to consider the effect that the other adsorbates in a multi-component feed stock may have on the equilibrium of each component and the method by which the adsorbent is to be regenerated, if it is not going to be discarded after the adsorption step. In this case, water plays an important role.

- **Adsorbate/adsorbent kinetic relationships including appropriate interaction data for multi-component systems;** separations are rarely controlled by equilibrium considerations alone and it is therefore necessary to determine whether or not the selected adsorbent has the required kinetic properties. The rate of adsorption will determine the size of the equipment for those separations, which do not have extremely fast kinetics, i.e. those which cannot be described as being equilibrium controlled.
- **Heat of adsorption as a function of the operating conditions, including the composition;** whether the process can be considered to be isothermal or not depends on the magnitude of the heat of adsorption per mole and the concentration of the adsorbate in the feed stock. The design process using rigorous methods, is simplified considerably if the heat released on adsorption is low.
- **Hydrodynamic data;** such data are required to determine pressure gradients and to evaluate the importance of dispersion in the design process.
- **Physical property data;** basic information required over the ranges of temperature. Pressure and composition to be encountered in the process, includes the density, viscosity, thermal conductivity, specific heat and molecular diffusivities of fluids together with the specific heat of the adsorbent and the bulk voidage and bulk density of the adsorbent bed. Determining thermodynamic conditions and properties in the system is difficult. In this study a simulator will be used to determine stream properties. The simulator input and output are provided as well as motivation for its use.

2.9.1 Design parameters for a basic PSA process

The performance of a PSA system depends on the design and proper functioning of all the system components. The three critical design parameters that needs to be considered are the pressure gradient, purging for desorption and bed dimensions.

The pressure gradient influences the power required to operate the system, the adsorbent life and the flow distribution. Sizing the bed is based on retaining both heat-and mass transfer fronts in the bed. The methods of White and Barkley^[76] are used for adsorber design purposes.

Velocity effects

The fluid stream flows through interstitial passages between the granules in an adsorbent bed, resulting in viscous and kinetic energy losses that create pressure gradients within the bed. These pressure gradients can be determined by the modified Sabri Ergun equation.

$$\frac{\Delta P_a}{L_a} = E_1 \mu v_s + E_2 \rho_o v_s^2 \quad (2.27)$$

where

$$E_1 = 1471(1-\varepsilon)^2 / (\varepsilon^3 D_p^2 g) \quad (2.28)$$

and

$$E_2 = 17.16(1-\varepsilon) / (\varepsilon^2 D_p g) \quad (2.29)$$

with

$$v_s = \frac{w_o}{\rho_o A} \quad (2.30)$$

Equation. 2.5 is expressed in terms of the superficial fluid velocity which is based on the total cross sectional area of the adsorber. The fluidisation velocity determines the minimum bed diameter.

$$v_s(\max) = -\frac{\mu E_1}{2\rho_o E_2} + \sqrt{\left(\frac{\mu E_1}{2\rho_o E_2}\right)^2 + \frac{\rho_o g}{\rho_o E_2}} \quad (2.31)$$

The ratio of differential pressures can be determine by:

$$\frac{\Delta P_b}{\Delta P_a} = \frac{E_{2b} \left[D_a^2 \left(\frac{1}{D_b} - \frac{1}{D_a} \right) - \frac{(D_a - D_b)^2 \cdot (5D_a + 3D_b)}{3D_a(D_a + D_b)} \right]}{8LaL_b^2 \cdot \left[\left(\frac{\pi E_{1a} \mu}{w_o} \right) + \left(\frac{4E_{2a}}{D_a^2} \right) \right]} \quad (2.32)$$

The minimum regeneration purge flow rate is given by:

$$w_2(\text{min}) = w_o \left(\frac{t_a}{t_p} \right) \cdot \left(\frac{P_{j0}}{P_{j3}} \right) \cdot (P_3 - P_{j3}) / P_o \quad (2.33)$$

more commonly used in PSA systems:

$$w_2(\text{min}) = 1.15 w_o \left(\frac{t_a}{t_p} \right) \cdot \left(\frac{P_3}{P_o} \right) \quad (2.34)$$

Adsorbent bed size

Heat is liberated during adsorption and the temperature of the bed is raised. The magnitude of the temperature elevation in the heat transfer front is determined by an energy balance in the bed.

$$\Delta T_a = \frac{(X_o - X_1)H - (q/w_o)}{c_o - c_a(X_o/Y^*)} \quad (2.35)$$

The bed length required to prevent emergence of the heat front at the bed exit is given by the following expression.

$$L = c_o \left(\frac{w_o}{A} \right) \cdot \left[\frac{C}{Ua} + \frac{t_a}{c_a \rho_a} + 2 \sqrt{\frac{Ct_a}{Uac_a \rho_a}} \right] \quad (2.36)$$

where

$$C = -0.88105 \ln \left(\frac{\Delta T_1}{\Delta T_a} \right) - 1.221 \left(1 - \left(\frac{\Delta T_1}{\Delta T_a} \right) \right); \quad \frac{\Delta T_1}{\Delta T_a} < 0.5 \quad (2.37)$$

A 5 % relative temperature rise at the bed outlet , which is equivalent to an axial dispersion factor (C) of 1.48, is adequate to ensure retention of the heat front. The adsorbent bed length to prevent the emergence of the mass transfer front is given by the following expression.

$$L = \frac{w_o(X_o - X_1)t_a}{AY^* \rho_a} + \frac{w_o(Y^*/\bar{Y})C}{A\rho_o aK} \quad (2.38)$$

Where

$$C = -0.88105 \ln\left(\frac{X_1}{X_o}\right) - 1.221 \left(1 - \left(\frac{X_1}{X_o}\right)\right) ; \frac{X_1}{X_o} < 0.5 \quad (2.39)$$

Heat transfer rate equations

Laminar layer conductance

$$h_o = 0.61\Psi v_s (c_o \rho_o) (N_{Pr})^{-2/3} (N_{Re})^{-0.41} ; (N_{Re} \geq 50) \quad (2.40)$$

$$h_o = 0.91\Psi v_s (c_o \rho_o) (N_{Pr})^{-2/3} (N_{Re})^{-0.51} ; (N_{Re} < 50) \quad (2.41)$$

based on

$$N_{Re} = \frac{(w_o/A)}{a\mu\Psi} \quad (2.42)$$

Adsorbent granule conductance

$$h_a = \frac{60k_a}{D_p^2 a} \quad (2.43)$$

Overall heat transfer coefficient

$$U = \frac{1}{h_o^{-1} + h_a^{-1}} \quad (2.44)$$

2.9.2 Major improvements on the basic pressure swing adsorption process

2.9.2.1 Cocurrent depressurisation (CD)

The first major process improvement after the invention of the pressure swing adsorption cycle, was the introduction of the cocurrent depressurisation step. To incorporate this step into the Skarstrom cycle, the adsorption step is cut short well before the breakthrough occurs, that is the concentration front is far from reaching the outlet of the bed. The adsorption step is then immediately followed by cocurrent depressurisation before the bed is desorbed by further blowdown and purging^[78]. Cocurrent depressurisation increases the concentration of the most strongly adsorbed component in the bed. This is achieved by removing the gas contained in the adsorbent voids which, following the initial two steps, will have entrapped gas at the same composition as the feed.

The pressurisation and feed steps during which adsorption occurs, are shortened in duration so that the cocurrent depressurisation step can be initiated before breakthrough of components from the bed. The bed is subsequently desorbed by blowdown and purge steps in the cycle. The net benefit of cocurrent depressurisation is increased purity of the most strongly adsorbed component in the product, which in consequence enhances the recovery of the least strongly adsorbed component^[13]. This technique also prevents the contaminant (methanol and water in this case), to adsorb at the bed exit.

2.9.2.2 Pressure equalisation (PE)

The term pressure equalisation refers to the action by which the pressures in two interconnected beds, are equalised. The main purpose of the PE step, is to conserve the mechanical energy that is contained in the gas of the high-pressure bed. With the PE step, the pressure in a regenerated bed is

increased in a sequence of steps by the gases admitted from other beds, which are in various stages of depressurisation. The energy reduction as well as other improvements resulting from the PE step, made large-scale PSA separations economically feasible. Benefits of PE include increased product recovery and steadier continuous flow of the most strongly adsorbed component from the unit. For the purpose of this study and its design, both cocurrent depressurisation as well as pressure equalisation will be used in the process cycle (see Table 4.1 later).

Industrial PSA systems are designed to repeat the cycle of pressurisation / adsorption and depressurisation / desorption as to provide gas separation on a continuous basis. Figure 2.20 illustrates this in which (as is usually the case in PSA) the non-adsorbed component is the desired product. This basic cycle sequence forms the basis of the vacuum swing adsorption process, which will be discussed in chapter 4. Figure 2.20 can be evaluated against the actual plant pressure output (Figure 5.6).

The general rule for sizing the beds is 15 – 30 actual v/v of feed per bed per cycle when the actual purge/feed ratio is 1.1. One actual v/v of feed represents its amount at the feed pressure in the empty bed. The feed throughput can be increased substantially if a high purge/feed ratio is employed. A high purge/feed ratio can also have negative effects, like the need for a bigger vacuum system to maintain conditions during regeneration.

The following rules from Skarstrom^[78] for the PSA cycle were also incorporated into the final design:

- short cycle and low throughput per cycle should be used to conserve the heat of adsorption and thereby maintaining an isothermal operation.
- obey the 1:1 volume rule for the purge/feed ratio. The volume ratio is measured at their respective pressures, thus the 1:1 ratio ensures complete displacement.

The purge / feed ratio is a key parameter in determining the product purity. It is usually between 1.1 and 2.0 in practice.

- According to Yang^[78] for a pure product the absolute pressure ratio between the high and low pressures should be greater than the reciprocal of the mole fraction of the product contained in the feed (purge/feed = 1):

$$\frac{P_{HI}}{P_{LO}} > \frac{1}{\text{mole fraction of product in feed}} \quad (2.45)$$

Equation 2.23 holds also true for the design discussed in chapter 4.

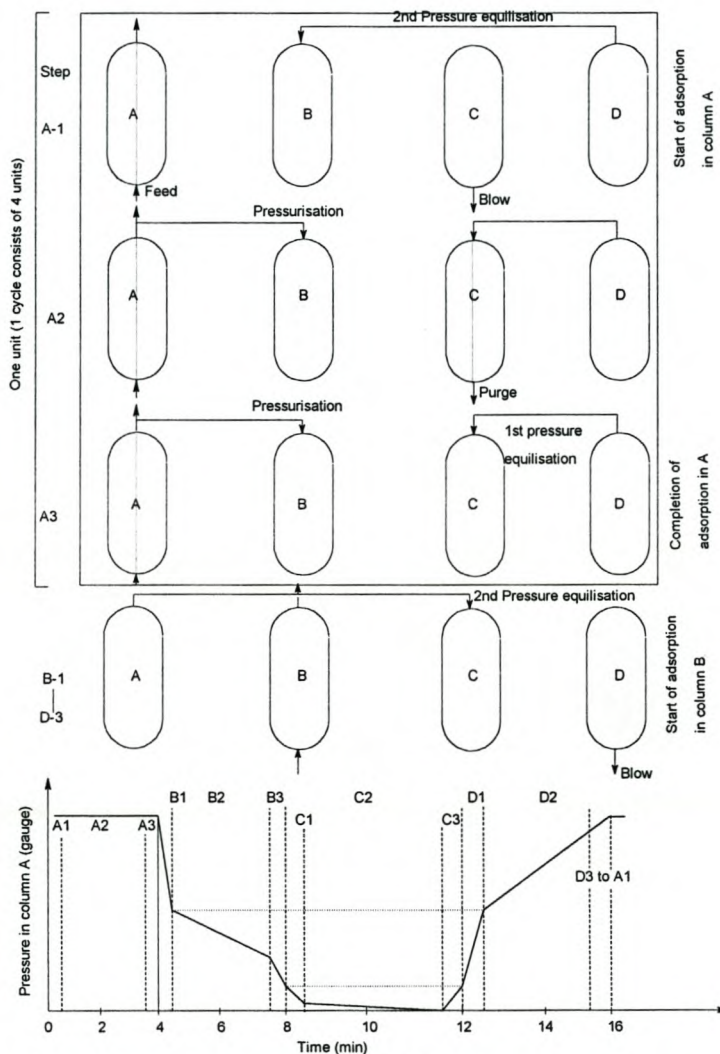


Figure 2.20. Basic steps in a multiple-bed PSA to ensure continuous production.^[67]

2.9.3 Desorption and regeneration of adsorbents

In certain applications, it may be economic to discard the adsorbete after use in which case it may be necessary to describe it as a waste. Disposal would be favoured when the adsorbent is of low cost, very difficult to regenerate and the non-adsorbed products of the adsorptive separation are of very high value.

However, in the majority of process applications, disposal of the adsorbent as a waste, is not an economic option and therefore regeneration is carried out either in-situ or external to the adsorption vessel to an extent sufficient that the adsorbent can be re-used. Practical methods of desorption and regeneration include one or more, usually a combination of the following:

- increase in temperature;
- reduction in partial pressure;
- reduction in concentration;
- purging with an inert fluid;
- displacement with a more strongly adsorbing species;
- change of chemical conditions such as pH;

As a variable for changing thermodynamic potential, a change in temperature is much more effective than a change in pressure. The most common methods are changes in temperature (thermal swing adsorption) and changes in pressure (pressure swing adsorption).

Advantages and disadvantages of each method together with some examples are shown in Table 2.8.

Table 2.8. Methods of regeneration with process examples

Method	Advantages	Disadvantages	Process	Adsorbent	Selectivity
Thermal swing	Good for strongly adsorbed species. Advantages high concentrations. For gases and liquids.	Thermal ageing of sorbent. Heat loss leads to thermal inefficiency. Long cycle times mean inefficient use of sorbent. High latent heat for liquids.	Drying of gases. Drying of solvents.	3A,4A, 13X 4A	Equilibrium Equilibrium
Pressure swing	Good for weakly adsorbed species required in high purity.	Very low P may be required. Mechanical energy is expensive.	Drying of gases. Hydrogen recovery. Air separation. Air separation.	3A,4A, 13X Mol sieve Carb mol sieve Zeolite	Equilibrium Equilibrium Kinetic Equilibrium
Vacuum swing (special case of pressure swing)	Rapid cycling gives efficient use of sorbent.	Desorbate recovered at low purity.	Separation of linear paraffins.	5A mol sieve	Shape selective sieving.
Displacement	Good for strongly held species. Avoid risks of cracking reactions during regen. Avoids thermal ageing of sorbent.	Product separation and recovery needed (choice of desorbent fluid is crucial.)	Separation of linear from branched and cycling paraffins.	5A mol sieve	Shape selective sieving.
Purge gas stripping	Essentially at constant T & P.	Only for weakly sorbed species, purge flow is high. Not normally used when desorbate needs recovery.	Relatively uncommon without thermal swing since purging alone is only suitable for weakly adsorbed species.		
Steam stripping (combining thermal swing and displacement)	As for thermal swing and displacement above.		Waste water purification. Solvent recovery.		Equilibrium

2.9.3.1 Reduction in partial pressure

The following figure indicates the effect of three process variables on the adsorption equilibrium for a type I isotherm.

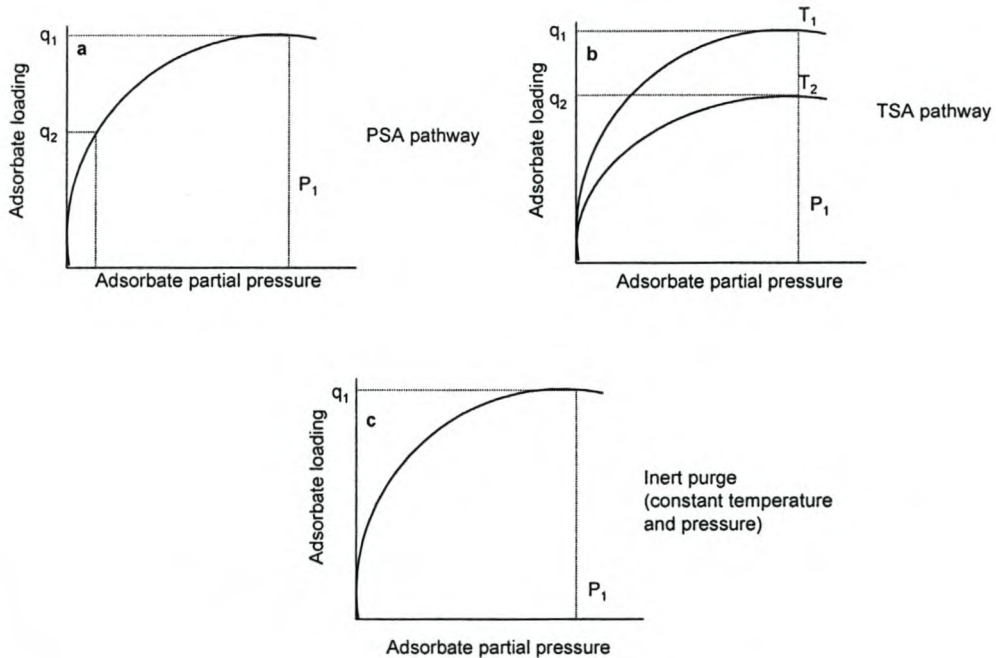


Figure 2.21. The effect of process variables on the adsorption equilibrium for a Type I isotherm: (a) the effect of adsorbate partial pressure, (b) the effect of temperature and (c) the effect of an inert purge.^[13]

Figure 2.21(a) shows schematically the effect of partial pressure on equilibrium loading for a Type I isotherm with a temperature T_1 reducing the partial pressure from $p_1 - p_2$ causes the equilibrium loading to be reduced from $q_1 - q_2$. Partial pressure can either be reduced by reducing the total pressure in the system or an inert gas can be used to lower the partial pressure while maintaining the total system pressure. The use of a purge fluid alone is unusual. Changes of pressure can be effected much more quickly than changes of temperature and therefore cycle times of pressure swing adsorption processes are typically of the order of minutes and for rapid cycle systems, of the order of seconds. The faster the cycle time, the lower the size of the equipment and the inventory of the adsorbent.

PSA processes are attractive for bulk gas separations and purifications for those situations in which the adsorptive forces are relatively weak.

Some PSA processes are based on kinetic rather than on equilibrium effects, in which case it can be important not to allow sufficient time for the gases in the bed to reach thermodynamic equilibrium with the adsorbent. In a PSA process, the production step may occur at a pressure greater than atmospheric with the desorption pressure being atmospheric. Alternatively, the production step could be carried out at atmospheric pressure and the desorption step under vacuum. Vacuum is used in this case to regenerate the bed. The purge step is very important for efficient operation, because the use of a purified component flowing in the reverse direction, causes the strongly adsorbed species to be pushed back towards the bed inlet for the subsequent adsorption step. In commercial PSA applications, the adsorbent is selected so that the most desired product is the least adsorbed species.

2.9.3.2 Increase in temperature

In the previous figure (b) one sees schematically the effect of temperature on the adsorption equilibrium of a single adsorbate. Clearly an increase in temperature leads to a decrease in the quantity adsorbed. Hence increasing the temperature from $T_1 - T_2$ will decrease the equilibrium loading from $q_1 - q_2$, assuming that the partial pressure in the gas phase remains constant. Because the most strongly adsorbed species have the greatest heats of adsorption, a relatively large decrease in loading can be achieved by a relatively modest increase in temperature.

Adsorption isotherms tend to become unfavourable for adsorption at increased temperature and hence they become more favourable to desorption. It is however important to ensure that the regeneration temperature does not exceed that required to degrade the adsorbent, or cause it to behave catalytically with the chemicals involved in the process.

Passage of a hot purge gas through the equipment to sweep out the desorbed species, is almost always used in conjunction with an increase in temperature. The heating and desorption steps must provide sufficient energy to perform a number of functions. First the adsorbent, its associated adsorbate and the containment vessel must be raised to the desorption temperature. Secondly, the heat of desorption must be provided. Thirdly, the adsorbent and vessel temperature must be raised to the final regeneration temperature if this needs to be higher than that used for desorption. Energy will also be required if there are heat losses and if vapourisation of liquid is necessary.

Normally TSA cycles therefore consumes large amounts of energy per unit quantity of adsorbate. Because beds of adsorbent cannot normally be heated and cooled quickly, the cycle time of a typical TSA process may range from several hours for a bulk separation to several days for a purification. Long cycle times inevitably mean large bed lengths with consequential high adsorbate inventories. A practical problem in thermal swing processes is the reduction in the capacity or life of the adsorbent when it is subjected to repeated thermal cycling. A further problem is the formation of coke in applications in which reactive hydrocarbons are exposed to elevated temperatures during the regeneration step.^[13]

2.9.3.3 Displacement fluid

The temperature and pressure are maintained essentially constant as in purge gas stripping but instead of an inert purge, the adsorbed species are displaced by a stream containing a competitively adsorbed species as in displacement chromatography. The mechanisms for desorption of the original adsorbate involves two aspects. First, the partial pressure of the original adsorbate in the gas phase surrounding the adsorbent is reduced. Secondly there is competitive adsorption of the displacement fluid. One advantage of the displacement fluid method of regeneration, is that the net heat generated or consumed in the adsorbent will be close to zero because the heat of adsorption of the displacement fluid is likely to be close to that of the original

adsorbate. Thus the temperature of the adsorbent should remain more or less constant throughout the cycle.

2.9.4 Increasing the energy efficiency of the adsorption cycle

The dehydration of the ethanol water azeotrope can be accomplished with less capital and lower energy cost (< 560kJ/ℓ) than conventional azeotropic distillation methods^[17]. Significant energy reductions can be achieved if the desorption step uses the stored heat for regeneration energy and thereby reduces the volume and temperature of the regeneration purge gas required. By taking full advantage of the significant heat of adsorption from streams with high adsorbate concentrations, a fixed bed adsorption cycle can be made more energy efficient and thereby extend the nominal range of applicability of adsorptive processes.

2.9.5 Performance of adsorbers

Analytical and numerical analysis of non-isothermal adsorption are highly useful in describing the basic behaviour of such systems. An empirical design parameter known as the cross over ratio (R) is useful in understanding the design of adiabatic fixed bed adsorbers. R is defined by the following^[17]:

$$R = \frac{C_{pG}}{(Y_i - Y_o)} \bigg/ \frac{C_{pS}}{(X_i - X_o)} \quad (2.46)$$

The performance of large fixed bed adiabatic adsorbers can be correlated with R. This term defines the approximate location of the heat front relative to the position of the mass transfer front. The numerator roughly describes the rate of heat removal out of the mass transfer font by the carrier fluid. The denominator roughly describes the rate at which heat is stored by the adsorbent. For a given adsorption system, the value of R depends not only on the values in the expression but the initial bed temperature, total pressure and type of adsorbent. The following table indicates the values of the crossover ratio.

Operating an adsorption cycle corresponding to case B in Table 2.9, results in a reduction of dynamic adsorption capacity as would be predicted from isothermal data. This reduction in operating capacity can be correlated with R .

Table 2.9. Values of crossover ratio^[17]

Case	R	Location of heat front
A	$\gg 1$	It is far ahead of the mass transfer front, and the heat will normally leave the adsorbent bed before the leading edge of the adsorbate MTZ exits the bed.
B	≥ 1	It is located within the mass transfer front between the leading edge and the stoichiometric point of the first concentration wave.
C	$\ll 1$	It is located behind the stoichiometric point of the first mass transfer front.

Thus, the heat generated both lengthens the mass transfer front and lowers the equilibrium capacity because of the higher local operating temperature. The heat generated can be distributed throughout the bed as a broad pulse or as a narrow spike. The maximum temperature experienced is a function of R , the adsorption dynamics and the initial conditions.

Operating conditions that lead to highly non-isothermal adsorption steps are generally avoided due to the reduction in capacity of the adsorbent bed. By the correct selection of cycle conditions, the heat of adsorption can be stored within and behind the mass transfer zone, such that heat is not lost out of the bed prior to adsorbate breakthrough. This makes the desorption step more efficient and compensates for the inefficiencies of the non-isothermal adsorption step.

2.9.6 Ethanol/water azeotrope dehydration

Alternative processes such as extractive or vacuum distillation techniques are more complicated than simple distillation and these processes are normally more energy intensive. This is also apparent from the following citation from Sowerby:

“Of all the energy required to proceed from around 10 wt. % to 99.95 wt. % by simple and azeotropic distillation, around 33 % is required to proceed upwards from the azeotrope, a concentration change which represents a mere 4.5 %”.

Continuous adsorptive cycles for bulk adsorbate removal normally requires short adsorption and regeneration cycle times. Product recovery also becomes critical for short cycles because of the void space present in the adsorbent bed. Thus, one bed volume is lost or has to be recycled for reprocessing during the regeneration step. This restriction normally rules out a liquid phase adsorption cycle because of the high molar density of a liquid which significantly reduces the recovery of the desired product. A vapour phase adsorption cycle will generally be more efficient and easy to operate in short cycle times. The heat of adsorption of water is the source of the heat generated during the dehydration step. Up to 4.2 MJ are liberated for every kilogram of water adsorbed^[17].

For low water concentrations (ppm – 2.5 vol. %) the heat generated in the mass transfer front, is generally carried ahead of the front by the carrier fluid, which is moving at a much higher velocity than the water adsorption front in the bed. ($R > 1$). This normally causes the product fluid to be slightly warmer than the feed fluid but does not affect the adsorption dynamics within the mass transfer front, which will remain isothermal. For high water concentrations (2.5 – 50 vol. %) the heat generated can remain within or behind the front and the adsorbent temperature rises significantly ($R \approx 1$). In this case, the rate of heat generated by adsorption is greater than the rate at which it is carried out of the mass transfer front by the carrier fluid.

For these situations, adsorption is occurring at a temperature higher than that of the feed. This reduces the efficiency of the adsorbent for water removal by both lowering the effective water equilibrium capacity and elongating the mass transfer front. This can possibly cause early breakthrough of water into the product. For these cases, the mass transfer front is termed unstable and is correspondingly less predictable for design purposes ^[17].

During the dehydration of the ethanol/water azeotrope by adsorption, the thermal effects can be used to a distinct advantage during the subsequent regeneration step. During a typical thermal swing regeneration, a major heat input is required to provide for the heat of desorption of water. This can account for up to 75 % of the total heat requirements of the regeneration step. If the heat of adsorption generated can be used to provide the heat of desorption during regeneration, less heat is required as an input to the system. In Figure 2.22 the adsorption step for the ethanol/water azeotrope is shown.

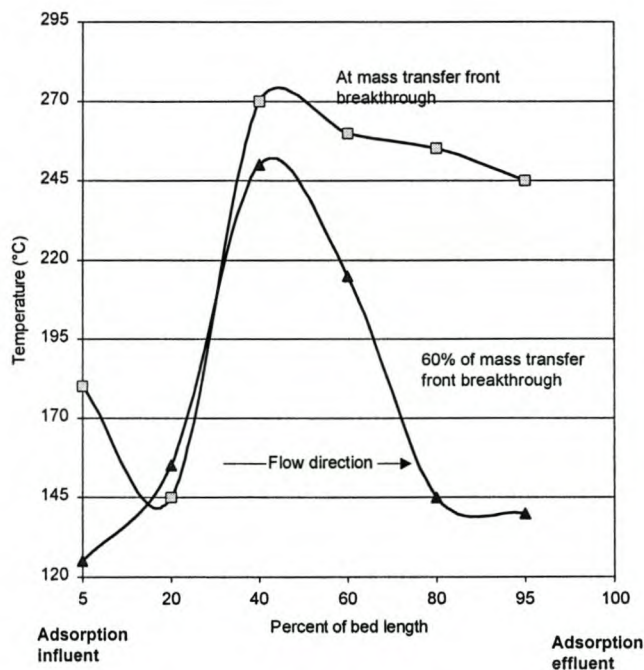


Figure 2.22. Temperature profile during non-isothermal adsorption.^[17]

If regeneration with a purge gas at 230 °C is carried out immediately after the adsorption step and in a countercurrent flow direction, the regeneration

temperature profiles are shown in the Figure 2.23. In this case, the peak internal temperature falls back to the original bed temperature before exiting from the bed and therefore the heat associated with the temperature peaks which was stored within the bed, is used to provide the heat of desorption of the adsorbed water.

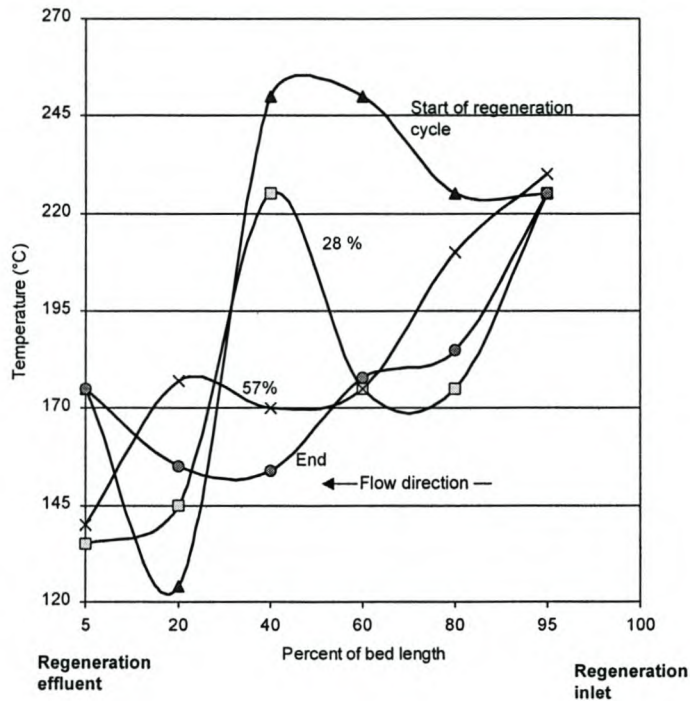


Figure 2.23. Regeneration temperature with heat of adsorption.^[17]

If the temperature peaks are allowed to escape to the surroundings after carrying out an adsorption step identical to that shown in Figure 2.22 and a regeneration carried out as before, the resulting temperature profiles are thus shown in the Figure 2.24. It can be expected that conditions in Figure 2.24 occur when breakthrough is allowed to occur.

For this situation, if one compares the water breakthrough times on the subsequent adsorption steps (35 minutes vs. 60 minutes), it can be seen that a 70 % improvement in the use of the regeneration gas is achieved when the heat of adsorption stored in the bed is used to augment the regeneration.

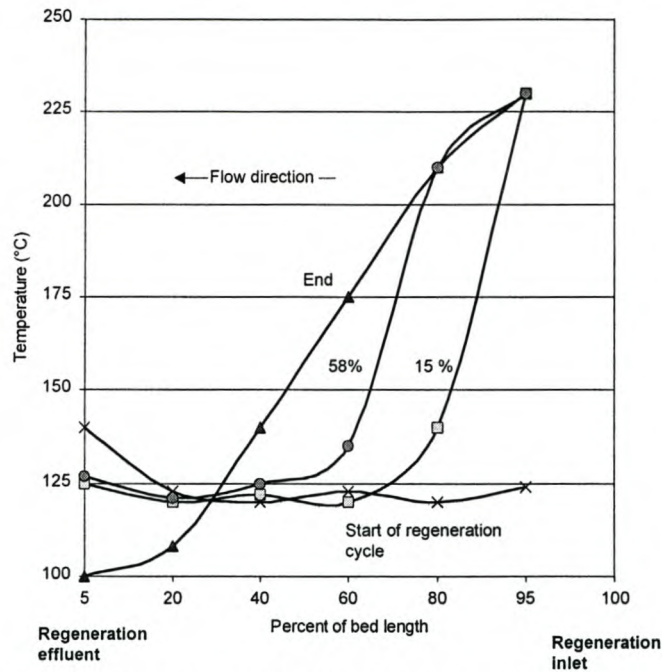


Figure 2.24. Regeneration without the heat of adsorption.^[17]

The choice of a suitable cycle time is based on an analysis of several factors. Shorter cycle times increase the purge to feed ratio requirement, which increases the operating cost. On the other hand, longer cycle times reduce the purge to feed gas ratio, but the bed sizes increase. This in return raises the capital cost.

During the regeneration process, a fixed amount of ethanol is normally lost during the purge cycle because of storage within the adsorbent bed voids. Alcohol losses need to be evaluated in this case. During the purge step a non-condensable gas, for example nitrogen or carbon dioxide, can be circulated in the purge loop by a blower. The gas is heated to the regeneration temperature and passed throughout the adsorber, after which it is cooled and the desorbed water condensed and collected in the knock-out vessel. The purge gas, saturated at the knock-out conditions can then be recirculated and used again for purge, after it is reheated to the regeneration temperature.

CHAPTER THREE

METHANOL ADSORPTION IN A SINGLE SMALL COLUMN

Various experimental runs were performed as part of a previous study to investigate the adsorption of methanol onto molecular sieves. These methanol separation experiments were performed on the same single adsorption column as described in chapter 2 for water adsorption. The results provided in this chapter were not published as part of the previous study.

3.1 EXPERIMENTAL PROCEDURES AND CONDITIONS

The adsorption column was operated on a discontinuous (batch) process, allowing for regeneration at the end of every adsorption cycle. The following diagram is a schematic of the apparatus that was used by the author in his previous study to investigate the adsorption of water and methanol onto 3A and 4A molecular sieves.

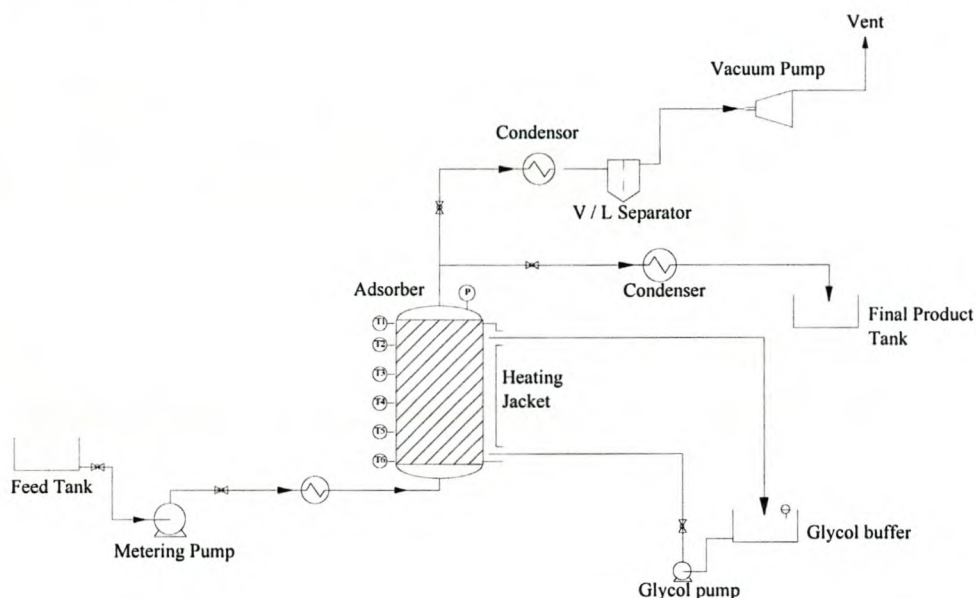


Figure 3.1. Experimental apparatus used to: (a) dehydrate the ethanol / water azeotrope and (b) selectively remove methanol from the feed stream.^[19]

The apparatus consisted of a single 0.026 m inner diameter carbon steel adsorption column. The primary objective of this adsorption experiment, was to produce absolute alcohol on laboratory scale with an ethanol content in excess of 99.95 wt % and to reduce the methanol content to < 5 mg/100 mlAA from a vapour feed of composition around that of the azeotrope. At the time of the trial runs, scale-up of the adsorber to a practical dual bed system with automated control and a continuous production rate did not fall within the scope of the study.

Energy was fed into the column by means of heating glycerol through an external heating jacket with a temperature controlled heating coil and pumping it at a constant flow rate through the annular section. A maximum vapour velocity of 0.86 m/s was obtained throughout the bed. Adsorption was carried out in an upward direction at an initial bed temperature of 88 °C – 94°C, depending on which molecular sieve was used. The following table shows the adsorption experimental conditions used by the author.

Table 3.1 Experimental conditions for a single small column

Experiment no	Feed no	Flowrate cm ³ /s	Zeolite type	Zeolite mass (g)	Initial bed temp (°C)
1	1	1.4	3A	695	88
2	1	1.4	3A	695	88
3	1	1.4	4A	643	92
4	1	1.4	4A	643	92
5	2	1.4	3A	695	88
6	2	1.4	4A	643	92
7	2	1.4	4A	643	92
8	3	1.4	3A	695	88

Desorption experiments were performed immediately following the adsorption experiment. For desorption, the bed was heated to a final temperature of 170°C and evacuated to 0.5 Bar. The desorption process stream was condensed in a condenser and forced through a vapour-liquid separator before it entered the vacuum pump.

The liquid fraction was removed from the separator and recycled to avoid any losses. The flow for desorption took place in a downward direction which is countercurrent to the adsorption cycle. This ensured that the heat of adsorption was contained in the bed and assisted in regeneration of the sieve. Upon condensation in a water-cooled condenser, the final product was analysed by gas chromatography. During the adsorption stage, temperature variations throughout the column were monitored to follow the movement of the mass transfer front as it approached the outlet.

Breakthrough was accepted to occur as soon as thermocouple 1 registered its maximum temperature. A typical temperature profile of the bed packed with zeolite 3A is shown in Figure 3.2.

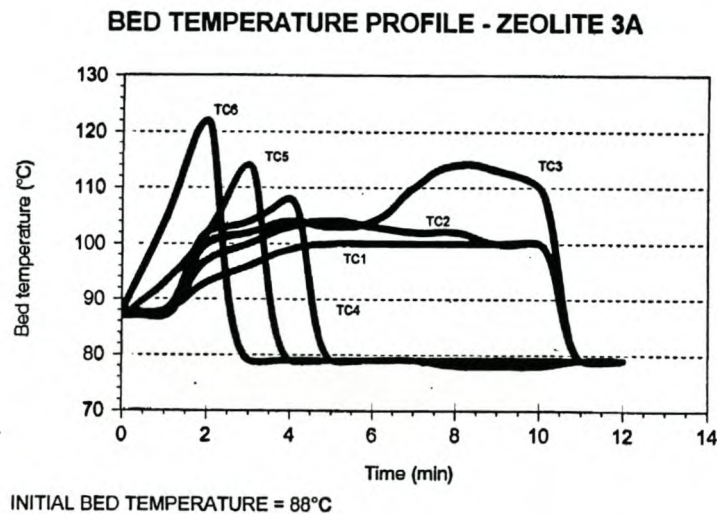


Figure 3.2. Typical temperature profile during adsorption onto molecular sieve 3A.^[19]

For the experiments, neutral wine spirits from the Paarl and Worcester regions were respectively used to investigate the adsorption of water and methanol onto the molecular sieve bed. The methanol content of these two products, are indicated in Table 3.2.

Table 3.2. Methanol variation

Feed	Ethanol (vol. %)	Methanol*
1	96.4	0
2	96.4	11.8
3	96.4	81.8

*mg/100ml AA

Experiments 5 - 8 were performed to evaluate the effectiveness of methanol removal from wine spirits by means of adsorption in a single small column. The experimental conditions for these adsorption runs were indicated in Table 3.1. The methanol containing ethanol vapour was forced in an upward direction through the molecular sieve bed.

3.2 RESULTS AND DISCUSSION

Table 3.3 clearly indicates that there was a significant reduction in the amount of methanol present in the wine spirits after the vapour was brought into contact with the molecular sieve bed.

Table 3.3. Results for single column adsorption.^[19]

Experiment	Raffinate moisture (vol. % H ₂ O)	Avg bed loading (g/g)	Initial methanol loading*	Exit methanol loading*
1	0.05	0.043	11.8	
2	0.05	0.043	11.8	
3	0.02	0.052	11.8	
4	0.02	0.052	11.8	
5	0.08	0.047	11.8	<1
6	0.05	0.047	81.8	3.96
7	0.05	0.052	81.8	1.36
8	0.19	0.039	81.8	<1

*mg/100ml AA

Experiment 8 showed that the Worcester feed stock with a methanol content of 81.76 mg/100 ml AA was reduced to < 1 mg / 100ml AA. This reduction is significant and demonstrates the success of methanol removal by means of adsorption.

The breakthrough curves for three adsorption experiments are shown in Figures 3.3 and 3.4.

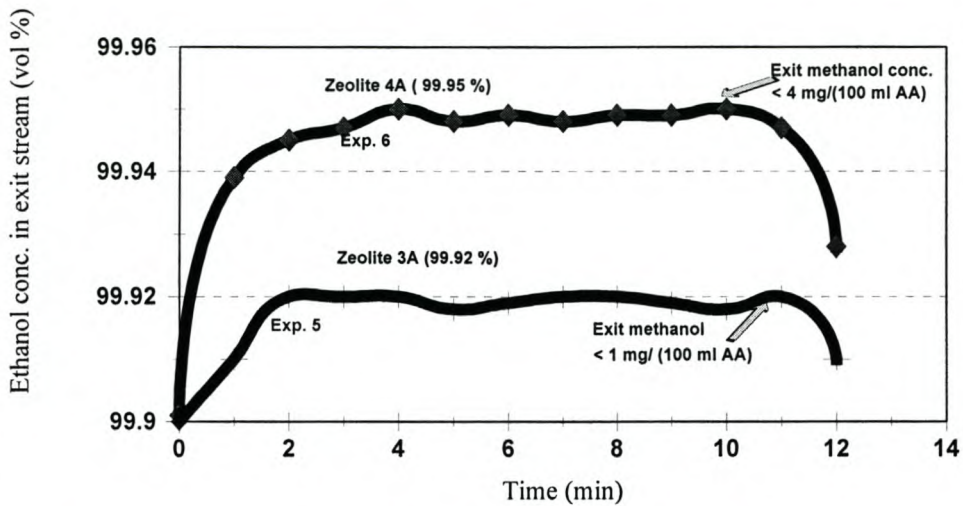


Figure 3.3. Breakthrough curves for water and methanol adsorption onto molecular sieve 3A and 4A at different feed concentrations (experiments 5 and 6).^[19]

Figure 3.3 clearly indicates that molecular sieve 4A has a higher affinity for water adsorption than molecular sieve 3A. However, at the same time, molecular sieve 3A indicated a lower exit concentration of methanol than molecular sieve 4A. This interesting phenomena supports the theory that water and methanol compete for adsorption sites. It could therefore be deduced that since zeolite 4A has the highest capacity for water adsorption, zeolites 3A will by preference, adsorb methanol due to a relative lack of competition with water molecules for an adsorption site.

In experiment 8 (Figure 3.4) which was performed at the highest methanol content feedstock, the methanol content was reduced to < 0.5 mg/100 ml AA.

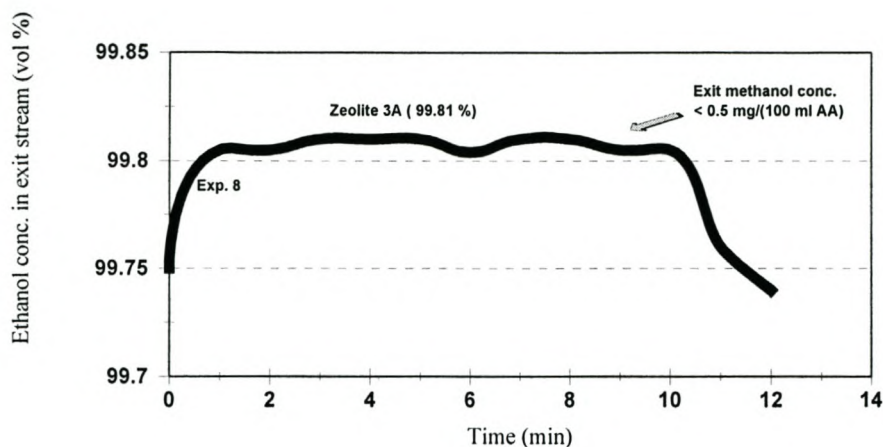


Figure 3.4. Breakthrough curves for water and methanol adsorption onto molecular sieve 3A (experiment 8).^[19]

It is the selectivity of these molecular sieves that will serve as a basis for the design of the vacuum swing adsorption demonstration plant, which will be discussed in chapter 4. As these results were obtained on relatively small scale and is of little value to the company in the existing form, a larger scale facility needs to be designed and built. The success in such a facility will be measured by its:

- ability to perform the predicted separation;
- ability to produce on a continuous basis.

For these reasons, the design consumed an extensive part of the project time.

CHAPTER FOUR

DESIGN OF A DUAL BED VACUUM SWING ADSORPTION DEMONSTRATION PLANT

The term vacuum swing adsorption (VSA) is often used to denote a PSA cycle with desorption at sub-atmospheric pressure. The benefits of using this form of adsorption have been discussed in detail in chapter two. The performance of any PSA process is governed by the ratio of absolute rather than gauge pressures. The desorption at sub-atmospheric pressure often leads to improved performance due to the form of the equilibrium isotherm, rather than any intrinsic effect of a vacuum. Because of this, the principles of VSA have been incorporated into the design of this demonstration plant.

4.1 DESIGN OBJECTIVES

The demonstration plant had to adhere to the following design principles:

- continuous operation;
- the creation of beneficial results to the company;
- ease of scalability ;
- automated control;
- possibilities for integration with the existing process;
- economic viability.

4.2 DESIGN CONSIDERATIONS FOR THE ADSORPTION PLANT

Theoretical considerations for the design of an adsorption system were discussed in great detail in chapter 2. The challenge was to make use of these theoretical principles and apply it to a practical and workable adsorption production facility. Due to this practical and application approach as well as the points set out above as design objectives, Table 2.7 will be used as a basis for design of the pilot plant.

This adsorption design approach of Knaebel^[29] was selected, as it makes provision for an array of practical and required design issues pertaining to an adsorption system. Table 2.7 was adapted and expanded to make provision for all aspects of this particular design. As was mentioned in chapter 2, the adsorber column design is based on the adsorber design philosophies of White and Barkley^[76]

It should be noted that the final demonstration plant was the result of a multi-disciplinary approach, which required the author to manage and direct the following type of contractors/suppliers: mechanical engineering, electrical engineering, instrumentation engineering, software programming, process engineering, adsorbent manufacturers. During the course of this study, the author interacted with various leading adsorption specialists / companies in Germany, Italy, the United States of America and the United Kingdom. All design work was directly performed by the author as indicated in this study. Individual detail equipment design for equipment such as heat exchangers, the separator and the steam generator was specified by the author in terms of its engineering duty and acquired from others. Contributions by other parties are consistently acknowledged.

4.2.1 Selection of molecular sieve

As can be deduced from Figure 3.3 in chapter 3, the author indicated that molecular sieve 4A was superior to 3A in water adsorption while at the same time molecular sieve 3A was superior to 4A with regards to methanol adsorption. This supports the theory that water and methanol compete for an adsorption site^[19]. It is therefore sensible to use molecular sieve 4A to remove the bulk of the water, while using 3A to remove the traces of methanol in the feed stream. However, following the author's work on the adsorption of methanol onto a single column as discussed in chapter 3, the products from this process were not only evaluated analytically but also organoleptically.

Although the methanol content has been reduced dramatically by the use of molecular sieve 3A (therefore analytical acceptance), it was clear that

organoleptically the product did not retain its neutral character. It seemed to have drawn from the molecular sieve or due to the adsorption process a soil / cement like aroma on the nose. Since organoleptic evaluation of products in the wine industry carries a significant level of importance when compared to chemical analysis, it was crucial for the success of this adsorption process that the source of this taint or foreign odour in the neutral wine spirits had to be established. In-depth discussions with the manufacturer (W.R. Grace & Company) revealed that the problem could be traced down to the binder used during the manufacturing process. As discussed in chapter 2, binders used in the manufacturing of molecular sieves usually are sepiolite, kaolin or attapulgite. These types of binders are known to normally affect organoleptic properties of products.

If organoleptic characteristics of the product therefore is not important, then clearly a molecular sieve could be used that does not have a specially treated binder in order to prevent contamination of the product in terms of its organoleptic quality. However, due to the sensitivity of this issue and the fact that this is a potable product produced for human consumption, the organoleptic quality is crucially important. The challenge was therefore to select a molecular sieve that could successfully adsorb both water and methanol, as well as be completely inert to the product. Grace then suggested that molecular sieve 3A was used for this application, but with a special binder. The special binder is only used on molecular sieve 3A and not 4A. Taints are formed due to the reaction between the ethanol molecule and the Lewis and Brönstedt acid sites on the binder of the molecular sieve. In this special molecular sieve, the acid sites were removed from the binder but not from the crystal of the molecular sieve.

As the pore openings of molecular sieve 4A allow for the ethanol molecule to penetrate the pores of the zeolite, the ethanol molecule in the case of molecular sieve 4A would be in contact with the crystal, while in the case of molecular sieve 3A only in contact with the binder. It would therefore be a senseless exercise to use a special binder in the case of molecular sieve 4A, as the ethanol molecule will in any event make contact with the crystal and

react with the Lewis and Brönstedt acid sites. The special binder (CS) is therefore only applicable on the molecular sieve 3A and not the 4A. The molecular sieve selected for this application, was therefore MS 564 CS. The product characteristic sheet of MS 564 CS (produced exclusively by W.R. Grace in Germany), is given in appendix C5

MS 564 CS is a high performance 3 Å, 1.6 – 2.5 mm spherical molecular sieve specifically formulated for the dehydration of cracked gas, propylene, butadiene and other unsaturated hydrocarbons. The proprietary and enhanced formulation of MS 564 CS, provides maximum retained cyclic water capacity, minimal attrition or material break-up, low unit pressure drop, maximum resistance to coking, no green oil formation and long service life in severe service cracked gas dehydration applications. MS 564 CS provides superior water adsorptive mass transfer efficiency. MS 564 CS is also known to be used in pharmaceutical applications.

This as well as the fact that MS 564 CS is known to create less loss of ethanol to the adsorbent and more efficient separation from water (i.e. higher concentration of end product) make this molecular sieve the best suited for the separation of water from ethanol. Although it has a slightly lower capacity to methanol adsorption, this molecular sieve will therefore be used in the proposed process to remove both water and methanol from the feed stream. MS 564 CS however is known to adsorb methanol because of the presence of water. Methanol is therefore co-adsorbed onto the molecular sieve. Because of this, as a safety precaution a certain amount of molecular sieve 4A was also packed into the bed on top of the 3A molecular sieve. The detail will be discussed further where the bed dimensions are calculated.

I BASIC ADSORBENT PROPERTIES

A Isotherm data

Adsorption equilibrium data are usually gathered at a fixed temperature and plotted or tabulated as isotherms: adsorption capacity (loading) vs. fluid phase concentration (partial pressure for gases and vapours). Adsorption isotherms

for W.R. Grace molecular sieves 3A and 4A are listed in appendices C7 and C8.

When compared to Figure 2.12, it would appear that the adsorption of water onto molecular sieve 3A is of the Type 1 or 2 isotherm. As was indicated, the possible occurrence of hysteresis should be taken cognisance of. The uptake or water capacity for MS 564 CS is minimum 20.5 wt. %. However, to understand even better the adsorption capacity and performance of MS 564 CS in the presence of water from ethanol, one should look at the breakthrough curves in this particular case. The breakthrough performance of MS 564 CS at different inlet water concentrations from ethanol is shown in appendix C2.

Clearly the higher the inlet water concentration, the shorter the cycle time required to adsorb a higher concentration of water on to the molecular sieve bed. This however also means that the bed will become saturated quicker and that high quantities of adsorption heat will be released from the bed, decreasing the adsorption potential. Applicable to this case would be the breakthrough curve at 4.8 wt. % and this already, even prior to the design, indicates that the cycle time should be shorter than 8 minutes to prevent any breakthrough of contaminants taking place.

Pre-treatment conditions

Pre-treatment of a molecular sieve bed prior to starting the adsorption cycle is crucial for the successful operation of the plant. Pre-treatment in this case will be discussed in detail under the operational start-up and shut-down procedures later.

Ageing upon multiple cycles

As was indicated earlier, MS 564 CS provides maximum retained cyclic water capacity, minimal attrition or material break-up, low unit pressure drop, maximum resistance to coking and long service life in severe service conditions.

Because of this the average life cycle of MS 564 CS under the conditions of water adsorption from ethanol, is estimated to be between 7 and 10 years.

B Mass transfer behaviour

Mass transfer characteristics like intra-particle diffusion, film diffusion and dispersion are crucially important in the design of an adsorber. These characteristics are fully taken into consideration in the actual design of the columns later.

C Particle characteristics

In order to totally understand the behaviour of MS 564 CS in the presence of the azeotropic composition of ethanol and water, all particle characteristics as listed in Table 2.7 are taken into consideration in the final design of the columns discussed later.

II APPLICATION CONSIDERATIONS

A Operating conditions

Operating conditions for this specific part of the plant was carefully selected. As the principle of methanol adsorption onto molecular sieves has been demonstrated earlier by the author, at a flow rate of a few cubic centimeters per second, it was crucial in this case to design the system at a flow rate that had significance in terms of production quantities. However, due to the intrinsic value of neutral wine spirits together with the value in terms of Customs and Excise purposes, an optimum flow rate for the adsorption plant had to be selected. This flow rate was selected to be 40 kg/hr, making this plant more suitable for real production purposes than a mere laboratory experiment.

In terms of the thermodynamic operating conditions, the following conditions were designed for. Adsorption would be taking place at ± 100 °C and atmospheric pressure while desorption and regeneration would take place at

an absolute pressure of ± 17 kPa. Although a temperature increase would be beneficial for regeneration, a raise in the bed temperature during the short cycle time would not be possible. It is desired to dehydrate completely this feed stream as well as remove all traces of methanol present. A crucial factor in the design of an adsorber is the cycle time. Normally, the longer the cycle time, the bigger the bed and therefore the higher the stock of molecular sieve on hand. Cycle time should therefore be considered carefully.

Figure C1 in the appendices indicates the principle of syneresis for MS 564 CS while adsorbing water vapour from ethanol. By definition, syneresis is graphically the gap that exists between the adsorption and desorption curve. In practical terms, this actually means that for example at an adsorption cycle of 1000 seconds an amount of 62 % of all water from the feed stream will be adsorbed. In this case, if one looks at the regeneration curve at 1000 seconds, of this amount adsorbed only 34 % of this total amount will be removed through desorption or regeneration and 28 % of this water will remain on the molecular sieve.

As the adsorption process continues, this effect of syneresis will accumulate resulting in a regeneration cycle that is insufficient to regenerate the bed to its required levels. A crucial design factor is to, at all times after an infinite amount of cycles, before adsorption and after regeneration, keep the water content of the bed constant. From Figure C1 it is clear that the only points where the amount of water adsorbed as well as desorbed is equal, occur at $T = 4$ minutes as well as $T = \infty$.

If one looks at the performance at $T = 4$ minutes, the Figure C1 indicates that syneresis at that point does not exist. From this point as well as Figure C2, a cycle time of 4 minutes is selected and will be built into the column design, which is to follow shortly. Therefore in theory, if the adsorption cycle time is maintained at 4 minutes, even after continuous production, no accumulation of water or other contaminants should take place on to the bed and the water content should always remain constant.

A further design consideration is contamination of the bed. Contamination of the bed reduces the adsorptive capacity and performance of an adsorber. It is therefore crucial to ensure that the contamination from other constituents in the feed stream should remain at a minimum. In this case, in the feed material which is neutral wine spirits and which is a product from the distillation process discussed in Chapter 2, contaminants are controlled to a minimum.

B Regeneration

The disposal of the adsorbent is not an economic option and therefore regeneration needs to be carried out on the bed. Six practical methods or modes of desorption / regeneration have been discussed in chapter 2. As was indicated, the two most prominent modes or methods are temperature swing adsorption and pressure swing adsorption. From the cycle time discussion it was clear that, due to the short cycle time for adsorption, the parallel cycletime for regeneration should be similar.

Temperature swing adsorption (TSA)

The use of the temperature swing cycle to regenerate the bed, has the following problematic areas:

- Although a change in temperature is more effective than a change in pressure as a variable to change thermodynamic potential, the response for a temperature change is relatively slow.
- As the temperature for adsorption and regeneration was 100 °C and 170 °C respectively, thermal inertia became a serious problem for the bed. It was just not possible to increase or decrease the temperature of the bed in such a short space of time. Regeneration temperature will therefore remain at 100 °C.
- Apart from the thermal inertia of the packed bed, thermal inertia within the heat exchanger to provide the low and high temperature, also posed a design problem.

Calculations indicated that the temperature within the heat exchanger would not be able to adapt sufficiently to the design parameters within a cycle time of 4 minutes.

- Problem of thermal inertia in the bed is increased even more due to the relatively low thermal conductivity of molecular sieves.
- TSA cycles normally consume large amounts of energy per unit quantity of adsorbate. Due to thermal inertia and low thermal conductivity, TSA cycles in general range from several hours for bulk separation to several days for a purification.
- Long cycle times for the TSA means larger bed lengths with a consequential high adsorbent inventory. Since the time for adsorption and desorption must be equal in a TSA process, the cycle time will therefore be controlled by the events in the desorption part of the cycle. The required 4 minute cycle as discussed previously, will therefore not be possible.

TSA will in this instance not be appropriate to effectively regenerate the bed to ensure continuous production.

Pressure swing adsorption (PSA)

Since changes of pressure can be effected much more quickly than changes in temperature, and thus cycle times of pressure swing adsorption processes, are typically of the order of minutes, the process of PSA will be preferential as regeneration method in the design of this pilot plant. As defined earlier, the vacuum swing adsorption (VSA) is often used to denote a special PSA cycle with desorption taking place at sub-atmospheric pressure.

The PSA for this pilot plant was initially designed at a high pressure of approximately 5 bar and a low pressure of approximately 2 bar. However, the gain in raffinate recovery is achieved here at the expense of the additional mechanical energy required by the compressing step. A significant energy saving is possible however if the cycle is operated with a higher pressure slightly above atmospheric and a very low desorption pressure.

The latter option was decided upon and the high pressure was selected as atmospheric pressure and the low pressure as 17 kPa (abs).

Figure C3 and pressure curves generated by Sowerby and Crittenden^[63] were used to determine the boundaries of low pressure for the vacuum swing adsorption cycle. From these sources, the lowest regeneration pressure used was at 40 kPa (abs). A final regeneration pressure of 17 kPa (abs) was selected for the following reasons:

- a regeneration pressure lower than 40 kPa was required as Sowerby and Crittenden also used elevated regeneration temperatures in excess of 200 °C;
- desorption needed to be more efficient than that depicted in Figure C3;
- a practical regeneration pressure of 17 kPa(abs) required a minimum nitrogen purge flow rate of 7.8 kg/hr (as calculated in appendix D1)

It is known that adsorption isotherms tend to become unfavourable for adsorption at increased temperature and therefore more favourable for desorption. For this reason it was decided not only to make use of a vacuum swing adsorption to regenerate the bed, but in addition to that, also increase the bed temperature to as high as would be allowed for during the regeneration cycle time using an inert purging gas like nitrogen. The purge gas therefore has the following functions:

- increases the bed temperature to as high as possible in the 4 – 5 minute cycle time;
- remove the molecules that has been desorbed due to the vacuum condition;
- it causes the strongly adsorbed species (water and methanol) to be pushed backwards towards the bed inlet for the subsequent adsorption step.

The mass of the minimum purge gas (nitrogen) for this purposes was calculated to be ± 8 kg/hr (refer to the appendix D1).

The purity of the purging gas used is of vital importance to the effective regeneration of the molecular sieve bed. This purity in terms of water content is depicted by Figure C9.

The nitrogen purge gas temperature was approximately 170 °C. The purity grade of nitrogen used is of the type nitrogen 4.5, with a dew point of -72° (provided by Afrox). From Figure C9, at a gas temperature of 170 °C and a dew point of -72° the achievable residual water loading < 0.5 %. According to W R Grace & Company, a residual water loading of 1 % is an industry norm and anything lower than that is exceptional.

C Energy requirements

As was indicated in chapter 2, adsorption is a competitive low energy alternative to more traditional separation processes. An energy analysis is discussed in chapter 5.

D Adsorbent Life

The typical life span of a molecular sieve bed is between 7 – 10 years. Due to the enhance formulation of MS 564 CS problems with attrition, ageing, fouling and swelling, is minimised. Attrition and abrasion of the bed is further avoided by the inclusion of the pressure equalisation and repressurisation steps, preventing pressure shocks to the beds. The beds are also heated at a rate < 3 °C /min to prevent thermal shocks.

III EQUIPMENT

A Contactor type

In the selection of the contactor or the reactor it was decided to make use of a fixed bed adsorption column with axial rather than radial flow. From a practical point of view, this seemed to be the better option.

Pulsed or fluidized beds were not considered at all. Due to the cost involved, the moving bed adsorption column was not considered either.

B Geometry

One of the design objectives of this demonstration plant was to have continuous production. PSA or VSA systems are normally designed in banks of 4, 8 or even more adsorbers. Process benefits from these multiple banks of adsorbers had to be evaluated against the addition in capital cost. Because of the latter reason, it was decided to design and make provision for two fixed bed adsorbers operating in parallel, one in adsorption mode whilst the other is regenerating. The design of the adsorbers was based on velocity effects, adsorbent bed size, regeneration purge as well as heat transfer rate equations. This design philosophy was proposed by White^[76]. Design calculations for the two adsorbers can be found in appendix D1. The design indicated that given the operating conditions as discussed earlier, the adsorber required a diameter of 0.4 m and a total packed height of 1.71 m.

C Column internals

Each adsorber has to support the weight of the molecular sieve. A 20 mesh screen (1mm) is mounted at the lower end of the bed and was designed to carry a total weight of 160 kg. The mesh was reinforced by a corrugated steel plate with slots to allow vapour flow and assist with distribution. Directly above the mesh support is a 30 mm layer of ceramic balls (3 mm in diameter) which provides optimum distribution of vapour through the molecular sieve bed, which is essential for efficient operation. This flow distribution system, as well as the fact that no resistance to flow is experienced anywhere in the

adsorber, ensures that dead volumes are almost completely eliminated, as shown in Figure 4.1.

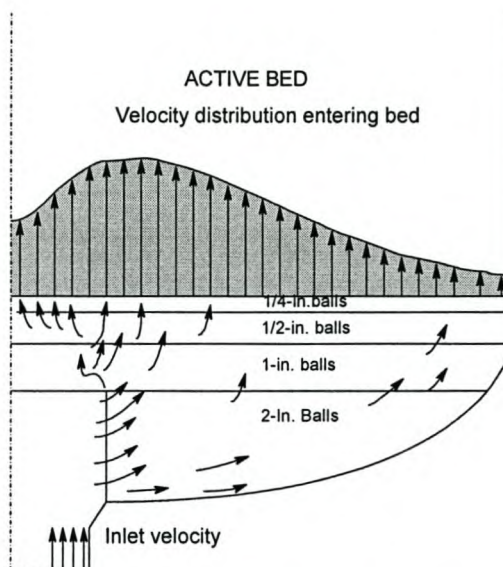


Figure 4.1. Arrangement involving layers of inert ceramic balls provide good flow distribution across adsorbent bed

A gas distribution plate (appendix F4) was mounted in the upper cones of the columns to ensure more uniform flow and heating through the beds. In order to remove the molecular sieve from the bed when required, a flanged stainless steel plug was manufactured and installed at the lower end of the columns. The plug ensured that no molecular sieve forms part of a dead space within the bed. Both adsorbers and piping were insulated to prevent excessive heat loss and consequent premature vapour condensation.

IV PROCESS FLOWSHEET

All the issues discussed so far in the design of the vacuum swing adsorber are crucially important for its successful operation. However, even if all these parameters were designed and selected appropriately, without proper process control of the VSA system, the following problems could be expected:

- premature breakthrough;
- variable content of strongly adsorbable component on bed;
- contamination of the bed;

- variable product purity;
- unsynchronized bed switching;
- loss of the heat of adsorption.

Process control for this VSA demonstration plant was based on the following flow chart shown in Figure 4.2. The cycle sequencing as indicated in this figure, was compiled specifically for this demonstration plant and based on sound theoretical and engineering principles.

The cycle sequence chart allows for all of the required sequential process steps to ensure continuous production, required purity, reduction in mechanical input energy as well as preservation of the molecular sieve.

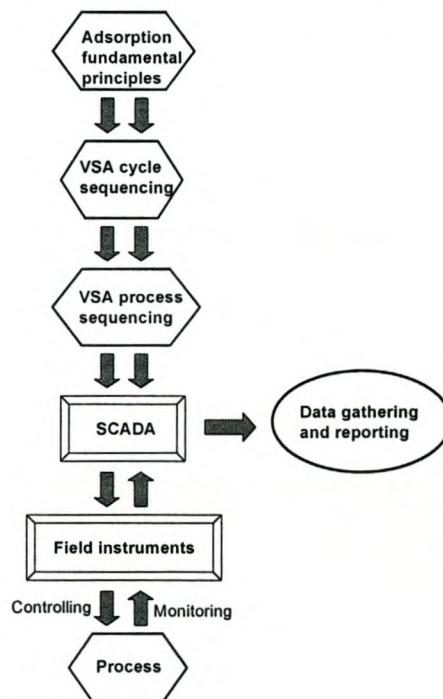


Figure 4.2 Process control flowchart

The following cycle sequence chart is at the heart of the process control of the VSA plant and was used as direct input into the process sequence chart.

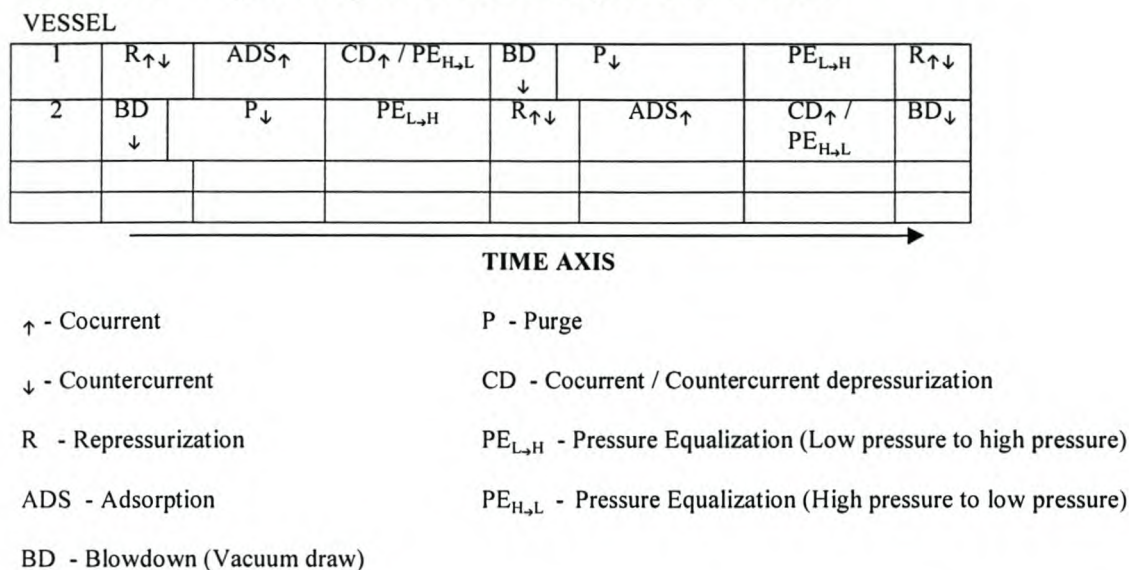
Table 4.1. Cycle sequence chart for process control

Figure 4.2 showed that the process will be controlled by means of a SCADA system. The interface between the cycle sequence chart and the SCADA is known as the process sequence chart. This process sequence chart will be discussed together with the final process and instrumentation flow diagram of the VSA process. It is this process sequence chart that was used to program the control loops for the plant. The specifications for the supply and installation of this software monitoring and control system are listed in the appendix E2.

B CONFIGURATION

Configuration progression

The process configuration for this demonstration plant went through various stages of development. From literature as well as other commercial adsorption applications, various configurations were initially built into the design of the demonstration plant. These configurations were based on sound adsorption engineering principles and are depicted in the following table.

Table 4.2 Development of design configurations

Stage	n _{columns}	Layout	Adsorption	Regen type	Purge	Mixed bed	Operational pairs	Continuity
1	4	Series	↓	TSA		No	2	Yes
2	2	Series	↓	TSA		No	1	No
3	2	Parallel	↓	TSA		Yes	1	Yes
4	2	Parallel	↓	PSA	Product & N ₂ ↑	Yes	1	Yes
5	2	Parallel	↑	PSA	↓ Product & N ₂	Yes	1	Yes
6	2	Parallel	↑	PSA	N ₂ - closed loop	Yes	1	Yes
7	2	Parallel	↑	VSA	N ₂ - single pass	Yes	1	Yes

This progression in process configuration was time consuming and together with the column design and selection of appropriate molecular sieves were the most challenging issues in this design.

Risk issues and safety

In alcohol production, the presence of flammable vapours in certain areas and at certain times are inevitable.

It is therefore important that certain stringent precautions are taken to prevent the occurrence of fires or explosions. It is also essential to ensure the safe design, installation maintenance and operation of the plant and its ancillary equipment. For this reason it was requested that the Risk Manager of KVV conduct a risk analysis on the design of the demonstration plant. The analysis set out to establish whether the demonstration plant design met the requirements of the Occupational Health and Safety Act (Act 85 of 1993).

Due to the evaluation of the risk and safety issues of the demonstration plant design against the Occupational Health and Safety Act, the Manager: Inspection and Enforcement Services, Department of Labour, assisted with the risk analysis. The task at hand was to ensure that a negligible probability of a means of ignition and any significant quantity of a potentially explosive atmosphere could occur in the same location at the same time while the demonstration plant was operated.

Due to the size of the demonstration plant and the volume of product envisaged to be used during the project, the initial design did not call for safe electrical components. During the risk analysis, the following became apparent:

- even with low volumes of product, a situation could arise where the optimum conditions for an explosion could occur. (Refer to Figure 4.3 for gas combustion versus concentration);
- the demonstration plant itself, in being mobile, could be transported into an area where flameproof electrical equipment was a requirement;

- the classification of the equipment in terms of SABS 0108 would be either zone 1 or zone 2.

In light of these findings of the analysis, a requirement of classified electrical apparatus was placed on the plant design with a resulting cost increase. Due to these findings, the following disciplines had to be applied:

- area classification: a risk analysis to identify both the level of explosion risk (frequency of occurrence) and type of selection of suitable equipment
- certification of the equipment
- installation, maintenance and the repair of equipment to ensure that the integrity of the explosion protection is maintained.

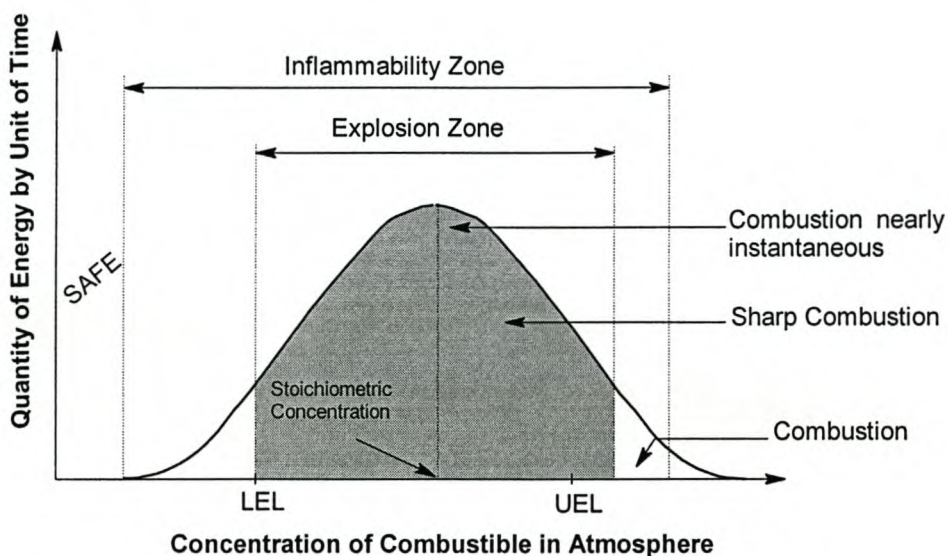


Figure 4.3. Relationship between gas combustion and concentration.^[3]

Due to this risk analysis and area and equipment classification, all electrical equipment had to carry a type “E” classification. The type “E” classification was therefore built into the total design of the demonstration plant with a significant increase in the capital cost .

A further risk and safety issue was whether the two adsorption columns were to be classified as pressure vessels. A pressure vessel by law is defined as any vessel of which the interior or jacket is under pressure or in which a

cushion of gas or vapour can form above the liquid at a pressure in excess of that of the atmosphere. It exclude the following vessel conditions:

- a vessel of which the product of the design pressure in pascal and the capacity in cubic metres is less than the figure 15 000;
- a vessel of which the design pressure is less than 40 kPa (gauge);
- a vessel with a nominal internal diameter of less than 150 mm.

Conditions were selected to adhere to the above conditions and the columns needed not be certified as pressure vessels.

4.2.2 Final process flow

The result of all the design considerations in this chapter as well as the theoretical considerations in chapter 2, led to the final design of the VSA plant of which the P&ID is depicted in appendix A2.

4.2.2.1 Process flow description

To facilitate mobility, the plant is constructed in two skid mounted portions, suitable for maneuvering by means of a forklift truck. The major portion consists of the process plant and the other of the chilled water system. The split between these two major portions was necessary since the chiller system was not suitable for operation in a hazardous area. The process plant needed to be suitable for a Zone 2 classified area, as discussed earlier under the risk analysis. The total installed electrical capacity of the plant is 20 kW.

The feed stream is pumped from tanks TK700 and TK800 with pump (PP302) at a flowrate of 50 *l*/hr. The feed flowrate is indicated on a local flowmeter FI301, while line pressure is monitored at local pressure gauge PI301. Manual valve V301 allows for complete isolation of the feed line should it be required. The liquid phase azeotropic ethanol feed is vaporised at a constant flowrate of \pm 40 kg/hr in HX300.

Sensible and latent heat to HX300 is provided by means of steam, generated in HX301. HX301 is a combination of a tubular heat exchanger and an electrically heated steam generator.

Vaporisation occurs on the shell side of the vertical heat exchanger. The steam temperature is set by means of a temperature transmitter, switching the three heating elements of 5 kW each to maintain a setpoint. The vapour is slightly superheated to ± 105 °C, after which it is fed through a liquid/vapour separator SP301 to prevent the potential entrainment of droplets into the adsorbers. The tangential inlet of the separator ensures complete separation of potential droplets.

This serves as an additional safety precaution to protect the beds, as superheating in HX300 already ensures the complete phase change from liquid to vapour. The vapour temperature in SP301 is monitored by the SCADA ensuring that the entrance temperature into the base of the adsorbers is 95 °C – 100°C. Safety valve V302 protects HX301 from over-pressurisation.

The azeotropic vapour is fed into the bottoms of either adsorber (AD100 or AD200), depending on the process mode. Adsorption takes place in an upward direction at an initial bed temperature of ± 95 °C, with the movement of the mass transfer zone at the actual line of adsorption being tracked by 12 thermocouples (TT101–TT106) and (TT201 – TT206) along the length of each adsorbing column. These thermocouples record temperatures along the central axis of the columns. To evaluate radial temperature effects, 2 additional thermocouples on each adsorber at position 4 provide the radial gradient information.

The adsorbers were designed to an inner diameter of 0.4 m, with a total packing height of 1.71 m. The beds are packed with 1.6 m of Sylobead™ MS 564 CS (3A) and 0.11 m of Sylobead™ MS 512 (4A) as manufactured by W.R. Grace & Co., with a total weight of 160 kg. The molecular sieve bed is supported by a slotted corrugated plate, covered with 20 mesh (1mm) wire. The molecular sieve bed was packed onto 8 kg of small ceramic beads of different diameters according, minimising flow uniformity problems.

Regeneration/desorption of the beds takes place under vacuum (17 kPa abs) at normal bed temperature.

Countercurrent (downward) purging with N₂ gas was done at a flowrate of ± 10 kg/hr, as measured by flow transmitter FT 501. The liquid nitrogen is drawn off a bulk N₂ storage tank at the KWW Paarl premises. The liquid nitrogen was filled under the required safety precautions into a portable cryogenic container (PCC) and transported by forklift to the adsorption plant as required. A special transport skid was designed for the PCC. The PCC carries a capacity of 130 kg N₂.

Besides an internal vaporiser, the PCC was also fitted with an additional external vaporiser, ensuring adequate vapor draw-off to the plant. The pressure of the N₂ gas is reduced in 2 stages at regulators (V502 and V504), after which it is heated in (HX500 and HX520) to 100 °C and 170 °C respectively, depending on the process mode of the adsorbers. The temperatures of oil heaters HX500 and HX520 are controlled by heating elements, ensuring that the required N₂ gas temperature is achieved at TT502 before entering the beds. Bed selection for N₂ purging is done by solenoid valves V523 and V503.

The desorption step also uses the stored heat for regeneration energy, reducing the volume and temperature of the required purge gas. Both adsorption and desorption step are performed in cycle times of ± 5 minutes. The raffinate which exits at the upper end of the columns is cooled in the condenser HX400 with chilled water. Samples were also drawn off at sample valve V401 and sent for analysis. The final product was collected in tanks TK900 and TK 950.

AD100 and AD200 were not designed or certified as pressure vessels and safety valves V106 and V206 ensured that the pressure limit as stipulated by the OHS Act were not exceeded as discussed earlier under “risk and safety”.

In order to reduce the size of the vacuum pump VP600, the volume of the contaminated purge gas exiting the bottoms of the adsorbers needed to be cooled prior to entering the vacuum intake. This was achieved by injecting directly into the line a water spray HX 602. The water spray in contact with the hot contaminated purge gas evaporates instantly and simultaneously extracts latent heat from the environment.

The evaporation effect led to the cool down of the gas stream prior to the vacuum intake, which in return reduced the volume of gas and consequently the size of the vacuum pump. The water for this spray condenser was drawn off just before the seal-water intake on the vacuum pump VP600 discharges into separator (SP601) which also serves as seal-water tank. This tank was equipped with a loose lid and a float valve to maintain the desired water level. The seal-water was cooled to $< 15^{\circ}\text{C}$ in a plate heat exchanger HX601 prior to entering the vacuum pump.

4.2.2.2 Process control

Effective process control is at the heart of the successful operation of the VSA plant. The objectives of the process sequence chart was:

- ensuring constant vapour flow to the adsorbers
- controlling heat of adsorption within the boundaries of the adsorber
- preventing premature breakthrough
- preventing exit bed and product contamination
- preventing accumulation of contaminants onto the molecular sieves following successive cycles
- ensuring all cycle modes operate as indicated by the cycle sequence chart (Table 4.1)
- ensuring adequate vapour and gas flow rates in the required directions
- preventing propagation of mechanical shocks into the molecular sieve bed

The interface between the cycle sequence chart and what actually takes place in the plant is depicted by Table 4.3.

TABLE 4.3. Process cycle sequence chart

TABLE 4.3. Process cycle sequence chart																	
Step	Comments	AD100			Valves at AD100				AD200			Valves at AD200					
		Process	Start	Stop	V101	V102	V103	V105	Process	Start	Stop	V201	V202	V203	V205	V303	
Warmup	WU1	Upper piping (same start & stop)	Warm up	Start	Manual	Closed	Closed	Open	Open							Closed	
	WU1a	Upper piping (same start & stop)								Warm up	Start	Manual	Closed	Closed	Open	Open	Closed
	WU2		Warm up	E of PP	TT101 >= T ₁	Closed	Open	Open	Closed				Closed	Closed	Closed	Closed	Closed
	WU3	Feed piping	Warm up	E of PP	Manual	Open	Closed	Open	Closed				Closed	Closed	Closed	Closed	Open
	WU4	Piping	Warm up	E of PP	Manual	Open	Closed	Open	Closed	Warm up	E of PP	Manual	Open	Open	Closed	Closed	Closed
WU5					Closed	Closed	Closed	Closed	Warm up	E of PP	TT201 >= T ₁	Closed	Open	Open	Closed	Closed	
Startup	SU1	Maintain PT101 <= P ₁	BD ₁₀₀ down	Operator	PT101 <= P ₁	Closed	Open	Closed	Closed				Closed	Closed	Closed	Closed	Closed
	SU2	Switch V503 & V523 (time ₁ before E of P)	Regen	E of PP	TimerP >= time ₂	Closed	Open	FIRC501	Closed				Closed	Closed	Closed	Closed	Closed
	SU3					Closed	Closed	Closed	Closed	BD ₂₀₀ down	E of PP	PT201 <= P ₁	Closed	Open	Closed	Closed	Closed
	SU4	Switch V503 & V523 (time ₁ before E of P)				Closed	Closed	Closed	Closed	Regen	E of PP	TimerP >= time ₂	Closed	Open	FIRC501	Closed	Closed
	SU5	Regen piping				Open	Open	Closed	Closed	Regen	E of PP	TimerSU5 >= time ₂	Open	Closed	FIRC501	Closed	Closed
Process	PR1		BD ₁₀₀ down	E of PP	PT101 <= P ₁	Closed	Open	Closed	Closed	RP ₂₀₀ down	E of PP	PT201 >= P ₂	Closed	Closed	PIRC201 Flow rate 10kPa / s	Closed	Open
	PR2	Switch V503 & V523 (time ₁ before E of P)	P ₁₀₀ down	E of PP	TimerP >= time ₂	Closed	Open	FIRC501	Closed	ADS ₂₀₀ up	E of PP	TT205 >= ave + T ₂ or TimerA >= time ₂	Open	Closed	Closed	Open	Open
	PR3	Same start & stop	PEI-h	E of PP	ABS (PT201 - PT101) <= P ₃	Closed	Closed	PIRC101 Flow rate 10kPa / s	Closed	CD up / PEH-l	E of PP	ABS (PT201 - PT101) <= P ₃	Closed	Closed	Open	Closed	Open
	PR4		RP ₁₀₀ down	Start	PT101 >= P ₂	Closed	Closed	PIRC101 Flow rate 10kPa / s	Closed	BD ₂₀₀ down	Start	PT201 <= P ₁	Closed	Open	Closed	Closed	Open
	PR5	Switch V503 & V523 (time ₁ before E of P)	ADS ₁₀₀ up	E of PP	TT105 >= ave + T ₂ or TimerA >= time ₂	Open	Closed	Closed	Open	P ₂₀₀ down	E of PP	TimerP >= time ₂	Closed	Open	FIRC501	Closed	Open
	PR6	Same start & stop	CD up / PEH-l	E of PP	ABS (PT201 - PT101) <= P ₃	Closed	Closed	Open	Closed	PEI-h	E of PP	ABS (PT201 - PT101) <= P ₃	Closed	Closed	PIRC201 Flow rate 10kPa / s	Closed	Open
Shut down	SD1	Procedure starts after P5, before pressure equalisation	BD ₁₀₀ down	Operator	PT101 <= P ₁	Closed	Open	Closed	Closed	Close valves	Operator	PT101 <= P ₁	Closed	Closed	Closed	Closed	Open
	SD2		P ₁₀₀ down	E of PP	Timer >= time ₂	Closed	Open	FIRC501	Closed	Close valves	E of PP	same as AD100	Closed	Closed	Closed	Closed	Open
	SD3	Fill column with N2 to exclude moisture	RP ₁₀₀ down	E of PP	PT101 >= P ₂	Closed	Open	FIRC501	Closed	Close valves	E of PP	same as AD100	Closed	Closed	Closed	Closed	Closed
	SD4	Fill column with N2 to exclude moisture	Close valves	E of PP	Stop	Closed	Closed	Closed	Closed	RP ₂₀₀ down	E of PP	PT201 >= P ₂	Closed	Open	FIRC501	Closed	Closed
	SD5	Process stopped				Closed	Closed	Closed	Closed	Close valves	E of PP	Stop	Closed	Closed	Closed	Closed	Closed

It defines the operational sequences and relationship between various equipment components of the VSA system. This process sequence chart (PSC) required careful and detailed planning to ensure the successful operation of the plant.

The PSC was categorised in the following four operation modes. These modes could be accessed both manually and automatically, depending on the operator requirement:

- Warm-up
- Start-up
- Process
- Shutdown

Warm-up

The purpose of the warm-up mode was to prepare the total reticulation system for adsorption and regeneration. The reticulation was warmed with hot N₂ gas after passing through HX520. The warm-up mode consisted of five steps (WU₁ – WU₅). These operational steps warmed the system in a sequential and structured manner, starting with the upper piping, the adsorber beds and finally the feed piping.

Start-up

The purpose of this mode was to prepare the two beds of molecular sieve for the first adsorption cycle. As the sieves were imported from Germany and subjected to various environmental conditions, it was important to start the process with a complete regeneration. This would ensure that the beds are properly cleaned and uncontaminated prior to its first cycle. The start-up step would always be performed following a complete shutdown, or in the event of bed contamination or a power failure. The mode consists of five operational steps (SU₁ – SU₅).

Process

This operational mode is the actual process ensuring the various cycle modes as indicated below. It consists of six steps (PR₁ – PR₆). The actual modes of operation and philosophy of control for this VSA system is formulated in the adsorption cycle sequence chart (Table 4.1). This stipulates the cycle order for an adsorber as follows:

1. Countercurrent blowdown
2. Countercurrent purge
3. Pressure equalization
4. Countercurrent repressurisation
5. Adsorption
6. Cocurrent depressurisation
7. Pressure equalisation

Apart from controlling the individual column cycles above, the PSC also controls the relative status of the parallel operations between AD100 and AD200. This means that the two adsorbers while operated in the automatic mode are fully synchronised, which ensures continuous production.

Shutdown

The shutdown mode would only be activated at the end of a production run. The mode consists of five steps (SD₁ – SD₅), which regulates the flow of cold N₂ gas into both adsorber beds. Cold N₂ gas is obtained by opening valve V506 and bypassing the oil heaters. The positive pressure of N₂ gas in the adsorbers prevent the possible contact of the molecular sieve beds with moist air during the shutdown period. Cold N₂ gas was used for sieve preservation, preventing unnecessary thermal expansion and shrinkage of the bed.

This concludes the aspects that were considered in the design of the VSA plant. Various design information including technical drawings of some process equipment, as well as actual pictures of the plant are shown in appendix F.

CHAPTER FIVE

EXPERIMENTAL PROCEDURES AND RESULTS

Actual operation of the VSA demonstration plant was much more than running a mere laboratory experiment. Operational procedures took place on the premises of KVV in Paarl. The plant was erected within the existing alcohol and brandy distillation facilities and was operated with the same level of involvement and responsibility as that of any other full-scale production facility.

The experimental procedures were divided into two experimental groups and designed to achieve the following **objectives**:

Group I experiments

1. To confirm on larger scale the experimental work discussed in chapter 3 and the concept that water and methanol are selectively adsorbed from the bulk ethanol stream onto molecular sieve 3A.
2. To evaluate the adsorption and desorption efficiency of the designed vacuum swing adsorption system.
3. To determine and solve potential commissioning and operational problems.

Group II experiments

4. To determine the sensitivity of the methanol breakthrough profile to a variety of process conditions in the presence of water.
5. To demonstrate the extent of methanol adsorption from ethanol in the absence of water and confirming the suitability of the methanol molecule characteristics for adsorption as discussed in chapter 2.8.2.
6. To define the process boundaries of operation.
7. To demonstrate stability of the process over a period of time

The plant was operated by the author only, indicating the ease of running this complex system by a single operator.

5.1 EXPERIMENTAL METHODS

5.1.1 Group I experimental runs

The plant was taken through various steps of commissioning prior to the commencement of production. Successful commissioning was pertinent to the efficiency of the system and was performed to test the integrity of all process equipment, determine certain production parameters and evaluate the efficiency of the process control loops and SCADA. The commissioning schedule that was followed consisted of pre-commissioning, engineering commissioning and process commissioning. The detail of this commissioning schedule is listed in appendix G.

Various problems were experienced during commissioning and needed to be solved prior to starting up the production process. These included:

- destruction of steam heating elements
- inefficient control of chilled water system
- inadequate pressure head on chilled water reticulation
- application of incorrect sealant material reacting with ethanol
- delay in oil heating
- incorrect electrical connections
- vapour feed cooling prior to entering the bed
- incorrect moisture analyser application
- incorrect temperature probe lengths
- incorrect nitrogen gas regulator to provide the required pressure and flow
- inadequate vacuum with increasing nitrogen flow rate
- difficulty in uniformly heating the bed
- maintaining effective vacuum on adsorbers

The latter posed a simple but significant technical problem. The plant had to be commercially vacuum tight, since inadequate vacuum during regeneration would lead to a decrease in desorption efficiency as discussed later. Searching for and establishing a vacuum leak was difficult.

The vacuum depletion curves before and after the vacuum checks show the vacuum behaviour of the columns (*note: all process curves in this section were generated directly by the Scada as the operational runs were performed. Format of curves are therefore affected*)

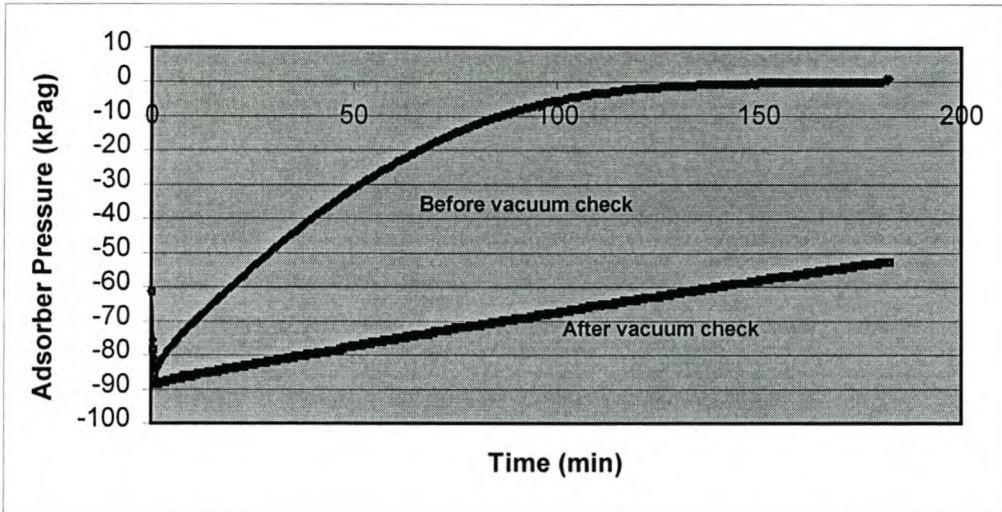


Figure 5.1. Vacuum depletion in adsorbers before and after doing a search for leaks.

Operation of the plant was performed in accordance to the process description in the previous chapter. Alcohol vapour was forced through the dual bed adsorbers at a constant vapour feed flow rate of 50 ℓ /hr and at known composition. This vapour flow rate was adequately below the fluidisation and attrition limits (see design calculations in appendix D).

Adsorption was carried out with flow in an upward direction and an initial bed temperature of ± 100 $^{\circ}\text{C}$. For desorption, the beds were heated and purged with purified nitrogen gas at ± 170 $^{\circ}\text{C}$ at a flow rate of ± 10 kg/hr in a downward direction. The nitrogen gas was heated in two oil baths (HX500 & HX520). The following oil heating curves show the response of the thermal oil heated by the 1.5 kW heating elements.

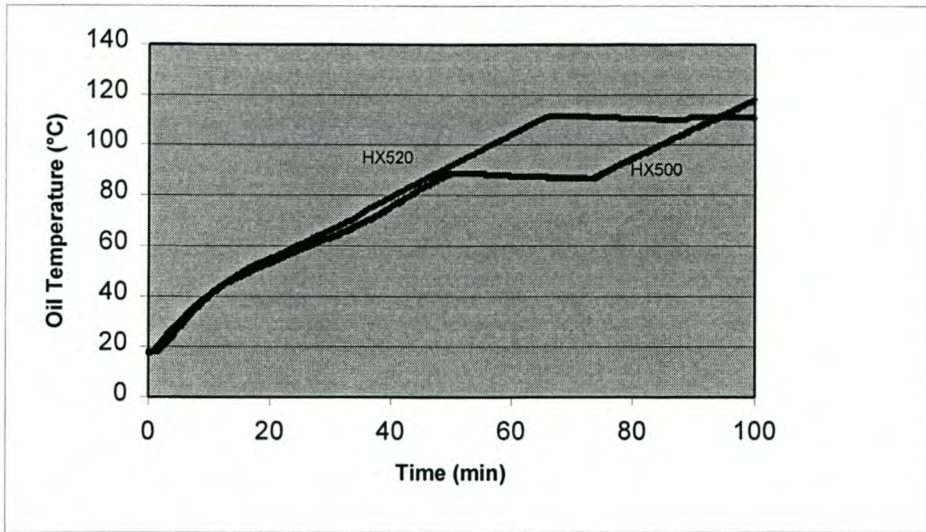


Figure 5.2. Thermal oil heating curve in heat exchangers HX500 and HX520

Normal equipment and pipe heating was also achieved by nitrogen heating. A typical bed heating curve is depicted in Figure 5.3.

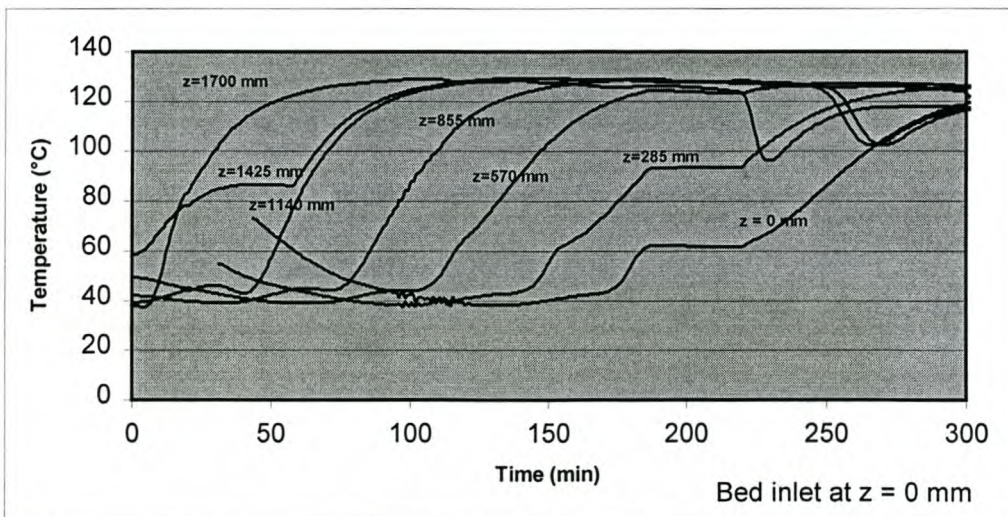


Figure 5.3 Typical bed heating curve for AD100 (axial temperature positions)

The following figures indicate the problematic effect of a radial temperature gradient of $\pm 26^\circ$ between the axial and outer section of the bed. TT107 is inserted 200 mm from the adsorber inner surface, while TT108 and TT109 are 80 mm and 15 mm respectively from the adsorber walls (same axial position).

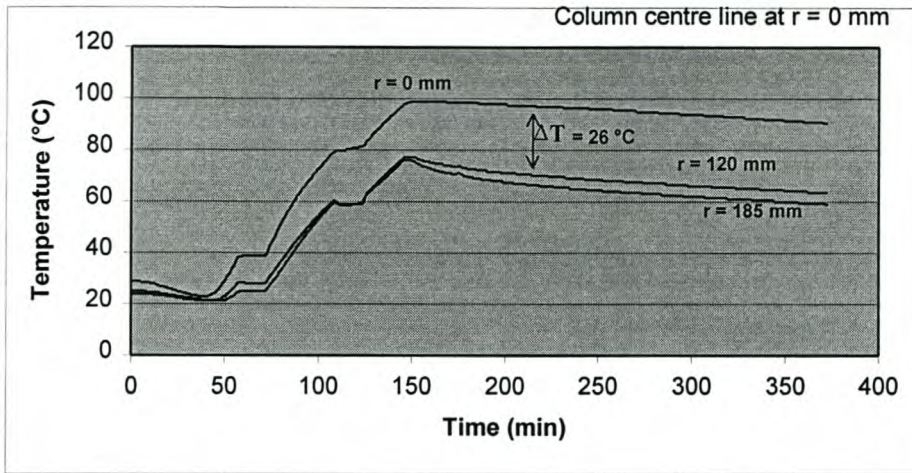


Figure 5.4. Radial temperature effect before gas distribution plate was mounted in adsorbers.

Figure 5.4 shows that the temperature closest to the column wall took 3 hours to reach 80 °C. This slow heating pattern indicates inadequate heating and nitrogen gas distribution.

This increases the risk of vapour condensation in the outer annulus of the bed and a higher consumption of nitrogen gas for heating. The adsorbers were reopened and a gas distribution plate was mounted into the upper conical sections of each adsorber (appendix F4 & F5). The following Scada curve shows that gas distribution and subsequent bed heating were improved.

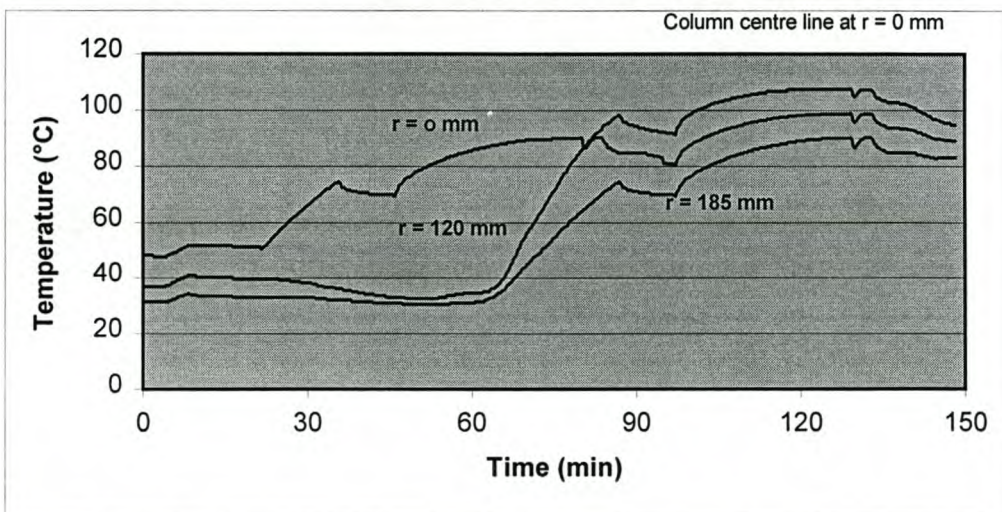


Figure 5.5. Radial temperature effect after gas distribution plate was mounted in adsorbers

Vacuum of 20 kPa (abs) was drawn on the adsorbers during regeneration. Both adsorption and desorption steps occurred simultaneously over a 5 minute period, as indicated by the design of the adsorbers (appendix D1). These process conditions were created and maintained by following the steps of synchronisation as depicted by the process sequence chart as discussed earlier (Table 4.3).

The VSA process has a distinctive pressure fingerprint, as can be seen in the following figure taken directly from the Scada recorded data. The pressure curves are derived from pressure transmitters PT101 and PT201 readings for AD100 and AD200 respectively.

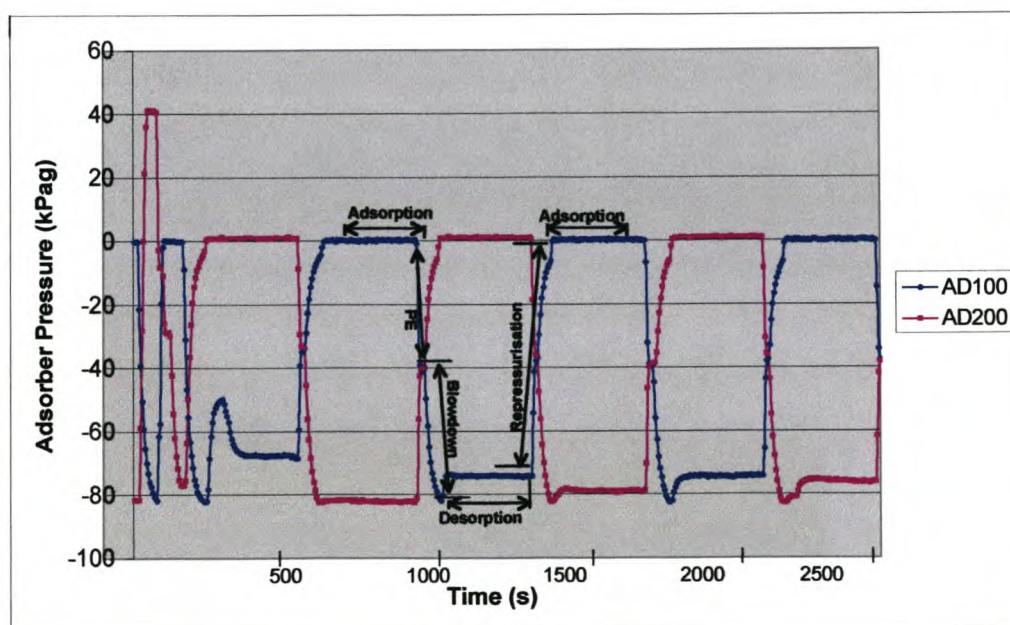


Figure 5.6 Pressure conditions in both adsorbers going through the synchronised steps as suggested by the process sequence chart.

The steps of pressure equalisation, blowdown, desorption, repressurisation and subsequent adsorption can clearly be distinguished. The pressure curves for the two adsorbers are exactly 180° out of phase, ensuring continuous production of purified ethanol.

Various aspects of the adsorption and regeneration cycles were evaluated. These did not just include product characteristics, but also variation in process conditions. These variables consisted of:

- feedstock quality and concentration;
- purge flow rate;
- depth of vacuum;
- repeatability;
- adsorption and desorption efficiency;
- radial temperature effects;
- heating effects.

60 Samples were drawn over 120 adsorption cycles, with 5 samples drawn at every 10th cycle according to the following table.

Table 5.1. Schedule of experimental runs (Group I)

Batch	Variable	Cycle No.	Samples taken over time				
			t1 = 1 min	t2 = 2 min	t3 = 3 min	t4 = 4 min	t5 = 5 min
1	Feed 1 ; N ₂ = 10 kg/hr	10	1	2	3	4	5
		20	6	7	8	9	10
2	Feed 1 ; N ₂ = 15 kg/hr	30	11	12	13	14	15
		40	16	17	18	19	20
3	Feed 2 ; N ₂ = 10 kg/hr	50	21	22	23	24	25
		60	26	27	28	29	30
4	Feed 2 ; N ₂ = 15 kg/hr	70	31	32	33	34	35
		80	36	37	38	39	40
5	Feed 3 ; N ₂ = 10 kg/hr	90	41	42	43	44	45
		100	46	47	48	49	50
6	Feed 3 ; N ₂ = 15 kg/hr	110	51	52	53	54	55
		120	56	57	58	59	60

Maximum sampling time (5 minutes) was limited to the design adsorption cycle time. Not only does this agree with the design period, but also adheres to the principle depicted in Figure C2. It indicates that a residual loading of contaminant will remain on the bed following regeneration, should the cycle time become significantly longer than 4 minutes. This also ensures enough time during the cycle for cocurrent depressurisation and prevents contamination of the bed exit.

Breakthrough during adsorption was therefore not allowed in the Group I experimental runs. The 120 adsorption cycles were varied over different feed concentrations and nitrogen purge flow rates.

5.1.2 Group II experimental runs

The Group II of experimental runs were performed according to the schedule shown in Table 5.2. Since organoleptic problems were evident in the product produced in Group I, molecular sieve 4A (with the untreated binder discussed earlier) was removed from both columns. Molecular sieve 4A was therefore not used in the Group II experiments and will not be investigated / discussed further.

Table 5.2 Schedule of experimental runs (Group II)

Batch #	Variable	Sample Number				
		t1 = 360 s	t2 = 720 s	t3 = 1080 s	t4 = 1440 s	t5 = 1800 s
	Feed concentration (mass %)					
1	C1	4	5	6	7	8
2	C2	9	10	11	12	13
3	C3	14	15	16	17	18
	Feed flowrate (l/hr)					
4	F1	19	20	21	22	23
5	F2	14	15	16	17	18
6	F3	24	25	26	27	28
	Regeneration pressure (kPa)					
7	P1	8	30	31	32	33
8	P2	34	35	36	37	38
9	P3	39	40	41	42	43
	Purge flowrate (kg/hr)					
10	m1	44	45	46	47	48
11	m2	49	50	51	52	53
12	m3	54	55	56	57	58
	Feed conc (synthetic) (mass %)					
13	CS1	59	60	61	62	63
14	CS2	64	65	66	67	68
15	CS3	69	70	71	72	73
	Initial bed temperature (°C)					
16	T1	74	75	76	77	78
17	T2	14	15	16	17	18
18	T3	79	80	81	82	83

The methanol mass transfer front was allowed to break through at the bed exit. Due to high analytical costs, the number of samples drawn were kept as low as possible. A number of 86 samples were drawn while varying the conditions as shown in Table 5.2.

For the purpose of the sensitivity analysis, the following critical process parameters were selected for evaluation: feed concentration, feed flow rate, regeneration pressure, nitrogen purge flow rate, initial bed temperature as well as methanol concentration in the absence of water. Only one parameter was varied per batch in order to demonstrate its effect on the methanol breakthrough curve. Although the water content was monitored at the bed exit, the Group II runs were primarily focused on assessing the sensitivity of separating methanol from the bulk ethanol stream. This is really where the contribution of this study is based. The Group II experiments were done over a period of 8 days, allowing as much as 12 hours of continuous production between each changed variable. Each batch represented an adsorption cycle of 1800 seconds (30 minutes) as opposed to the 5 minute cycles of Group I.

Since breakthrough was allowed to occur each time (and deviation from Figure C2), it was anticipated that gradual build-up of the contaminant would occur, impeding adsorption efficiency. There was also a delay of ± 10 days before results from the analyses became available. This made it difficult to pro-actively adjust the process conditions. As a precautionary measure, production was halted following batch 12. A 24 hour thermal regeneration at 150 °C was performed on both columns to allow for the removal of possible residual contaminant due to breakthrough.

A significant aspect of Group II experiments was the induction of a synthetic methanol state in the adsorption columns. Natural neutral wine spirits, as explained in chapter 2, contains water at or just below the azeotropic composition. Chapter 2 also discussed the dominance of the water molecule in comparison with methanol. If therefore the adsorption sensitivity of methanol on its own was to be investigated, it needed to be performed in the absence of water. Since absolute alcohol is expensive to purchase, the dehydrated product from some of the batches 1 – 12 was collected in a separate product tank.

This dehydrated product was then dosed at 3 different concentrations with synthetic methanol. The analytic specification of the synthetic methanol is given in appendix H5. This “synthetic” feed was then passed through the columns for batches 13 – 15. The dosages were far higher than one would expect to find in natural neutral spirits. This was done to evaluate high concentrations of methanol adsorption in the absence of water. The synthetic dosing was also done since it would, from a practical point of view, be difficult to source this type of product at the time these experiments were done from the Wine Industry.

5.2 METHOD OF ANALYSES

The samples were analysed on a Varian CP-3380 gas chromatograph with a Flame Ionisation Detector (FID) using a 50 m BP1 column. The FID was required for its wide linear range and high sensitivity. The low quantities of methanol could otherwise not be detected. The FID flame ignites and ionizes the combustible sample components as the carrier gas passes into it, after which the ions are collected at the electrodes, producing a current.

Temperature program

- initial temperature 60°C;
- initial time 6 minutes;
- temperature increased at 10 °C/min to a final temperature of 135°C;
- final column hold time: 2 min

Internal standard

n-Butanol

The water content was determined by means of volumetric Karl Fischer titrations using a Metrohm 701 Titrino. All relevant analytical information are listed in appendix H2.

Group I analyses were done in the Department of Chemical Engineering at The University of Stellenbosch and Group II analyses at Saybolt Laboratories in Durban.

5.3 RESULTS AND DISCUSSIONS

5.3.1 Group I experimental runs

Adsorption

During adsorption runs, the axial temperature variation was monitored throughout the adsorbers. Complete breakthrough of the mass transfer front was not allowed to occur. Breakthrough causes contamination of the bed exit and is detrimental to product purity and bed regeneration. The use of pressure equalisation principles also inhibited breakthrough. The adsorption of water and methanol onto the bed is reflected by the exothermic heat of adsorption and consequential rise in bed temperature, as the mass transfer front move through the beds in an upward direction. Bed temperatures of up to 180 °C were observed. A typical bed temperature profile for Group II experiments is shown later in chapter 5.3.2.

The 60 samples, in accordance with Table 5.1, were drawn just after the product condenser (HX400). The Karl Fischer and gas chromatography results for water and methanol adsorption onto MS 564 CS are listed in the table of analytical results in appendix H1. A typical ethanol adsorption curve for adsorption cycles 30 and 40 is shown in the following figure.

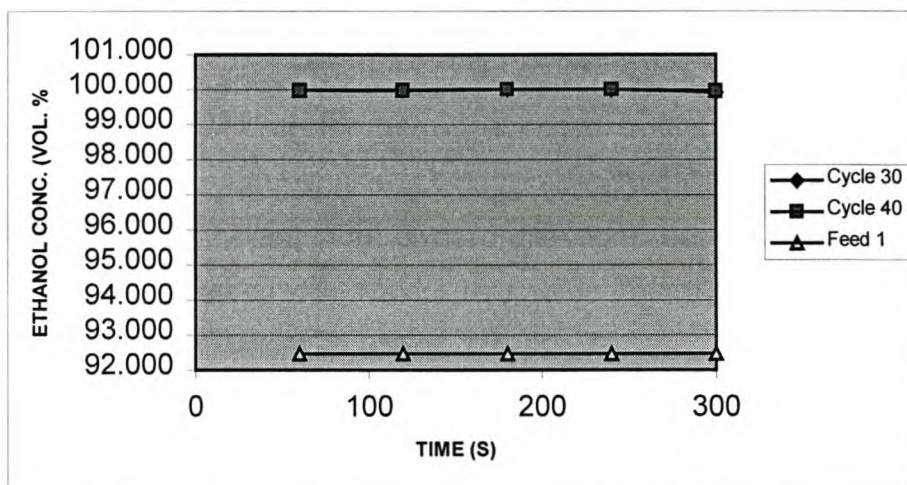


Figure 5.7. Ethanol adsorption curves during adsorption cycles 30 and 40.

Further ethanol adsorption curves are listed in appendix H3. The above figure shows no breakthrough after 5 minutes even with feed 1, which carries an initial water content of 7.47 wt. % water.

Table 5.2 shows that the water content of the exit streams was consistently reduced to < 0.05 wt. % on average. These results compares very well with the experimental work of Sowerby and Crittenden^[63] as well as with the results discussed in chapter 3.

This shows that the ethanol / water azeotrope was successfully broken, producing dehydrated potable alcohol. Due to the feed water content higher than that of the azeotrope, the adsorption step did not just break the azeotrope, but also removed excess water up to the azeotrope concentration. This expands even more the applications and points of integration of the adsorption step with conventional distillation.

The adsorption at higher water content without breakthrough after 5 minutes, also indicates that the VSA plant is able to handle a throughput > the theoretical design capacity of 40 kg/hr, without additional capital cost. This aspect will later be investigated further as part of the sensitivity analysis for Group II. The consistent adsorption efficiency over the 120 cycles (99.24 %), shows that the VSA process and its operating conditions were under control.

Table 5.3 Adsorption experimental conditions and results (Group I)

Batch	Feed	Cycles	Initial H ₂ O (% mass)	Exit H ₂ O (% mass)	η H ₂ O (%)	Water bed loading (g/100 g sieve)	Initial methanol (mg/100mlAA)	Exit methanol (mg/100mlAA)	η methanol (%)	Methanol bed loading (mg/100 g sieve)
1	1	10	7.47	0.1400	98.13	0.0153	66.4	3.8	94.28	0.1550
	1	20	7.47	0.0780	98.96	0.0154	66.4	4.6	93.07	0.1531
2	1	30	7.47	0.0693	99.07	0.0154	66.4	1.9	97.14	0.1598
	1	40	7.47	0.0288	99.61	0.0155	66.4	2.5	96.23	0.1583
3	2	50	5.26	0.0468	99.11	0.0109	85.3	2.6	96.95	0.2076
	2	60	5.26	0.0027	99.95	0.0109	85.3	2.8	96.72	0.2071
4	2	70	5.26	0.1474	97.20	0.0106	85.3	50.7	40.56	0.0869
	2	80	5.26	0.0103	99.80	0.0109	85.3	10.9	87.22	0.1868
5	3	90	8.39	0.0526	99.37	0.0174	12.2	23.5	-92.62	-0.0278
	3	100	8.39	0.0046	99.95	0.0175	12.2	2.9	76.23	0.0228
6	3	110	8.39	0.0236	99.72	0.0174	12.2	15.9	-30.33	-0.0091
	3	120	8.39	0.0019	99.98	0.0175	12.2	1.8	85.25	0.0255

 η = adsorption efficiency

effect of liquid surge

The principle of methanol adsorption onto molecular sieve 3A was demonstrated successfully on the VSA plant. The following methanol adsorption curves for adsorption cycles 50 and 60 show that the initial methanol content of 114.1 mg/100 mL AA were reduced to 3.4 mg/100 mL AA on average over the adsorption cycle of 5 minutes.

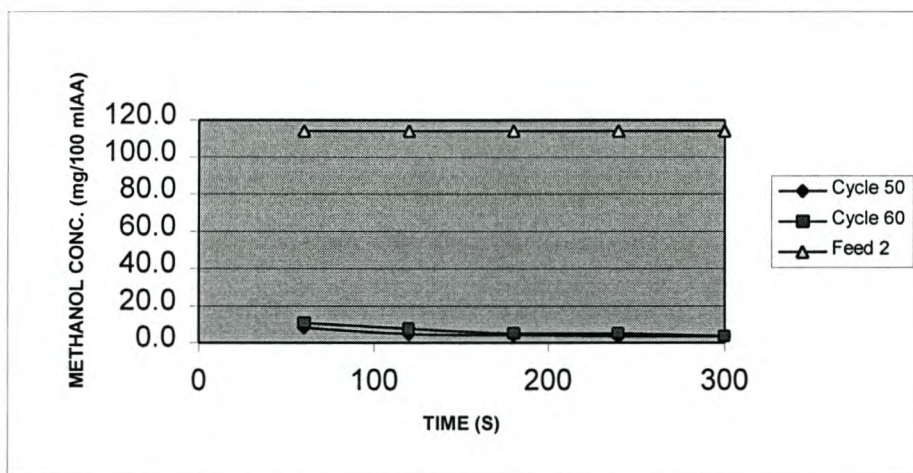


Figure 5.8. Methanol adsorption curves during adsorption cycles 50 and 60.

The methanol removal was consistent and supports the findings of the author as discussed in chapter 3. The following figure indicates the efficiency of water and methanol adsorption over 120 adsorption cycles.

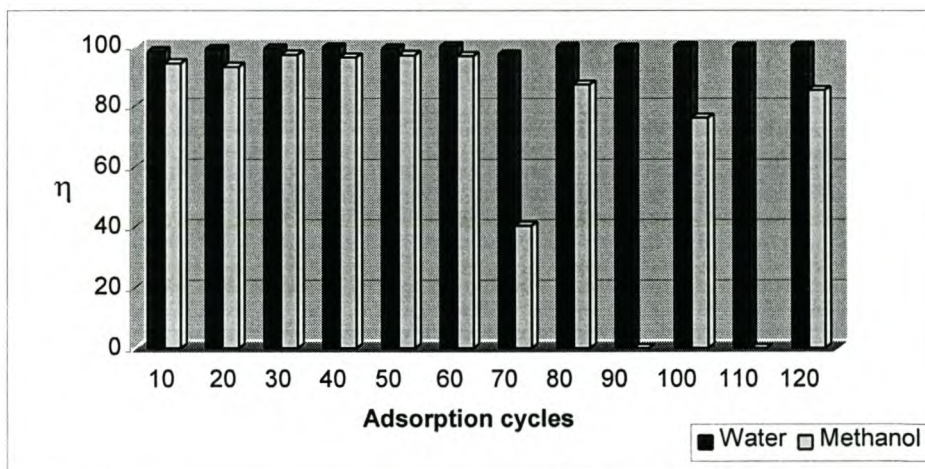


Figure 5.9. Efficiency of water and methanol adsorption over 120 experimental adsorption runs.

Clearly, methanol adsorption was consistent over the first 60 cycles, with a significant reduction as from cycle 70. The following ethanol adsorption curve for cycle 70 also indicates a reduction in adsorptive capacity.

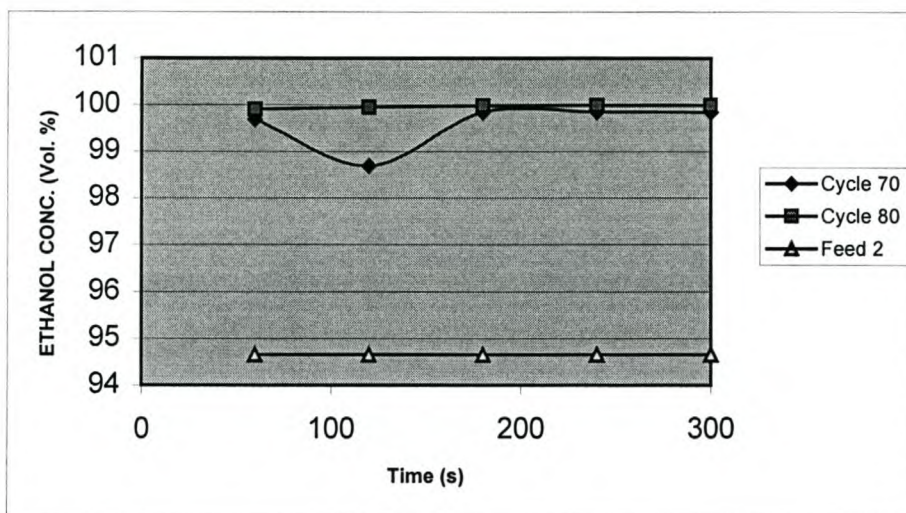


Figure 5.10. Ethanol adsorption curves during adsorption cycles 70 and 80.

This pattern also repeats in the following methanol adsorption curve. Although at considerably lower efficiency, methanol is still removed at cycles 70 and 80.

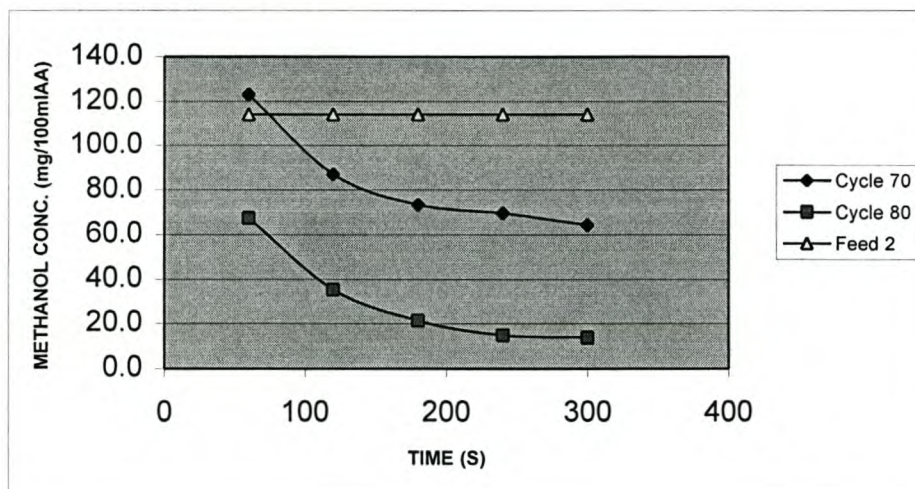


Figure 5.11. Methanol adsorption curves during adsorption cycles 70 and 80.

These patterns of a reduced methanol adsorptive capacity is however not linked to an inability of the system to separate methanol, as this would then have taken place prior to cycle 70.

The reduction at cycle 70 and thereafter was traced back to a liquid surge that took place in adsorber AD100 due to inadequate repressurisation of the column following vacuum regeneration. This took place only once and was the consequence of an error in the control program. The error was immediately rectified. An increase in efficiency was observed towards cycle 120, which indicates that the liquid caught in the adsorbent bed was gradually removed. The effects of the liquid surge are clearly marked in Table 5.2.

The following bed loading curves for water and methanol were derived from Table 5.3.

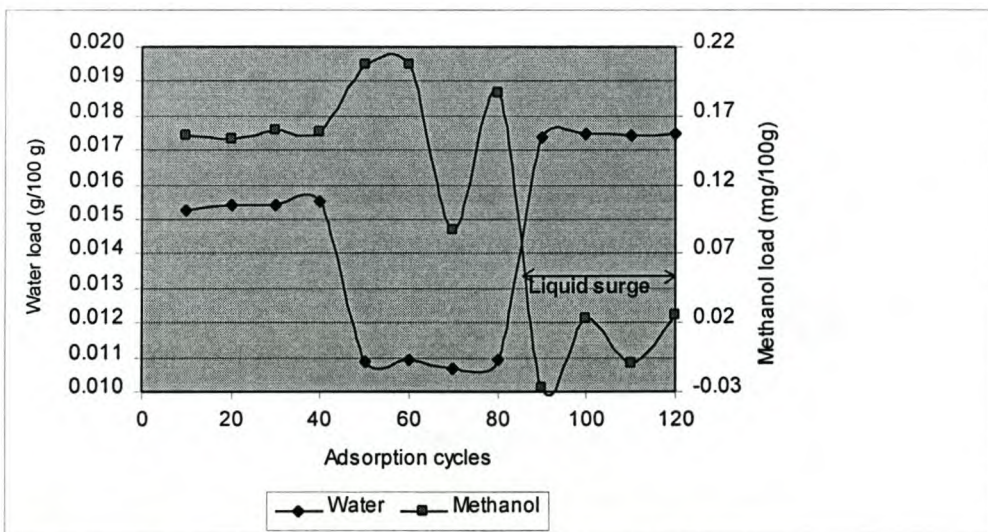


Figure 5.12. Water and methanol bed loading curves (Group I)

The water bed loading curve clearly shows a decrease between cycles 50 and 80. It was already indicated that the liquid surge that occurred during cycle 70 adversely affected both water and methanol adsorption. This is clearly depicted by the bed loading curves. Although the water bed loading recovers again after cycle 80, the methanol loading remains low.

Figure 5.9 however indicates that the methanol adsorption efficiency is only affected in cycles 70, 90 and 110. This was to be expected, as the liquid surge took place in one adsorber. The adsorbers were alternated for sampling. The high efficiency for cycles 100 and 120 as opposed to the low bed loadings for the same cycles is due to a low feed 3 methanol inlet quantity.

Another phenomenon is also clear from the bed loading curves and that is for a higher methanol content, the water loading on the bed is lower and vice versa. This supports the author's theory that water and methanol compete for adsorption sites.

The adsorption temperature profiles indicate that adsorption does not take place under isothermal conditions, as is normally the case for feed streams with a water content < 1 wt. % where the heat of adsorption is usually small and swept out of the bed easily. In this case, the operating conditions were chosen in such a way that this caused the heat of adsorption to be stored in the adsorbent bed. This stored energy was used in the subsequent desorption step to provide part of the heat of desorption.

Desorption

Desorption took place after every adsorption step. The regeneration was performed at vacuum conditions and nitrogen was the purging medium. The conditions and efficiency of desorption is shown in Table 5.3.

Table 5.4 Desorption conditions and efficiency

Batch	Feed	Cycles	N ₂ flow (kg/hr)	Vacuum (kPag)	$\Delta\eta$ H ₂ O (%)	$\Delta\eta$ methanol
1	1	10	10	-75	0.00	0.00
	1	20	10	-75	0.85	-1.28
2	1	30	15	-65	0.12	4.37
	1	40	15	-65	0.55	-0.93
3	2	50	10	-75	-0.51	0.75
	2	60	10	-75	0.85	-0.24
4	2	70	15	-65	-2.75	-58.06
	2	80	15	-65	2.68	115.03
5	3	90	10	-75	-0.43	-206.19
	3	100	10	-75	0.58	-182.30
6	3	110	15	-65	-0.23	-139.78
	3	120	15	-65	0.26	-381.08

effect of liquid surge

The change in adsorption efficiency ($\Delta\eta$) as the cycles progressed is depicted in the following figure.

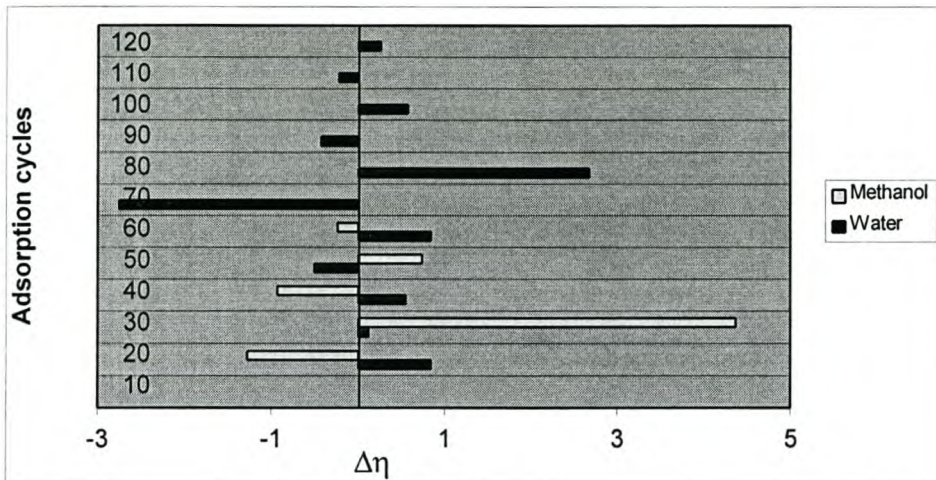


Figure 5.13 Change in adsorption efficiency over 120 adsorption cycles

As to be expected, the biggest negative change on efficiency takes place at cycle 70. The efficiency of desorption can be directly assessed by taking samples of the exit purge gas and analysing for contaminants. Desorption in this case however was indirectly assessed by repeating adsorption steps every tenth cycle, monitoring the depletion of adsorption efficiency. The negligible depletion indicates that the residual loading on the bed remains relatively constant and contaminant build up did not take place over the cycles.

The use of variation in vacuum conditions and purge flow rate influences the pressure ratio of the VSA cycle. The higher the pressure ratio (lower vacuum) the better $\Delta\eta$ over cycles. In this case there was not a considerable improvement linked to the additional 10 kPa vacuum from 35 to 25 kPa (abs). The explanation for this is found in the reduction of purge flow rate with an increased vacuum. The design regeneration conditions call for a vacuum of at least 17 kPa (abs). This was however not achievable due to the incorrect capacity of the vacuum pump. This problem was addressed later and a different vacuum pump was installed for the Group II experiments.

The repeatability of the bed loading curve (Figure 5.12) and the adsorption efficiencies (Figure 5.13) indicates that the desorption mode of 5 minutes is adequate to maintain product quality.

5.3.2 Group II experimental runs

A typical adsorption temperature bed profile over the 1800 s is shown in the following figure (compare to Figure 3.2):

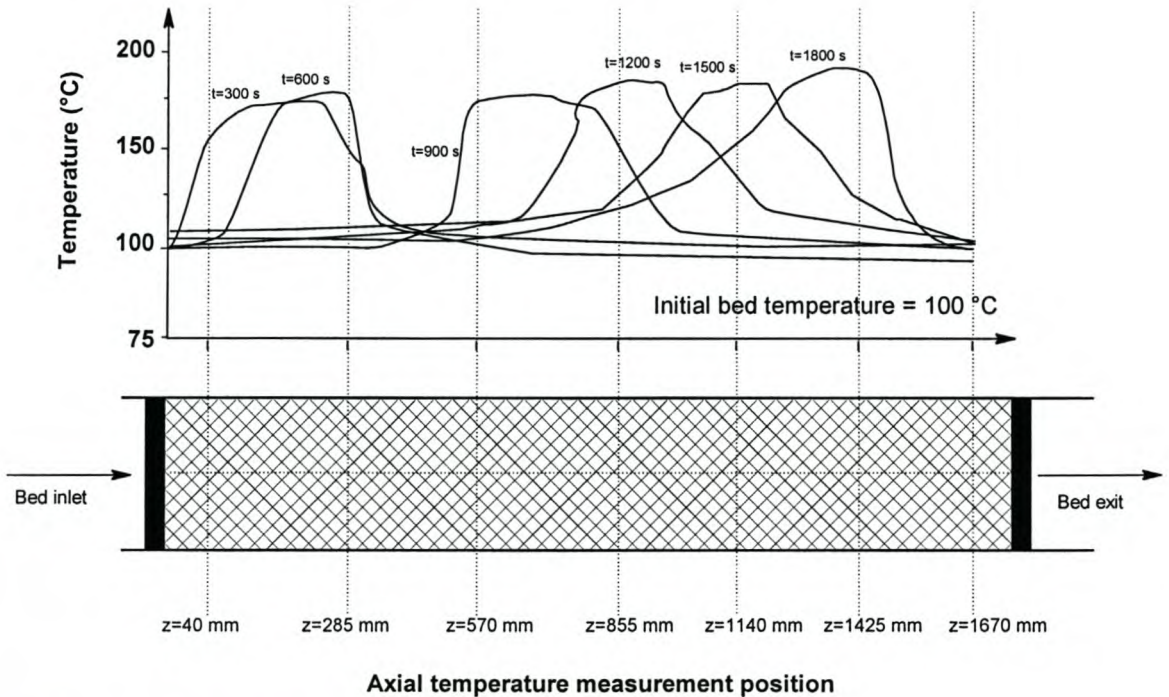


Figure 5.14. Typical temperature profile as a function of axial position.

The Group II experiments analysed the sensitivity of methanol adsorption to changes of various process parameters. All analytic information for methanol and water over the 18 batches and 86 samples are given in appendix H4. The table shows that water remained dominant in its adsorption and did not break through following any of the 18 adsorption cycles. Significant differences in the profiles of methanol adsorption are however evident.

Figure 5.15 shows the effect of varying the feed concentration on the normalised breakthrough curves.

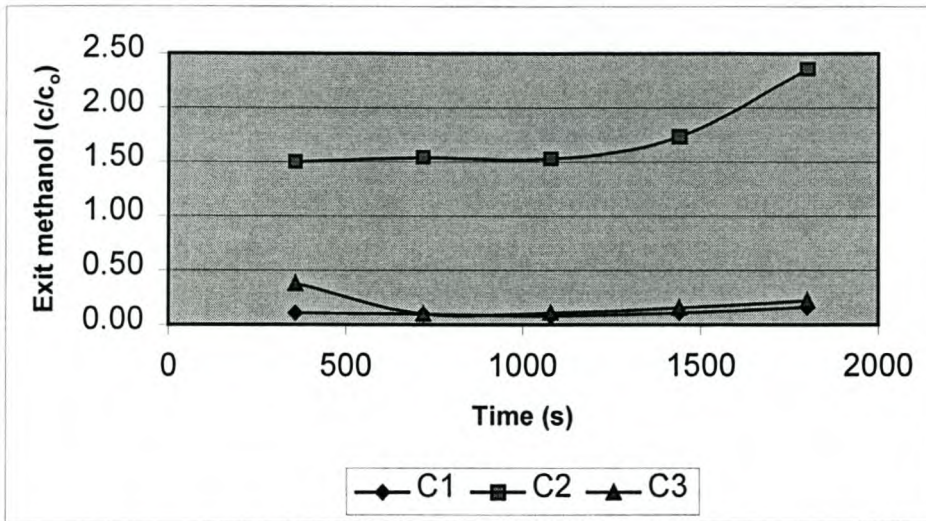


Figure 5.15. Effect of variation in feed concentration on the methanol breakthrough curve (C1 = 57.9 ; C2 = 13.6 ; C3 = 81 mg/100mLAA).

It is clear that even with the highest natural methanol concentration (Feed C3 ; methanol = 81 mg/100 mLAA), the adsorbers still delivered a product at an average methanol concentration of 9.8 mg/100 mLAA. Although water was not primarily evaluated as part of the Group II experiments, the significance of a high water presence in the adsorbate is demonstrated in the breakthrough curve for feed concentration C2. Although feed C2 contained a methanol concentration as low as 13.8 mg/100 mLAA, at a strength of 94.3 vol. % it contained as much as 58% more water than feed C3.

This leads to a normalised breakthrough curve at values > 1 , which indicates that the bed exit concentration was higher than the feed content. The bed loading for this experiment (discussed later) also indicates a negative loading. As anticipated, this confirms the ability of water, especially in concentrations larger than that of the azeotrope to displace the residual methanol loading. The displaced residual methanol is detected as part of the bed exit concentration. This experimental observation indicates that an abundance of water negatively affects the selective removal of methanol and that the water concentration in the feed streams should remain as close as possible to the azeotropic composition.

Figure 5.16 shows the effect of varying feed flow rate to the VSA plant. The maximum flow rate of 70 ℓ/hr was the maximum that the steam generator allowed for in its evaporating capacity.

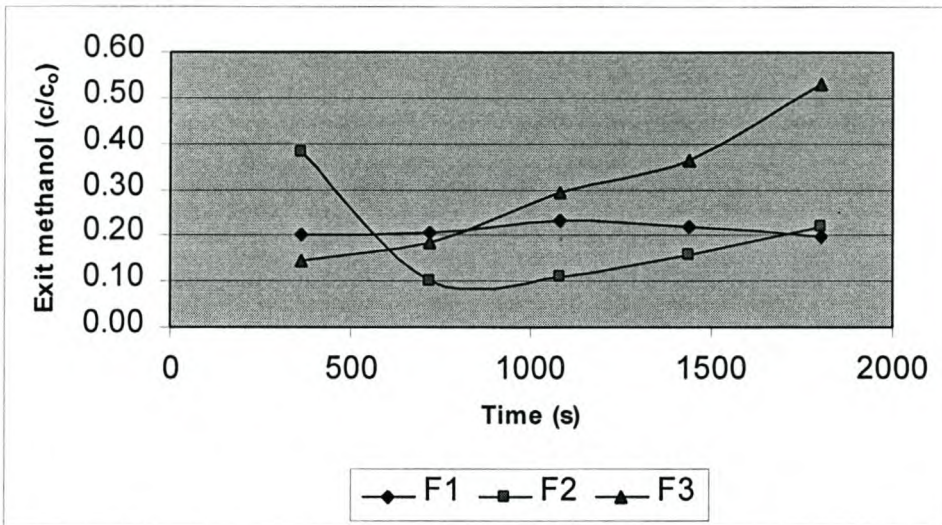


Figure 5.16. Effect of variation in feed flow rate on the methanol breakthrough curve (F1 = 20 ; F2 = 50 ; F3 = 70 ℓ/hr).

Figure 5.16 shows that increasing the feed flow rate decreases the time for methanol breakthrough. This happens because more adsorbate is exposed to the available adsorbent per unit time. The lowest flow rate curve (F1) shows a consistent bed loading over the 1800 s and it clearly shows that a low flow rate has flat breakthrough curve, taking the column capacity far beyond the assessed adsorption cycle time. The F3 curve shows a sharp increase in the gradient after 700 s. It can be deduced that with an adsorption cycle shorter than 700 s, the existing plant would comfortably be able to treat a feed flow rate of 70 ℓ/hr . This represents an additional capacity of 40 % when compared to the theoretical capacity of 50 ℓ/hr .

Regeneration pressure effects are indicated in the following figure. As expected, the highest pressure curve P1 (25 kPa (abs)) showed the biggest build-up of contaminant in the exit stream over time.

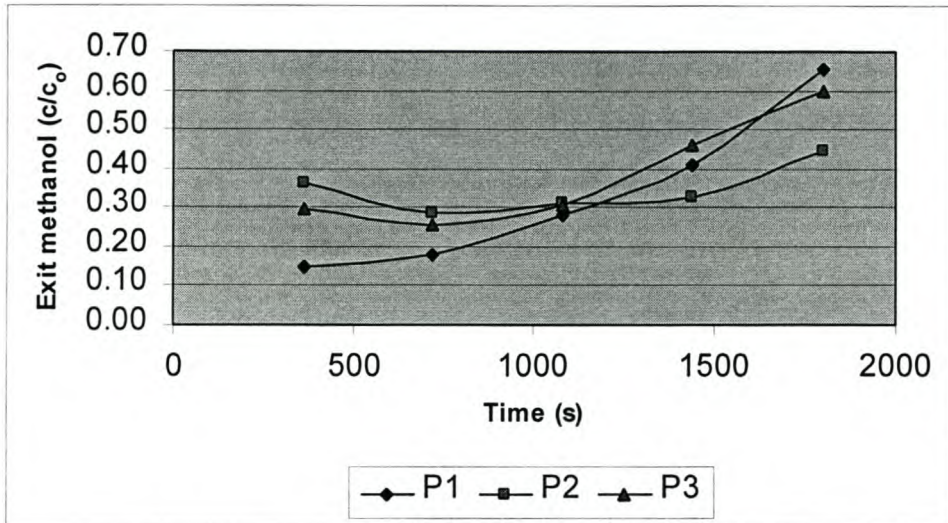


Figure 5.17. Effect of variation in regeneration pressure on the methanol breakthrough curve (P1 = 25 ; P2 = 16 ; P3 = 10 kPa (abs)).

Curve P2 (16 kPa) which is at the design regeneration pressure, showed that the adsorption cycle following the P2 regeneration was consistent to 1500 s. This certainly was the best profile in the group and confirms the design regeneration pressure of 17 kPa (abs). Curve P3 was only favourable to 1000 s, after which the breakthrough gradient increased. This shows that even at very good vacuum conditions (10 kPa), the adsorption cycle time needed to be limited to a maximum of 1000 s, should breakthrough be allowed to occur.

The effect of varying the nitrogen purge flow rate is depicted in Figure 5.18.

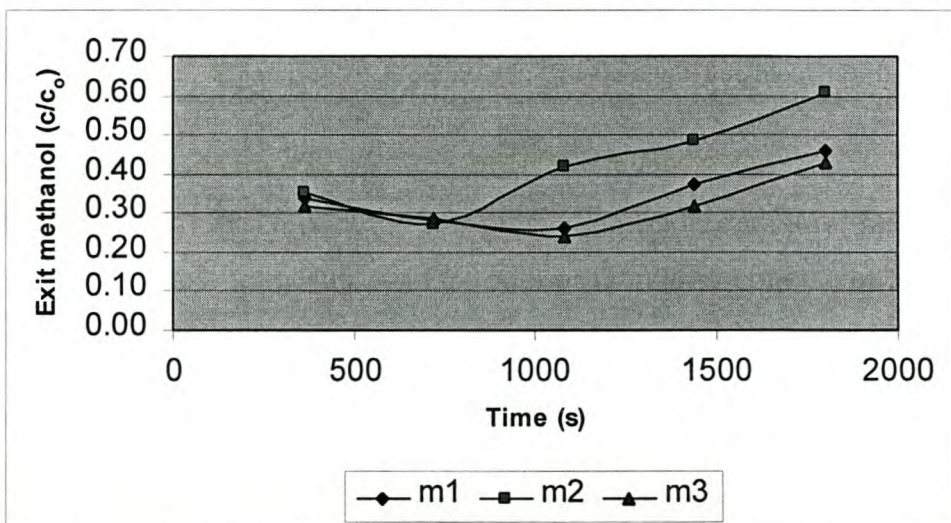


Figure 5.18. Effect of variation in purge flow rate on the methanol breakthrough curve (m1 = 7 ; m2 = 12 ; m3 = 18 kg/hr).

The higher the purge flow rate, the flatter the breakthrough profile and a subsequent longer breakthrough time is evident. As to be expected, the profiles were less sensitive to a variation in purge flow rate than regeneration pressure. The design minimum purge flow rate of 7.8 kg/hr is clearly adequate for regeneration purging. Differentiation between the 3 profiles only occurred after 500 s. This indicated that the effects of the variation in purge flow rate is dominant at the bed exit and not so much at the bed entrance. This, together with the fact that the breakthrough curves started at a c/c_0 ratio of 0.35, indicated that the allowance of breakthrough in an adsorber is unhealthy and promotes the gradual build-up of contaminants.

As discussed in chapter 2, contamination of the bed exit leads to poor adsorption efficiencies. It should be noted that this build-up did not occur in the Group I experiments, as breakthrough was not allowed and cycle times were kept to the design period of 5 minutes. A 24 hour thermal regeneration at 160 °C was performed and a further 24 hours were allowed for bed cooling.

Following the thermal regeneration, experiments 13, 14 and 15 were performed. The breakthrough profiles for methanol adsorption in the absence of water is shown in Figure 5.19.

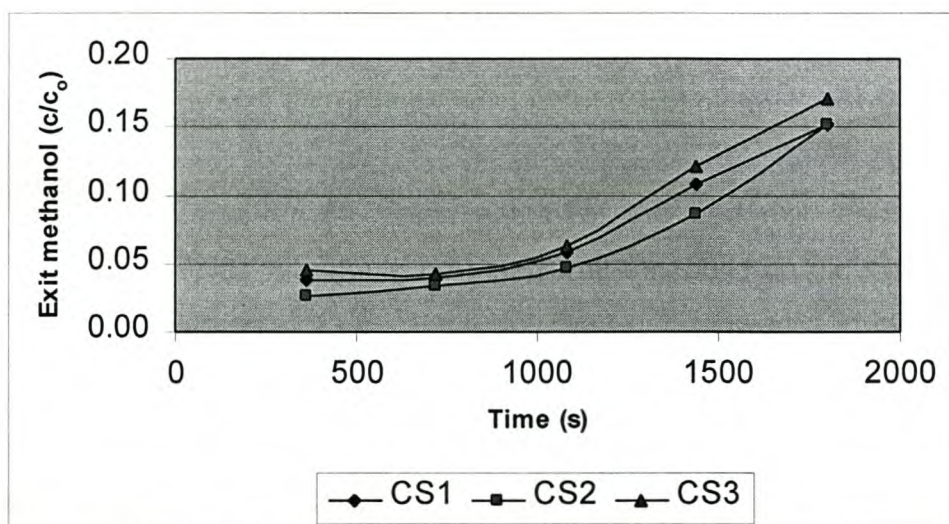


Figure 5.19. Effect of variation in synthetic methanol feed concentration on the methanol breakthrough curve (CS1 = 499.8 ; CS2 = 809.8 ; CS3 = 1117.6 mg/100mLAA).

The positive effect of the thermal regeneration is evident as the initial methanol c/c_0 ratio is 0.03. These three experiments confirm that methanol adsorption does not take place as a coincidence due to the presence of water. The combination of chemical and physical adsorption for the methanol molecule as well as complex formation, as discussed in chapter 2, continues to take place and do not require the presence of water. Adsorption is clearly favourable up to 1000 s and even after this, the breakthrough takes place very gradually indicating the adsorption ability for the separation of methanol from ethanol.

The adsorbers easily separated methanol with concentrations as high as 1118 mg/100 mLAA, confirming the competition between water and methanol for an adsorption site. The profiles in Figure 5.19 with extremely high methanol concentrations are considerably more favourable than that of Figure 5.15. Generally, as was also shown in Figure 5.15, an increase in contaminant feed concentration causes earlier breakthrough. These experiments (13,14 and 15) ultimately demonstrates the ability of the process to separate methanol from ethanol.

The effect of variation in initial bed temperature is shown in Figure 5.20.

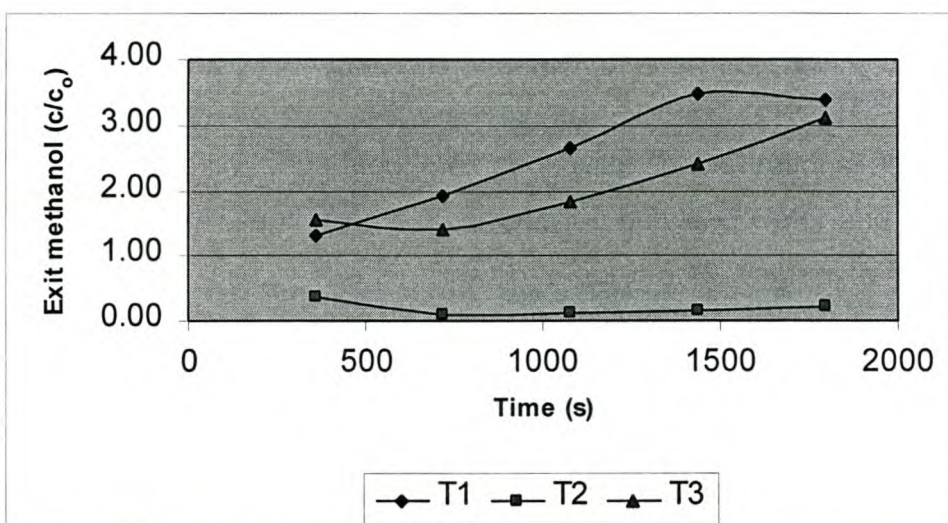


Figure 5.20. Effect of variation in initial bed temperature on the methanol breakthrough curve (T1 = 110 ; T2 = 90 ; T3 =125 °C).

The profiles show that curve T2 (90 °C) was most favourable methanol adsorption. T1 and T3 at 110 °C and 125 °C respectively showed similar curves to C2 in Figure 5.15. This was due to the reduction in adsorption ability at elevated temperatures and the release of residual loading methanol to the exit stream.

Table 5.5 is a summary of the sensitivity analysis for methanol adsorption in the presence and absence of water. The analysis also shows the effect of condition variation on methanol bed loadings. As the methanol profiles were not linear as in Group I experiments, the area under each profile (Figures 5.15 – 5.20) was integrated over the adsorption cycle time to determine the accumulated methanol at the exit. The mathematical function for each of the 18 curves first needed to be formed. The mathematical approach of the La Grange interpolation was used to create the functions before integrating. The general form of the expressions with 5 concentration points over time is given in appendix H6.

The methanol bed loadings are depicted in Figures 5.21 and 5.22.

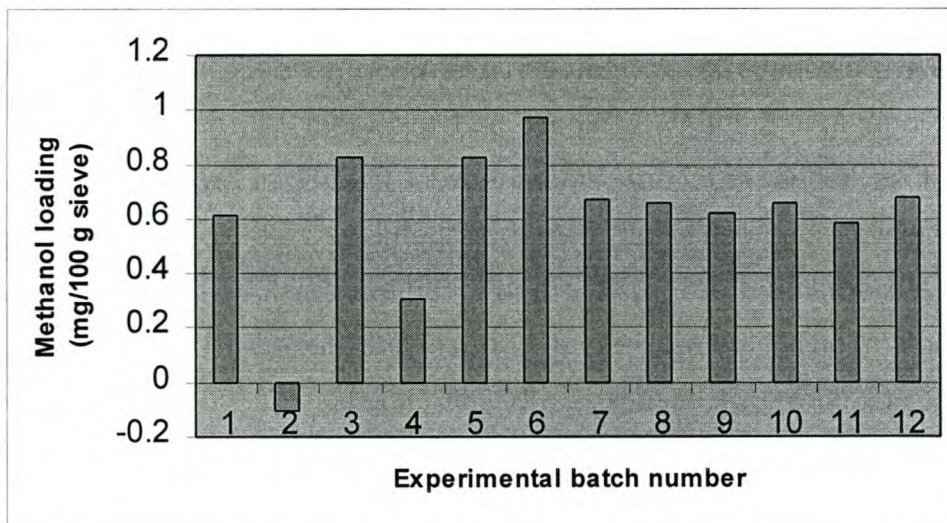


Figure 5.21. Methanol bed loadings for batches 1 – 12.

Table 5.5 Sensitivity analysis (Group II)

Batch #	Variable	Variable value	Variable unit	Initial bed temp (° C)	Feed flow rate l/hr	Feed methanol concentration (mg/100mLAA)	Feed ethanol concentration (vol . %)	Methanol in feed (g)	Area under methanol profile (mg/100mLAA).s	Accumulated methanol at exit (g)
FEED CONCENTRATION (NATURAL METHANOL)										
1	C1	57.9	(mg/100mLAA)	90	50		95.1	11.01	8796.9	1.16
2	C2	13.6	(mg/100mLAA)	90	50		94.3	2.57	32635.2	4.28
3	C3	81.0	(mg/100mLAA)	90	50		96.4	15.62	17882.3	2.40
FEED FLOW RATE										
4	F1	20	l/hr	90		81.0	96.4	6.25	24880.2	1.33
5	F2	50	l/hr	90		81.0	96.4	15.62	17882.3	2.40
6	F3	70	l/hr	90		81.0	96.4	21.87	33614.9	6.31
REGENERATION PRESSURE										
7	P1	25	kPa (abs)	90	50	81.0	96.4	15.62	36116.2	4.84
8	P2	16	kPa (abs)	90	50	81.0	96.4	15.62	37741	5.06
9	P3	10	kPa (abs)	90	50	81.0	96.4	15.62	42412.4	5.68
NITROGEN PURGE FLOW RATE										
10	m1	7	kg/hr	90	50	81.0	96.4	15.62	38313.5	5.13
11	m2	12	kg/hr	90	50	81.0	96.4	15.62	46845.4	6.28
12	m3	18	kg/hr	90	50	81.0	96.4	15.62	35404.9	4.74
FEED CONCENTRATION (SYNTHETIC METHANOL)										
13	CS1	499.8	(mg/100mLAA)	90	50		96.4	96.37	53666.9	7.19
14	CS2	809.8	(mg/100mLAA)	90	50		96.4	156.14	73012.1	9.78
15	CS3	1117.6	(mg/100mLAA)	90	50		96.4	215.49	134384.6	18.01
INITIAL BED TEMPERATURE										
16	T1	110	°C		50	81.0	96.4	15.62	307616.9	41.22
17	T2	90	°C		50	81.0	96.4	15.62	17882.3	2.40
18	T3	125	°C		50	81.0	96.4	15.62	228837.9	30.66

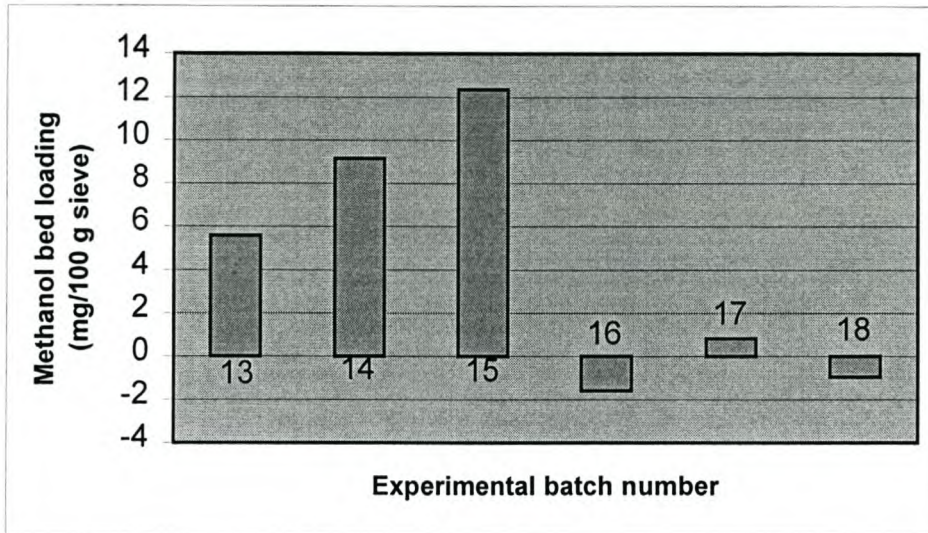


Figure 5.22. Methanol bed loadings for batches 13 – 18.

The effect of high water content in the feed is evident from batch 2. In general, the adsorber beds could comfortably treat an average methanol loading of ± 0.6 mg/100 g sieve in the presence of water and as much as 12.3 mg/100 g sieve in the absence of water. Negative bed loading values on batches 16 and 18 were due to excessive initial bed temperatures discussed earlier. The consistency in bed loadings confirms that the selected process conditions for adsorption and regeneration were adequate in treating neutral wine spirits.

5.4 ENERGY ANALYSIS

A reduction in operating costs is one of the various benefits discussed earlier in chapter 2. The purpose of the following table was not to draft a detailed analysis of economic feasibility, but to provide an overview of the energy consumption of conventional distillation and to compare that on a unit basis to the proposed process.

Table 5.6 compares the total steam consumption for conventional distillation to total installed electrical capacity of the VSA plant. The steam consumption figures in Table 5.6, are actual steam measurements taken on vortex-type steam flow meters which the author had installed for energy analyses

purposes. The vortex-type steam flow meters were installed on each of the columns depicted in appendix A1.

Table 5.6 Energy analysis and comparison

Process	Steam (kg/hr)	Unit steam (kg/LAA)	Energy (MW)	Unit energy (kW/LAA)	Contribution (%)
CONVENTIONAL					
Wine	2225	2.8	1.4	1.7	36
Hydroselection	510	0.6	0.3	0.4	8
Impurities	220	0.3	0.1	0.2	4
Spirits	2232	2.8	1.4	1.7	36
Final	1013	1.3	0.6	0.8	16
Total	6200	7.8	3.8	4.7	100
VSA (installed)			0.02	0.4	

The energy calculations for distillation are based on the actual plant capacity of 800 LAA/hr. The analysis shows that the distillation process energy requirement is 3.8 MW to produce azeotropic ethanol. The total energy requirement for the VSA plant is 20 kW. These 2 figures are however not comparable, and one should rather compare the unit energy consumption.

Depending on the strategy and point of, various degrees of savings can be achieved. Two options will be evaluated in the following chapter (refer to Table 5.6): option 1 – integration at final column ; option 2 – integration at spirits column. For option 1 integration, the unit energy comparison for the VSA = 0.4 kW/LAA vs distillation = 0.8 kW/LAA. Similar for option 2 integration, the VSA = 0.4 kW/LAA vs distillation = 2.5 kW/LAA. It should be noted that although the above mentioned energy savings are of value to the company, the financial benefits from this are negligible when compared to the benefit of improved separation due to the adsorption process. This important aspect will be discussed in detail in chapter 5.5.

A further benefit of the process is the production losses when compared to distillation. The conventional process reports a consistent alcohol distillation loss of 4 % on a single distillation and an over-all loss of as high as 15 % over the production season (see Figure 5.23 (a) later). Experimental runs for both Group I and Group II experiments were done under the supervision of the Department of Customs and Excise. Actual feed tank and product tank readings were taken in conjunction with an officer from the Department of Customs and Excise before and after experimental work. This is normal procedure for any form of alcohol production. Official readings from the Department confirmed negligible losses.

5.5 FINANCIAL ANALYSIS AND FEASIBILITY

Due to the nature of this project, a complete financial analysis would contain sensitive information not open for public scrutiny. Only selective information is hereby given and diagrams are over-simplified. Prior to evaluating the potential financial benefits from the suggested scheme, one needs to understand the production routing of the spirits manufacturing process. The standard routing for spirits production is shown in Figure 5.23 (a).

The distillation process indicated on the figure was earlier discussed in chapter 2(refer to appendix A1 for P&ID). The routing shows that 3 separate distillations are performed over a production period, with losses and production ratios as indicated. These values are strongly influenced by the physical condition and age of equipment. Figure 5.23 (b) shows the proposed production routings and how the VSA process is to be integrated with the conventional process. Two separate suggestions for integration are depicted in the figure:

- Option 1 – integrate before the Final Column
- Option 2 – integrate at the Spirits Column

Figure 5.23 (a). Standard spirits production routing

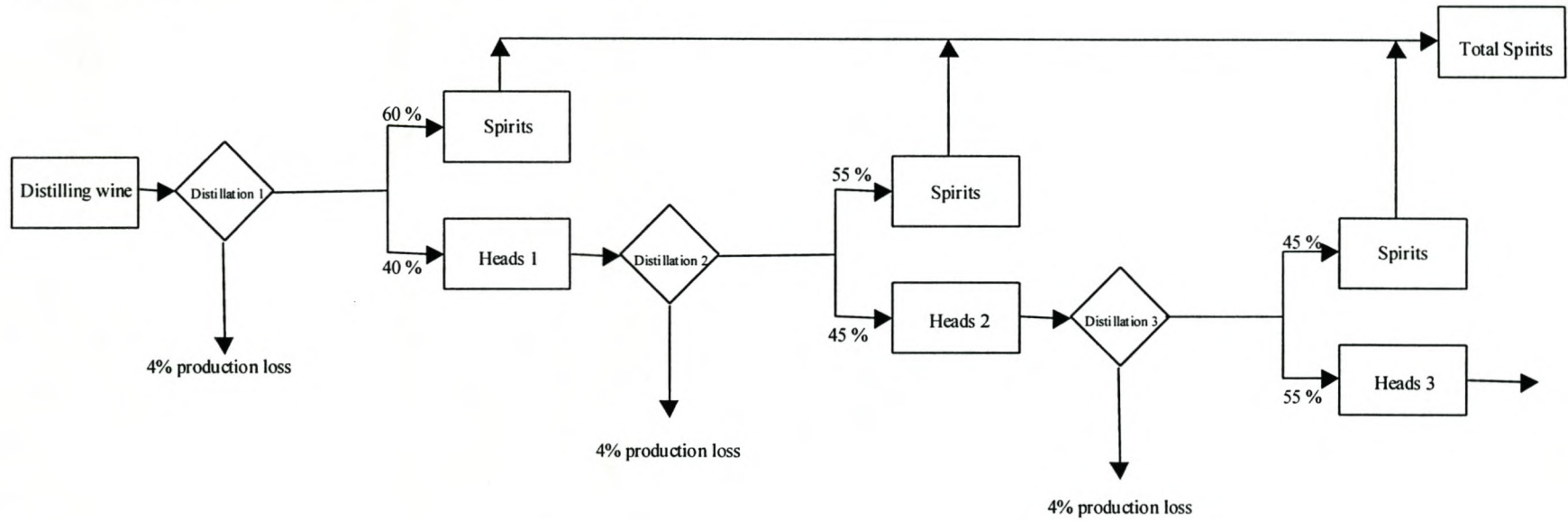
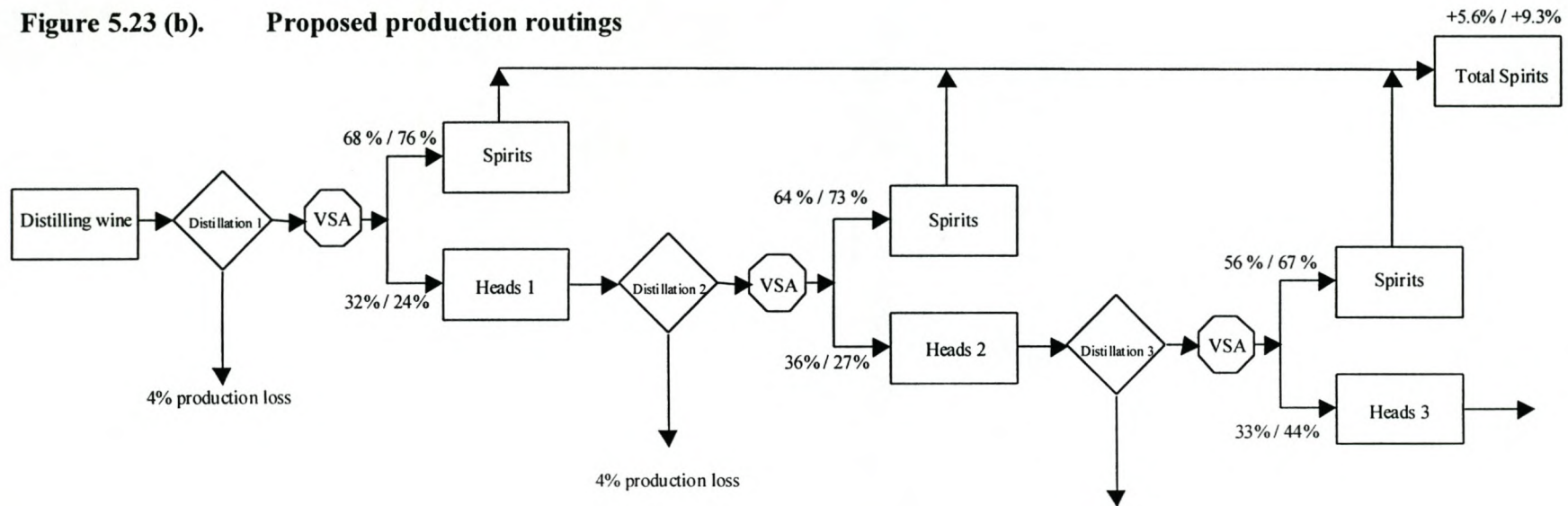


Figure 5.23 (b). Proposed production routings



The effect of integrated treatment between distillation and adsorption is shown and values are given in the format: option 1 / option 2. The significance of these options at a conservative wine intake of 1 500 000 LAA is evident from the following profitability analyses (all volumetric quantities expressed in LAA). The advantage of the proposed process is clearly in its ability to separate more efficiently the ethanol from the heads fractions and to a much lesser extent the energy saving.

5.5.1 Profitability due to additional product

Here the financial benefit is derived from the production of additional product that would otherwise be part of a distillation production loss. The production quantities (as calculated against the ratios in Figure 5.23) for such a scheme is shown in Table 5.7.

Table 5.7 Production quantities (additional product)

	STANDARD	OPTION 1	OPTION2
Distilling wine in	1 500 000	1 500 000	1 500 000
1st Distillation	1 440 000	1 440 000	1 440 000
Spirits	864 000	979 200	1 094 400
Heads 1	576 000	460 800	345 600
2nd Distillation	552 960	442 368	331 776
Spirits	304 128	283 116	242 196
Heads 2	248 832	159 252	89 580
3rd Distillation	238 879	152 882	85 997
Spirits	107 496	85 614	57 618
Heads 3	131 383	67 268	28 379
Spirits out	1 275 624	1 347 930	1 394 214
Overall loss	15.0%	10.1%	7.1%

The additional product represents 5.6% and 9.3% more against the standard for option 1 and 2 respectively. The profitability is derived at by making use of the existing selling price of neutral wine spirits (Table 5.8).

Table 5.8 Profitability analysis (additional product)

	Option 1	Option 2
Additional spirits - LAA	72 306	118 590
Additional turnover (R10.92/LAA)	R789 582	R1 295 003
Additional costs	R 42 602	R 69 871
- Variable	R 36 457	R 59 793
- Fixed (depreciation over 10 years)	R 6 145	R 10 078
Additional profit	R 746 980	R1 225 132
Investment	R 554 751	R 554 751
Return on investment	134.7%	220.8%

For options 1 and 2, the return on investment due to the additional product benefit are 134.7 % and 220.8 % respectively.

5.5.2 Profitability due to reduced wine purchasing

A different perspective of gaining financial benefit, would be to calculate the equivalent distilling wine that need not to be purchased in that period of production. The production routings for this scenario are shown in Table 5.9.

Table 5.9 Production quantities (reduced wine purchasing)

	STANDARD	OPTION 1	OPTION2
Distilling wine in	1 500 000	1 419 536	1 372 411
1st Distillation	1 440 000	1 362 755	1 317 515
Spirits	864 000	926 673	1 001 311
Heads 1	576 000	436 082	316 204
2nd Distillation	552 960	418 639	303 556
Spirits	304 128	267 929	221 596
Heads 2	248 832	150 710	81 960
3rd Distillation	238 879	144 682	78 682
Spirits	107 496	81 022	52 717
Heads 3	131 383	63 660	25 965
Spirits out	1 275 624	1 275 624	1 275 624
Overall loss	15.0%	10.1%	7.1%

The profitability analysis shows an ROI of 110.1 % and 174.7 % for options 1 and 2 respectively (Table 5.10) Normally an ROI of 18 % for a project is seen as being profitable.

Table 5.10 Profitability analysis (reduced wine purchasing)

	Option 1	Option 2
Reduced wine purchasing - LAA	80 464	127 589
Reduced purchasing cost (R7.00/LAA)	R563 248	R 893 123
Saving in cost	R 47 796	R 76 181
- Variable (saving because of reduced purchasing)	R 40 570	R 64 330
- Fixed (depreciation over 10 years)	R 7 226	R 11 851
Additional profit	R 611 044	R 969 304
Investment	R 554 751	R 554 751
Return on investment	110.1%	174.7%

The proposed VSA process, when integrated with conventional distillation, is a highly feasible option in the production of neutral wine spirits.

5.5.3 Issues of capital layout

Following the feasibility analyses, it is also of importance to assess the requirements of capital layout. It would not be possible at this stage to determine exactly the requirements of capital. The following two figures however give an indication of what the capital expenditure and distribution for a larger scale plant would be.

The information is the author's best prediction with the existing information at hand. Figure 5.24 shows the distribution of capital for equipment in larger dual bed VSA plants. The cost of columns and piping/fittings are more prominent than that of the other equipment.

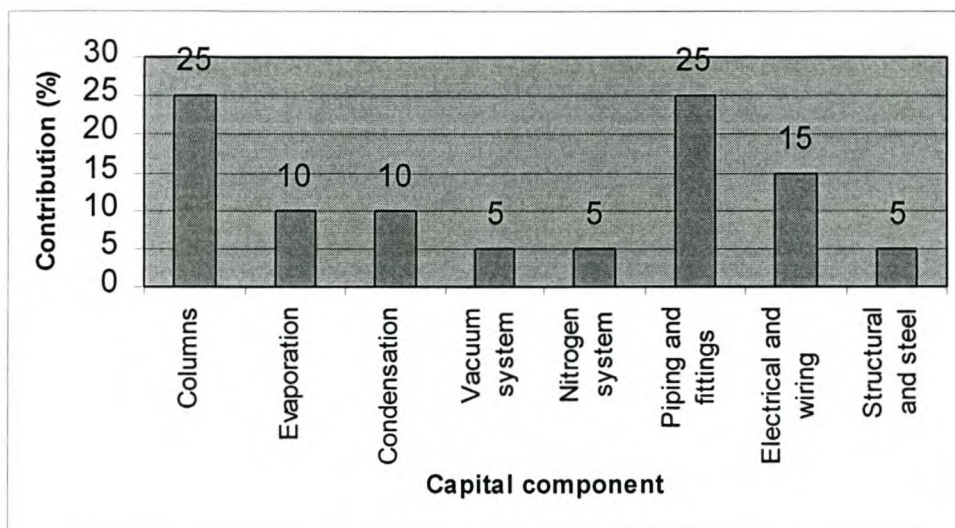


Figure 5.24. Distribution of capital costs for VSA plant on a larger scale.

The following figure is a projection of capital layout against installed production capacity.

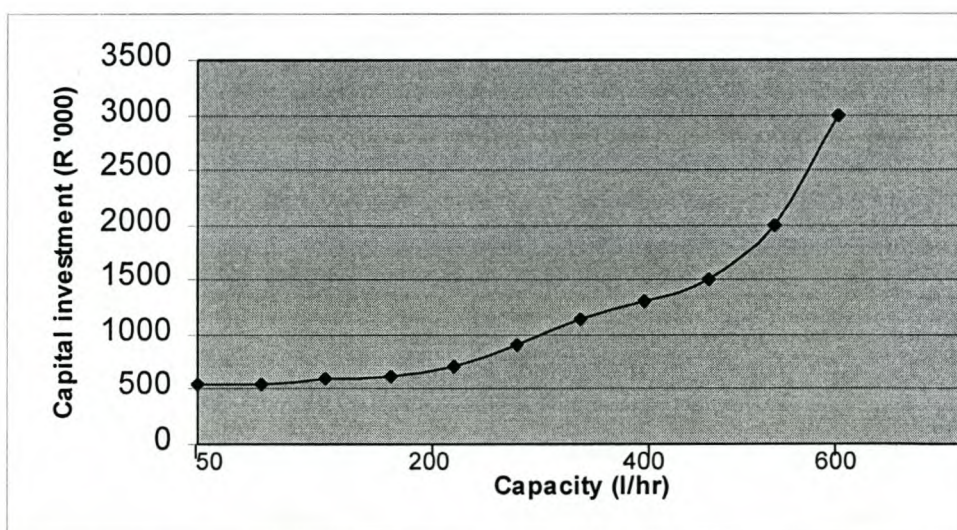


Figure 5.25. Projected capital / capacity layout.

As a rough guide, a full-scale plant ten times larger than the existing one is projected to cost between 4 – 5 times more.

CHAPTER SIX

FUTURE WORK AND PROPOSALS FOR INTEGRATION

The design objectives for the VSA plant was set out in chapter 4 prior to the actual design of the plant. From the results discussed in the previous chapter, these objectives were clearly met. This however does not imply that all possible combinations and permutations of the variables on the VSA plant have been adequately investigated. A schedule of future work with regards to the plant and its applications was drawn up. Some of these issues are discussed below.

6.1 ADDITIONAL RUNS

The trial runs that were performed during operational procedures investigated:

- water / methanol removal from the azeotrope;
- breakthrough conditions on MS564 CS;
- bed loading and capacities;
- temperature profiling;
- heat- and mass transfer zone retention;
- energy utilisation;
- radial effects by measurement;
- regeneration efficiency.

These investigations gave good insight into the dynamics of atmospheric adsorption and sub-atmospheric desorption of water and especially methanol onto the bed of molecular sieve 3A. The following additional runs should be performed.

- higher concentrations of water content (> 20 vol. %) needs to be investigated. The high water content adsorption has been confirmed by Garg^[G5] and will allow for earlier integration of the adsorption plant with the existing distillation facility.

Here the benefit is the removal of water to concentrate the feed stream. Earlier integration will lead to further reduction in the wine spirits operating costs.

- **intermediate distillate separations:-** these trial runs will be important to determine the ability of the existing configuration, conditions and adsorbent to separate fractions at different locations in the atmospheric distillation process. This would however depend on the other components present at these locations.

6.2 IMPROVEMENTS TO PLANT

As is apparent from the literature survey (chapter 2) and the principles that was followed, thorough and detailed reasoning and consideration have been given to the design of the VSA plant. Operating the plant and comparison to the paper design, however emphasized that certain adaptations could be beneficial in order to improve the process. The following modifications should be investigated:

- **nitrogen gas recycle for purging:-** N₂ gas was readily available and at low cost. It was therefore justified to run the gas as a once-through purging medium, without make provision for recycling. As the closed loop recycle option would unnecessarily complicate the plant, it was omitted and did not form part of the design objectives. It would however be sensible to recycle the gas and put it through a cooling and knock-out cycle to separate the contaminants from the purging gas. This would be advisable when scaling-up the plant.
- **option for regenerating with product:-** this principle is often used in PSA / VSA systems. Instead of using an external gas for purging and regeneration, a fraction of the raffinate product (normally $\pm 15\%$) could be drawn off and used as purging medium. The purified product is inert relative to the molecular sieve and effectively drives back the strong adsorptives to the inlet side of the bed. The benefit of saving in nitrogen cost should be carefully weighed up against the potential increase in alcohol losses and the risk of catalysis to acetaldehyde and diethyl ether. A further intermediate product vapour tank will also need to be installed.

The effluent product purge stream can either be recycled back to the adsorption column or alternatively be fed back into the distillation process.

- **contaminant condensation:-** desorbed contaminant vapour should be separated and condensed from the N₂ purge gas. The amount of contaminant removed and prediction of the residual contaminant after every cycle, can then be easily determined. This would also quantify the efficiency of consecutive bed purging steps. Bed contamination or coking would immediately be identified.
- **recovery of void ethanol:-** reducing alcohol losses was one of the plant design objectives. The biggest possible alcohol loss (still negligible in comparison with traditional distillation and confirmed by Customs and Excise) occurs after the pressure equalisation step. PE is followed by blowdown, which simply means that the untreated feed material trapped in the bed voids of the saturated bed is drawn off into the vacuum pump and dissolved in the seal water, or lost by entrainment with nitrogen as carrier gas.
- **the use of dried air:-** in order to cut down on nitrogen consumption, the warm-up procedure for preheating piping sections and the packed bed as set out in the process sequence chart could be performed by heating dry air. Possible contamination of the beds should be investigated first.
- **position of the moisture analyser:-** the position for the moisture analyser and the sample point for gas chromatography should preferably be shifted to the nitrogen exit side. This should allow direct assessment of the regeneration efficiency.

6.3 INTEGRATION WITH EXISTING PROCESSES

Adsorption will never completely replace distillation. The challenge is therefore to make use of the benefits which adsorption offers, but at the same time connecting them intimately into the distillation facility. Additional work is required to finalise the integration scheme. Various options are however given (refer to appendix A1 – P&ID of KWW distillation)

(a) final product refining:- it often happens that a final product is produced from the final column and adheres partially to the required specification. Normally non-conformance in the final column is almost certainly linked to a high methanol concentration. The infrastructure and plant layout is of such that further refining of that specific product can only be done by a complete redistillation as described in chapter 2. This however would be a significant waste, as the product has to go through the whole cycle of dilution, rectification, hydro selection and further rectification with the accompanying costs. The dual bed VSA would be useful in this application as the product from the final column could be fed directly into the adsorbers where methanol would be removed. A further saving could be achieved if the vapour stream was drawn directly from the final column. Not only is this an energy saving by not having to condense the product, but also to revaporise prior to adsorption (HX301 in plant).

(b) fault-product refining:- similar to the above product, a fault product which was formed due to some deviating specification parameter in the process needs to be re-distilled. This product would however already be at high alcohol concentration and can be fed to the adsorbers where a component like methanol could be easily separated.

(c) crude spirits refining:- crude spirit is the single rectified product from distilling wine as discussed in chapter 2. It is already at 96 vol.%, but remains high in methanol and other components. The VSA can in this case be integrated much more stream-up than in the previous two cases. This issue offers various benefits to the distillation process. Crude spirit distillation forms an essential part of the operations at KVV.

(d) intermediate products :- they can be drawn at the liquid draw-off between the spirits and final column. This product is typically concentrated with methanol. This methanol would be removed in the final column (also called the methanol column). The VSA system would replace the final column

(e) tray draw-off based on simulator:-tray-by-tray simulations has been performed and provide detail of liquid and vapour component compositions on the different plates in the distillation column. Based on the results in chapter 5,

one can determine exactly which plate along the spirits column can be used to supply feed to the adsorbers.

6.4 APPLICATION TO OTHER SEPARATION PROBLEMS

It is important that the final proposal to KVV should not be superficial in its applicability to core production processes. In order to bring forth a more value-added proposal, the application of the suggested separation principle and process configuration should be further investigated for use in other production areas with problematic separations. These could typically include the following:

- concentration of brandy flavours during potstill distillation;
- the selective removal of colour over wood character from brandy to produce colourless matured brandies study provides useful information;
- the selective removal of hydroxy methyl furfural and polyphenols from grape juice;
- the removal of SO₂ compounds from grape juice;
- the separation of grape-sugars in juice and semi-concentrate;
- the selective removal of water from grape juice;
- selective taint removal from any alcoholic beverage;
- dealcoholising wines ;
- the removal of unwanted components from effluent streams;
- the direct separation of ethanol from distilling wine at 10 vol.%.

The latter remains an important challenge and the work performed in this study provides the basis for such a separation concept.

CHAPTER SEVEN

CONCLUSIONS AND RECOMMENDATIONS

- 7.1** Methanol is naturally present in products from the vine and its separation by conventional distillation is costly. A split bed of molecular sieves 3A (MS 564CS) and 4A (MS 512) proved to be effective in separating methanol and water molecules from the bulk ethanol stream at considerable lower energy cost and higher purity. Adsorption curves (Group I) suggest that the proposed design, configuration and selected adsorption and regeneration conditions were adequate to consistently reduce the water and methanol content in the wine spirits to < 0.05 wt % and < 4 mg/100 mLAA respectively. Molecular sieve MS 512 (4A) caused organoleptic taints in the product. Since its use was of no commercial value, it was removed from the columns and not evaluated any further.
- 7.2** Methanol breakthrough curves derived from Group II experiments over 30 minute cycles, demonstrated that molecular sieve 3A (MS 564 CS) was capable of loading an average of ± 0.6 mg/100 g sieve in the presence of water. In the absence of water, a loading of 12.3 mg/100 g sieve was achieved as a maximum, with a feed concentration of 1118 mg/100mLAA. Methanol adsorption onto molecular sieve is not dependent on the presence of water to take place, but is influenced by it. Results suggest that at water concentrations higher than that of the azeotrope, the methanol bed loading becomes negative. This confirms that water can displace residual loading methanol on molecular sieve 3A, prior to exiting the bed.
- 7.3** Breakthrough information confirmed that water is preferentially adsorbed and that both methanol and water compete for adsorption

sites. This again shows good agreement with the results from single column adsorption experiments as discussed in chapter 3.

- 7.4** In general, the higher the feed concentration and feed flow rate, the quicker breakthrough occurs.
- 7.5** The VSA plant is capable of treating a maximum feed flow rate of 70 ℓ/hr, provided that adsorption cycle time remains less than 700 s. This represents a capacity 40 % higher than the theoretical.
- 7.6** The allowance of continuous breakthrough increases residual bed loading and affects breakthrough curves negatively.
- 7.7** The adsorption of methanol onto 3A molecular sieves appeared to be due to a combination of different mechanisms and characteristics. Due to molecule configuration and polarity (adsorption forces), methanol adsorption takes place in a balanced way between chemical and physical adsorption. Molecular sieving also plays a role due to the differences in molecule configuration and critical diameter when compared with the ethanol molecule (steric effect). The kinetic effect appears to be of less significance in this case, since the adsorption cycles were short, normally not allowing enough time for selectivity to be based upon differences in diffusion rates.
- 7.8** The typical life span of a molecular sieve bed is between 7 – 10 years. Due to the enhance formulation of MS 564 CS, problems with attrition, ageing, fouling and swelling are minimised. Attrition and abrasion of the bed is further avoided by the inclusion of the pressure equalisation and repressurisation steps, preventing pressure shocks to the beds. The beds are also heated at a rate $< 3 \text{ }^{\circ}\text{C /min}$ to prevent thermal shocks.
- 7.9** Adsorption temperature curves for Group I indicate that the peak bed temperature falls back to the initial bed temperature prior to exiting from

the bed. This suggests that the heat associated with the temperature peaks that was stored in the bed, is used to provide some of the energy for desorption. This was not the case for Group II, since breakthrough was allowed to occur. The loss of stored energy and an increase in contaminant residual loading are good examples of reasons why breakthrough should not be allowed to occur.

- 7.10** Nitrogen appears to be completely inert to the molecular sieve and serves as an effective purging medium. Adsorption curves over 120 cycles (Group I) showed little effect of deterioration, which suggest that regeneration by using the vacuum swing principle together with a nitrogen purging medium was adequate in removing the strongly adsorbed molecules. It can therefore be concluded that the residual bed loading between cycles remained constant.
- 7.11** The addition of cocurrent depressurisation and equalisation to the typical Skarstrom cycle not only increased the concentration of the purified product, but also minimised pressure and attrition shocks to the molecular sieve beds. The cocurrent depressurisation step also ensured that the mass transfer front was retained in the active bed.
- 7.12** Vacuum swing adsorption is superior to pressure swing adsorption. Although PSA was not investigated in this application, literature suggests a much higher critical pressure ratio than that used in this case. Even with the same pressure ratio and bed penetration, the VSA is able to process a higher feed rate than PSA.
- 7.13** The process cycle sequences that define the process control of the VSA plant, were successful in achieving the initial process control objectives that were set out. Process control is at the heart of the plant and close valve timing ensures continuous production.
- 7.14** Amongst other things, this study suggests that adsorption is superior to distillation in removing methanol from wine spirits. This is supported by

the energy analysis of the VSA plant and its comparison to the energy contribution due to methanol separation during conventional distillation. Energy depends on the strategy of integration with the conventional process.

- 7.15** Benefits derived from adsorption's separation ability when compared to distillation far exceeds that from energy savings. When integrated at the final column and at a conservative feed flow rate of 1 500 000 ℓ AA, the VSA delivered 5.6 % more product against the standard. At current selling price, this integration option delivers an ROI of 134.7 % for the project. Integration at the spirits column delivered an addition of 9.3 % more product, with a calculated ROI of 220.8 %. If profitability is assessed from the point of view of reduced wine purchasing, final column integration delivers an ROI of 110.1 %, while on spirits column integration the ROI is calculated at 174.7 %.
- 7.16** The successful operation and production of the plant indicate that the practical design objectives as set out in chapter 4 have been met. Adsorption has various advantages over distillation. These features were also evident in the demonstration plant during production and include flexibility, reliability, ease of operation, short start-up cycles, higher purity and portability.
- 7.17** Adsorption is a proven technology and has been in use for decades. However, the application of methanol / ethanol separation, the specific configuration, the combination of process conditions, the selection of molecular sieve and the process control sequences are unique.
- 7.18** Following this study, it was concluded that the high level of innovation and chemical engineering technology that were applied during the complete development chain of the VSA plant, emphasized the importance of chemical engineering in the wine industry.

As is the norm in innovative environments, this achievement should also lead to other innovative and technological breakthroughs at KVV. The wine industry in general is focussed on product improvements, while fundamental process improvements in order to produce products of higher purity and at lower cost does not take place as would be expected. Process improvements remain part of normal operational changes, based on the experience of renowned masters, rather than sound engineering principles.

- 7.19** The low cost removal of methanol from wine spirits by means of an innovative process unknown to the wine industry and other than distillation, will give KVV a benefit in the marketing of its spirituous products. Lower production costs should also enable KVV to offer a more competitive cost structure to potentially new customers, as well as winning back previous customers. This is true not only for potential wine spirits and blended brandy customers, but also customers to whom KVV offers a distillation service at a fixed production cost and profit margin.
- 7.20** The existing plant configuration can easily be extended to other applications and product categories e.g. grape juice concentration. These types of applications could add even more value to the importance of this contribution.

RECOMMENDATIONS

The following recommendations will be made to management:

- a) Patent protection needs to be extended. The completion of this study was required to determine with more certainty the boundaries of the process, prior to furthering patent protection.
- b) Marketing benefits should be quantified.
- c) Scale up of the plant to an agreed production level should be investigated.

REFERENCES

1. Amerine, M. A. and Berg, M. S., ***"The Technology of Wine Making"***, 3rd ed., AVI Publishing Company, Connecticut (1972).
2. Amerine, M. A. and Joslyn, M. A., ***"Table Wines: Technology of their Production"***, 2nd ed., UCLA Press, California (1970).
3. Brodie, A. ***"Explosion Protection of Electrical Apparatus in Hazardous Areas"***, Electricity and Control, 33 – 38 (March 2001).
4. Buck, D, M, ***"Vacuum Swing Adsorption – An Alternate Nitrogen Supply System "***, Air Products and Chemicals, Inc, Allentown, 429 – 437.
5. Budner, Z. and Dula, W., ***"Study and Modelling of the Vacuum Swing Adsorption Process Employed in the Production of Oxygen"***, Institution of Chemical Engineers Trans IChemE, Vol. 77, Part A, 405 - 412 (July 1999).
6. Carton, A. and Gonzalez, G., ***"Separation of Ethanol-Water Mixtures Using 3A Molecular Sieve"***, J. Chem. Tech. Biotechnol., Society of Chemical Industry (1987).
7. Chemstations Inc., ***"ChemCad II User Guide"***, Texas (1988).
8. Chi, C. W. and Wasan, D. T., ***"Fixed Bed Adsorption Drying"***, AIChE Journal, Vol. 16, No. 1, 23 - 31 (January 1970).
9. Christian, G. D. and O'Reilly, J. E., ***"Instrumental Analysis"***, 2nd ed., Allyn and Bacon, Inc., Boston (1986).
10. Cooney D., ***"Numerical Investigation of Adiabatic Fixed-Bed Adsorption"***, Ind. Eng. Chem., Process Des. Develop., Vol. 13, No. 4, 368 - 373 (June 1974).
11. Coulson, J. M. and Richardson, J. F., ***"Chemical Engineering – Particle Technology and Separation Processes"***, Vol 2, 4th ed., Pergamon Press, Oxford (1991).
12. Crab, C., ***"No zz's for Zeolites"***, Chemical Engineering, 59 - 61 (May 2001).
13. Crittenden, B. and Thomas, W. J., ***"Adsorption Technology and Design"***, Butterworth-Heinemann, Oxford (1998).

14. Crittenden, B. and Sowerby, B., **"Scale-up of Vapour Phase Adsorption Columns for Breaking the Ethanol-Water Azeotrope"**, IChemE Symposium Series, No. 118, 55 - 69 (April 1990).
15. Engelbeen, F., **"Toxicity of Methanol"**, www.csf.colorado.edu/envtecsoc/2000/msg00541.html (November 2000).
16. Fosbrook, M. and Faraday, D. B., **"Potable Spirits Distillation Employing Clean Technology"**, The 1997 Jubilee Research Event, IChemE, 1125 - 1128 (April 1997).
17. Garg, D. R. and Ausikaitis, J. P., **"Molecular Sieve Dehydration Cycle for High Water Content Streams"**, CEP, 60 - 65 (April 1983).
18. Goliath, E. M., **"The Optimisation of an Ethanol Distillation Plant"**, M-Thesis, University of Stellenbosch (December 1996).
19. Goliath E. M., **"Methanol Adsorption onto Molecular Sieves"**, University of Stellenbosch, unpublished material (August 1996).
20. Grace W. R. & Co., **"Davison Molecular Sieves"**, Davison Chemical Division, Worms – Germany.
21. Grace W. R. & Co., **"Ethanol Drying Using Davison Molecular Sieves"**, Davison Chemical Division, Worms – Germany.
22. Grace W. R. & Co., **"Molecular Sieves for Dynamic Applications"**, Davison Chemical Division, 3-1-0.6 WW MS DA 1E, Worms – Germany (April 1995).
23. Heftmann, E., **"Chromatography"**, Reinhold Publishing Corporation, New York (1963).
24. Holland, C. D. and Liapis, A. I., **"Computer Methods for Solving Dynamic Separation Problems"**, McGraw-Hill Book Company, New York (1983).
25. Incropera, F. P. and De Witt, D. P., **"Introduction to Heat Transfer"**, John Wiley and Sons, New York (1990).
26. Jeřábek, K. and Prokop, Z., **"Polymer Adsorbents for Methanol Separation from a Hydrocarbon Stream"**, Reactive Polymers, Elsevier Science Publishers B. V., Vol. 18, 221 – 227, Amsterdam (Sept. 1992).
27. Kern, D. Q., **"Process Heat Transfer"**, McGraw-Hill Book Company, Auckland (1965).

28. Kirk-Othmer Encyclopedia, **"Encyclopedia of Separation Technology"**, Vol 1, John Wiley & Sons, New York.
29. Knaebel, K. S., **"The Basics of Adsorber Design"**, Chemical Engineering, 92 - 101 (April 1999).
30. Kumar R. and Golden, T. C., **"Novel Adsorption Distillation Hybrid Scheme for Propane/Propylene Separation"**, Separation Science and Technology, Vol. 27, No. 25, 2157 - 2170 (1992).
31. Kumar R., **"Vacuum Swing Adsorption Process for Oxygen Production – A Historical Perspective"**, Separation Science and Technology, Vol. 31, No. 7, 877 - 893 (1996).
32. Kurihara K. and Nakamichi M., **"Isobaric Vapour-Liquid Equilibria for Methanol + Ethanol + Water and the Three Constituent Binary Systems"**, J. Chem. Eng. Data, Vol. 38, No. 3, 446 - 449 (April 1993).
33. Kvamsdal, H. M. and Hertzberg, T., **"Pressure Swing Adsorption – Optimisation of a Trace Separation System"**, European Symposium on Computer Aided Process Engineering, S339 – S344.
34. LaCava, A. I. and Ramachandran, R., **"How to Specify Pressure Swing Adsorption Units"**, Chemical Engineering, 110 - 118 (June 1998).
35. Lea, A. G. and Piggot, J. R., **"Fermented Beverage Production"**, Blackie Academic & Professional, London (1995).
36. Leavitt K. W., **"Non-Isothermal Adsorption in Large Fixed Beds"**, Chemical Engineering Progress, Vol. 58, No. 8, 54 - 59 (August 1962).
37. Loudon, G. M., **"Organic Chemistry"**, The Benjamin/Cummings Publishing Company, California (1988).
38. Lyons, T. P. and Jacques, K., **"The Alcohol Textbook"**, 3rd ed., Nottingham University Press, Nottingham (1999).
39. **"Methanol and its Properties"**, www.holisticmed.com (1998).
40. Mersmann, A. B. and Scholl, S. E., **"Fundamentals of Adsorption"**, 3rd International Conference, United Engineering Trustees Inc., Germany (1991).
41. Mettler-Toledo GmbH, **"Karl Fischer – Basic Knowledge at a Glance"**, www.mt.com, Switzerland (June, 1998).
42. Meyer O. A., **"Non-Isothermal Adsorption in Fixed Beds"**, AIChE Journal, Vol. 13, No. 3, 457 - 465 (May 1967).

43. Notaro, F. and Ackley, M. W., **"Recover Industrial Gases via Adsorption"**, Chemical Engineering, 104 - 108 (April 1999).
44. Ondrey, G, **"Making Much More Methanol"**, Chemical Engineering, 29 - 37 (May 2001).
45. Ondrey, G and Armesto, C., **"A Renewed Boost for Ethanol"**, Chemical Engineering, 35 - 39 (February 1999).
46. Pal, T. K. and Majumder, A., **"Evaluation of Standard Thermodynamic Parameters for the sorption of n-Hexane and Methanol in Zeolites"**, Chem. Eng. Technol., Vol. 13, 298 - 303 (1990).
47. Pan, C. Y. and Basmadjian, D., **"Constant-Pattern Adiabatic Fixed-Bed Adsorption"**, Chemical Engineering Science, Vol. 22, 285 - 297 (1967).
48. Pan, C. Y. and Basmadjian, D., **"An Analysis of Adiabatic Sorption of Single Solutes in Fixed Beds: Pure Thermal Wave Formation and its Practical Implications"**, Chemical Engineering Science, Vol. 25, 1653 - 1664 (1970).
49. Pascal Biotech, **"Technologies for the Treatment of Grape Musts and Wines"**, Paris (1992).
50. Perry, R. H. and Green, D. W., **"Perry's Chemical Engineer's Handbook"**, 6th ed., McGraw-Hill Book Company, New York (1984).
51. Piggot J. R. and Paterson, A., **"Distilled Beverage Flavour"**, Ellis Horwood, Chichester (1989).
52. Rep, M. and Palomares, A. E., **"Interaction of Methanol with Alkali Metal Exchanged Molecular Sieves – IR Spectroscopic Study"**, J. Phys. Chem. B, Vol. 104, No. 35, 8624 - 8630 (May 2000).
53. Ritter, J. A. and Liu, Y., **"New Vacuum Swing Adsorption Cycles for Air Purification with the Feasibility of Complete Cleanup"**, Ind. Eng. Chem. Res, Vol. 37, No. 5, 1970 - 1976 (1998).
54. Ruthven, D. M., **"Principles of Adsorption and Adsorption Processes"**, John Wiley and Sons, New York (1984).
55. Ruthven, D. M. and Shamsuzzaman, F., **"Pressure Swing Adsorption"**, VCH Publishers Inc., New York (1994).

56. SABS 0108, ***"The Classification of Hazardous Locations and the Selection of Apparatus for Use in Such Locations"*** (1995).
57. Schreiner, H., ***"The Mannheim Adsorption Project"***, IChemE Symposium Series, No. 118, 25 - 34.
58. Schwuger, M. J. and von Rybinski, W., ***"Adsorption of Cationic Surfactants on Zeolite A"***, Symposium on Adsorption from Solution, 185 – 195, Academic Press, London (1983)
59. Seader, J. D., ***"Separation Process Principles"***, John Wiley and Sons, New York.
60. Shah, R. ***"Acid-Base Catalysis in Zeolites from First Principles"***, www.tcm.phy.cam.ac.uk
61. Shah, R. and Gale, J., ***"Methanol Adsorption in Zeolites – A First-Principle Study"***, J. Phys. Chem., Vol. 100, No. 28, 11688 – 11697 (April 1996).
62. Shah, R. and Payne, M. C., ***"Understanding the Catalytic Behaviour of Zeolites: A First-Principles Study of the Adsorption of Methanol"***, Science, Vol. 271, 1395 - 1397 (March 1996).
63. Sowerby, B. and Crittenden, B. D., ***"An Experimental Comparison of Type A Molecular Sieves for Drying the Ethanol-Water Azeotrope"***, Gas Separation and Purification, Vol. 2, 77 - 83 (June 1988).
64. Sowerby, B. and Crittenden, B. D., ***"A Vapour Phase Adsorption and Desorption Model for Drying the Ethanol-Water Azeotrope in Small Columns"***, Institution of Chemical Engineers Trans IChemE, Vol. 69, Part A, 3 - 11 (January 1991).
65. Sundaram, N., ***"A Non-Iterative Solution for Periodic Steady States in Gas Purification Pressure Swing Adsorption"***, Ind. Eng. Chem. Res., Vol. 32, No. 8, 1686 - 1691 (1993).
66. Sundaram, N., ***"Training Neural Networks for Pressure Swing Adsorption Processes"***, Ind. Eng. Chem. Res., Vol. 38, No. 11, 4449 - 4457 (1999).
67. Suzuki, M., ***"Adsorption Engineering"***, Elsevier, Amsterdam (1990).
68. Swain, R. L., ***"Molecular Sieves – A New Option for Ethanol Dehydration"***, Alcohol Outlook, (December 1987).

69. Swain, R. L., **"Ethanol Dehydration Technology: State of the Art"**, National Alcohol Fuels Meeting and Exhibition (1988).
70. Swain, R. L., **"Molecular Sieve Dehydrators – How They Became the Industry Standard and How They Work"**, Delta-T Corporation, Virginia (1990).
71. Teo, W. K. and Ruthven, D. M., **"Adsorption of Water from Aqueous Ethanol Using 3A Molecular Sieves"**, Ind. Eng. Chem. Process. Des. Dev., Vol. 25, No. 1, 17 - 21 (1999).
72. Tsunoda, R., **"Adsorption of Water Vapour on Active Carbon Preadsorbed with Methanol and Benzene"**, Journal of Colloid and Interface Science, Vol. 188, 224 - 228 (1997).
73. **"Ullman's Encyclopedia of Industrial Chemistry"**, Vol A28.
74. Wankat, P. C., **"Equilibrium Staged Separations"**, Elsevier, New York, (1988).
75. Weast, R. C., **"CRC Handbook of Chemistry and Physics"**, CRC Press, Florida, (1984).
76. White, D. and Barkley, P., **"The Design of Pressure Swing Adsorption Systems"**, Chemical Engineering Progress (January 1989).
77. Wineland, **"SA Wine Industry Directory 2001"**, Ampersand Press, South Africa (2000).
78. Yang, R. T., **"Gas Separation by Adsorption Processes"**, Butterworths, Boston, (1987).

APPENDICES

CONTENTS

APPENDIX A	Process and Instrumentation Diagrams
APPENDIX B	Adsorbent Properties and Applications
APPENDIX C	W.R. Grace Molecular Sieve Characteristics
APPENDIX D	Adsorber Design
APPENDIX E	Engineering Specification
APPENDIX F	Plant Design Information
APPENDIX G	Commissioning Schedule
APPENDIX H	Experimental Results
APPENDIX I	VLE Data for Methanol/Ethanol Systems

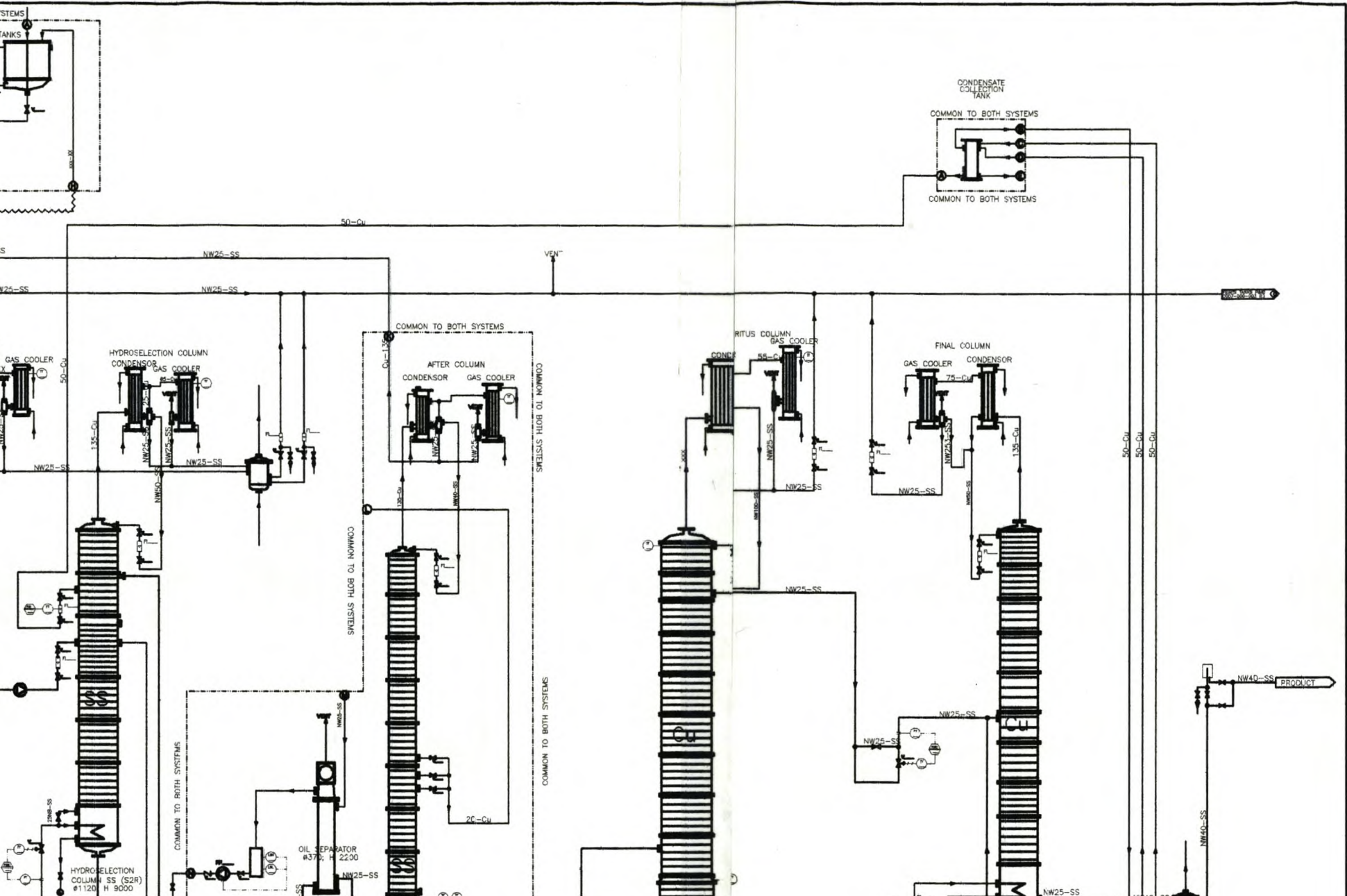
APPENDIX A

PROCESS AND INSTRUMENTATION DIAGRAMS

A1. Conventional Distillation P&ID

A2. Vacuum Swing Adsorption Demonstration Plant P&ID

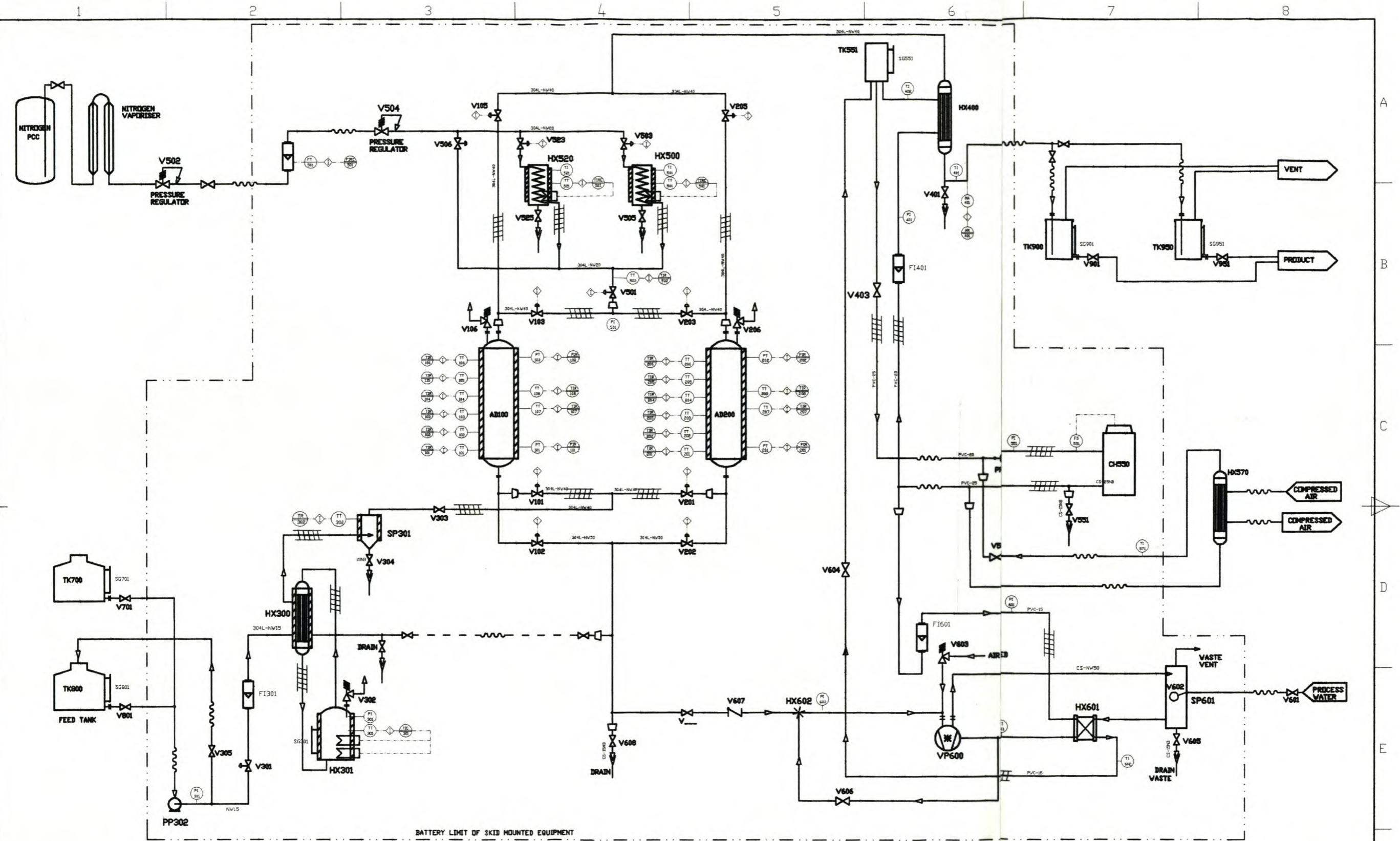
Appendix A1. KWV Distillation P&ID



Appendix A1. KWV Distillation P&ID

Appendix A2. VSA Demonstration Plant P&ID

Appendix A2. VSA Demonstration Plant P&ID



◇ DENOTES CONNECTION TO SCADA

DATE	REV	DESCRIPTION	Itemref	Quantity	Title/Name, design, material, dimension etc	Article No./Reference
31/8/00	1	ADDED VACUUM SEPARATION TANK				
31/8/00	1	ADDED T1803				
31/10/00	2	CHANGED DESIGN				
01/11/00	3	HX500 CW CHANGED TO STEAM				
01/11/00	3	CHANGED INSTRUMENTATION				
16/11/00	4	CHANGED INSTRUMENTATION				
25/03/01	5	CHANGED FLOW DIRECTION, ADDED N2, CHILLER				
30/03/01	6	CHANGED DRAWING				
04/04/01	7	REMOVED PRODUCT REGION				
30/05/01	8	- HX850, + HX820, +HX570, +V504, +TT301, +V506, PIPING (H-X400, TK900)				
20/07/01	9	PIPING AT PP551, FS 651				

DESIGNED_BY E M GOLIATH	CHECKED_BY	APPED_BY_DATE	FILENAME	DATE SEPTEMBER 2001	SCALE N.T.S.
PAARL			TITLE ADSORPTION DEMONSTRATION PLANT		
DRAWING_NUMBER FIGURE A2			EDITION SHEET		

APPENDIX B

ADSORBENT PROPERTIES AND APPLICATIONS

Appendix B1. Typical Adsorbent Applications

Appendix B2. Adsorbent Properties

Appendix B1. Typical Adsorbent Applications

B1.

Type	Typical application
Silica gel	Drying of gases, refrigerants, organic solvents, transformer oils; desiccant in packings and double glazing; dew Point control of natural gas.
Activated alumina	Drying of gases, organic solvents, transformer oils, removal of HCl from hydrogen;
Carbons	removal of fluorine and boron-fluorine compounds in alkylation processes. Nitrogen from air; hydrogen from syn-gas and hydrogenation processes; ethene from methane and hydrogen; vinyl chloride monomer (VCM) from air; removal of odours from gases; recovery of solvent vapours; removal of SO ₂ and NO _x ; purification of helium; clean-up nuclear off-gases; decolourising of syrups, sugars and molasses; water purification, including removal of phenol, halogenated compounds, pesticides, caprolactam, chlorine.
Zeolites	Oxygen from air; drying of gases; removing water from azeotropes; sweetening sour gases and liquids; purification of hydrogen; separation of ammonia and hydrogen., recovery of carbon dioxide; separation of oxygen and argon., removal of acetylene, propane and butane from air, separation of xylenes and ethyl benzene, separation of normal from branched paraffins; separation of olefins and aromatics from paraffins; recovery of carbon monoxide from methane and hydrogen, purification of nuclear off-gases; separation of cresols; drying of refrigerants and organic liquids; separation of solvent systems; purification of silanes; pollution control, including removal of Hg, NO _x and SO ₂ from gases; recovery of fructose from corn syrup.
Polymers and resins	Water purification, including removal of phenol, chlorophenols, ketones, alcohols, aromatics, aniline, indene, polynuclear aromatics, nitro- and chlor-aromatics, PCB, pesticides, antibiotics, detergent emulsifiers, wetting agents, kraftmill effluents, dyestuffs; recovery and purification of steroids, amino acids and polypeptides, separation of fatty acids from water and toluene; separation of aromatics from aliphatics; separation of hydroquinone from monomers; recovery of proteins and enzymes; removal of colours from syrups; removal of organics from hydrogen peroxide.
Clays (acid treated and pillared)	Treatment of edible oils; removal of organic pigments; refining of mineral oils; removal of polychlorobiphenyl (PCB).

Appendix B2. Adsorbent Properties

Material and uses	Shape* of particles	Size range, U.S. standard mesh†	Internal porosity χ , %	Bulk dry density, kg/L	Average pore diameter, μm	Surface area, km^2/kg	Sorptive capacity, kg/kg (dry)
Aluminas							
Low-porosity (fluoride sorbent)	G, S	8-14, etc.	40	0.70	~7	0.32	0.20
High-porosity (drying, separations)	G	Various	57	0.85	4-14	0.25-0.36	0.25-0.33
Desiccant, CaCl_2 -coated	G	3-8, etc.	30	0.91	4.5	0.2	0.22
Activated bauxite	G	8-20, etc.	35	0.85	5		0.1-0.2
Chromatographic alumina	G, P, S	80-200, etc.	30	0.93			~0.14
Silicates and aluminosilicates							
Molecular sieves							
Type 3A (dehydration)	S, C, P	Various	~30	0.62-0.68	0.3	~0.7	0.21-0.23
Type 4A (dehydration)			~32	0.61-0.67	0.4	~0.7	0.22-0.26
Type 5A (separations)			~34	0.60-0.66	0.5	~0.7	0.23-0.28
Type 13X (purification)			~38	0.58-0.64	1.0	~0.6	0.25-0.36
Mordenite (acid drying)				0.88	0.3-0.8		0.12
Chabazite (acid drying)				0.72	0.4-0.5		0.20
Silica gel (drying, separations)	G, P	Various	38-48	0.70-0.82	2-5	0.6-0.8	0.35-0.50
Magnesium silicate (decolorizing)	G, P	Various	~33	~0.50		0.18-0.30	
Calcium silicate (fatty-acid removal)	P		75-80	~0.20		~0.1	
Clay, acid-treated (refining of petroleum, food products)	G	4-8		0.85			
Fuller's earth (same)	G, P	<200		0.80			
Diatomaceous earth	G	Various		0.44-0.50		~0.002	
Carbons							
Shell-based	G	Various	60	0.45-0.55	2	0.8-1.6	0.40
Wood-based	G	Various	~80	0.25-0.30		0.8-1.8	~0.70
Petroleum-based	G, C	Various	~80	0.45-0.55	2	0.9-1.3	0.3-0.4
Peat-based	G, C, P	Various	~55	0.30-0.50	1-4	0.8-1.6	0.5
Lignite-based	G, P	Various	70-85	0.40-0.70	3	0.4-0.7	0.3
Bituminous-coal-based	G, P	8-30, 12-40	60-80	0.40-0.60	2-4	0.9-1.2	0.4
Organic polymers							
Polystyrene (removal of organics, e.g., phenol; antibiotics recovery)	S	20-60	40-50	0.64	4-9	0.3-0.7	
Polyacrylic ester (purification of pulping wastewaters; antibiotics recovery)	G, S	20-60	50-55	0.65-0.70	10-25	0.15-0.4	
Phenolic (also phenolic amine) resin (decolorizing and deodorizing of solutions)	G	16-50	45	0.42		0.08-0.12	0.45-0.55

*Shapes: C, cylindrical pellets; F, fibrous flakes; G, granules; P, powder; S, spheres.

†U.S. Standard sieve sizes (given in parentheses) correspond to the following diameters in millimeters: (3) 6.73, (4) 4.76, (8) 2.98, (12) 1.68, (14) 1.41, (16) 1.19, (20) 0.841, (30) 0.595, (40) 0.420, (50) 0.297, (60) 0.250, (80) 0.177, (200) 0.074.

NOTE: To convert kilograms per liter to pounds per cubic foot, multiply by 6.238×10^{-1} ; to convert square kilometers per kilogram to square feet per pound

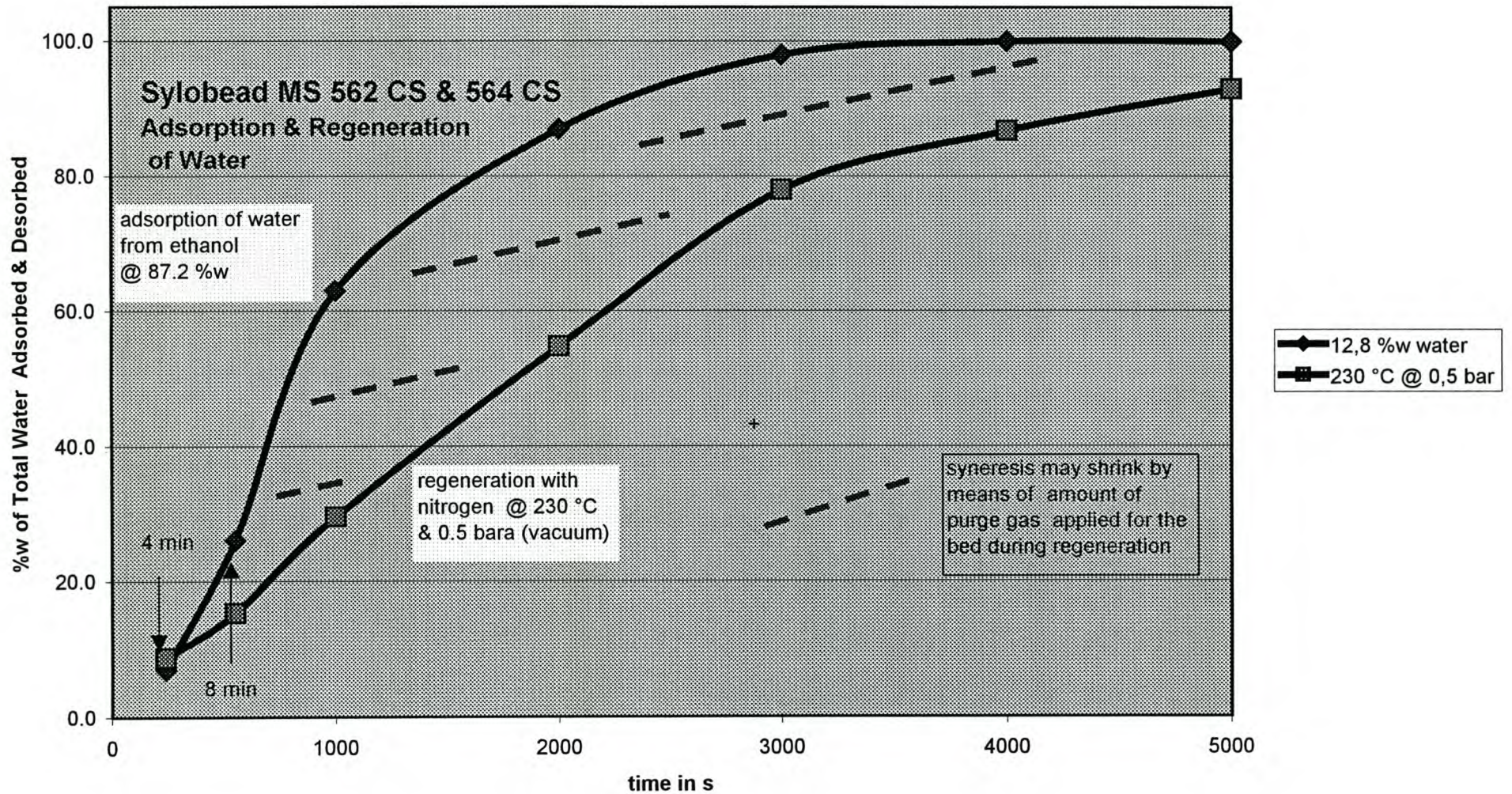
APPENDIX C**W.R. GRACE MOLECULAR SIEVE CHARACTERISTICS**

Appendix C1	Adsorption and Regeneration on MS 564 CS
Appendix C2	Breakthrough Curves of Different Concentration Water on MS 564 CS
Appendix C3	Desorption of Water from MS 564 CS at Different Pressures
Appendix C4	Desorption of Water from MS 564 CS at Different Temperatures
Appendix C5	MS 564 CS Data Sheet
Appendix C6	MS 512 Data Sheet
Appendix C7	Isotherms for Water Adsorption on Molecular Sieve 3A
Appendix C8	Isotherms for Water Adsorption on Molecular Sieve 4A
Appendix C9	Dewpoint of Regeneration Gas

Appendix C1. Adsorption and Regeneration on MS 564 CS

GRACE Davison

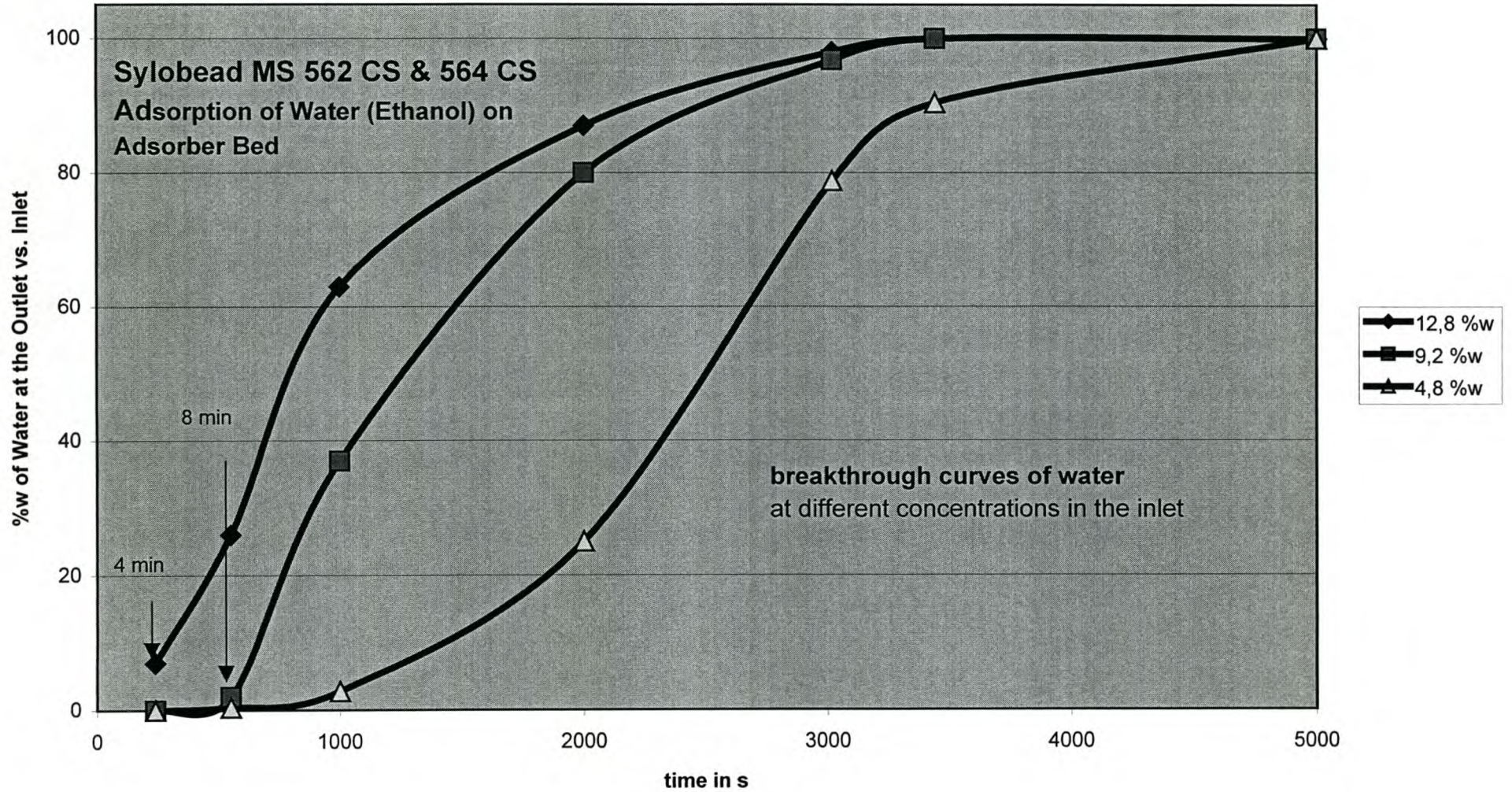
Ethanol Dehydration with Zeolite

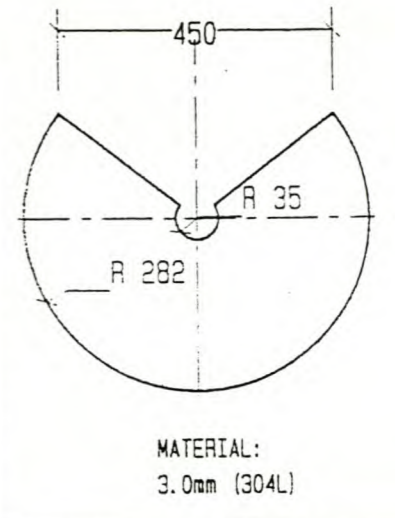
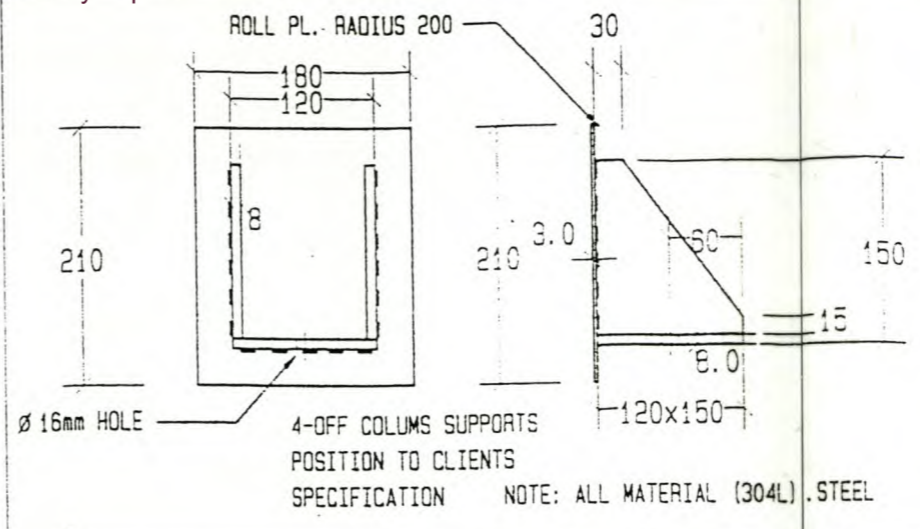
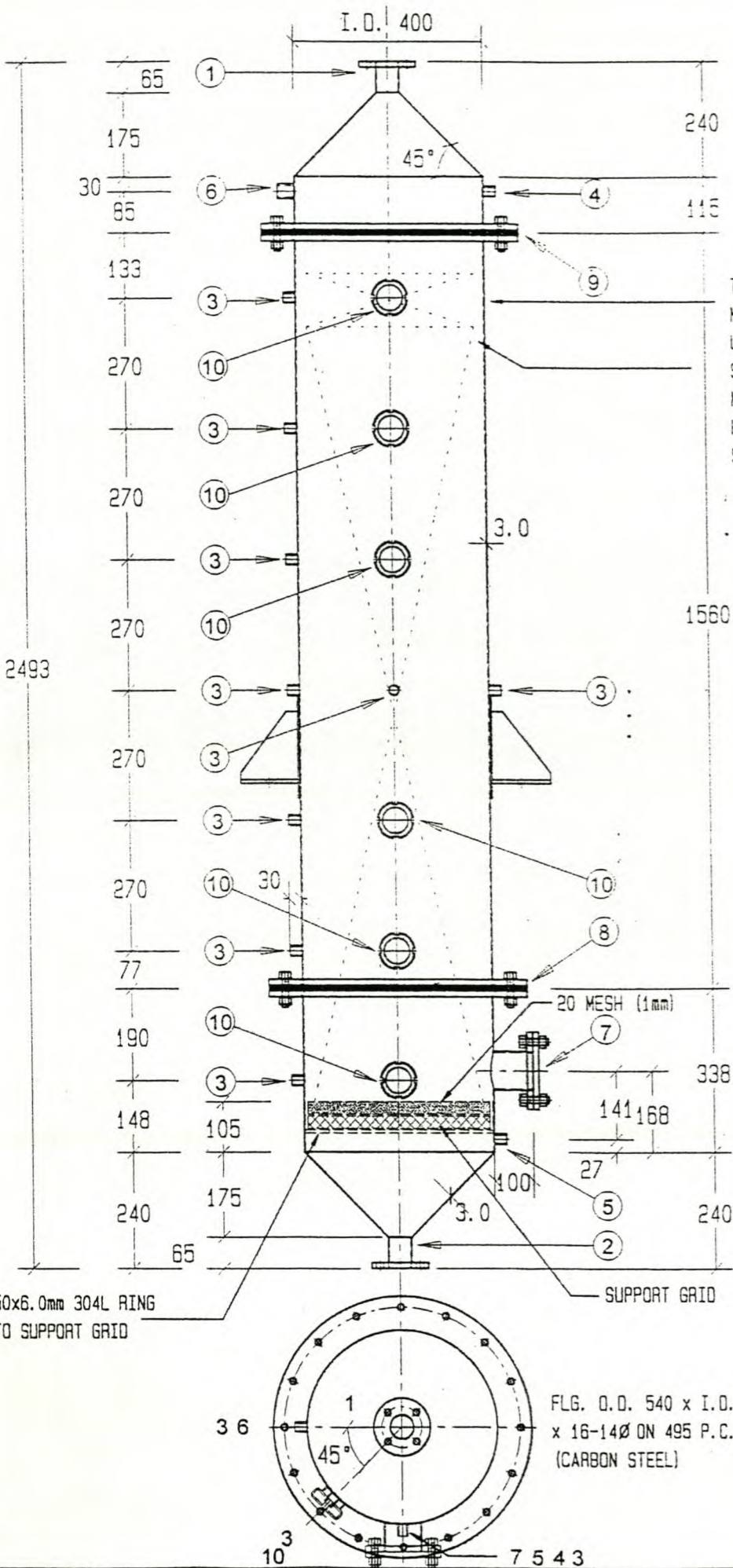


Appendix C2. Breakthrough Curves of Water on MS 564 CS

GRACE Davison

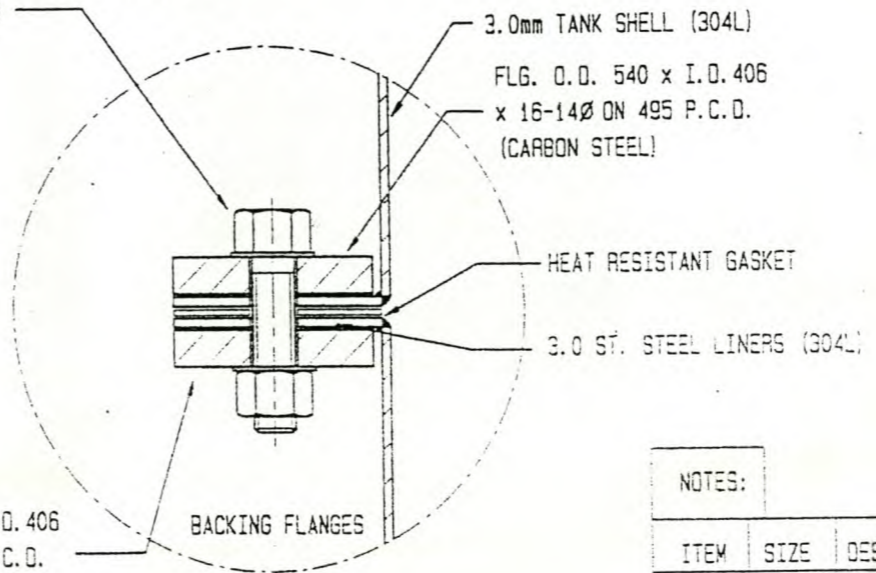
Ethanol Dehydration with Zeolite



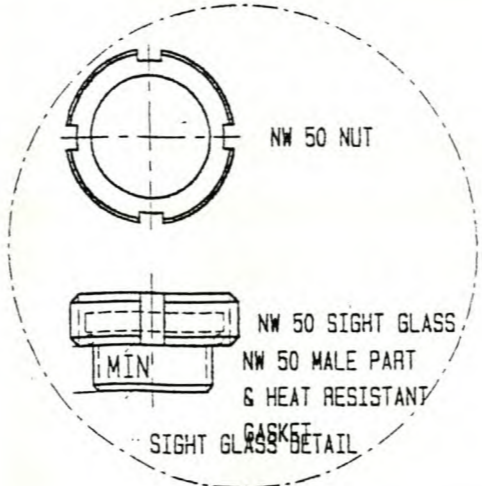


TOP OF UPPER MOLECULAR SIEVE
UPPER AND LOWER MOLECULAR SIEVES ARE SEPERATED WITH MESH. MESH FITTED WITH HANDLES EXTENDING ABOVE SIEVE TOP

M12x60 SST. BOLTS & NUTS (16-OFF)



FLG. O.D. 540 x I.D. 406 x 16-14Ø ON 495 P.C.D. (CARBON STEEL)



SIGHT GLASS GASKET DETAIL

NOTE: SOCKET & HOLE CONCENTRIC

TEMPERATURE SOCKET 15NB NTP

Ø 4mm HOLE TO ACCOMMODATE TEMPERATURE PROBE SHAFT

TYPICAL TEMPERATURE SOCKET DETAIL

NOTES:

ITEM	SIZE	DESCRIPTION
1.	50 NB	IN & OUT FLG. BS 4504 6/3 10 THK, HOLES Ø11
2.	50 NB	OUTLET MAIN FLG. BS 4504 6/3 10 THK, HOLES Ø11
3.	15 NB	TEMPERATURE SOCKET
4.	15 NB	PRESSURE SOCKET
5.	15 NB	PRESSURE SOCKET
6.	25 NB	SAFETY YE SOCKET
7.	80 NB	HAND HOLE BLANK
8.	-	FLG. BS 4 6/3 12 THK, HOLES Ø14
9.	-	SEE DET. DRW.
10.	NW 50	MALE PART GASKET, SIGHT GLASS & NUT

APPROVED FOR CONSTRUCTION
Date 1/06/01

NOTE: ALL SOCKETS MUST HAVE NYLON PLUG

REV.	DATE	BY	DESCRIPTION
C	1.06.01	A.KEA	MATERIAL (304L)

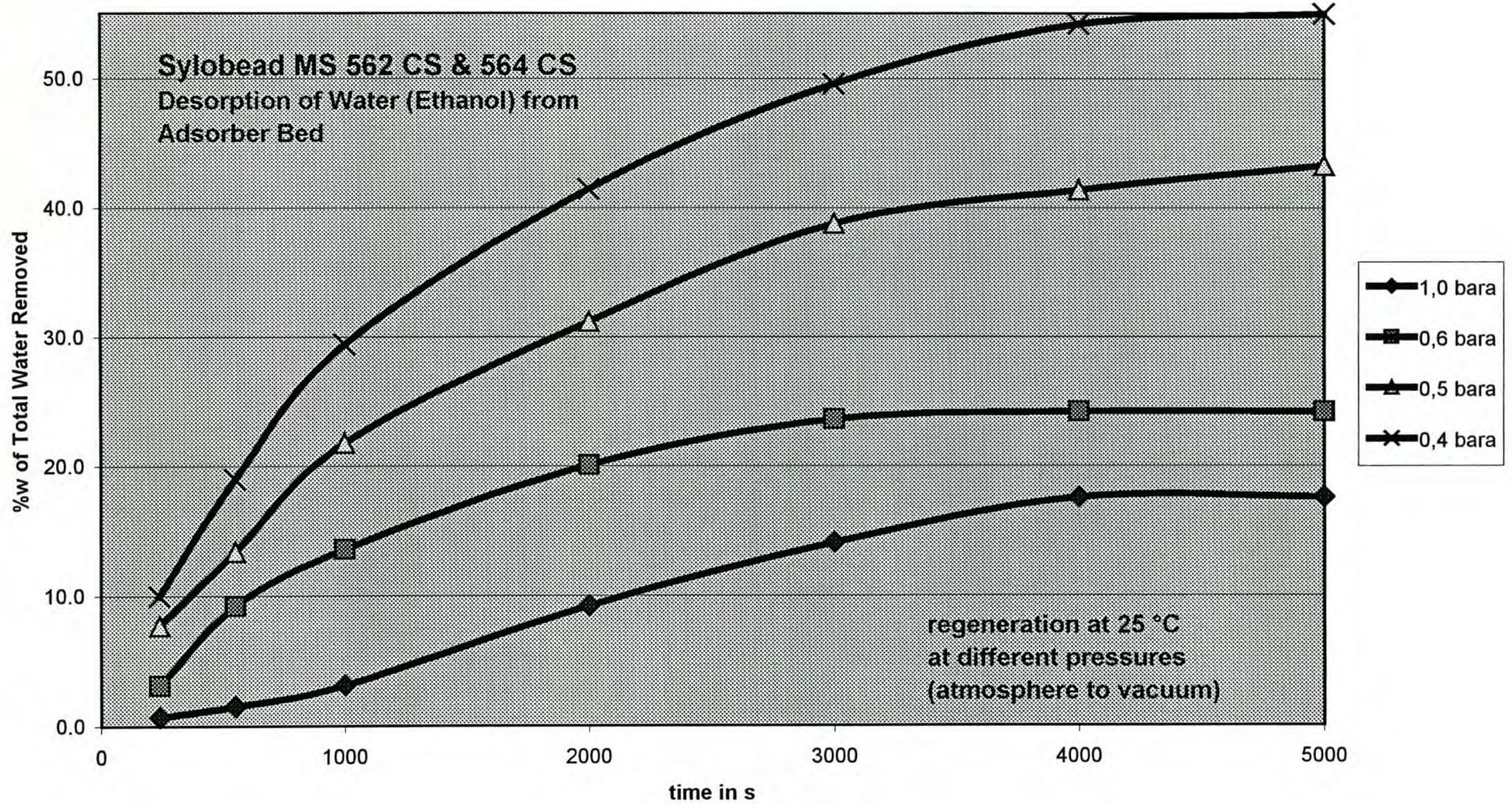
DESIGN PRESSURE FULL VAC. - 40 kPa	PAPER SIZE: A3	TITLE: BIADSOPTION COLUMNS	SATURN STAINLESS IND. 9 KAPLAN STREET HUGUENOT 7645
WORKING PRESSURE 40 kPa		CLIENT: I-CHEM	
HYDRAULIC TEST PRESS. 60 kPa			
WORKING TEMP. 180 °C	DRW. NO.: C422E-001	SCALE: 5 DRAWN BY A.KEARN	DATE 2001 05 23
CONSTRUCTED IN ACCORDANCE WITH CODE: RSA-CIF-81-98-0 (NOT CODED)		REV. NO.: N/A DATE: N/A	CHECKED BY:



Appendix C3. MS 564 CS Desorption at Different Pressures

GRACE Davison

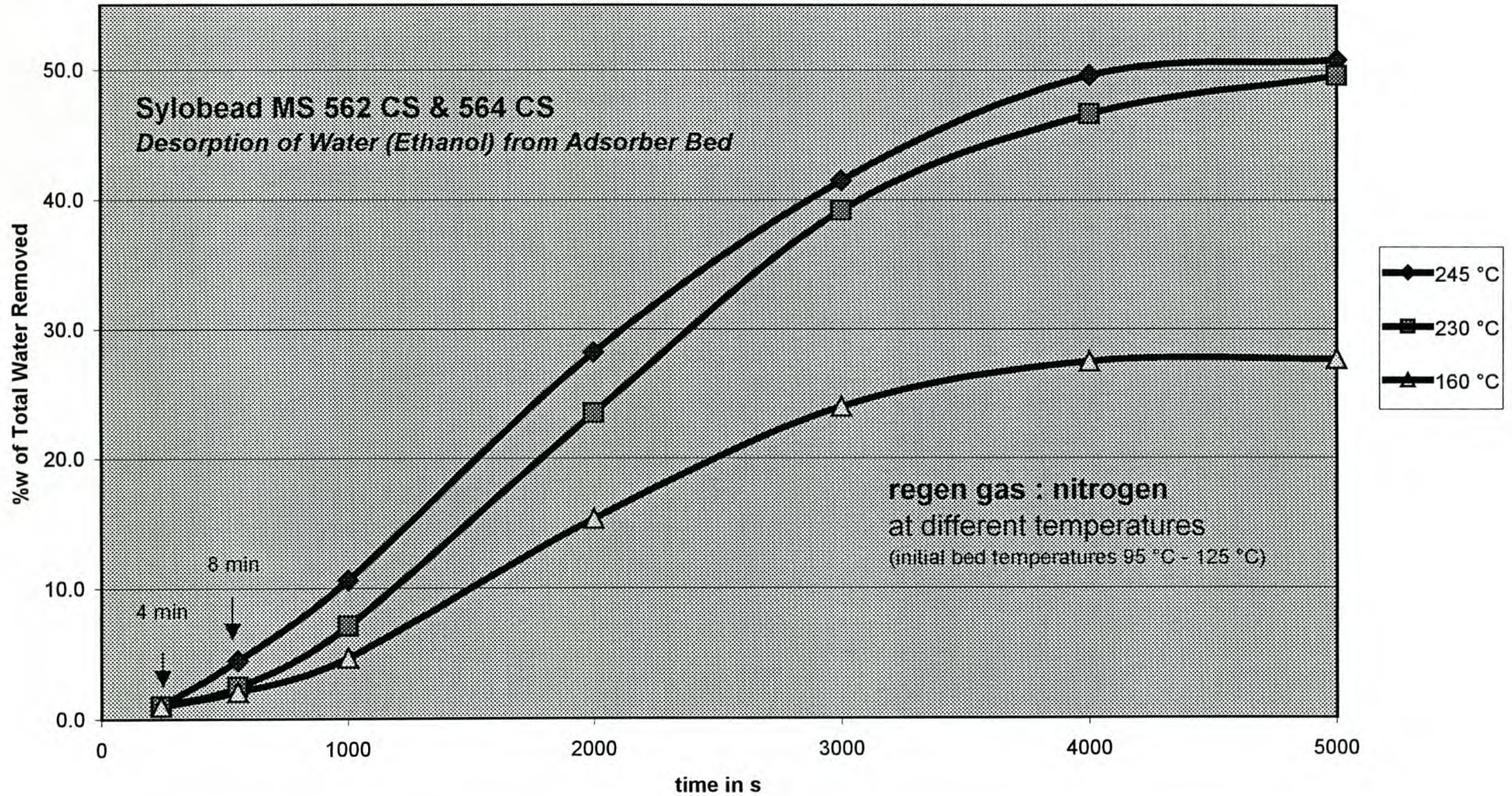
Ethanol Dehydration with Zeolite



Appendix C4 MS 564 CS Temperature Desorption

GRACE Davison

Ethanol Dehydration with Zeolite



Appendix C5. MS 564 CS Data Sheet

SYLOBEAD™ MS 564 CS

Adsorbent for the Dehydration of Cracked Gas and Olefins

1) PRODUCT DESCRIPTION

SYLOBEAD™ MS 564 CS (8X12 mesh beads) is a highly porous, high performance crystalline aluminosilicate in spherical form. The pore openings in the crystals have a diameter of approximately 3 Å. Sphere size is a nominal 1/16" diameter.

2) PRODUCT SPECIFICATION

<i>Property</i>	<i>Unit</i>	<i>Specification</i>	<i>Test Method</i>
Total Volatile (1000°F)	%	2.0 max.	GRACE 002040
H ₂ O-Adsorption Capacity a)	%	20.5 min.	GRACE 025090
Screen Analysis:			
on 8 US mesh	%	20.0 max.	GRACE 029400
on 12 US mesh	%	90.0 min.	GRACE 029420
on 20 US mesh	%	99.5 min.	GRACE 029460

a) 80 % r.h., 77°F

3) TYPICAL PROPERTIES

The following data are given for information purposes only:

<i>Property</i>	<i>Unit</i>	<i>Typical Value</i>	<i>Test Method</i>
Bulk Density	lbs./cu.ft.	46.0 avg.	GRACE 022010
Crush Strength	lbs.	4.5 avg.	GRACE 501161
Heat of Adsorption, H ₂ O	BtU/lb.	1800	

4) RECOMMENDED APPLICATIONS

SYLOBEAD™ MS 564 CS is a high performance 3 Å, 1.6-2.5mm spherical molecular sieve specifically formulated for the dehydration of cracked gas, propylene, butadiene and other unsaturated hydrocarbons. The proprietary, enhanced formulation of MS 564 CS provides maximum retained cyclic H₂O capacity, minimal attrition or material breakup, low unit pressure drop, maximum resistance to coking, no green oil formation and long service life in severe service cracked gas dehydration applications. MS 564 CS provides superior H₂O adsorptive mass transfer efficiency.

5) PACKAGING INFORMATION

SYLOBEAD™ MS 564 CS is supplied in steel drums, big bags or silo trucks.

150 kg/216.5 l drum	4 drums/pallet	600 kg/pallet	pallet: 1200 x 1000 mm
800 kg/big bag on pallet			pallet: 1000 x 1000 mm

Details of silo truck delivery (pneumatic loading) on request.

6) HANDLING AND STORAGE RECOMMENDATIONS

SYLOBEAD™ MS 564 CS should be handled so as to avoid generation of dusty conditions at the workplace. When pouring into a container in the presence of flammable liquids, gases or dust, earth both containers electrically to prevent a static electric spark and the risk of explosion. Additional information can be found in our Safety Data Sheet. Storage in a dry warehouse is recommended. Extended exposure to UV light degrades the big bag material and this should be avoided. Open packages should be resealed to prevent contamination and adsorption of water or other gases and vapors. The material in drums should be used within 4 years, the material in big bags within 6 months (from the date of production).

7) HEALTH AND SAFETY INFORMATION

SYLOBEAD™ MS 564 CS is a synthetic aluminosilicate bound with a mineral clay. In active conditions it will release heat when adsorbing water or other substances. If a large quantity of sieve quickly adsorbs water, the molecular sieve can become hot enough to cause thermal burns of the skin; contact has to be avoided under these conditions. Information to date indicates that the synthetic aluminosilicate is not toxic and does not cause fibrosis. The product contains, however, a small amount (ca. 1 %) of quartz carried over from the mineral binders. At present, EU Regulations do not require safety labelling of products containing quartz. However, quartz has been recently classified by IARC (International Agency for Research on Cancer) as carcinogenic to humans by inhalation (Group 1). Furthermore, quartz can cause silicosis or other lung diseases on prolonged exposure. When handling Molecular Sieve Beads the concentration of respirable quartz in the working environment is expected to be well below the limits allowed by the worker protection regulations. Nevertheless, the user is responsible for controlling the working environment according to local regulations, e.g. in the UK: COSHH Regulations; in Germany: Gefahrstoffverordnung and TRGS 900. The Occupational Exposure Limit for synthetic aluminosilicate in Germany is 6 mg/m³ for fine dust (MAK). The Occupational Exposure Limit for quartz in Germany is 0.15 mg/m³ for fine dust (MAK). Additional information can be found in our Safety Data Sheet. Please refer also to national laws and regulations.

8) OTHER INFORMATION

We hope the information given here will be helpful. It is based on data and knowledge which we believe to be true and accurate and is offered for the user's consideration, investigation and verification. Accordingly, save in the event of gross negligence or willful misconduct of ourselves and our agents, we will not be liable for any damages resulting from errors, omissions or non-compliance of the information set forth herein. Further, please read all statements, recommendations or suggestions in conjunction with our General Conditions of Delivery, Performance and Payment which limit our liability with respect to all goods supplied by us. Test methods are available on request.

9) PRINCIPAL SALES OFFICES

GRACE GmbH, D-67545 Worms, Tel.: 6241/403 0, Tlx: 467724, Fax: 6241/403 211

W.R. GRACE Italiana S.p.A., Via Trento 7, I-20017 Passirana di Rho, Tel.: 02/93537444, Tlx: 332512, Fax: 02/93537581

GRACE S.A., Calle Riera de Fonollar 12, E-08030 San Boi de Llobregat (Barcelona), Tel.: 3/635 10 00, Fax: 3/635 11 11

GRACE Davison, Clifton House, 1 Marston Road, GB-St. Neots, Cambridgeshire PE19 2HN, Tel.: 1480/22 40 89, Fax: 1480/22 40 60

GRACE AB, Box 622, S-25106 Helsingborg, Tel.: 42/25 61 00, Tlx: 72445, Fax: 42/25 61 15

W.R. GRACE S.A.S., 33, route de Gallardon, Boîte Postale 39, F-28234 Epernon Cédex, Tel.: 237/188841, Fax: 237/188690

W.R. GRACE & Co., Lab Washington Research Centre, 7500 Grace Drive, Columbia, 21044 Maryland, USA, Tel.: 410/531-4047, Fax: 410/531-4309

W.R. GRACE (Hong Kong) Ltd., Units 1001-4, 10/F, AXA Centre, 151 Gloucester Road, Wanchai, Hong Kong, Tel.: 25 90 28 28, Fax: 28 56 07 12

GRACE Brasil Ltda., Av. Mofarrej 619, Vila Leopoldina, 05311-902 Sao Paulo, SP, Brasil, Tel.: 55 (11) 3649-2700, Fax: 55 (11) 3649-2783

The above information is given in good faith, but without guarantee. No patent liability is assumed.

Appendix C6. MS 512 Data Sheet

SYLOBEAD™ MS 512

Adsorbent for Drying and Purification of Gases and Liquids

1) PRODUCT DESCRIPTION

SYLOBEAD™ MS 512 is a highly porous, crystalline aluminosilicate in beaded form. The pore openings in the crystals have a diameter of approximately 4 Å.

2) PRODUCT SPECIFICATION

<i>Property</i>	<i>Unit</i>	<i>Specification</i>	<i>Test Method</i>
Total Volatile (950°C)	%	3.0 max.	GRACE Q 107
H ₂ O-Adsorption Capacity a)	%	17.5 min.	GRACE Q 102
Crush Strength	N	40 min.	GRACE Q 104
Screen Analysis:			GRACE Q 101
> 6.3 mm	%	0	
> 5.0 mm	%	7.0 max.	
> 2.5 mm	%	95.0 min.	
> 1.6 mm	%	99.0 min.	

a) 10 % r.h., 25°C

3) TYPICAL PROPERTIES

The following data are given for information purposes only:

<i>Property</i>	<i>Unit</i>	<i>Typical Value</i>	<i>Test Method</i>
Bulk Density	g/l	680-730	GRACE Q 110

4) RECOMMENDED APPLICATIONS

SYLOBEAD™ MS 512 is a product for dynamic drying of most gases and vapors. It can also be used to remove other impurities with effective molecule diameters smaller than 4 Å. Typical applications for SYLOBEAD™ MS 512 are drying/purification of natural gas, reformer gas and air.

5) PACKAGING INFORMATION

Stellenbosch University <http://scholar.sun.ac.za>

SYLOBEAD™ MS 512 is supplied in steel drums, big bags or silo trucks.

150 kg/216.5 l drum

4 drums/pallet

600 kg/pallet

pallet: 1200 x 1000 mm

800 kg/big bag on pallet

pallet: 1000 x 1000 mm

Details of silo truck delivery (pneumatic loading) on request.

6) HANDLING AND STORAGE RECOMMENDATIONS

SYLOBEAD™ MS 512 should be handled so as to avoid generation of dusty conditions at the workplace. When pouring into a container in the presence of flammable liquids, gases or dust, earth both containers electrically to prevent a static electric spark and the risk of explosion. Additional information can be found in our Safety Data Sheet. Storage in a dry warehouse is recommended. Extended exposure to UV light degrades the big bag material and this should be avoided. Open packages should be resealed to prevent contamination and adsorption of water or other gases and vapors. The material in drums should be used within 4 years, the material in big bags within 6 months (from the date of production).

7) HEALTH AND SAFETY INFORMATION

SYLOBEAD™ MS 512 is a synthetic aluminosilicate bound with a mineral clay. In active conditions it will release heat when adsorbing water or other substances. If a large quantity of sieve quickly adsorbs water, the molecular sieve can become hot enough to cause thermal burns of the skin; contact has to be avoided under these conditions. Information to date indicates that the synthetic aluminosilicate is not toxic and does not cause fibrosis. The product contains, however, a small amount (ca. 1 %) of quartz carried over from the mineral binders. At present, EU Regulations do not require safety labelling of products containing quartz. However, quartz has been recently classified by IARC (International Agency for Research on Cancer) as carcinogenic to humans by inhalation (Group 1). Furthermore, quartz can cause silicosis or other lung diseases on prolonged exposure. When handling Molecular Sieve Beads the concentration of respirable quartz in the working environment is expected to be well below the limits allowed by the worker protection regulations. Nevertheless, the user is responsible for controlling the working environment according to local regulations, e.g. in the UK: COSHH Regulations; in Germany: Gefahrstoffverordnung and TRGS 900. The Occupational Exposure Limit for synthetic aluminosilicate in Germany is 6 mg/m³ for fine dust (MAK). The Occupational Exposure Limit for quartz in Germany is 0.15 mg/m³ for fine dust (MAK). Additional information can be found in our Safety Data Sheet. Please refer also to national laws and regulations.

8) OTHER INFORMATION

We hope the information given here will be helpful. It is based on data and knowledge which we believe to be true and accurate and is offered for the user's consideration, investigation and verification. Accordingly, save in the event of gross negligence or willful misconduct of ourselves and our agents, we will not be liable for any damages resulting from errors, omissions or non-compliance of the information set forth herein. Further, please read all statements, recommendations or suggestions in conjunction with our General Conditions of Delivery, Performance and Payment which limit our liability with respect to all goods supplied by us. Test methods are available on request.

9) PRINCIPAL SALES OFFICES

GRACE GmbH, D-67545 Worms, Tel.: 6241/403 0, Tlx: 467724, Fax: 6241/403 211

GRACE Italiana S.p.A., Via Trento 7, I-20017 Passirana di Rho, Tel.: 2/933 21, Tlx: 332512,

Fax: 2/933 25 81

GRACE S.A., Calle Riera de Fonollar 12, E-08030 San Boi de Llobregat (Barcelona), Tel.: 3/635 10 00,

Fax: 3/635 11 11

GRACE Davison, Clifton House, 1 Marston Road, GB-St. Neots, Cambridgeshire PE19 2HN,

Tel.: 1480/22 40 89, Fax: 1480/22 40 60

GRACE AB, Box 622, S-25106 Helsingborg, Tel.: 42/25 61 00, Tlx: 72445, Fax: 42/25 61 15

W.R. GRACE S.A.S., 33, route de Gallardon, Boîte Postale 39, F-28234 Epernon Cédex,

Tel.: 237/18 92 39, 237/18 94 26, Tlx: 760022, Fax: 237/18 96 60

W.R. GRACE & Co., Davison Chemical Division, 10E Baltimore Street, Baltimore, 21202 Maryland, USA,

Tel.: 410/659 90 00, Fax: 410/659 92 13

W.R. GRACE (Hong Kong) Ltd., 20/F Devon House, 979 King's Road, Taikoo Place, Quarry Bay,

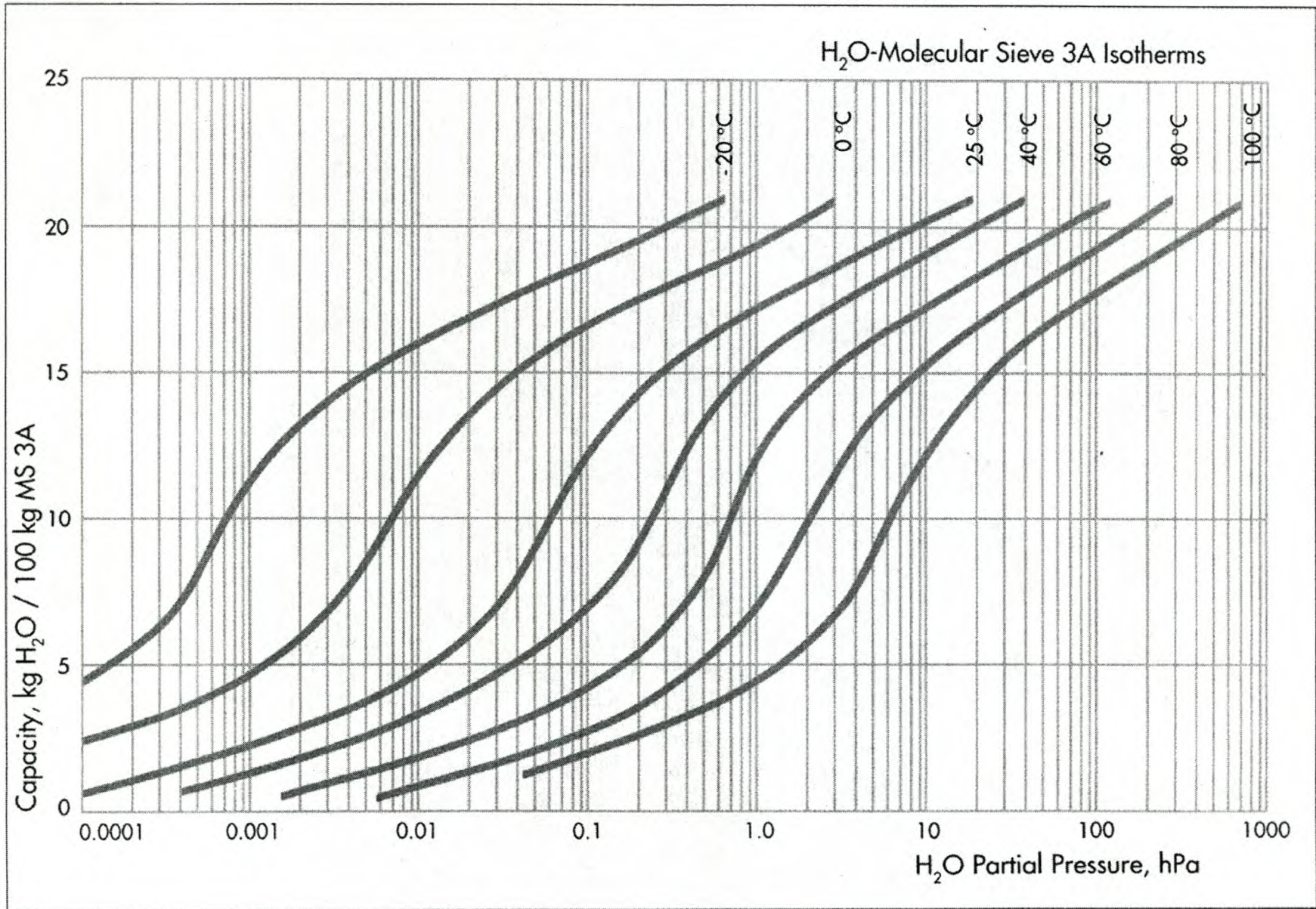
Hong Kong, Tel.: 259 08 28, Tlx: 73663, Fax: 28 56 07 12

GRACE Brasil Ltda., Av. Mofarrej 619, Vila Leopoldina, 05311-902 Sao Paulo, SP, Brasil,

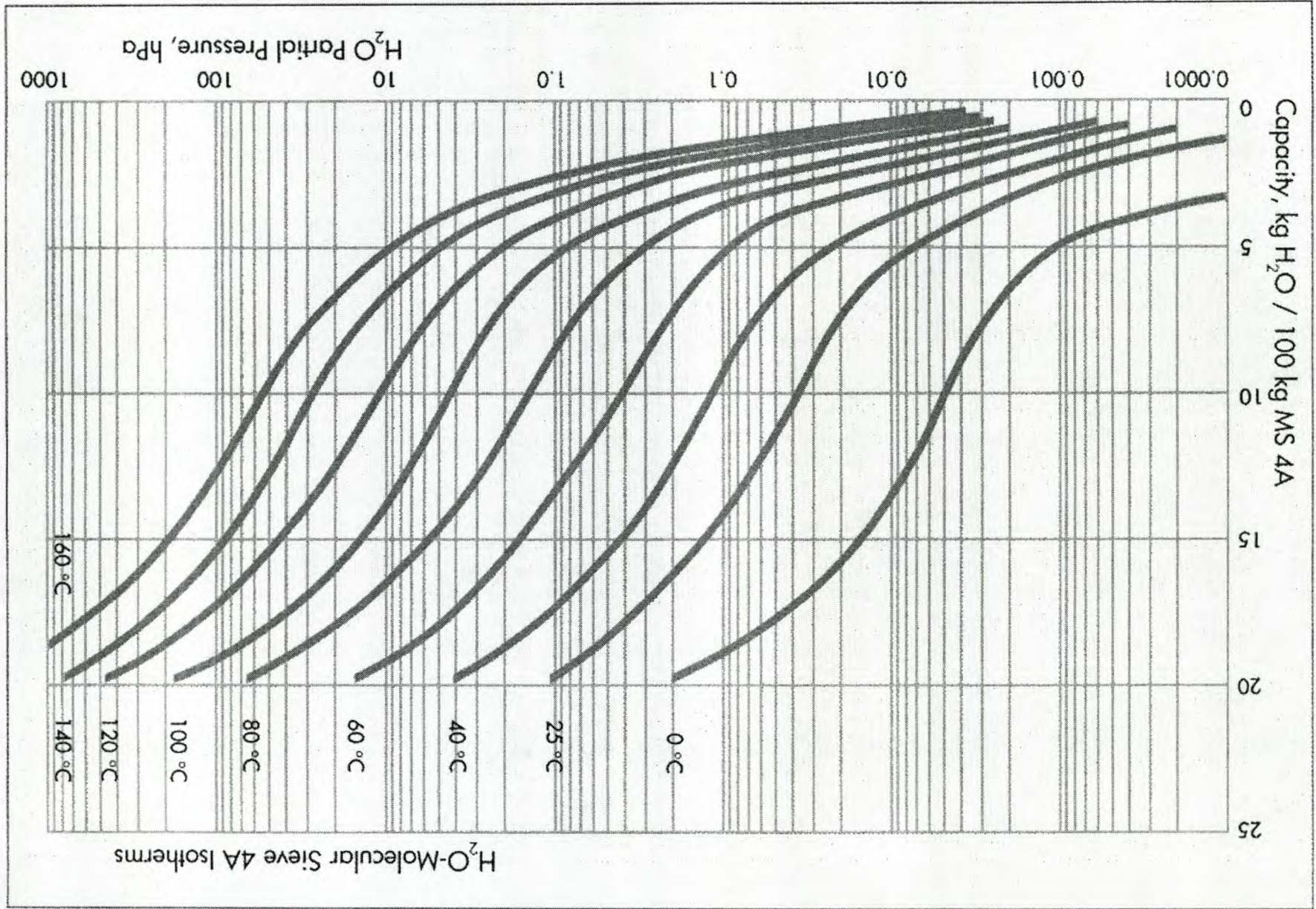
Tel.: 11/833 27 60 (-65), Tlx: 5511-83502, Fax: 11/260 44 02

The above information is given in good faith, but without guarantee. No patent liability is assumed.

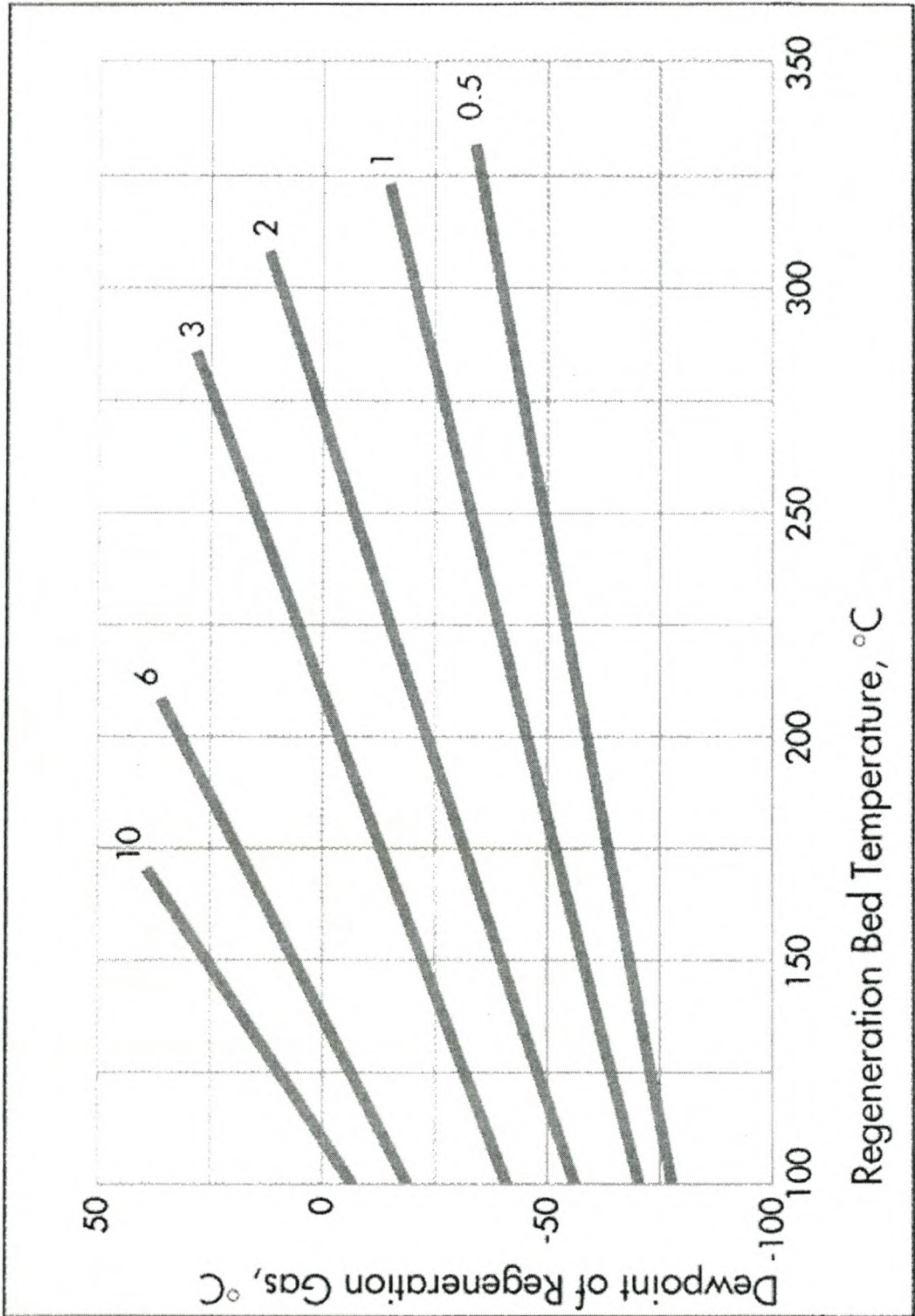
Appendix C7. Water Isotherms-Molecular Sieve 3A



Appendix C8. Water Isotherms-Molecular Sieve 4A



Appendix C9. Dewpoint of Regeneration Gas



APPENDIX D

ADSORBER DESIGN

- D1. Design Methodology and Calculations**
- D2. ChemCad Simulation Input**
- D3. ChemCad Simulation Output**

D1 Design methodology

As explained in chapter 2, the principles for design of the adsorbers were based on the methodology of White ^[W1]. Thermodynamic conditions in the adsorbers during operating conditions were simulated by Chemcad and were used in the design. The input and output files used are provided in appendices D2 and D3. Motivation for the use of these values are also given. The simulator was used, as it estimated the thermodynamic conditions in the adsorber under specific conditions more accurate than the literature. Vapour stream 4 being (appendix D3) is equivalent to the actual adsorption conditions. The design methodology is based on the design equations in chapter 2.9.1.

Physical properties

The following values were used in the calculations:

$$\varepsilon = 0.393 \text{ (for spheres with a diameter of } 0.0032 \text{ m)} \quad [11]$$

$$a = 6/D_p = 6/0.0032 = 1875 \text{ m}^{-1} \quad [11]$$

$$\psi = 1 \text{ (W.R. Grace)}$$

$$D_p = 0.0032 \text{ m}$$

$$c_a = 53 \text{ J}\cdot\text{kg}^{-1} \quad [64]$$

$$k_a = 1.3 \text{ W}\cdot\text{m}^{-1}\cdot\text{K}^{-1} \quad [25]$$

Reference

Thermodynamic conditions (from ChemCad output file)

$$\mu = 1.1157\text{E-}5 \text{ Pa}\cdot\text{s}$$

$$\rho_o = 1.412 \text{ kg}\cdot\text{m}^{-3}$$

$$k_o = 0.0226 \text{ W}\cdot\text{m}^{-1}\cdot\text{K}^{-1}$$

$$c_o = 1688.52 \text{ J}\cdot\text{kg}\cdot\text{K}^{-1}$$

Operating conditions

$$w_o = 0.0111 \text{ kg}\cdot\text{s}^{-1} \quad (40 \text{ kg/hr})$$

$$t_a = 240 - 300 \text{ s}$$

$$T_{\text{ads}} = 100 \text{ }^\circ\text{C}$$

$$P_{\text{ads}} = 100 \text{ kPa}$$

$$T_{\text{des}} = 100 \text{ }^\circ\text{C} \text{ (> } 100^\circ\text{C is not possible in short cycle times)}$$

$$P_{\text{des}} = 17 \text{ kPa}$$

Velocity effects

$$E_1 = 88\,978\,764,56 \quad (\text{From Eq. 2.5})$$

$$E_2 = 2150,56 \quad (\text{From Eq. 2.7})$$

$$v_s (\text{max}) = 1.39 \text{ ms}^{-1} \quad (\text{From Eq. 2.9})$$

$$v_s (\text{attrition}) = 0.75v_s (\text{max}) = 1.04 \text{ ms}^{-1}$$

$$v_s = 0.6v_s (\text{attrition}) = 0.62 \text{ ms}^{-1}$$

$$A_{\text{min}} = 0.0133 \text{ m}^2 \quad (\text{From Eq. 2.8})$$

$$D_b(\text{min}) = 0.13 \text{ m}$$

Pressure gradients

$$\Delta P_a/L_a = 3 \text{ kPa} \quad (\text{From Eq. 2.5})$$

Heat transfer

$$N_{\text{Re}} = 4.22 \quad (\text{From Eq. 2.20})$$

$$N_{\text{Pr}} = 0.834$$

$$h_o = 704.8 \text{ W}\cdot\text{m}^{-2}\cdot\text{K}^{-1} \quad (\text{From Eq. 2.19})$$

$$h_a = 4062.5 \text{ W}\cdot\text{m}^{-2}\cdot\text{K}^{-1} \quad (\text{From Eq. 2.21})$$

$$U = 600.6 \text{ W}\cdot\text{m}^{-2}\cdot\text{K}^{-1} \quad (\text{From Eq. 2.22})$$

Final bed dimensions

$$\text{At } t_a = 300 \text{ s and } D_b = 0.35 \text{ m}$$

$$L = 1.5 \text{ m} \quad (\text{From Eq. 2.14})$$

Both the length and diameter were increased by an additional 15%, bringing the final bed dimensions to:

$$L = 1.7 \text{ m and } D_b = 0.4 \text{ m}$$

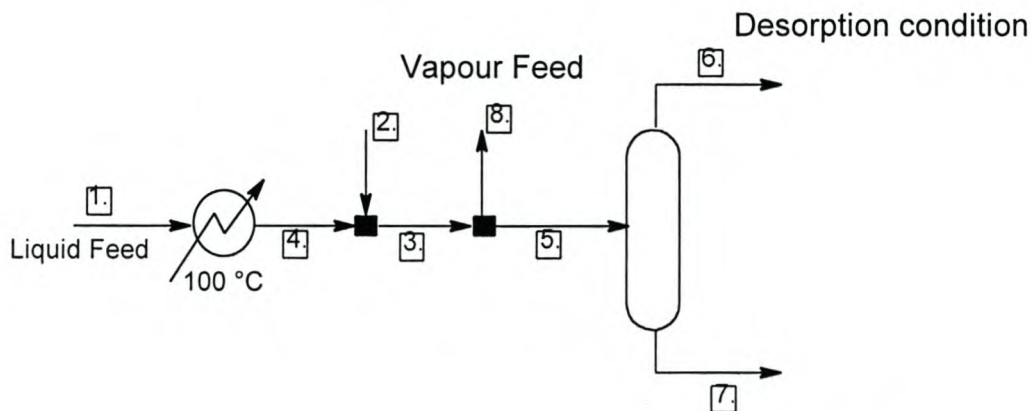
This allowed for retention of both heat-and mass transfer fronts.

Purge gas

$$W_2(\text{min}) = 7.8 \text{ kg/hr} \quad (\text{From Eq. 2.12})$$

D2. ChemCad input file

The following process flow diagram shows the structure of the simulation that was used to determine stream properties for use in the design of the adsorber columns (appendix D3). This PID was fed into the simulator.



The thermodynamic model used for the simulation is the Unifac method. The method is predictive and does not require the input of binary interactive parameters. The Unifac equation is based on the group contribution method for estimating activity coefficients. It has the following characteristics which determined its use for simulating the feed stream in this case.

- Based on versatile Uniquac equation
- Parameters are almost independent of temperature
- Temperature range = 275 – 425 °K
- Pressure range = 0 – 4 atm
- Can simulate non-ideal systems and 2 liquid phases

The Latent Heat model was used to determine enthalpy values. These two models are generally used in combination.

Stream 1 (feed) at a flowrate of 40 *l*/hr, represents the neutral wine spirits at 25 °C and atmospheric conditions. Composition of the stream was specified to a typical spirits (see output file - stream 1). To simulate the vapour, stream 1 is heated in Equipment 2, a fired heater to produce Stream 4, which is at

100 °C with a vapour fraction of 1. Stream 2 is a so-called zero stream (added to Stream 4 with Mixer 1), which could be used to simulate the process if a recycle was added. Since recirculation was not used to the adsorbers, this stream was omitted in the simulation. Stream 8 simulated the properties of the final product (equivalent to stream 3). Stream 5 was fed into a component separator which had a zero bottom stream (Stream 7). This was used to simulate the vacuum conditions at 17 kPa (abs) in Stream 6, which would represent the regeneration conditions. The values produced in the output file was then used in the design approach (appendix D3).

INPUT

CHEMCAD 2 Version 2.5

Filename : ADS.TLK
Date: 07-Feb-01 Time: 10:22 am

□□□□□□

FLWSHEET SUMMARY

Equipment	Stream Numbers
1 MIXE	2 4 -3
2 FIRE	1 -4
3 CSEP	5 -6 -7
4 DIVI	3 -8 -5

Stream Connections

Stream	Equipment	Stream	Equipment	Stream	Equipment
To	From To	To	From To	To	From
1		2		4	2 1
2		1		5	4 3
3	1	4		6	3

COMPONENTS

134 117 62

THERMODYNAMICS

K-value model :UNIFAC
Enthalpy model :Latent Heat
Liquid density :API
Water miscible

number	4
Mode	0
	Ratio
Flow rate/ratio	.850000
Flow rate/ratio	.150000

Page 3

Component Separator Summary

Equipment name	
number	3
P out / del P bars	.169996
Top temp. mode	0
	Temp out
Top spec. value C	170.000
Bottom temp. mode	0
	Temp out
Bottom spec. value C	170.000
Component split mode	0
Split destination	Top
Mol spl frac	
Ethanol	1.00000
Methanol	1.00000
Water	1.00000

Mixer Summary

Equipment name	
number	1
Outlet pres. bars	.999979

Page 4

Fired Heater Summary

Equipment name	
number	2
Rated duty Kw-hr/hr	.000000
Pres. drop bars	.000000
Temp. out C	100.000
Fuel val MJ/StdM3	.000000
Thermal efficiency	.000000
Q absorbed Kw-hr/hr	9.82540
Fuel usage SCFH	49.6797

D3. Chemcad simulation outputSTREAM PROPERTIES
Version 2.5

CHEMCAD 2 -

Stream No.	1	3	4	5
Phase	Liquid	Vapor	Vapor	Vapor
From Eqp #	Feed	1	2	4
To Eqp #	2	4	1	3
kgmol/hr	.744381	.744381	.744381	.111657
Temp C	25.0000	100.000	100.000	100.000
Pres bars	.999979	.999979	.999979	.999979
Enth Kw-hr/hr	-3.86901	5.95638	5.95638	.893457
Cp Vap J/g-C		1.68852	1.68852	1.68852
Cp Liq J/g-C	2.51203			
Mol Fraction Vapor	0.00000	1.00000	1.00000	1.00000
Average Mol Wt	43.0881	43.0881	43.0881	43.0881
- - Liquid only - -				
kg/hr	32.0739			
Std Liq m3/hr	.399975E-01			
Sp Gr	.802001			
Actual m3/hr	.404814E-01			
kg/m3	792.253			
Sf tens dyne/cm	23.0895			
Th cond W/m-K	176348			
Visc cp	1.06168			
- - Vapor only - -				
kg/hr		32.0739	32.0739	4.81109
Std Vap m3/hr		16.6844	16.6844	2.50266
Actual m3/hr		22.7209	22.7209	3.40814
kg/m3		1.41164	1.41164	1.41164
Cp/Cv		1.11568	1.11568	1.11568
Compress. factor		.983932	.983932	.983932
Th cond W/m-K		.226391E-01	.226391E-01	.226391E-01
01				
Visc cp		111567E-01	.111567E-01	.111567E-01
Stream No.	6	8		
Phase	Vapor	Vapor		
From Eqp #	3	4		
To Eqp #	Product	Product		
kgmol/hr	.111657	.632724		
Temp C	170.000	100.000		
Pres bars	.169996	.999979		
Enth Kw-hr/hr	1.08476	5.06293		
Cp Vap J/g-C	1.90252	1.68845		
Mol Fraction Vapor	1.00000	1.00000		
Average Mol Wt	43.0881	43.0881		
- - Vapor only - -				
kg/hr	4.81109	27.2629		
Std Vap m3/hr	2.50266	14.1818		
Actual m3/hr	24.1608	19.3128		
kg/m3	.199128	1.41164		
Cp/Cv	1.11238	1.11564		
Compress. factor	.998483	.983932		
Th cond W/m-K	.302491E-01	.226391E-01		
Visc cp	.131147E-01	.111567E-01		

Page

6

FLOW SUMMARIES CHEMCAD 2 -

Version 2.5

Stream No.	1	3	4	5
Temp C	25.0000	100.000	100.000	100.000
Pres bars	999979	.999979	.999979	.999979
Enth Kw-hr/hr	-3.86901	5.95638	5.95638	.893457
Vapor mole fraction	0.00000	1.00000	1.00000	1.00000
Total kgmol/hr	744381	.744381	.744381	.111657
Flowrates in kgmol/hr				
Ethanol	665063	.665063	.665063	.997595E-01
Methanol	416454E-03	.416454E-03	.416454E-03	.624682E-04
Water	789017E-01	.789017E-01	.789017E-01	.118352E-01

Stream No.	6	8
Temp C	170.000	100.000
Pres bars	.169996	.999979
Enth Kw-hr/hr	1.08476	5.06293
Vapor mole fraction	1.00000	1.00000
Total kgmol/hr	.111657	.632724
Flowrates in kgmol/hr		
Ethanol	.997595E-01	.565304
Methanol	.624682E-04	.353986E-03
Water	.118352E-01	.670664E-01

From the output file, stream 8 is important to determine the azeotrope properties in the vapour form at atmospheric pressure and 100 °C. The vapour mole fraction = 1, which indicates that no liquid phase is present as input to the adsorber beds. Molar flow rates are less important, as the thermodynamic properties can be applied to any flow rate. The input mass flow of 40 kg/hr is thus of less importance. The compressibility factor (z) for both streams 8 and 6 \approx 1. This indicates that the azeotropic vapour flow to the adsorber under the specified conditions can be approximated with the ideal gas law. Stream 8 is simulated at 17kPa (abs), to determine properties under desorption conditions. The temperature of 170 °C is an over-estimation, as this high temperature is only reached in the purging gas and not the bed. The latter due to the short adsorption cycle. Other properties like thermal conductivity, enthalpy, densities and viscosity are also provided.

APPENDIX E

ENGINEERING SPECIFICATIONS

- E1. Adsorption Plant Specifications**
- E2. SCADA Specification for Process Control**

E1. Adsorption Plant Specifications

E1 ADSORPTION DEMONSTRATION PLANT SPECIFICATIONS

Introduction

Tenders are invited for the design, manufacture, installation and commissioning of an adsorption demonstration plant at KVV, Paarl.

The SCADA system and instrumentation are excluded from this tender request.

Tender documents shall be returned to KVV (fax 863 2933) marked for Elroy Goliath.

Quote on all equipment marked "pilot plant supplier" in the Equipment listing.

Applicable documents

The following are drawings applicable to the pilot plant:

B015-001-21-R4	B015 Adsorption Pilot Plant – Process & Instrumentation Diagram
B015-001-01-R2	B015 Adsorption Column

Standard

All work must be performed according to recognised and sound engineering principals.

The installation must conform to OHS act requirements.

Tenderers are hereby notified that the plant will be constructed and operated in a Zone 2 classified area and that a Hot Work Permit shall be obtained from the KVV before any work commences.

Description

A pump supplies ethanol (96.4% ambient temperature) from two feed tanks to the top of the adsorption columns via an evaporator.

The system alternates between the two columns. While adsorption of the impurities occurs in one column, the other column is regenerated. Adsorption pressure can be set between ambient and a specified maximum. Regeneration is performed under vacuum conditions.

Vacuum is created by means of a vacuum pump and the waste product is condensed in a condenser prior to the vacuum pump.

The columns operate for approximately 4 minutes where after the molecular sieve shall be regenerated for ± 4 minutes at the regeneration conditions.

Regeneration is done with purified and heated N₂ gas entering the column at the bottom.

Operation

The switching between the two columns is achieved by switching a set of valves. During adsorption in AD100 (pressurised), regeneration occurs in AD200 (vacuum). Before the start of the next cycle the column under vacuum must be pressurised.

The pressure in AD100 will be controlled by setting a set point on PRC 101, which in turn controls V105. The flow in FT 502 is measured and V104 is controlled to allow 15 – 20% of the measured flow in FT 502, through FT 501.

To achieve the vacuum in the other column, the pressure is lowered via pressure regulating valve V501. The vacuum pump evacuates the vapour and an air bleed valve maintains the vacuum at a constant vacuum.

Valve	Position / mode during adsorption of AD100	Position during pressurisation of AD200	Position / mode during adsorption of AD200
V101	Closed	Closed	Open
V102	Open	Open	Closed
V103	Closed	Closed	Open
V104	Ratio controlled by FRC 501 & FRC 502	Controlled rate of flow	Closed
V105	(Controlled by PRC 101) ¹	Closed	Closed
V201	Open	Closed	Closed
V202	Closed	Closed	Open
V203	Open	Closed	Closed
V204	Closed	Open	Ratio controlled by FRC 501 & FRC 502
V205	Closed	Closed	(Controlled by PRC 201) ²

SPECIFICATION

Design

The plant shall be designed for a feed rate of 40 kg/h ethanol (96.4%) at ambient conditions.

Both the product and waste shall be condensed to ambient conditions.

The pilot plant shall be mounted on a skid and provided with flexible connections to feed and product tanks as well as service liquids.

Process water at ambient conditions is available.

¹ During pressure adsorption. If atmospheric adsorption is performed this valve changes to a solenoid valve.

² See note 1

The access to the distillery in Paarl is via a double door. The dimensions and access route shall be checked on site.

The process temperature will fluctuate between ambient and 170°C. Installation of equipment and piping shall accommodate movement caused by thermal expansion and contraction.

Electrical equipment such as pumps shall be installed outside of the Zone 2 area where possible.

All piping and equipment shall be checked and any foreign material be removed before engineering commissioning.

Piping shall be properly supported.

Flange holes shall straddle main centrelines.

Relief valves shall be vented to a safe place

Process water outlets and drain outlets shall be piped to proper drains.

All instrument fittings shall be 15NB sockets.

Consideration shall be given to alternative ways of controlling the bleed stream (V104, V105, V204 and V205) and achieving expansion of the bleed stream.

Adsorption columns

The two vertical columns are each packed with two types of molecular sieves shall conform to the following specifications:

- | | |
|-------------------------------------|----------------------------------|
| 1. Internal diameter | ±400mm |
| 2. Material of construction | 304L stainless steel |
| 3. Pressure (processing) | Ambient to 4 bar (abs) (maximum) |
| 4. Pressure (regeneration) | 170 mbar (abs) |
| 5. Temperature (processing) | 107°C |
| 6. Temperature (regeneration) | 170°C |
| 7. Height of bottom molecular sieve | 1600mm |
| 8. Height of top molecular sieve | 110mm |
| 9. Mass of bottom molecular sieve | 150kg |
| 10. Mass of top molecular sieve | 10 kg |
| 11. Sieve diameter 99% > 1.0mm | |
| 12. Pressure drop (processing) | 40mbar |
| 13. Pressure drop (regeneration) | (to be specified) |

Provision shall be made for nine temperature probe sockets at various levels on the columns and two pressure sensors.

A support shall be fitted as indicated on the drawing and capable of supporting the mass of the both molecular sieves. In addition, the flow area through the support shall be the same or bigger than the flow area through the sieve. A loose mesh shall separate the two sieves.

The columns are pressure vessels according to the OHS act and shall conform to all requirements.

The nozzles for the sight glasses shall have a projection as indicated on the drawing or shorter if physically possible.

Supply the column complete with sight glasses, gaskets, nuts and bolts.

Piping

Stainless steel dairy tubing in NW range shall be used for the product piping of the plant.

Electrical

All electrical connection shall be made and a panel provided that houses all contactors, circuit breakers, stop / start buttons, lights. If the panel cannot be located outside of the hazardous area, the panel design shall be changed to conform to relevant SABS 0142 and 086 codes.

At least one NO and one NC auxiliary shall be provided with each contactor.

All equipment will be started either from the SCADA or manually. A voltage free contact shall be supplied by the SCADA system. Terminals shall be provided for connection to SCADA system.

One panel shall be supplied that houses the electrical switchgear for the electrical equipment.

Stop/start buttons and RUN lights for each electrical motor or heater element shall be fitted in the panel door.

This panel shall be supplied with gland holes to accept 6 mm Ø air purge line for pressurization as a means of achieving acceptance for Zone 2 areas.

Engineering commissioning

The plant shall be commissioned with water to ensure that the plant is leak-free, no undue vibrations occur and all piping and equipment properly installed.

Valves

All control valves and solenoid valves shall be supplied by others.

Gaskets

Gasket and seal material shall be compatible with the ethanol and capable of

withstanding at least 170°C where applicable.

Cleaning

All burrs and sharp edges shall be removed.

All welds on stainless steel shall be purged during welding and pickled & passivated afterwards.

Acceptance

The plant shall be demonstrated to deliver the design parameters.

Inspection

The pilot plant design shall be approved by KVV prior to manufacturing.

All work shall be inspected by KVV after installation and a snag list shall be drawn up for completion by the contractor.

Documentation

Tag and number all valves.

All documentation and nameplates required by the OHS act for pressure vessels shall be supplied.

Final payment

Final payment shall only be made after completion of the snag list(s).

Contact person

If any other information is required please contact Elroy Goliath 083 463 4187 or goliath@kwv.co.za.

Scope of work

1. Supply and install pilot plant according to specification
2. Perform equipment commissioning.

E2. SCADA Specification for Process Control

E2 SCADA SPECIFICATION FOR PROCESS CONTROL

Introduction

Tenders are invited for the supply and installation of the software monitoring system and the provision of hardware to monitor the Alcohol Pilot Plant at KWW Paarl.

The pilot plant shall be skid mounted with flexible connections to process piping.

Tender documents shall be returned to KWW (fax 863 2933) marked for the attention of Elroy Goliath. Quote on all equipment marked "instr supplier" in the Equipment listing.

Applicable documents

The following are drawings / documents applicable to the pilot plant:

B015-001-21-R7	B015 Alcohol Pilot Plant – Process & Instrumentation Diagram
B015-001-01-R3	B015 Alcohol Column
Equipment Listing Rev 7	
Process Sequence Rev 2	

1 Standard

All work must be performed according to recognised and sound engineering principals.

The installation must conform to OHS act requirements.

Tenderers are hereby notified that the plant will be constructed and operated in a Zone 2 classified area and that a Hot Work Permit shall be obtained from the KWW before any work commences.

The system shall be of the same standard as existing FIX SCADA systems.

Description

A pump supplies ethanol ($\pm 96.4\%$ ambient temperature) from two feed tanks to the Alcohol columns via an evaporator. The feed to the columns can be manually regulated.

The evaporator is heated by means of an external electrical boiler fitted with electrical controls and safety valve(s).

Ethanol vapour is fed to one of the columns via a separator, which shall remove any droplets entrained with the vapour. The vapour passes through the column where impurities are removed. Once through the column the product is condensed in a condenser and stored in the product tank.

The system alternates between the two columns. While processing of the impurities occurs in one column, the other column is regenerated. Regeneration is performed under vacuum conditions. The pilot plant shall be designed to operate with nitrogen as regeneration medium. Nitrogen is fed via a flow meter through a heat exchanger

designed to heat nitrogen from ambient to 170°C. The heated nitrogen enters the column to be regenerated, heats the column and removes impurities. Nitrogen is expelled into atmosphere via the vacuum pump.

Vacuum is created by means of a vacuum pump and the waste product is condensed in a condenser prior to the vacuum pump. A separator separates condensable and non-condensable vapours.

The columns operate for approximately 4 minutes where after the column shall be regenerated with the regeneration medium for ± 4 minutes at the regeneration conditions.

Operation

The switching is achieved by switching a set of actuated valves. The process status of each valve for each operation is indicated on the Process Sequence Chart.

Each cycle for a column consists of four processes, i.e. blow down (create vacuum), regeneration (purge), equalisation & pressurisation and alcohol processing. Additional process such as heating and cooling of the columns shall occur during the processes. This information is contained in the Process Sequence Chart.

The process sequence is divided into several operations. Each operation is started by the end of the previous operation / process. Each operation / process is stopped and the next process started when a set of conditions are met. The processes and conditions are indicated on the Process Sequence Chart.

SPECIFICATION

SCADA system design

- a) The system shall be designed to accept inputs from the temperature probes, pressure sensors flow meters and analysers as indicated on the P&ID; operate and control a number of valves and one heat exchanger; record all parameters on timer and real time; generate batch numbers;
- b) Unique batch ID numbers shall be generated by the system. A batch is the duration of one cycle from the start of blow down (AD100) and re-pressurisation (AD200) to the end of pressure equalisation (both columns). A lot shall be an operator defined number of batches and the start and stop of a lot is determined by the operator. Lot and batch numbers shall be recorded.
- c) The system shall generate sample numbers, which includes the lot, batch and sample number. The operator shall accept the number and this number shall then be recorded.
- d) It shall be possible to run only one column at a time.
- e) Warm-up and start-up procedures shall be manual or automatic. (Manual means manual operation via the SCADA system.)

- f) A real time clock shall run together with a timer for each cycle / batch.
- g) Two pause modes shall be incorporated into the design, one pause mode shall pause the system immediately and the other shall pause the system at the end of the current cycle. Pausing is done by closing all valves (actuated and control). The process can then be resumed or stopped. The timer shall be paused as well. Once stopped the system shall revert to manual mode where the operator can operate the plant manually.
- h) Switch over is achieved by switching a number of solenoid valves. The sequencing of the valves is indicated on the Process Sequence Chart.
- i) The system shall provide outputs to the various solenoids for pneumatic actuated valves.
- j) Any valve can be opened and closed manually via the SCADA
- k) Equipment (connected to the SCADA) individually started and stopped when the system is not in operation. HX 500 will have four contactors of various ratings. These contactors shall be operated individually or in combinations.

Module Enclosure

Module Enclosure shall be equipped with communication modules to accommodate the inputs of the sensors as indicated on the P&ID.

The enclosure shall be large enough to accommodate at least three additional field modules for future expansion. It shall be mounted onto the pilot plant skid frame.

Field module

If the modules are not marked according to SABS 0108, the contractor shall supply test certificates (issued by approved testing authority) stating that the modules can be connected to instruments in Zone 1 areas where ethanol is distilled.

Safety features

The system shall not open the valves V101 and V201 when TT302 is not above a certain definable temperature.

Display

Process overview on one screen.

Other screens for the following:

- Display to indicate equipment status
- Indication of process sequence step; AD100 (Alcohol processing, Purge, Equalisation, etc.)
- Temperatures, pressures, flows, moisture analysis on screen display.

Graphs

Graphs shall display the following:

- TT101 – 108, TT302, TT501 °C vs time (s)
- TT201 – 208, TT302, TT501 °C vs time (s)
- PP101 – 102, PP201 – 202 mbar vs time (s)
- Moisture analysis of product concentration (ppm) vs time

Reports

Reporting shall conform to the following:

- Data written to Excel or Access files.
- Reports shall include lot number, automatic batch ID, accepted sample numbers, real time clock, timer for each batch and timer for process time, temperatures, pressures, flows, equipment status, etc – all process parameters.
- Recording shall be done for all parameters at any change in status of any equipment valves, heater elements. For a continuous changing parameter recording shall be done at time intervals.
- Totalise flow for nitrogen per process and batch.
- Addition of text for comments on reports, such as flow rate, tank levels / volume.

General

The contractor shall be in possession of a Hot Work Permit be issued by the KVV **before attempting any welding, grinding, cutting or any other hot work.**

Inspection

All work shall be inspected by KVV after installation and a snag list drawn up for completion by the contractor.

Final payment

Final payment shall only be made after completion of the snag list(s).

Documentation

Supply system documentation and manuals.

Supply all drawings, diagrams and schedules.

Contact person

If any other information is required please contact Elroy Goliath at 021 - 8073179

Scope of work

1. Supply and install field modules enclosure.
2. Supply control and actuated valves.
3. Install temperature and pressure sensors.

4. Supply and connect cabling between sensors and modules.
 5. Supply and install cabling between enclosures and the SCADA system.
 6. Supply and install cabling between the SCADA system and electrical panel.
 7. Supply all cabling diagrams and loop schedules.
 8. Perform all required calibrations.
 9. Perform commissioning of system.
- Supply all required documentation.

APPENDIX F

PLANT DESIGN INFORMATION

- F1. Technical Equipment Design Information
(Logichem)**
- F2. Plant Equipment Listing**
- F3. Adsorber Columns – Engineering Drawing
(Saturn Stainless)**
- F4. Process Construction Drawings
(Logichem)**
- F5. Technical Images**
- F6. MS Project Schedule**
- F7. Vacuum Pump Technical Data Sheets
(SS Pumps)**
- F8. Plate Heat Exchanger Specification
(Alfa Laval)**
- F9. Thermal Oil Data Sheet**

F1 TECHNICAL EQUIPMENT DESIGN INFORMATION

F1.1 VAPORISER (HX300)

F1.1.1 Duty

13 kW to vaporise and superheat 50 ℓ/hr ethanol at 96.4 vol. % at ± 15 °C and atmospheric conditions to 110 °C, using steam from the steam generator

F1.1.2 Specifications

Shell and tube heat exchanger, not coded, single pass with steam condensing on tube side and ethanol vaporising on shell side.

Shell side volume: 0.0071 m³

Shell side vaporisation area: 0.968 m²

Tube side volume: 0.0139 m³

Tube side condensation area: 0.8385 m²

Shell side pressure tested to 30 Bar.

F1.1.3 Material of construction

Shell: 150NB Schedule 40 pipe 304 SS

Tubes: 15.9 mm OD x 1.2 mm wall thickness x 600 long 304 SS tubes
33 off

Cone: 6 mm Thick plate 304L SS

Tube sheets: 6 mm thick rolled plate 304L SS

End cover: 10 mm thick plate 304L SS

F1.2 STEAM GENERATOR(HX301)

F1.2.1 Duty

15 kW to supply steam to vaporiser HX300 at 1.5 Bar and ± 24 kg/hr.

F1.2.2 Specifications

Closed cycle – steam boiler not coded, 15 kW water heating electrical element.

Internal volume: 0.01778 m³

Water volume: 0.009 m³

Pressure tested to 30 Bar.

F1.2.3 Material of construction

Shell: 150NB Schedule 40 CS pipe and fittings

F1.3 SEPARATOR(HX301)

F1.3.1 Duty

To ensure dry and slightly superheated alcohol vapour.

F1.3.2 Specifications

Tangential entry, vortex separation vessel, not coded, with 10 mm copper steam tracing on exterior to ensure superheated state.

F1.3.3 Material of construction

Shell: 150NB Schedule 40 pipe 304 SS

Cone: 6 mm thick rolled plate 304L SS

F1.4 VACUUM PUMP HEAT EXCHANGER (HX601)

F1.4.1 Duty

4 kW to cool vacuum pump seal water from ±30 °C to ±15 °C using chilled water.

F1.4.2 Specifications

Alfa Laval CB14-14H copper brazed plate heat exchanger complete with 14 plates in AISI 316 SS.

F1.5 CHILLER (CH550)

F1.5.1 Duty

To chill process water for cooling purposes by utilising compressed coolant and ambient air.

F1.5.2 Specifications

Daikin EUWA8GW air-cooled chiller, fitted with one scroll compressor and operate on R22-refrigerant.

Cooling capacity:	20.4 kW
Chilled water flow rate:	3.5 m ³ /hr
Evaporator pressure drop:	58 kPa
Unit size:	1254 x 1440 x 373
Operational weight:	192 kg

F1.6 CHILLED WATER CIRCULATION PUMP (PP551)

F1.6.1 Duty

Supply 3.5 m³/hr cooling water at 170 kPa to chiller

F1.6.2 Motor

0.37 kW 380/3/50H² electric motor closed coupled to pump

F1.7 NITROGEN HEATERS (HX500 ; HX520)

F1.7.1 Duty

1.5 kW to heat a maximum flowrate of 20 kg/hr nitrogen gas from ± 25 °C to either 120 °C or 170 °C.

F1.7.2 Specifications

Oil immersed tube cooling and 1.5 kW electrical oil heating element, contained in SS vessel with lid, not coded.

Internal volume:	0.085 m ³
Coil length:	9 m
Oil volume:	± 65 m

F1.7.3 Material of construction

Shell and lid: 1.6 mm thick rolled plate 304L SS

Coil: NW20 tube 304L SS

F1.8 PRODUCT CONDENSER (HX400)

F1.8.1 Duty

11 kW to condense the purified product at 50 ℓ/hr and vent all non-condensables using chilled water at ethanol at ± 10 °C.

F1.8.2 Specifications

Shell and tube heat exchanger, not coded, single pass with ethanol condensing on tube side and chilled water on the shell side.

Shell side volume: 0.0036 m³

Shell side cooling area: 0.49 m²

Tube side volume: 0.0059 m³

Tube side condensation area: 0.42 m²

Shell side pressure tested to 30 Bar.

F1.8.3 Material of construction

Shell: 150NB Schedule 40 pipe 304 SS

Tubes: 15.9 mm OD x 1.2 mm wall thickness x 300 long 304 SS
tubes 33 off

Cone: 5 mm Thick plate 304L SS

Tube sheets: 6 mm thick rolled plate 304L SS

End cover: 10 mm thick plate 304L SS

F1.9 VACUUM PUMP (VP600)

F1.9.1 Duty

Evacuate 20 kg/hr nitrogen and maintain a pressure of 170 mBar in the columns.

F1.9.2 Pump

Stork model P308 liquid ring vacuum pump, cast iron housing, gland packed, with bronze impellers.

Flow rate: 93 m³/hr nitrogen at 170 mBar and 120 °C

Seal water flow rate: 20 ℓ/min at STP

F1.9.3 Motor

4 kW 4-Pole IP55 380/3/50 TEFC electric motor Class II Div II via a fenner coupling. All mounted on a pre-fabricated mild steel base plate complete with a totally enclosed coupling guard.

F2. Plant Equipment Listing

Type	#	Discipline	Size	Type equipment	Item Description	Specification	Contractor	Manufacturer	Revision	
FI	301	Instr		Flow indicator		20°C; 2 barg; 40kg/h; ethanol	pilot plant supplier		rev8	delete manufacturer
FT	501	Instr		Flow transmitter		amb; 2 bar; 20kg/h; nitrogen	(supplied by KVV)	Endress & Hauser		
FT	502			(deleted)					rev8	
HX	300	Mech		Evaporator		20- 107°C; 0-2 barg; 40kg/h; ethanol; s/s	pilot plant supplier			
HX	301	Mech		Boiler		20°C-120°C; water	pilot plant supplier			
HX	400	Mech		Condenser	Shell & tube	107°C; 1 barg; 40kg/h; ethanol, nitrogen; s/s	pilot plant supplier			
HX	500	Mech		Heater	Oil bath heater - low temperature	amb - 110°C????; 2 barg; 0 - 20kg/h; nitrogen	pilot plant supplier		rev8	
HX	520	Mech		Heater	Oil bath heater - high temperature	amb - 190°C????; 2 barg; 0 - 20kg/h; nitrogen	pilot plant supplier		rev8	
HX	570	Mech		Heat exchanger	Compressed air cooler	80 - 25°C air, chiller water	(supplied by KVV)		rev8	
HX	601	Mech		Heat exchanger	Plate??	20-15°C; atm; 12l/min; water	pilot plant supplier			
HX	602	Mech		Heat exchanger	Spray direct cooler		pilot plant supplier			
HX	650			(deleted)					rev8	
IN	601			(deleted)					rev8	
MA	401	Instr		Moisture analyser	Moisture Target Series 5 Analyser & sample well	Panel mount & safety barrier	(supplied by KVV)	Panametrics		
PI	401	Instr		Pressure indicator		0-±2bar (abs), 75mm dial, taper thread 15NB	pilot plant supplier		rev8	Correct range
PI	501	Instr		Pressure indicator		0-±2bar (abs), 75mm dial, taper thread 15NB	pilot plant supplier		rev8	Previously 2x PI401
PI	551	Instr		Pressure indicator		0-±4barg, 75mm dial, taper thread 15NB	pilot plant supplier			
PI	601	Instr		Pressure indicator		0-±4barg, 75mm dial, taper thread 15NB	pilot plant supplier			
PI	602	Instr		Pressure indicator		0 - (-1) bar (g), 75mm dial, taper thread 15NB	pilot plant supplier		rev8	
PI	651			(deleted)					rev8	
PI	301	Instr		Pressure indicator		0-±4barg, 75mm dial, taper thread 15NB	pilot plant supplier			
PP	302	Mech		Feed pump		40kg/h; 1.5barg; ethanol	pilot plant supplier			
PP	551	Mech		Circulation pump		3500l/h; ??barg; water	pilot plant supplier			
PT	101	Instr	15NB	Pressure sensor		0 - 2bar(abs); 4-20mA; 170°C; 20:1 td	instr supplier	E&H / Wika		
PT	102	Instr	15NB	Pressure sensor		0 - 2bar(abs); 4-20mA; 170°C; 20:1 td	instr supplier	E&H / Wika		
PT	201	Instr	15NB	Pressure sensor		0 - 2bar(abs); 4-20mA; 170°C; 20:1 td	instr supplier	E&H / Wika		
PT	202	Instr	15NB	Pressure sensor		0 - 2bar(abs); 4-20mA; 170°C; 20:1 td	instr supplier	E&H / Wika		
PT	301	Instr	15NB	Pressure sensor		0 - 2bar (g); 4-20mA; 170°C; 20:1 td	instr supplier	E&H / Wika	rev8	
PT	652			(deleted)					rev8	
SG	551	Mech		Sight glass	Tank, tube		pilot plant supplier			
SG	651			(deleted)					rev8	
SG	951	Mech		Sight glass	Tank, tube		(supplied by KVV)			
SG	701	Mech		Sight glass	Tank, tube		(supplied by KVV)			
SG	801	Mech		Sight glass	Tank, tube		(supplied by KVV)			
SG	901	Mech		Sight glass	Tank, tube		(supplied by KVV)			
SP	301	Mech		Separator	Liquid separator; s/s	150diam x 250	pilot plant supplier			
SP	601	Mech		Separator	Separator & water supply tank		pilot plant supplier			
SP	651			(deleted)					rev8	
TI	301	Instr		Temperature indicator		0-100°C, 75mm dial, taper thread 15NB	pilot plant supplier		rev8	
TI	401	Instr		Temperature indicator		0-60°C, 75mm dial, taper thread 15NB	pilot plant supplier			
TI	402	Instr		Temperature indicator		0-60°C, 75mm dial, taper thread 15NB	pilot plant supplier			
TI	501	Instr		Temperature indicator		0-200°C, 75mm dial, taper thread 15NB	pilot plant supplier		rev8	
TI	521	Instr		Temperature indicator		0-200°C, 75mm dial, taper thread 15NB	pilot plant supplier		rev8	

Type	#	Discipline	Size	Type equipment	Item Description	Specification	Contractor	Manufacturer	Revision	
TI	571	Instr		Temperature indicator		0-60°C, 75mm dial, taper thread 15NB	pilot plant supplier		rev8	
TI	601	Instr		Temperature indicator		0-60°C, 75mm dial, taper thread 15NB	pilot plant supplier			
TI	602	Instr		Temperature indicator		0-60°C, 75mm dial, taper thread 15NB	pilot plant supplier			
TI	651			(deleted)					rev8	
TK	551	Mech		Tank, expansion			pilot plant supplier		rev8	existing
TK	700	KWV		Tank		(± 2000l)	(supplied by KWV)			
TK	800	KWV		Tank		(± 2000l)	(supplied by KWV)			
TK	900	KWV		Tank		(± 350l)	(supplied by KWV)		rev8	change volume
TK	950	KWV		Tank		(± 350l)	(supplied by KWV)		rev8	change volume
TT	101	Instr	15NB	Temperature sensor	PT100, s/s; no pocket	0-200°C; 0-3bar(abs); 3mm stem	instr supplier	E&H / Wika	rev8	no bayonet fitting
TT	102	Instr	15NB	Temperature sensor	PT100, s/s; no pocket	0-200°C; 0-3bar(abs); 3mm stem	instr supplier	E&H / Wika	rev8	no bayonet fitting
TT	103	Instr	15NB	Temperature sensor	PT100, s/s; no pocket	0-200°C; 0-3bar(abs); 3mm stem	instr supplier	E&H / Wika	rev8	no bayonet fitting
TT	104	Instr	15NB	Temperature sensor	PT100, s/s; no pocket	0-200°C; 0-3bar(abs); 3mm stem	instr supplier	E&H / Wika	rev8	no bayonet fitting
TT	105	Instr	15NB	Temperature sensor	PT100, s/s; no pocket	0-200°C; 0-3bar(abs); 3mm stem	instr supplier	E&H / Wika	rev8	no bayonet fitting
TT	106	Instr	15NB	Temperature sensor	PT100, s/s; no pocket	0-200°C; 0-3bar(abs); 3mm stem	instr supplier	E&H / Wika	rev8	no bayonet fitting
TT	107	Instr	15NB	Temperature sensor	PT100, s/s; no pocket	0-200°C; 0-3bar(abs); 3mm stem	instr supplier	E&H / Wika	rev8	no bayonet fitting
TT	108	Instr	15NB	Temperature sensor	PT100, s/s; no pocket	0-200°C; 0-3bar(abs); 3mm stem	instr supplier	E&H / Wika	rev8	no bayonet fitting
TT	201	Instr	15NB	Temperature sensor	PT100, s/s; no pocket	0-200°C; 0-3bar(abs); 3mm stem	instr supplier	E&H / Wika	rev8	no bayonet fitting
TT	202	Instr	15NB	Temperature sensor	PT100, s/s; no pocket	0-200°C; 0-3bar(abs); 3mm stem	instr supplier	E&H / Wika	rev8	no bayonet fitting
TT	203	Instr	15NB	Temperature sensor	PT100, s/s; no pocket	0-200°C; 0-3bar(abs); 3mm stem	instr supplier	E&H / Wika	rev8	no bayonet fitting
TT	204	Instr	15NB	Temperature sensor	PT100, s/s; no pocket	0-200°C; 0-3bar(abs); 3mm stem	instr supplier	E&H / Wika	rev8	no bayonet fitting
TT	205	Instr	15NB	Temperature sensor	PT100, s/s; no pocket	0-200°C; 0-3bar(abs); 3mm stem	instr supplier	E&H / Wika	rev8	no bayonet fitting
TT	206	Instr	15NB	Temperature sensor	PT100, s/s; no pocket	0-200°C; 0-3bar(abs); 3mm stem	instr supplier	E&H / Wika	rev8	no bayonet fitting
TT	207	Instr	15NB	Temperature sensor	PT100, s/s; no pocket	0-200°C; 0-3bar(abs); 3mm stem	instr supplier	E&H / Wika	rev8	no bayonet fitting
TT	208	Instr	15NB	Temperature sensor	PT100, s/s; no pocket	0-200°C; 0-3bar(abs); 3mm stem	instr supplier	E&H / Wika	rev8	no bayonet fitting; changed supplier
TT	301	Instr	15NB	Temperature sensor	PT100, s/s; thermowell	0-200°C; 0-3bar(abs)	instr supplier	E&H / Wika	rev8	no bayonet fitting; changed from PT 301
TT	302	Instr	15NB	Temperature sensor	PT100, s/s; no pocket	0-200°C; 0-3bar(abs)	instr supplier	E&H / Wika	rev8	no bayonet fitting; changed supplier
TT	501	Instr	15NB	Temperature sensor	PT100, s/s; thermowell	0-200°C; 0-3bar(abs)	instr supplier	E&H / Wika	rev8	no bayonet fitting; changed supplier
TT	502	Instr	15NB	Temperature sensor	PT100, s/s; no pocket	0-200°C; 0-3bar(abs)	instr supplier	E&H / Wika	rev8	no bayonet fitting; changed supplier
TT	521	Instr	15NB	Temperature sensor	PT100, s/s; thermowell	0-200°C; 0-3bar(abs)	instr supplier	E&H / Wika	rev8	no bayonet fitting; changed supplier
V	101	Valve	40NB	Valve, solenoid	V-Flow 3-piece ball, butt weld; pneumatic; s/s	0 - 2barg; 170°C; ethanol; nitrogen; bi-direc	instr supplier	Worcester		
V	102	Valve	50NB	Valve, solenoid	V-Flow 3-piece ball, butt weld; pneumatic; s/s	0 - 2barg; 170°C; ethanol; nitrogen; bi-direc	instr supplier	Worcester		
V	103	Valve	40NB	Valve, control	V-Flow 3-piece ball, butt weld; pneumatic; s/s	0 - 2barg; 170°C; ethanol; nitrogen; bi-direc	instr supplier	Worcester		
V	105	Valve	40NB	Valve, solenoid	V-Flow 3-piece ball, butt weld; pneumatic; s/s	0 - 2barg; 170°C; ethanol; nitrogen; bi-direc	instr supplier	Worcester		
V	106	Valve		Valve	Safety	0.4 barg setting	pilot plant supplier			
V	201	Valve	40NB	Valve, solenoid	V-Flow 3-piece ball, butt weld; pneumatic; s/s	0 - 2barg; 170°C; ethanol; nitrogen; bi-direc	instr supplier	Worcester		
V	202	Valve	50NB	Valve, solenoid	V-Flow 3-piece ball, butt weld; pneumatic; s/s	0 - 2barg; 170°C; ethanol; nitrogen; bi-direc	instr supplier	Worcester		
V	203	Valve	40NB	Valve, control	V-Flow 3-piece ball, butt weld; pneumatic; s/s	0 - 2barg; 170°C; ethanol; nitrogen; bi-direc	instr supplier	Worcester		
V	205	Valve	40NB	Valve, solenoid	V-Flow 3-piece ball, butt weld; pneumatic; s/s	0 - 2barg; 170°C; ethanol; nitrogen; bi-direc	instr supplier	Worcester		
V	206	Valve		Valve	Safety	0.4 barg setting	pilot plant supplier			
V	301	Valve		Valve, control	Ball	0 - 3barg; 30°C; ethanol	pilot plant supplier		rev8	
V	302	Valve		Valve	Safety valve evaporator		pilot plant supplier			
V	303	Valve		Valve, shut off	Hand	0 - 2barg; 120°C; ethanol	pilot plant supplier			
V	304	Valve		Valve, drain		1 - 2barg; 100°C; ethanol	pilot plant supplier		rev8	Correct range
V	401	Valve	10NB	Valve, sample	Hand	0 - 2barg	pilot plant supplier		rev8	
V	403	Valve	25NB	Valve, control	Hand	0 - 2barg	pilot plant supplier			
V	404	Valve	15NB	Valve, air vent			pilot plant supplier			
V	501	Valve		Valve, solenoid	V-Flow 3-piece ball, butt weld; pneumatic; s/s	0 - 2barg; 170°C; ethanol; nitrogen	instr supplier	Worcester	rev8	

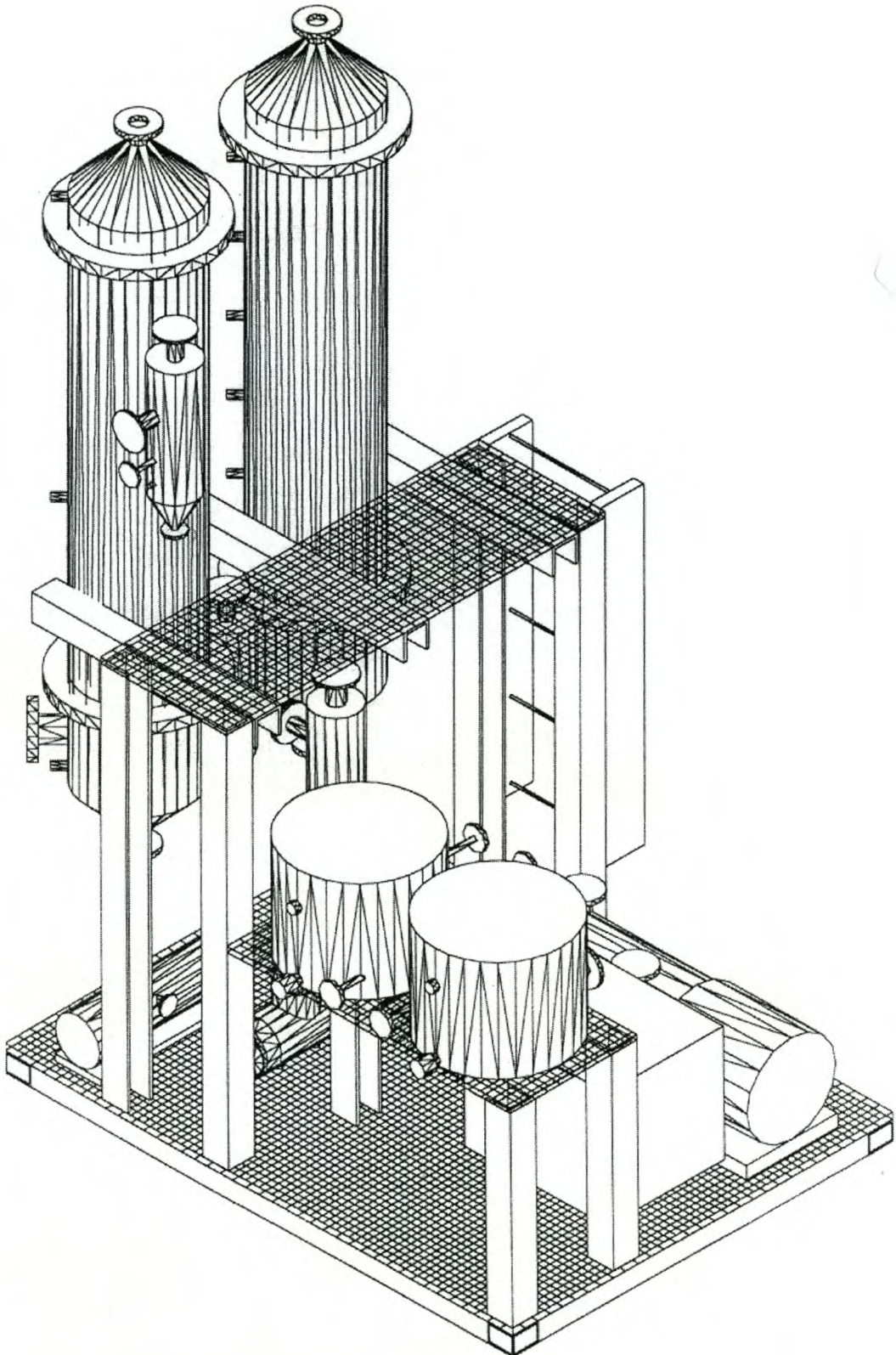
Type	#	Discipline	Size	Type equipment	Item Description	Specification	Contractor	Manufacturer	Revision
V	502	Valve		PRV	Pressure regulator valve	16 - 5bar (g) nitrogen	(supplied by KVV)	Afrox	rev8
V	503	Valve		Valve, solenoid		Nitrogen	instr supplier		rev8
V	504	Valve		PRV	Pressure regulator valve	5 - 0bar (g) nitrogen	(supplied by KVV)	Afrox	rev8
V	505	Valve		Valve, drain			pilot plant supplier		rev8
V	523	Valve		Valve, solenoid		Nitrogen	instr supplier		rev8
V	525	Valve		Valve, drain			pilot plant supplier		rev8
V	551	Valve		Valve, drain			pilot plant supplier		
V	552	Valve		Valve, drain			pilot plant supplier		rev8
V	601	Valve		Valve, shut off	Hand	Water	(supplied by KVV)		
V	602	Valve		Valve	Ball float	Water	pilot plant supplier		rev8
V	603	Valve	25NB	Valve	Air bleed	0 - 1 bar(abs)	pilot plant supplier		
V	604	Valve	15NB	Valve, control	Hand	0 - 2barg	pilot plant supplier		
V	605	Valve	15NB	Valve	Hand	0 - 2bar(abs)	pilot plant supplier		
V	605	Valve	15NB	Valve, drain	Hand	Water	pilot plant supplier		
V	606	Valve		Valve, control	Hand				rev8
V	607	Valve	50NB	Valve, non return					rev8
V	651	Valve		(deleted)					rev8
V	652	Valve		(deleted)					rev8
V	653	Valve		(deleted)					rev8
V	654	Valve		(deleted)					rev8
V	901	Valve	15NB	Valve, shut off	Hand	20°C; 0 - 1barg; ethanol	pilot plant supplier		
V	951	Valve	15NB	Valve, shut off	Hand	20°C; 0 - 1barg; ethanol	pilot plant supplier		
V	701	Valve	15NB	Valve, shut off	Hand	20°C; 0 - 1barg; ethanol	pilot plant supplier		
V	801	Valve	15NB	Valve, shut off	Hand	20°C; 0 - 1barg; ethanol	pilot plant supplier		
VP	600	Mech		Vacuum pump	liquid ring vacuum pump	20kg/h; 100mbar(abs); nitrogen;	pilot plant supplier		
		Consum		Molecular sieve	MS 564 CS		(supplied by KVV)	Grace Davison	
		Consum		Molecular sieve	MS 512 C		(supplied by KVV)	Grace Davison	
		Consum		Ceramic balls	3 mm		(supplied by KVV)	SAG Ceramics	
		Consum		Ceramic balls	6 mm		(supplied by KVV)	SAG Ceramics	
		Services		Nitrogen supply			(supplied by KVV)	Afrox	
		Services		Nitrogen rental			(supplied by KVV)	Afrox	rev8
		Services		Compressor			(supplied by KVV)		

F3. Adsorber columns – Engineering Drawing
(Saturn Stainless)

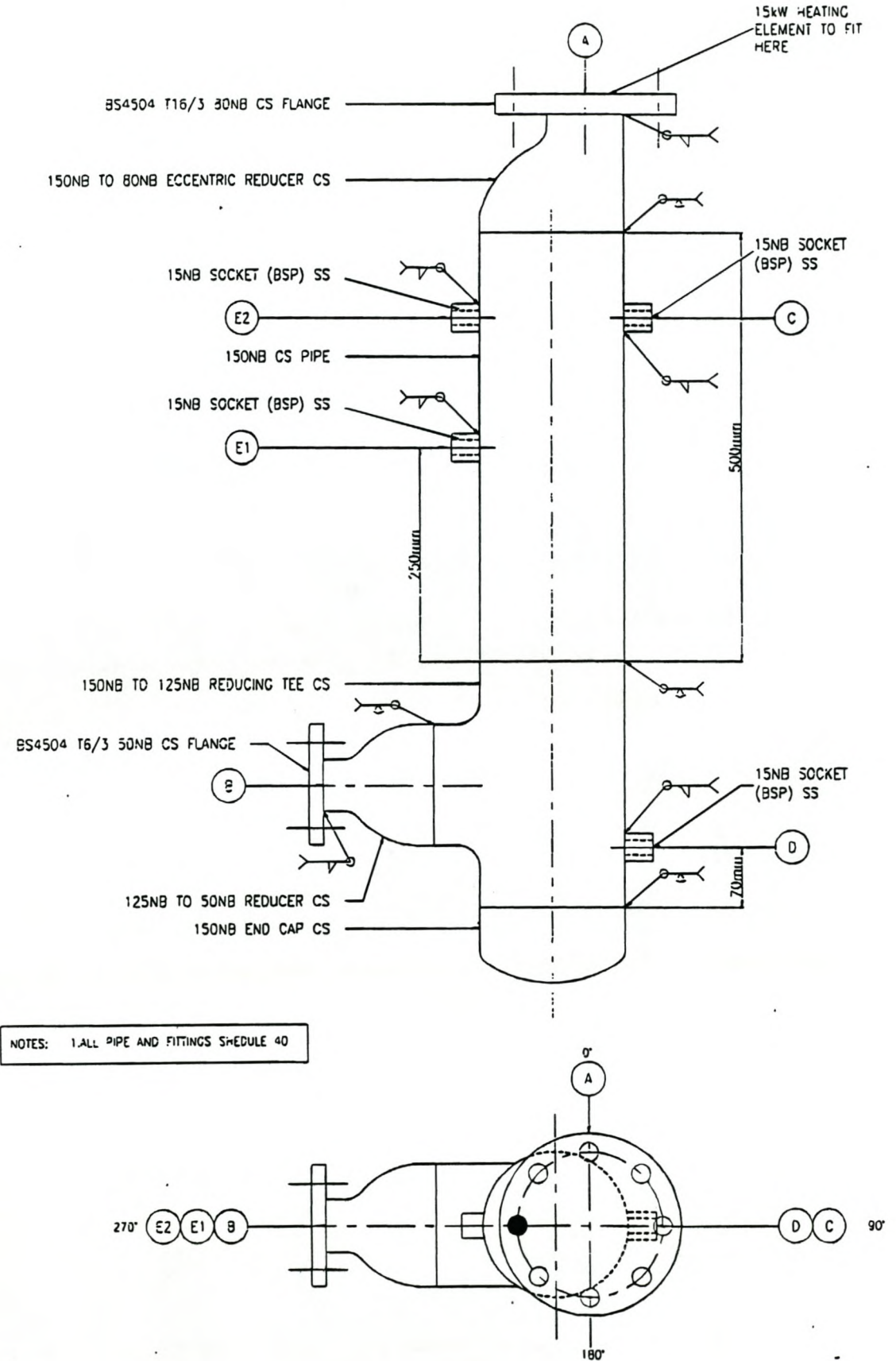
F3. Adsorber columns – Engineering Drawing
(Saturn Stainless)

**F4. Process Construction drawings
(Logichem)**

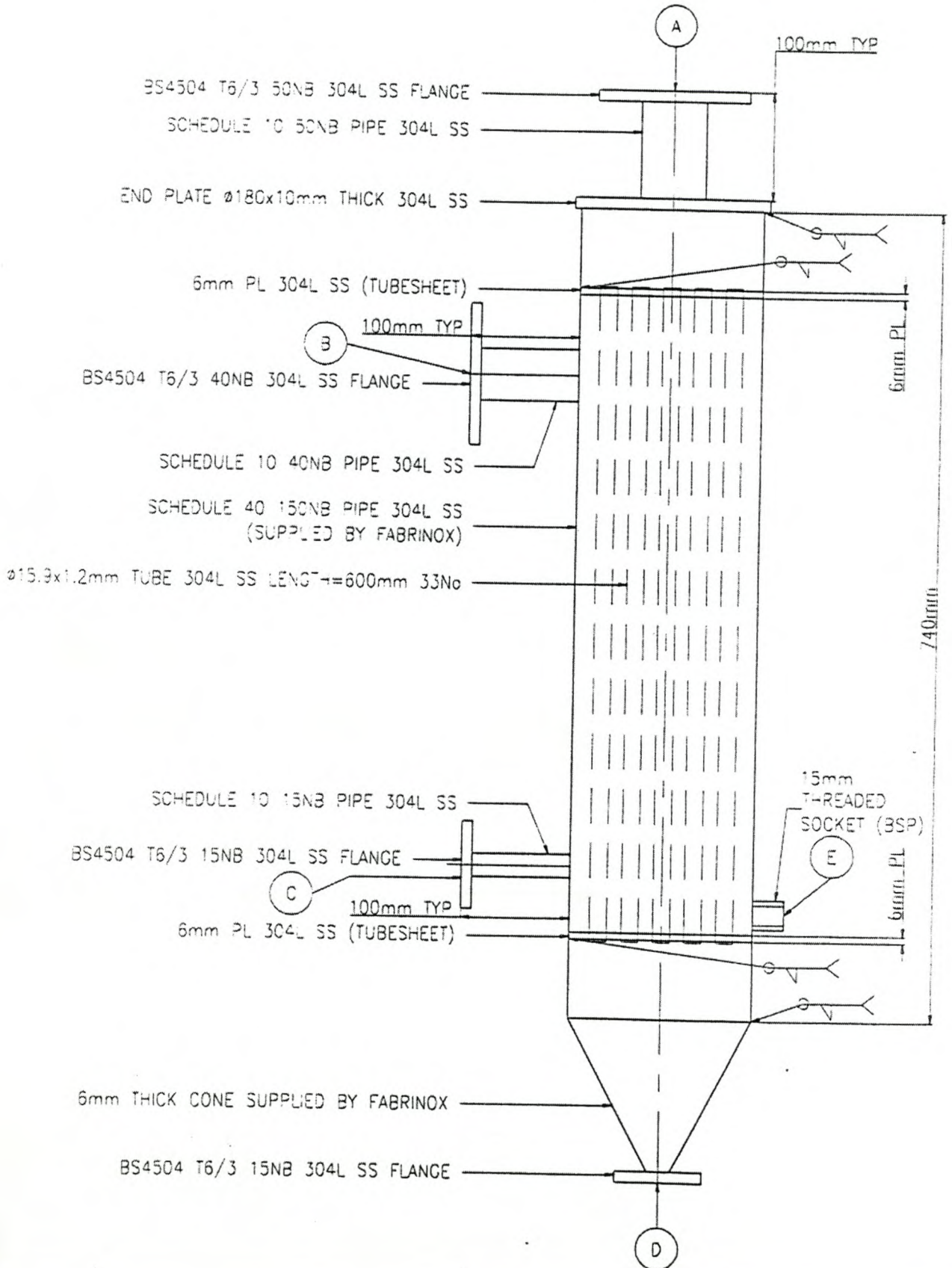
ISOMETRIC PLANT LAYOUT



STEAM GENERATOR - HX301

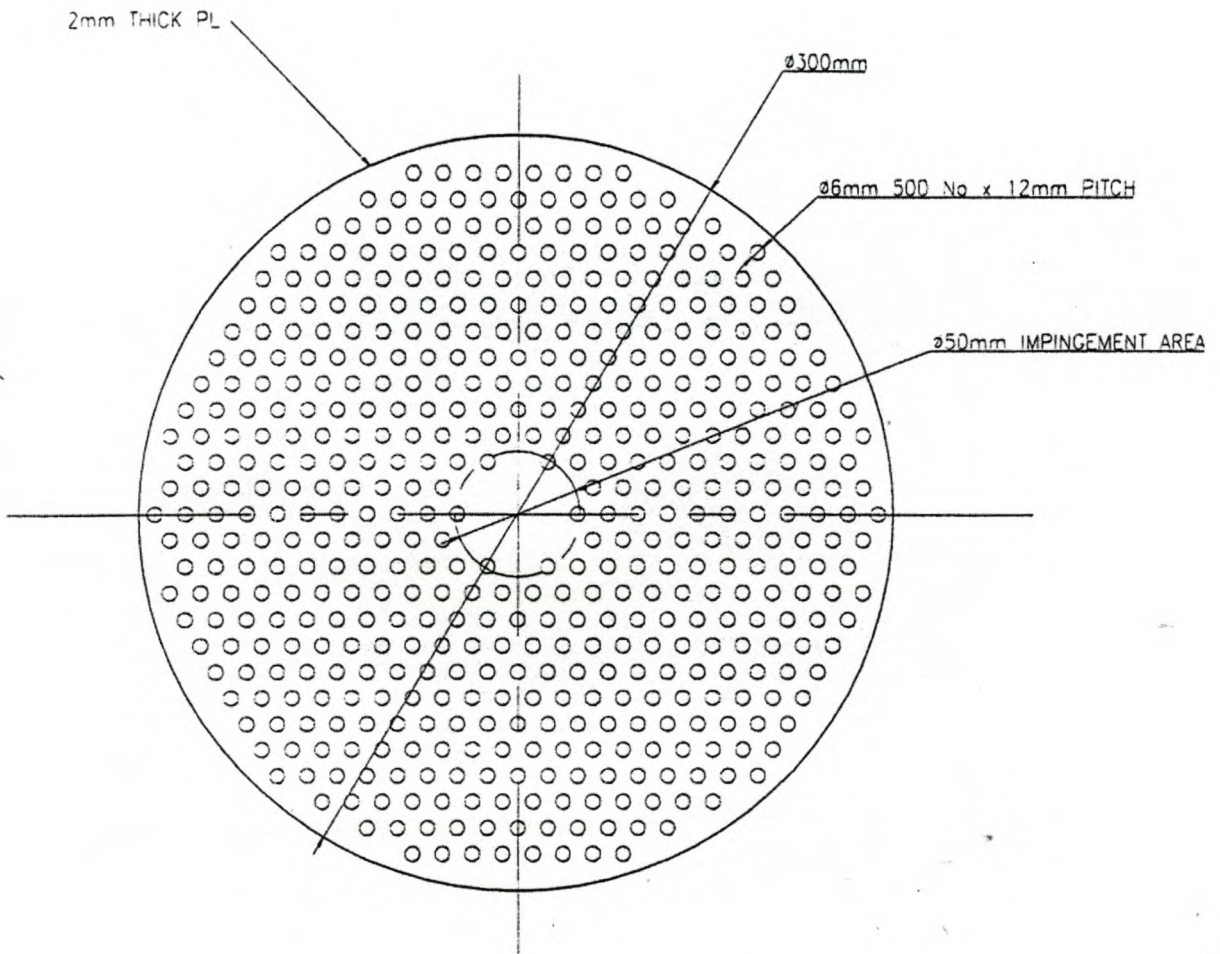


VAPORISER - HX300

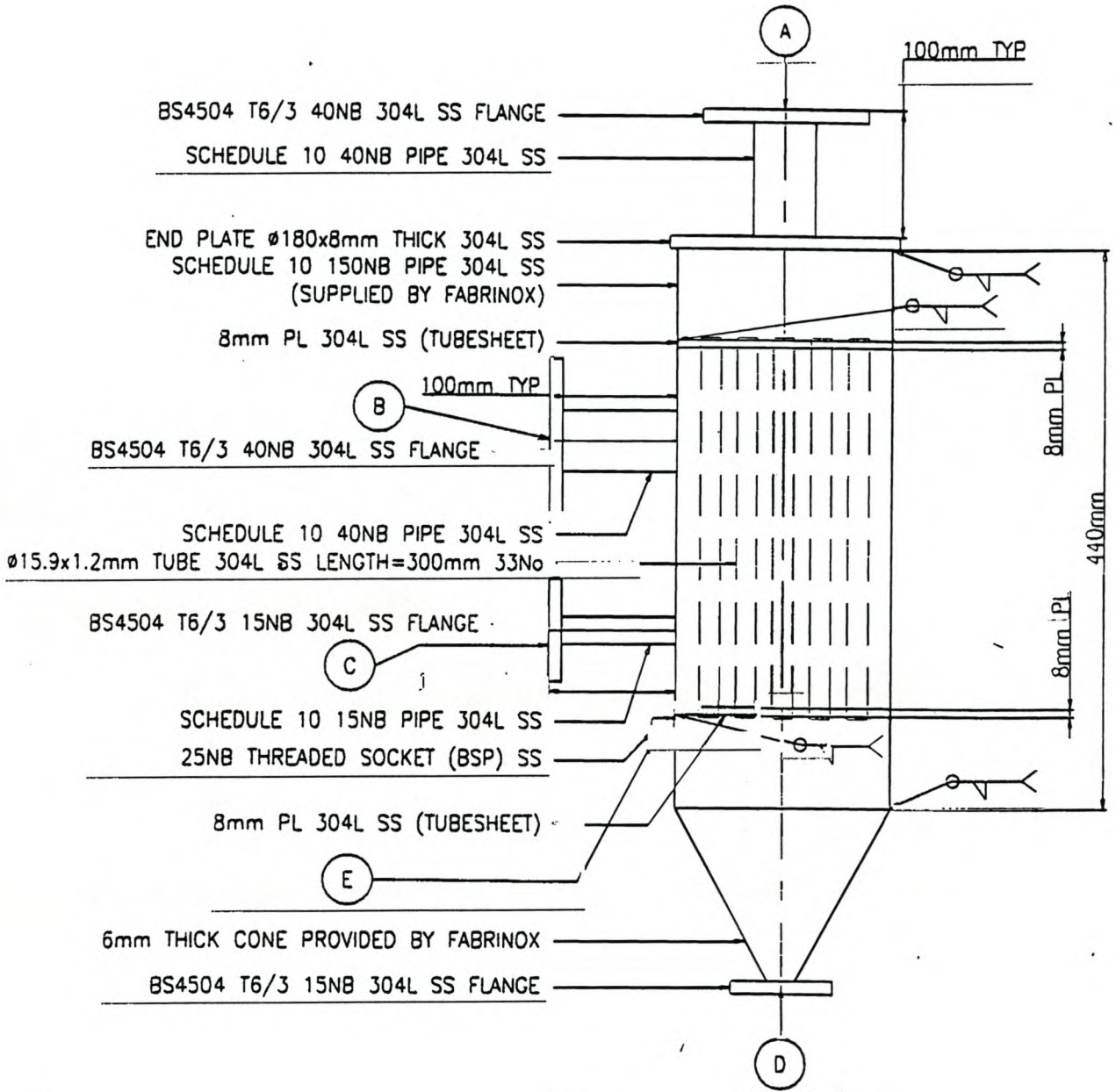


GAS DISTRIBUTION PLATE

NOTES: 1.MATERIAL 304L SS
2.QUANTITY 2



PRODUCT CONDENSER-HX400

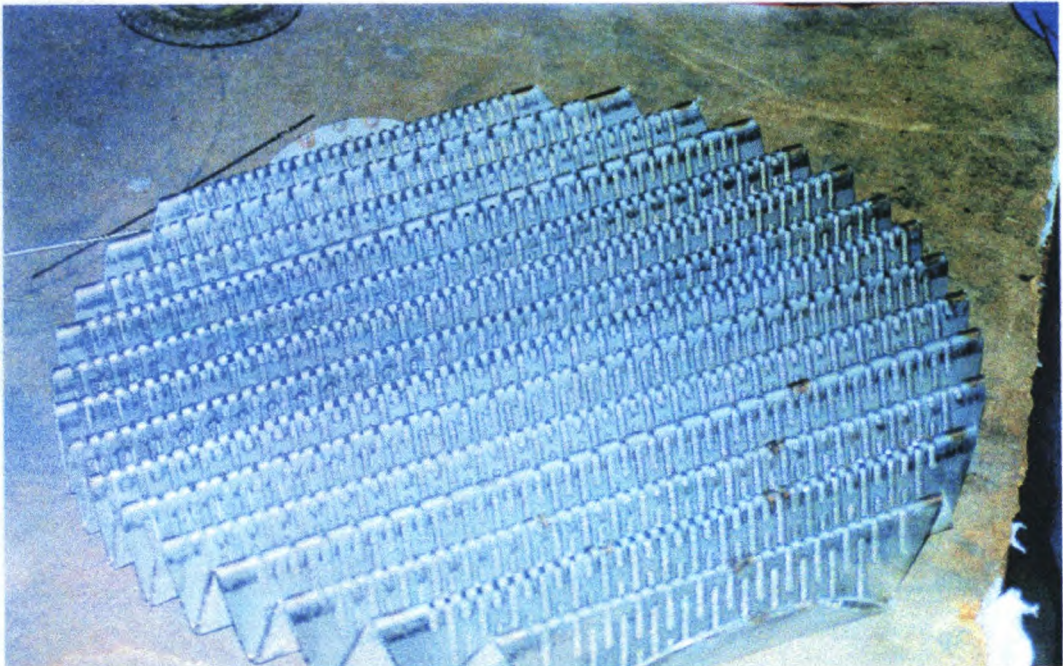


F5. Technical images

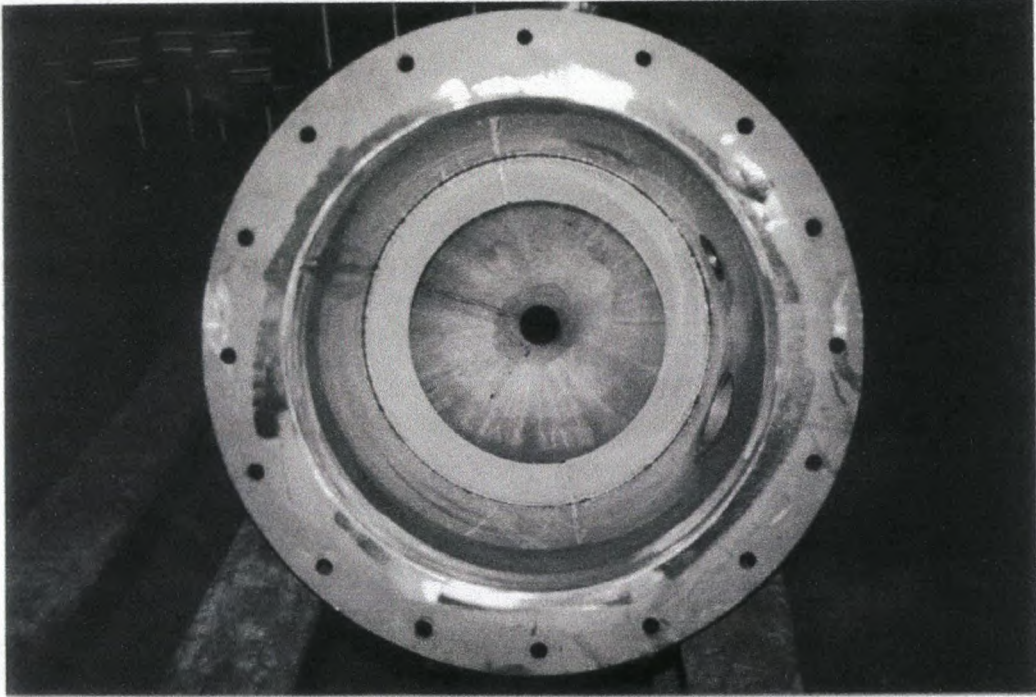
MOBILITY OF SKID



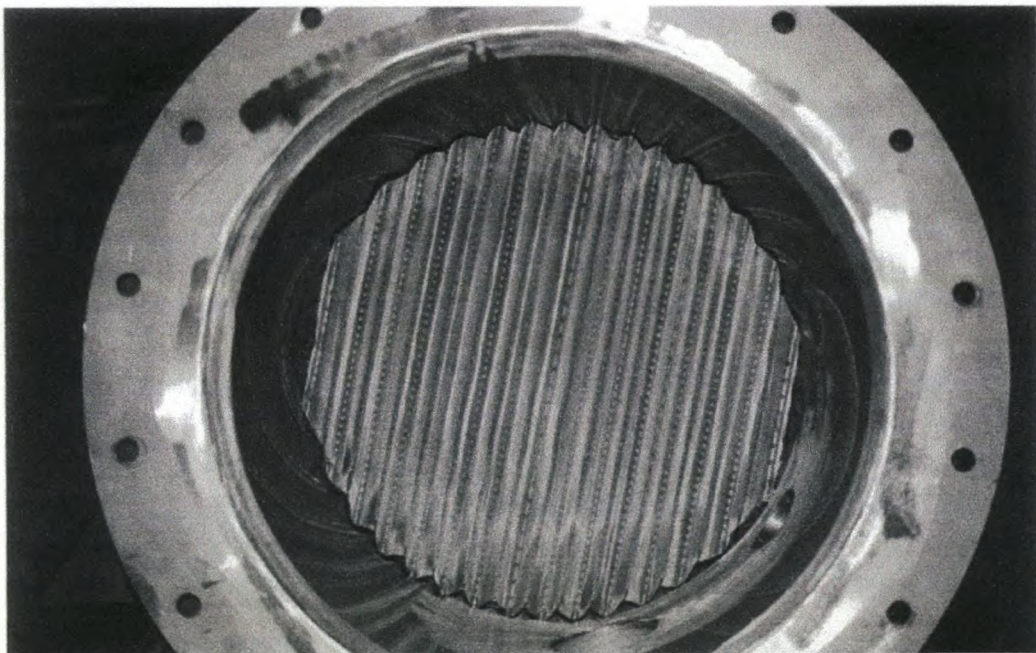
CORRUGATED BED SUPPORT



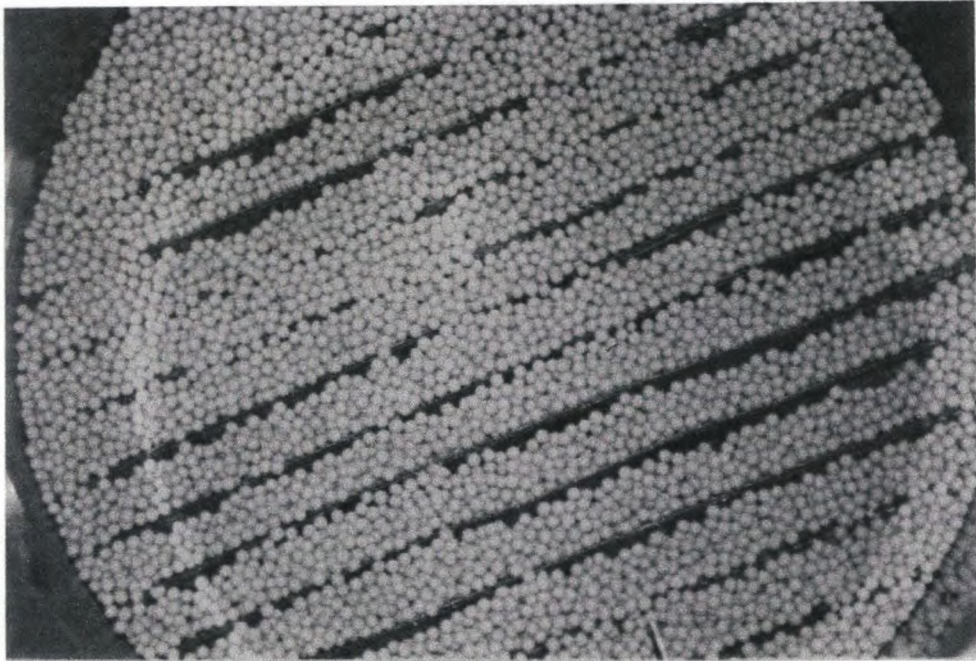
RING SUPPORT



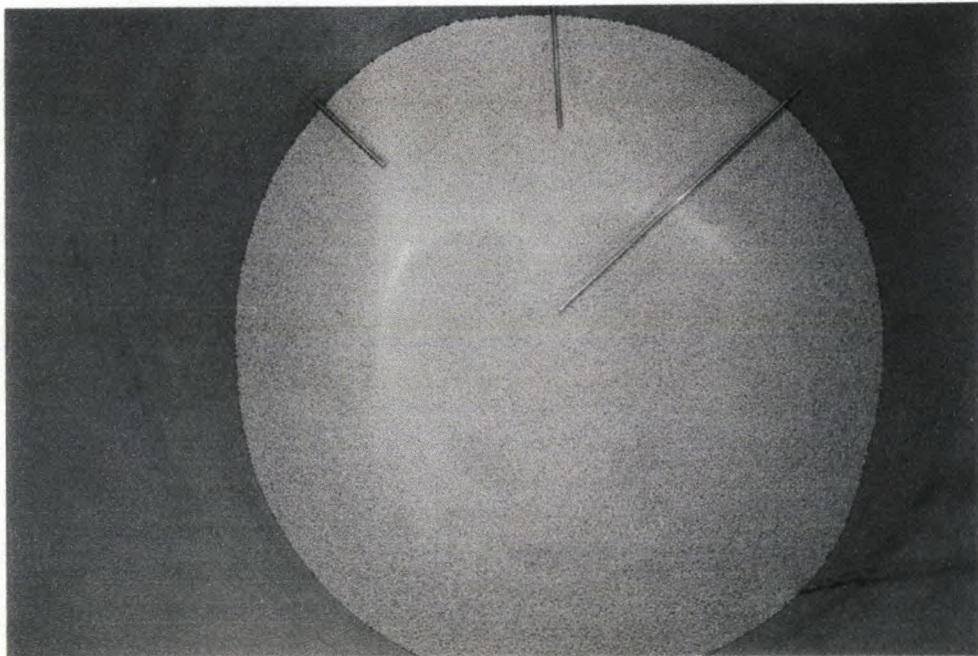
CORRUGATED PLATE FITTING



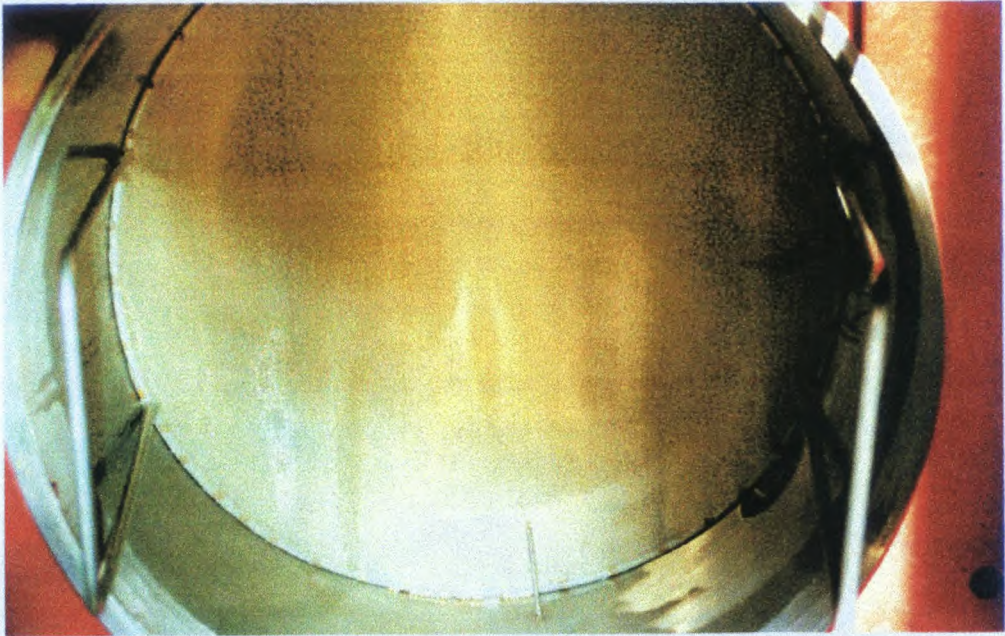
CERAMIC BEAD BED SUPPORT



POSITION OF RADIAL THERMOCOUPLES

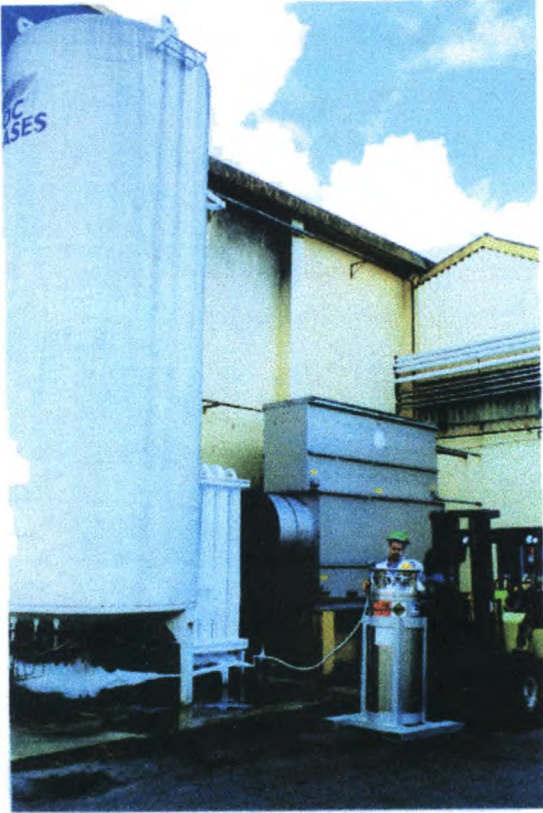


SEPARATION OF BEDS



OIL HEATER



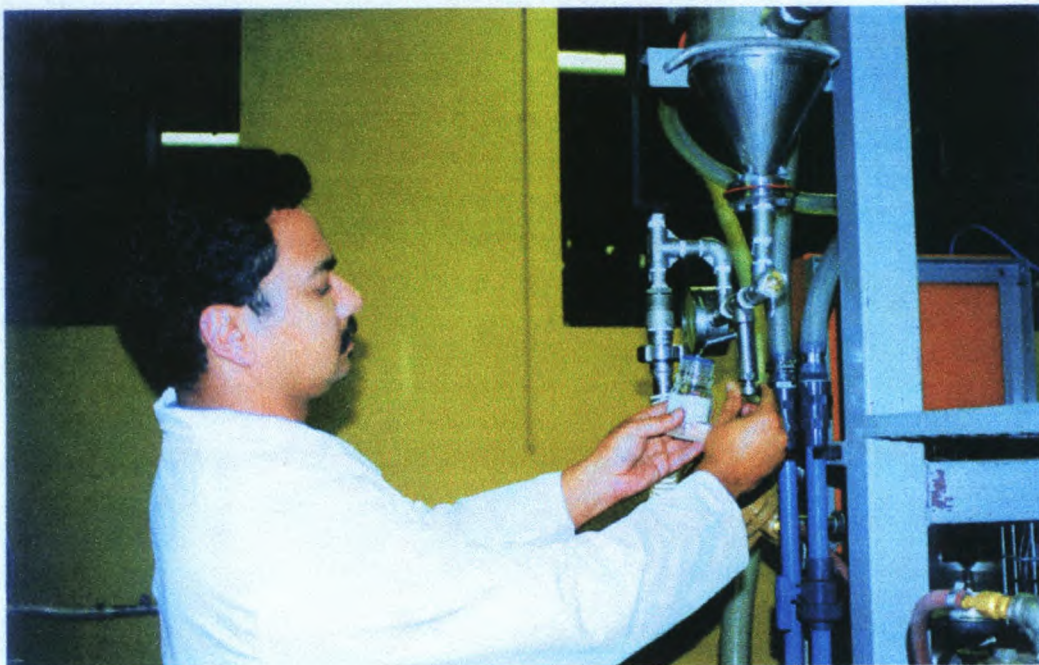


NITROGEN LOADING TO PCC

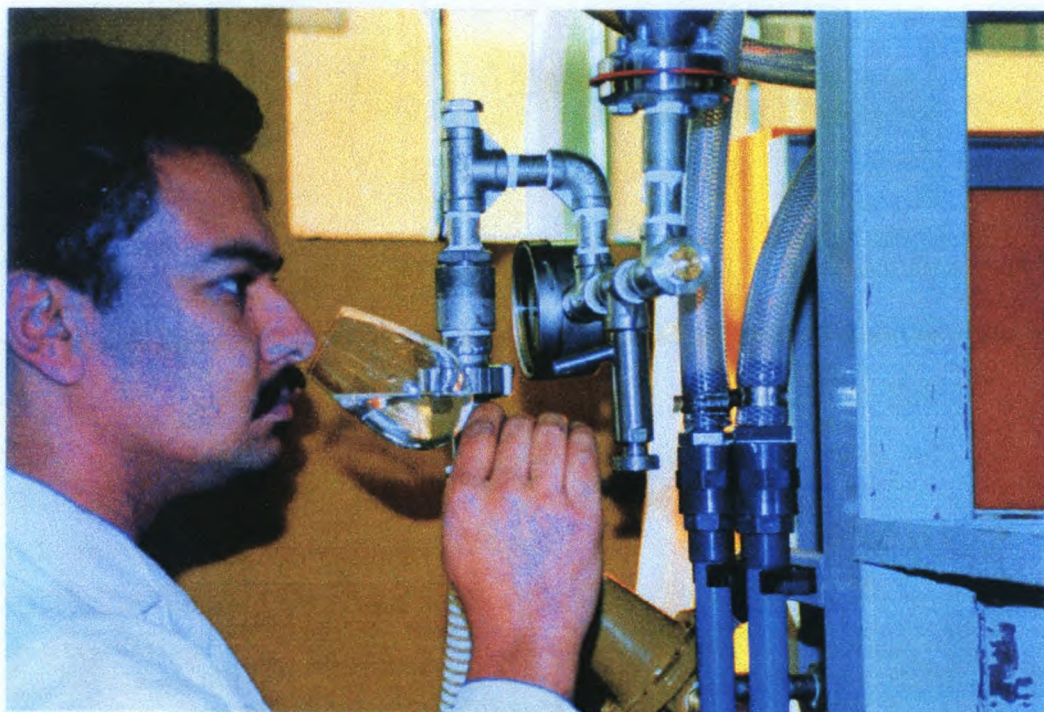


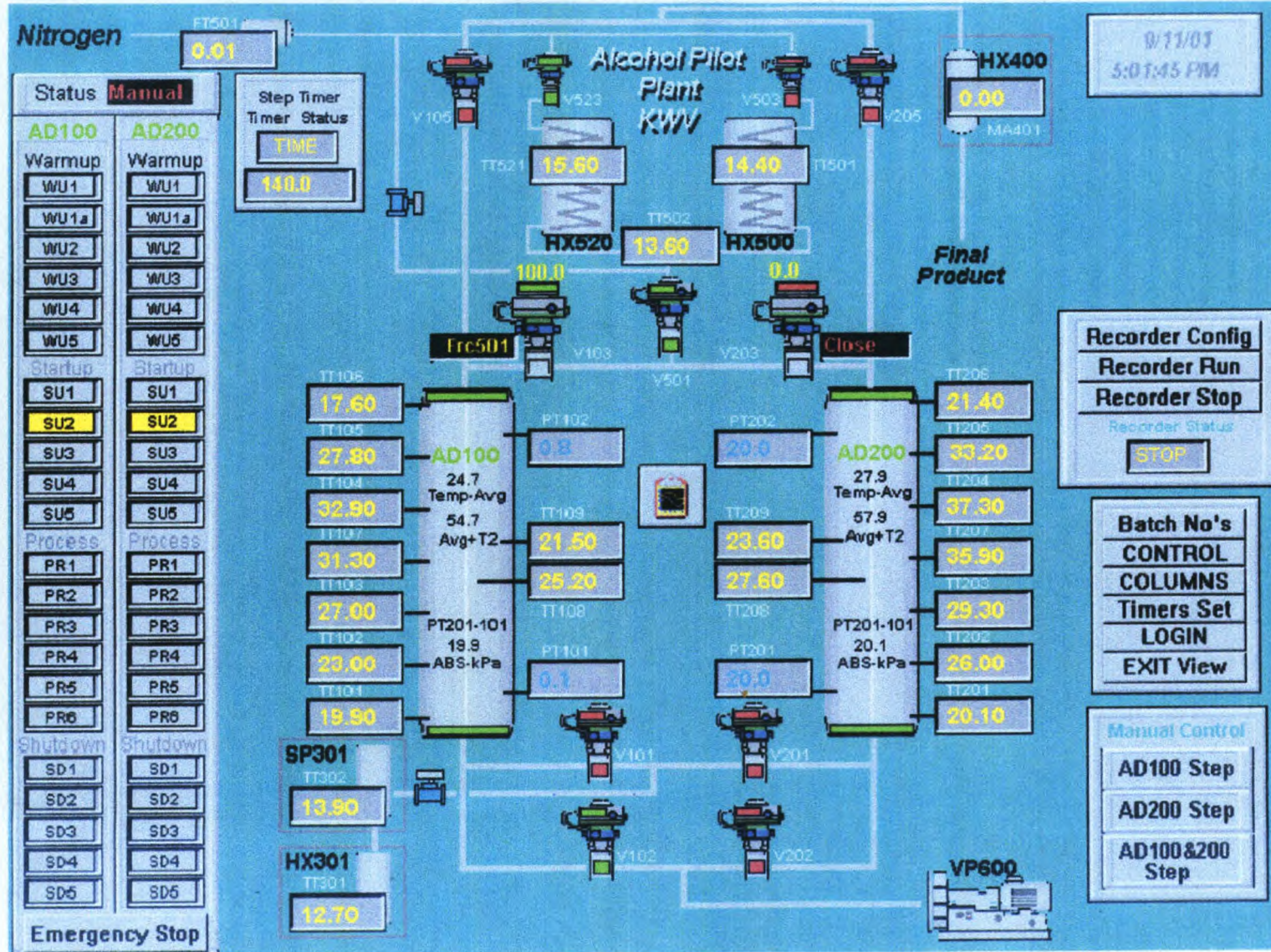
INSULATED COLUMNS

SAMPLING



ORGANOLEPTIC EVALUATION





PROCESS CONTROL SCREEN

F6. MS Project Schedule

F7. Vacuum Pump Technical Data Sheets
(SS Pumps)



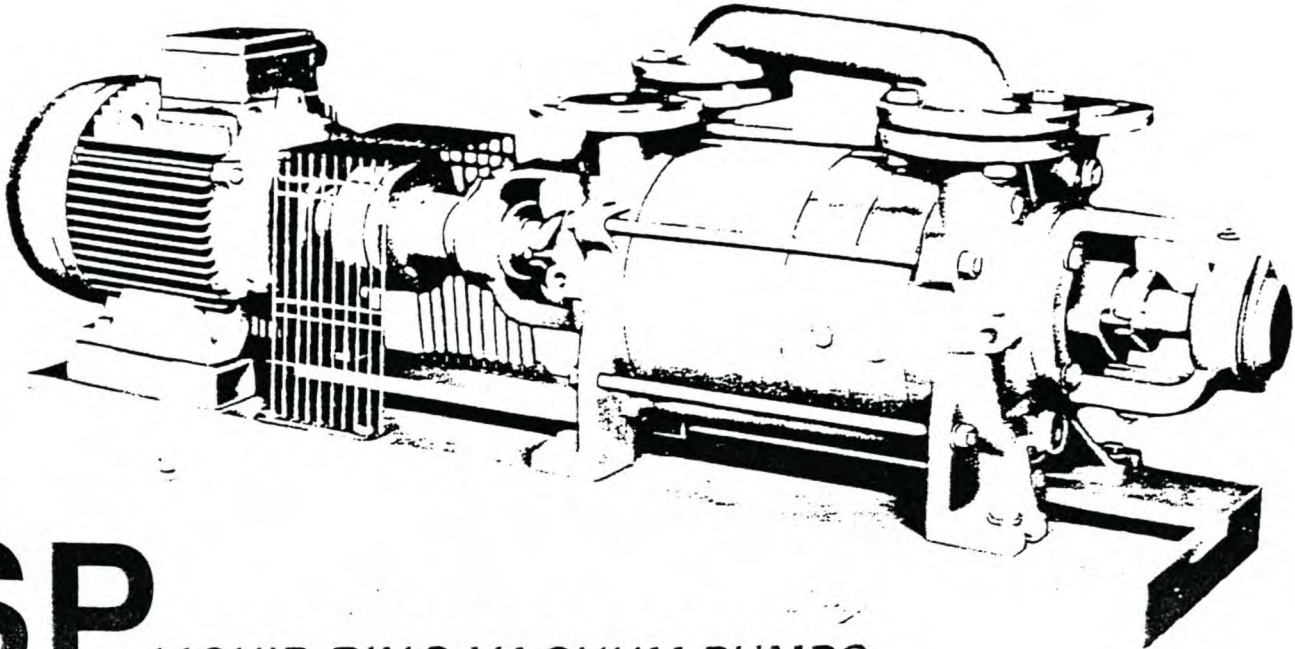
SOUTHERN PUMPS S.A. (PTY) LIMITED

Reg. No. 35/02322/07

P.O. Box 519 Milnerton 7435 Cape Town
48 Marconi Road Montague Gardens 7441
Telephone (021) 551-2490
Fax (021) 551-3088 / 551-5365
e-mail: sosa@ct.ia.net.za

JOHNSON PUMP

Branches: Johannesburg and Durban. Distributors throughout South Africa



SP LIQUID RING VACUUM PUMPS

APPLICATIONS

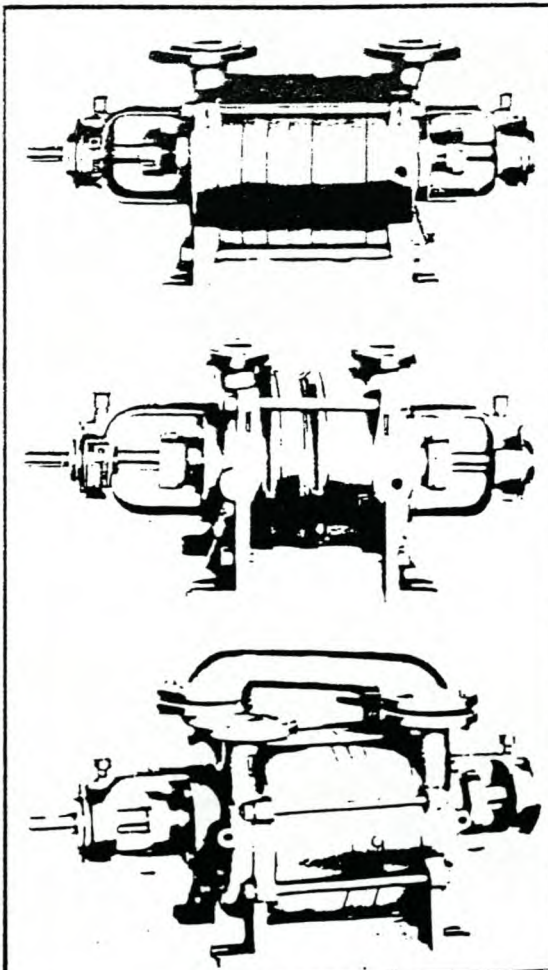
These pumps are designed to handle liquids, vapours also with liquid parts in suspension. They are used in chemical, pharmaceutical, food, textile, and paper industries and everywhere there is a necessity of evaporation, distillation, pulverization or impregnation vacuum and so on.

OPERATION

These liquid ring vacuum rotaries are pumps for high and middle vacuum.

ROTATION

Standard rotation, viewed from drive end, for P200 size rotation is anticlockwise.



STANDARD CONSTRUCTION

Casings, plates and impeller housings in high quality cast iron; impellers in gunmetal; 13% chromium stainless steel shaft (AISI 420); seals by packing rings, with easily adjustable glands, complete with lantern ring device for flushing and hydraulic barrage (with exception of P200 and P300 sizes).

BEARING

Two grease lubricated bearings, mounted in substantial cast iron bearing housings at both pump ends.

FLANGES

For P200 size: oval flanges with 1 1/4" gas threaded counter-flanges; for other sizes: round flanges in compliance with UNI 2223-29 PN 10 standards.

Performance data

(tolerance 10%)

SIZE	Ø Branches	R.P.M.	Vacuum (mmHg) measured on pump suction flange and relative to a barometric pressure of 760 mmHg. Capacity (m³/h) of rarified clean air, sucked using as service liquid water at temperature of 15 °C. Absorbed power (HP) measured at pump spindle.														Service liquid capacity liters/min (*)			
			500 mmHg		600 mmHg		650 mmHg		680 mmHg		700 mmHg		720 mmHg		730 mmHg				735 mmHg	
			m³/h	HP	m³/h	HP	m³/h	HP	m³/h	HP	m³/h	HP	m³/h	HP	m³/h	HP			m³/h	HP
SP 202	32	1450	13	0.95	14	0.95	14	0.95	15	1.05	14	1.05	9.5	1.05	6	1	-	-	2.5	4
SP 204	32		33	1.6	34	1.6	33	1.4	30	1.35	25.5	1.35	18.5	1.35	13	1.35	-	-	6	8
SP 304	40		53	3.3	53	3.3	52	3.3	51	3.3	47	3.3	38	3.3	29	3.3	22	3.3	12	19
SP 308	40		100	4.4	100	4.4	97	4.4	94	4.2	90	4	80	3.9	65	3.8	52	3.8	14	24
SP 412	40		130	4.8	132	4.8	138	4.8	140	4.6	143	4.5	122	4.4	95	4.2	76	4.2	19	30
SP 416	40		140	6	150	6	174	5.9	180	5.8	185	5.7	160	5.6	128	5.5	100	5.5	24	35
SP 512	50		275	10	285	9.8	285	9.5	275	9.3	255	9.3	220	9.2	185	9.1	162	9	32	50
SP 516	50		315	12	340	12	350	11.3	340	10.7	325	10.4	280	10.3	230	10.1	185	10	37	58
SP 520	50		380	14.7	415	14.7	420	13.6	415	13.2	390	12.7	330	12.6	265	12.1	213	12	45	75
SP 616	80		510	21	540	21	540	20.5	530	20.5	495	20.5	420	20	330	19.5	-	-	70	110
SP 624	80		720	30	780	28	785	27.5	750	27	690	26	530	26	415	25.5	-	-	90	130
SP 720	100		960	800	34	880	33	895	31.5	860	31	825	29.5	735	29	640	28	-	-	95
SP 730	100	1200		47	1270	45	1270	43	1230	43	1180	42.5	970	40	780	39	-	-	110	140
SP 740	100	1270		52	1470	51	1620	49	1620	47	1530	46.5	1280	45	1030	44.5	-	-	120	150
SP 835	150	735	1780	79	2020	78	2050	75	2050	70	2000	68	1770	64	1390	62	-	-	160	230
SP 845	150		2100	97	2410	94	2650	91	2610	87	2470	83	2100	79	1760	76	-	-	190	260
SP 855	150		2450	113	3000	113	3180	106	3160	100	3020	95	2650	90	2170	89	-	-	230	300

SPECIAL CONSTRUCTIONS

Main materials in contact with gas and service liquid:

B* = «304» stainless steel

C = «316» stainless steel

D* = Gunmetal with AISI 316 stainless steel shaft

E* = Tin bronze with AISI 316 stainless steel shaft

F = All cast iron and steel (copper and it's alloys excluded)

G = Nodular cast iron

L = Alloy «20» (ASTM A296 CN-7M) with shaft in ASTM B425

M = Alloy «C» (ASTM A494 CW-12M-1)

? = Other materials available

*) Available from P500 size on

The powers stated on the table refer to operation with service liquids having specific gravity = 1Kg/dm³ and viscosity = 1° Engler ; stated values increase using service liquids with higher specific gravity and viscosity and in case of removal of both air and liquid. Capacities decrease if the temperature of service liquid is higher than 15 °C, if barometric pressure is lower than 760 mmHg and if there is removal of both air and liquid.

During operation the service liquid must be sent to the pump continuously.

For the construction «B» - «C» - «L» - «M», the capacity values stated on the table bear an average decrease of 10%.

PECIAL FEATURES

= Impellers in «316» with shaft in AISI 420 stainless steel

= Special packing

= Chromium plated shaft

= Single mechanical seal

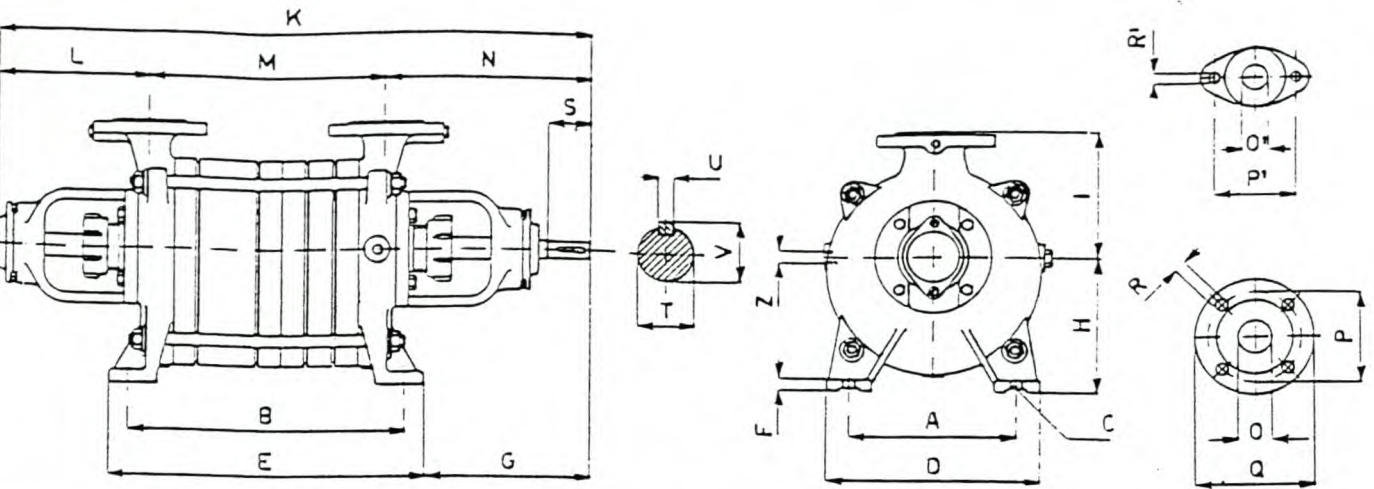
= Double mechanical seal

= Special flanges

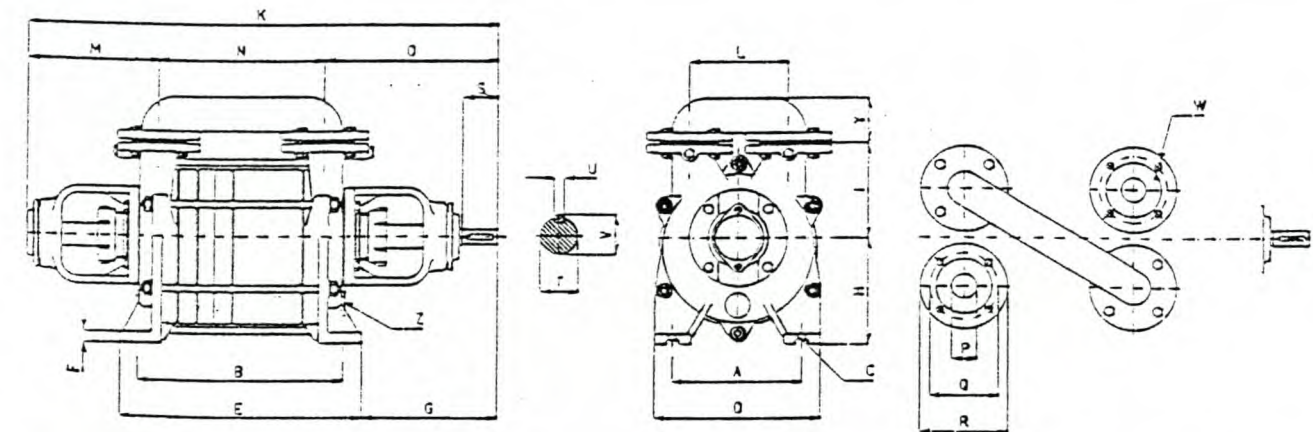
= Double drive shaft

= Other features on request

(*) N.B.: The values (il') stated on the table are respectively referred to: max fresh liquid consumption in case of partial re-circulation of service liquid (on the left); max fresh liquid consumption in case of direct feed with service liquid to lose (on the right).



SIZE	A	B	C	D	E	F	G	H	I	K	L	M	N	O	P	Q	R	O'	P'	R'	N.	S	T	U	V	Z	kg. Weight
SP 202	180	196	14	220	240	16	178	132	135	548	183	134	231	-	-	-	-	32	95	14	2	45	18	6	20.5	3/8"	34
SP 204	180	226	14	220	270	16	178	132	135	578	183	164	231	-	-	-	-	32	95	14	2	45	18	6	20.5	3/8"	38
SP 304	200	290	14	250	340	16	191	165	155	664	181	244	239	40	110	150	18	-	-	-	4	50	22	6	24.5	1/2"	63
SP 308	200	330	14	250	380	16	191	165	155	704	181	284	239	40	110	150	18	-	-	-	4	50	22	6	24.5	1/2"	73



SIZE	A	B	C	D	E	F	G	H	I	K	L	M	N	O	P	Q	R	S	T	U	V	W	N.	Y	Z	kg. Weight
SP 412	210	334	14	270	394	18	213	175	155	762	160	217	270	275	40	110	150	55	25	8	28	18	4	75	1/4"	97
SP 416	210	394	14	270	454	18	213	175	155	822	160	217	330	275	40	110	150	55	25	8	28	18	4	75	1/4"	111
SP 512	240	376	15	300	432	20	269	210	180	885	230	241	318	326	50	125	165	70	35	10	38.5	18	4	89	1"	155
SP 516	240	436	15	300	492	20	269	210	180	945	230	241	378	326	50	125	165	70	35	10	38.5	18	4	89	1"	171
SP 520	240	476	15	300	532	20	269	210	180	985	230	241	418	326	50	125	165	70	35	10	38.5	18	4	89	1"	180
SP 616	340	504	18	400	564	20	292	250	220	1049	290	255	440	354	80	160	200	90	45	14	49	18	4	120	1 1/4"	264
SP 624	340	524	18	400	584	20	292	250	220	1169	290	255	560	354	80	160	200	90	45	14	49	18	4	120	1 1/4"	278
SP 720	400	640	20	480	710	25	352	320	275	1285	370	306	545	434	100	180	220	120	60	18	55	18	8	150	1 1/2"	510
IP 730	400	790	20	480	860	25	352	320	275	1435	370	306	695	434	100	180	220	120	60	18	55	18	8	150	1 1/2"	600
IP 740	400	890	20	480	960	25	352	320	275	1535	370	306	795	434	100	180	220	120	60	18	55	18	8	150	1 1/2"	685
IP 835	520	960	24	650	1080	30	511	440	380	1939	500	473	830	636	150	240	285	160	80	18	85	22	8	204	2 1/4"	1460
IP 845	520	1110	24	650	1230	30	511	440	380	2089	500	473	980	636	150	240	285	160	80	18	85	22	8	204	2 1/4"	1580
P 855	520	1210	24	650	1330	30	511	440	380	2189	500	473	1080	636	150	240	285	160	80	18	85	22	8	204	2 1/4"	1700

pproximate dimensions (in mm). * Holes

STORK

P 3008

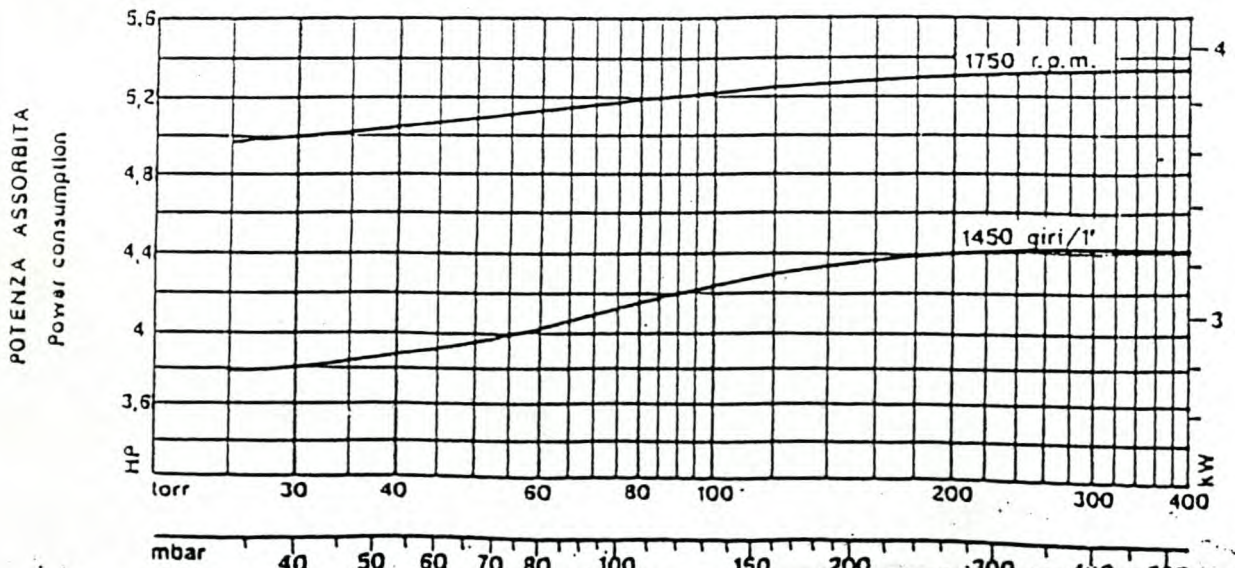
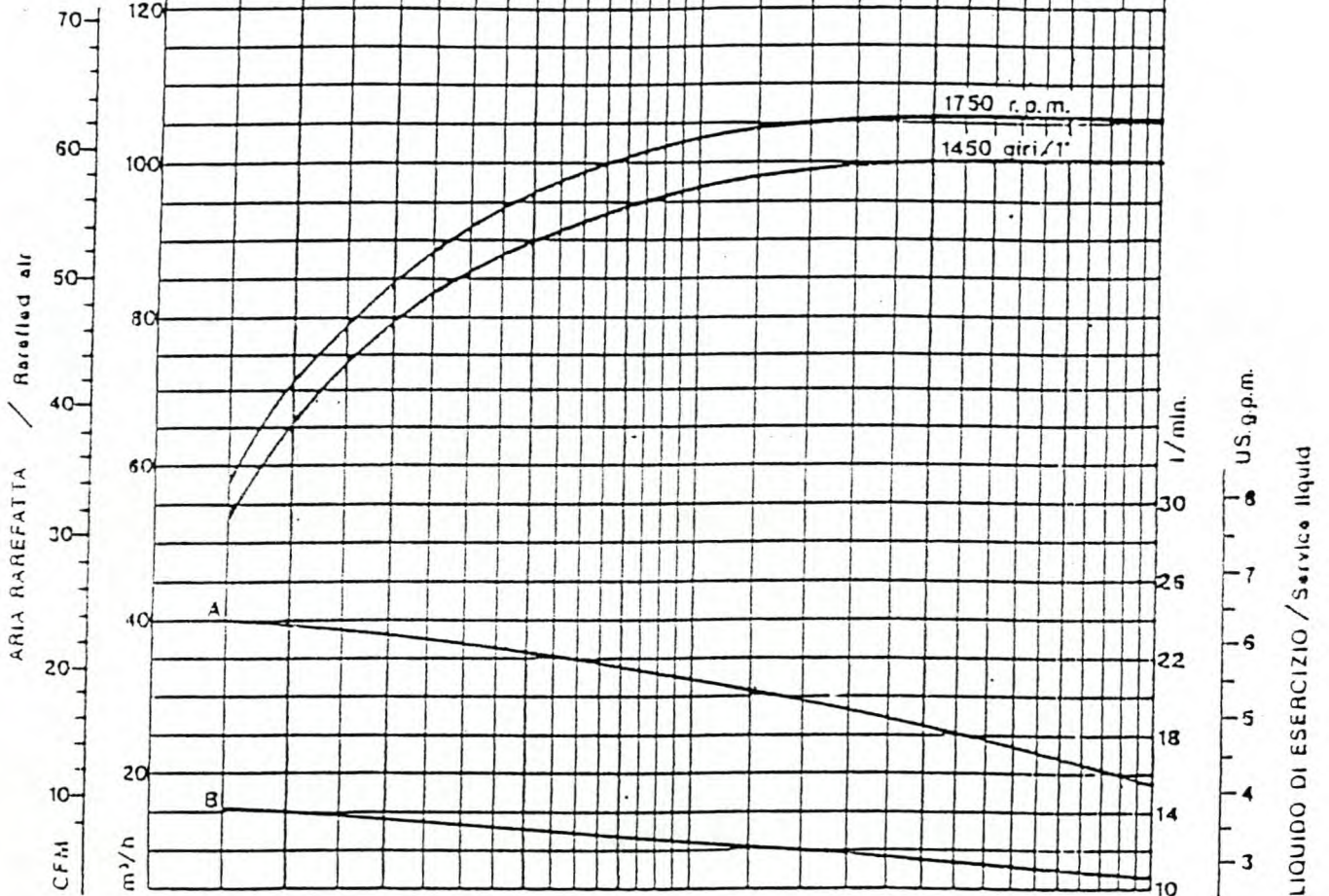
Stork Pumps South Africa (Pty) Ltd.

TEMPERATURA ARIA 20 °C	Air temperature 70 °F
TEMPERATURA LIQUIDO DI ESERCIZIO 15°C	Service liquid temperature 60 °F
PRESSIONE BAROMETRICA 760 mmHg	Barometric pressure 29.92 inches Hg

A	PORTATA ANELLO LIQUIDO RICHIESTA DALLA POMPA Service liquid capacity required by the pump
B	PORTATA LIQUIDO DI REINTEGRO PER RICIRCOLO PARZIALE Make up liquid capacity for partial recirculation

VUOTO / Vacuum

inches Hg 28.6 28 27 25 24 23 22 20 18 16
mmHg 730 720 700 660 560 460 360



**F8. Plate Heat Exchanger Specification
(Alfa Laval)**

Customer : LURGICHEM Model : CB14
 Project: : ED321
 Item : Option 2 Date : 04/06/2001

		<u>Hot side</u>	<u>Cold side</u>
Fluid		Water	Water
Density	kg/m ³	995.1	998.3
Specific heat capacity	kJ/(kg*K)	4.18	4.19
Thermal conductivity	W/(m*K)	0.614	0.598
Viscosity.inlet	cP	0.801	1.14
Viscosity.outlet	cP	0.877	1.05
Volume flow rate	m ³ /h	0.8400	1.000
Inlet temperature	°C	30.0	15.0
Outlet temperature	°C	25.9	18.4
Pressure drop	kPa	12.1	13.0
Heat exchanged	kW	4.000	
L.M.T.D.	K	11.2	
O.H.T.C clean conditions	W/(m ² *K)	5500	
O.H.T.C service	W/(m ² *K)	2127	
Heat transfer area	m ²	0.2	
Fouling resistance * 10000	m ² *K/W	2.9	
Duty margin	%	158.6	
Rel. directions of fluids		Countercurrent	
Number of plates		14	
Effective plates		12	
Number of passes		1	1
Extension capacity			
Plate material / thickness		AISI 316 / 0.35 mm	
Sealing material			
Connection material			
Connection diameter	mm	18	18
Nozzle orientation			
Pressure vessel code		SA	
Flange rating		DIN	
Design pressure	barg	5.0	5.0
Test pressure	barg	6.5	6.5
Design temperature	°C	30.0	20.0
Overall length x width x height	mm	x x	
Net weight, empty / operating	kg	/ 0.00	

Performance is conditioned on the accuracy of customer's data and customer's ability to supply equipment and products in conformity therewith.

F9. Thermal Oil Data Sheet

Product Data Sheet Mobiltherm 605

Heat Transfer Oil

Product Description

Mobiltherm 605 is a high quality heat transfer medium made from solvent refined mineral oil. It gives outstanding performance in indirect heating installations operating at bulk oil temperatures up to 315°C.

The high thermal stability of Mobiltherm 605 will reduce the tendency towards viscosity increase in correctly designed indirect heating systems and prevent formation of deposits which interfere with efficient heat transfer operations. The viscosity has been selected to provide quick circulation at start-up and the pour point gives good handling properties at low temperatures.

The density of the product gives good thermal properties, specific heat and thermal conductivity. These features all help to reduce circulating pump power input and enable systems to be built with smaller bore piping, thus contributing to lower initial installation costs and increased operating efficiency.

Benefits

Mobiltherm 605 provides:

High resistance to thermal cracking and decomposition. Excellent thermal stability reduces viscosity increase. Low viscosity gives easy start-up.

Non toxic in the event of leakage.

Good handling properties at low temperature.

Minimum heat transfer interference due to deposit formation.

Excellent thermal properties give improved operating efficiency.

Long trouble free service life giving improved operating profit.

Application

Mobiltherm 605 is recommended for use in indirect heating and cooling installations in all kinds of industrial processes operating at bulk oil temperatures up to 315°C.

The limitation of the upper temperature is based on the high temperature properties of Mobiltherm 605 at atmospheric pressure. If used above this level vapour lock may result unless the system is designed to operate at the higher temperature by pressurising with an inert gas, such as nitrogen.

At higher temperatures fluid life will be shortened because the rate of thermal degradation increases markedly as temperatures rise above the recommended limit. In well designed systems the temperature of the oil film surrounding the heating element will be about 15°C to 30°C above the bulk oil temperature. To ensure long service life and freedom from deposition of sludge and coke-like material, which interferes with heat transfer rates, the temperature of the oil film adjacent to the heater element should preferably not exceed 345°C.

Mobil Oil South Africa (Pty) Limited.

Sandton Square, West Tower, 4th Floor, Corner Fifth & Maude Street, Sandton
P.O. Box 78043, Sandton 2146. Tel (27)(11) 301 1800, Fax (27)(11) 301 1801,
Customer Service 0800 600 383



Stat Code C018

Health and Safety

Based on available toxicological information, it has been determined that this product poses no significant health risk when used and handled properly.

Details on handling, as well as health and safety information, can be found in the Material Safety Data Bulletin which can be obtained through Mobil Oil South Africa (Pty) Ltd., by telephoning 0800 600 383.

Characteristics

Typical physical characteristics of Mobiltherm 605 are given in the table. These are intended as a guide to industry and are not necessarily manufacturing or marketing specifications. They may be changed without notice due to continued product research and development.

	Mobiltherm 605
Relative Density 15/4 °C	0.874
Pour Point, °C max.	-6
Flash Point COC, °C min.	212
Viscosity cSt at 40 °C	29.5
Viscosity cSt at 100 °C	5.0
Viscosity Index	100
Colour - ASTM	2.5

Mobil Oil South Africa (Pty) Limited.

Sandton Square, West Tower, 4th Floor, Corner Fifth & Maude Street, Sandton
P O Box 78043, Sandton 2146. Tel (27)(11) 301 1800, Fax (27)(11) 301 1801,
Customer Service 0800 600 383



Stat Code C018

APPENDIX G

Commissioning Schedule

- G1. Pre-commissioning**
- G2. Engineering Commissioning**
- G3. Process Commissioning**

APPENDIX G

COMMISSIONING SCHEDULE

G1. PRE - COMMISSIONING

The following actions need to be performed prior to commissioning:

- Ensure all piping, columns, intersections and other process equipment are free from debris and any possible source of contamination
- All handvalves in close position. Sequence: V701, V801, V301, V303, V506, V606, V401, V403, V901, V951, V604, V551, V552, V601, V605
- Certify air receivers

SERVICES

1. Adequate water level in chilled water buffer tank TK551
2. Prime and bleed PP551
3. Adequate level of seal-water in SP601
4. Adequate water to ensure submersed elements in HX301
5. Adequate level of liquid nitrogen in PCC
6. Adequate level of thermal oil in oil heaters
7. Mains electricity to plant on
8. Required air pressure in receiver (switch on compressor) and air reticulation check
9. Check rotation of all pump motors for correct connections
10. SCADA on
11. Check leaks on all services lines

G2. ENGINEERING COMMISSIONING

The purpose of engineering commissioning was:

1. To test all systems and equipment without any product flowing through the columns:
2. to evaluate the efficiency by which the VSA system could provide driving forces for:
 - steam generation (HX 301)
 - nitrogen liquid vaporization
 - nitrogen gas heating (HX500 and HX 520)
 - drawing and maintaining vacuum on columns (VP600)
 - generation of chilled water (CH550)
 - condensation (HX400)

SCHEDULE

1. Check all valve positions in sequence: V101, V102, V201, V202, V105, V205, V503, V523, V501, - on/off positions for valve and feedback – on instrumentation panel (remote switches) and on SCADA
2. Manual switch all process equipment (evaluate temperatures, flows and pressures); sequence HX301, HX500, HX520, VP600 (set air bleed V603), CH550 etc (as on SCADA and electrical panel)
3. Purge electrical panels and heating elements with compressed air
4. Bleed air from the steam generator (HX301)
5. Switch on pump PP551 – chilled water circulation
6. Switch on pump PP302 with water (V301) closed
7. Adjust chilled water flowrate to HX400, HX601 and HX570
8. Check TI402 at HX400 (chilled water)
9. Check temperature of compressed air
10. Adjust pressure regulators V502 and V504 on N₂ line to working pressures
11. Purge with N₂ flow and set V103 and V203
12. Check seal-water temperature (TI601) < 15°C
13. Set air bleed V603 for VP600 to draw vacuum up to 170 mBar
14. Adjust V106 and V206 safety valves with N₂ gas to adsorber column design pressure
15. Check leaks on all lines

16. Run cycles with water vapour in columns to check all systems and to sterilise the inner surfaces of the piping and columns

G3. PROCESS COMMISSIONING

Process commissioning was performed to evaluate the individual process steps as well as synchronize the adsorbers.

SCHEDULE

- Open columns and remove sealant material around flanges
- Pack both columns with proper ceramic beads and molecular sieves

Single column operation (manual)

1. Run through process sequences (step manually and simulate stop conditions)
2. Adjust chilled water flow to compressor, seal-water and HX400
3. Determine time for: warm-up (all sections), complete breakthrough, regen/purge (timer3), time1 for bed cooling, time to TT105 and TT205(time2), PE and at which pressure and bed dT.

Dual bed operation (VSA)

1. Supply conditions determined above to SCADA
2. Manual step operation
3. Fully automate
4. Start sampling

APPENDIX H

EXPERIMENTAL RESULTS

Appendix H1.	Table of Analytical results (Group I)
Appendix H2.	Analytical Parameters
Appendix H3.	Additional Results (Group I)
Appendix H4.	Experimental Layout and Analytical Results (Group II)
Appendix H5.	Synthetic Methanol Specifications
Appendix H6.	La Grange Interpolation Function

Appendix H1. Table of Analytical results (Group I)

Sample #	GC		GC ?	KF		CONVERSION TO mg / mL absolute ethanol					
	[ppm]	[%]		[ppm]	[ppm]	ethanol 0.79 g / ml			PER 100 ml Ethanol		
	methanol	ethanol	2-propanol	water	water	PER 100 g sample====	PER 100 ml Ethanol		mg MeOH	mg 2-PrOH	
F1	664	92.462		25	74690	7.4690	73.0	66.4	2.5	90.9	3.4
F2	853	94.654		14	52594	5.2594	74.8	85.3	1.4	114.1	1.8
F3	122	91.585		91	83941	8.3941	72.4	12.2	9.1	16.9	12.6
1	116	99.884		16	1031	0.1031	78.9	11.6	1.6	14.7	2.1
2	57	99.993		15			79.0	5.7	1.5	7.3	1.9
3	50	99.994		13			79.0	5.0	1.3	6.3	1.7
4	41	99.995		13			79.0	4.1	1.3	5.2	1.6
5	38	99.854		19	1400	0.1400	78.9	3.8	1.9	4.8	2.4
6	126	99.987		8			79.0	12.6	0.8	16.0	1.0
7	67	99.993		4			79.0	6.7	0.4	8.5	0.5
8	52	99.994		4			79.0	5.2	0.4	6.6	0.6
9	45	99.995		9			79.0	4.5	0.9	5.7	1.2
10	46	99.914		30	780	0.0780	78.9	4.6	3.0	5.8	3.8
11	52	99.994		5			79.0	5.2	0.5	6.6	0.6
12	28	99.968		5	291		79.0	2.8	0.5	3.6	0.6
13	25	99.997		8			79.0	2.5	0.8	3.1	1.1
14	24	99.996		12			79.0	2.4	1.2	3.1	1.5
15	19	99.923		5	742		78.9	1.9	0.5	2.4	0.6
16	94	99.990		6			79.0	9.4	0.6	11.9	0.8
17	55	99.994		4			79.0	5.5	0.4	6.9	0.5
18	32	99.996		7			79.0	3.2	0.7	4.1	0.8
19	27	99.997		6			79.0	2.7	0.6	3.4	0.8
20	25	99.968		6	290		79.0	2.5	0.6	3.1	0.7
21	65	99.992		14			79.0	6.5	1.4	8.3	1.7
22	37	99.996		4			79.0	3.7	0.4	4.6	0.5
23	33	99.996		5			79.0	3.3	0.5	4.2	0.7
24	27	99.996		13			79.0	2.7	1.3	3.4	1.7
25	26	99.948		6	484		79.0	2.6	0.6	3.3	0.7
26	85	99.990		14			79.0	8.5	1.4	10.7	1.8
27	59	99.994		5			79.0	5.9	0.5	7.4	0.7
28	39	99.995		10			79.0	3.9	1.0	5.0	1.3
29	41	99.995		7			79.0	4.1	0.7	5.1	0.9
30	28	99.997		5			79.0	2.8	0.5	3.6	0.7
31	968	99.685	2178				78.8	96.8	217.8	122.9	276.5

32	678	98.692	12400	78.0	67.8	1240.0	87.0	1590.5
33	579	99.840	1018	78.9	57.9	101.8	73.4	129.0
34	549	99.8437	1014	78.9	54.9	101.4	69.6	128.6
35	507	99.8362	1131	78.9	50.7	113.1	64.3	143.4
36	532	99.9028	440	78.9	53.2	44.0	67.5	55.8
37	279	99.9507	213	79.0	27.9	21.3	35.4	27.0
38	169	99.9786	45	79.0	16.9	4.5	21.4	5.7
39	117	99.9875	8	79.0	11.7	0.8	14.8	1.0
40	109	99.9886	5	79.0	10.9	0.5	13.8	0.7
41	689	99.7747	1564	78.8	68.9	156.4	87.4	198.4
42	343	99.9214	442	78.9	34.3	44.2	43.5	56.0
43	287	99.9388	324	79.0	28.7	32.4	36.4	41.1
44	225	99.954	235	79.0	22.5	23.5	28.5	29.7
45	235	99.9416	349	79.0	23.5	34.9	29.7	44.2
46	243	99.9728	29	79.0	24.3	2.9	30.8	3.6
47	40	99.9948	12	79.0	4.0	1.2	5.0	1.5
48	38	99.9927	36	79.0	3.8	3.6	4.8	4.5
49	33	99.9962	5	79.0	3.3	0.5	4.2	0.6
50	29	99.9949	22	79.0	2.9	2.2	3.7	2.7
51	428	99.8789	783	78.9	42.8	78.3	54.3	99.2
52	200	99.9562	239	79.0	20.0	23.9	25.3	30.2
53	181	99.9684	135	79.0	18.1	13.5	23.0	17.1
54	173	99.9711	117	79.0	17.3	11.7	21.9	14.8
55	159	99.9738	103	79.0	15.9	10.3	20.2	13.1
56	67	99.9917	16	79.0	6.7	1.6	8.5	2.1
57	35	99.9944	21	79.0	3.5	2.1	4.4	2.7
58	22	99.9968	10	79.0	2.2	1.0	2.7	1.3
59	19	99.9972	9	79.0	1.9	0.9	2.4	1.1
60	18	99.9979	3	79.0	1.8	0.3	2.3	0.4

Appendix H2. Analytical Parameters (GC & KF)

	AREAS		peak cut off				MASS FRACTIONS			RESPONSE FACTORS			
	methanol	ethanol	2-prop tot	n-butanol	m sample	m IS	methanol	ethanol	2-propanol	methanol	ethanol	2-propanol	n-butanol
F1_1	20244	10588400	1544	2786878	4.483	0.248	0.00059		0.00004	0.68	1.19	0.76	1.00
F1_2	20706	10200559	316	2285762	4.483	0.248	0.00074		0.00001	0.68	1.19	0.76	1.00
F1_14/09	36487		405	3935177	4.483	0.248	0.00069			0.74	1.19	0.76	1.00
F2_1	25159	10439137	921	1886419	4.689	0.194	0.00081		0.00003	0.68	1.19	0.76	1.00
F2_2	35557	11854118	30	2418614	4.689	0.194	0.00089		0.000001	0.68	1.19	0.76	1.00
F2_15/09	104582	19581130	1402	7236014	5.787	0.234	0.000859		0.00001	0.68	1.19	0.76	1.00
F3_1	3512	10887198	3256	2096377	4.871	0.243	0.000123		0.000102	0.68	1.19	0.76	1.00
F3_2	4710	11225156	3474	2826132	4.871	0.243	0.000122		0.000081	0.68	1.19	0.76	1.00
F3_15/09	15754	18905240	5197	5497819	5.8	0.191	0.000128		0.000041	0.74	1.19	0.76	1.00
F1_ave							0.00066		0.00003	0.68	1.19	0.76	1.00
F1_14/09	36487		405	3935177	4.483	0.248	0.00069			0.74	1.19	0.76	1.00
F2_ave							0.00085		0.00001	0.68	1.19	0.76	1.00
F2_15/09	104582	19581130	1402	7236014	5.787	0.234	0.000859		0.00001	0.68	1.19	0.76	1.00
F3_ave							0.00012		0.00009	0.68	1.19	0.76	1.00
F3_15/09	15754	18905240	5197	5497819	5.8	0.191	0.000128		0.000041	0.74	1.19	0.76	1.00
1	4183	11743747	656	2889392	4.271	0.232	1.2E-04		1.6E-05	0.68	1.19	0.76	1.00
2	3473	13756740	995	4944733	4.443	0.247	5.7E-05		1.5E-05	0.68	1.19	0.76	1.00
3	2208	13016529	661	3176899	4.282	0.209	5.0E-05		1.3E-05	0.68	1.19	0.76	1.00
4	1708	12392837	603	3119495	4.352	0.221	4.1E-05		1.3E-05	0.68	1.19	0.76	1.00
5	1325	11992147	745	3284230	4.017	0.255	3.8E-05		1.9E-05	0.68	1.19	0.76	1.00
6	6438	13777339	442	3685262	4.143	0.204	1.3E-04		7.8E-06	0.68	1.19	0.76	1.00
7	3575	13624028	231	3581349	4.441	0.204	6.7E-05		3.9E-06	0.68	1.19	0.76	1.00
8	2348	12941548	221	3628099	4.02	0.22	5.2E-05		4.4E-06	0.68	1.19	0.76	1.00
9	2671	14043477	624	6775598	4.284	0.332	4.5E-05		9.4E-06	0.68	1.19	0.76	1.00
10	2016	13285447	1467	2974222	4.946	0.226	4.6E-05		3.0E-05	0.68	1.19	0.76	1.00
11	7451	22778314	745	9591696	4.376	0.218	5.2E-05		5.1E-06	0.74	1.19	0.76	1.00
12	1751	14315584	300	4693219	4.418	0.249	2.8E-05		4.7E-06	0.74	1.19	0.76	1.00
13	1780	15621985	622	4608864	4.718	0.224	2.5E-05		8.4E-06	0.74	1.19	0.76	1.00
14	2123	16556560	1040	6047880	3.91	0.201	2.4E-05		1.2E-05	0.74	1.19	0.76	1.00
15	1773	16524350	457	6228498	4.145	0.205	1.9E-05		4.8E-06	0.74	1.19	0.76	1.00
16	7802	16022200	542	4212182	4.742	0.178	9.4E-05		6.4E-06	0.74	1.19	0.76	1.00
17	3343	14460972	245	2719299	4.389	0.145	5.5E-05		3.9E-06	0.74	1.19	0.76	1.00
18	2318	15477195	486	4656864	5.029	0.241	3.2E-05		6.6E-06	0.74	1.19	0.76	1.00
19	1591	13937881	369	3874898	4.464	0.219	2.7E-05		6.1E-06	0.74	1.19	0.76	1.00
20	1682	14953453	408	4582927	4.55	0.227	2.5E-05		5.8E-06	0.74	1.19	0.76	1.00
21	4237	14748529	914	4198808	4.676	0.224	6.5E-05		1.4E-05	0.74	1.19	0.76	1.00
22	2901	15735182	311	6347229	4.191	0.249	3.7E-05		3.8E-06	0.74	1.19	0.76	1.00
23	2275	14553371	373	3774421	4.636	0.188	3.3E-05		5.3E-06	0.74	1.19	0.76	1.00
24	1730	14482425	872	4834056	4.289	0.238	2.7E-05		1.3E-05	0.74	1.19	0.76	1.00
25	1587	14146620	365	4106497	5	0.251	2.6E-05		5.9E-06	0.74	1.19	0.76	1.00
26	11108	19898732	1865	8003015	4.508	0.204	8.5E-05		1.4E-05	0.74	1.19	0.76	1.00

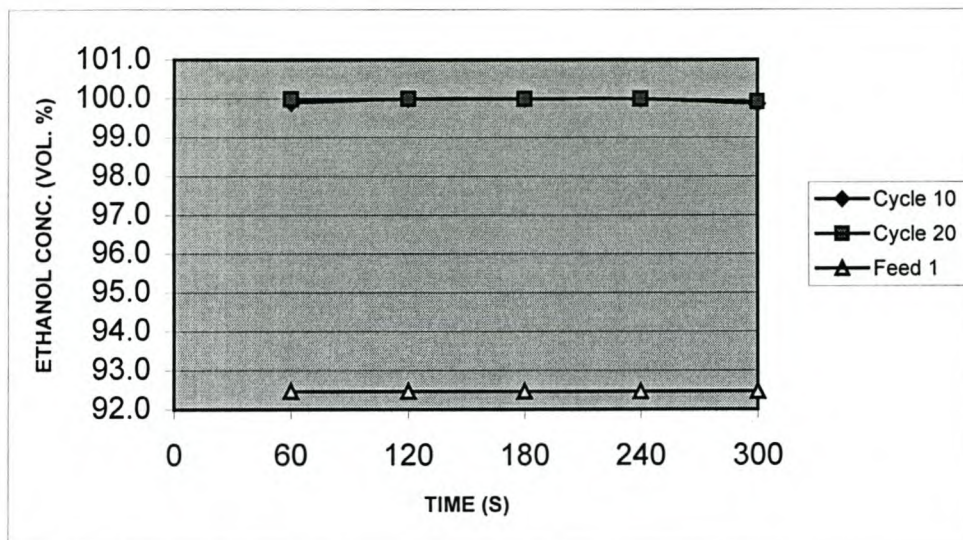
27	4385	14859842	400	4022119	5.068	0.202	5.9E-05	5.2E-06	0.74	1.19	0.76	1.00
28	2615	14982064	694	3123237	5.998	0.208	3.9E-05	1.0E-05	0.74	1.19	0.76	1.00
29	2704	14522897	471	2961932	5.65	0.186	4.1E-05	6.9E-06	0.74	1.19	0.76	1.00
30	1982	14825735	394	2848024	5.665	0.17	2.8E-05	5.5E-06	0.74	1.19	0.76	1.00
31	79946	15733635	184727	4397920	5.786	0.228	9.7E-04	2.2E-03	0.74	1.19	0.76	1.00
31a	120020	18683014	252923	6833946	5.786	0.228	9.4E-04	1.9E-03	0.74	1.19	0.76	1.00
32	42459	13530204	79745	2538350	5.967	0.179	6.8E-04	1.2E-03	0.74	1.19	0.76	1.00
33	40200	14477902	72629	3790518	6.044	0.244	5.8E-04	1.0E-03	0.74	1.19	0.76	1.00
34	29743	13181029	56468	2041866	6.386	0.178	5.5E-04	1.0E-03	0.74	1.19	0.76	1.00
35	29579	13706488	67719	3295951	5.81	0.243	5.1E-04	1.1E-03	0.74	1.19	0.76	1.00
36	32986	14222161	28004	3409664	5.28	0.215	5.3E-04	4.4E-04	0.74	1.19	0.76	1.00
37	29608	21138690	23221	5443757	5.55	0.211	2.8E-04	2.1E-04	0.74	1.19	0.76	1.00
38	17623	18055340	4778	3906037	5.912	0.164	1.7E-04	4.5E-05	0.74	1.19	0.76	1.00
39	17917	21782636	1227	7347635	5.863	0.208	1.2E-04	7.8E-06	0.74	1.19	0.76	1.00
40	13751	19384862	703	5592013	6.299	0.206	1.1E-04	5.4E-06	0.74	1.19	0.76	1.00
41	101768	2125268	237304	6072324	6.214	0.189	6.9E-04	1.6E-03	0.74	1.19	0.76	1.00
42	37236	18423644	49218	7647005	5.46	0.285	3.4E-04	4.4E-04	0.74	1.19	0.76	1.00
43	12729	12201963	14761	2151787	6.231	0.224	2.9E-04	3.2E-04	0.74	1.19	0.76	1.00
44	10604	12249109	11361	2510450	6.038	0.238	2.2E-04	2.3E-04	0.74	1.19	0.76	1.00
45	9958	11948952	15213	1929333	5.887	0.198	2.3E-04	3.5E-04	0.74	1.19	0.76	1.00
46	24482	18056432	2965	5654320	5.407	0.225	2.4E-04	2.9E-05	0.74	1.19	0.76	1.00
47	1876	12240540	579	3237173	6.193	0.315	4.0E-05	1.2E-05	0.74	1.19	0.76	1.00
48	2191	13356086	2135	2677400	5.51	0.187	3.8E-05	3.6E-05	0.74	1.19	0.76	1.00
49	1983	13610689	295	2937614	5.886	0.214	3.3E-05	4.8E-06	0.74	1.19	0.76	1.00
50	1624	13212382	1223	2234252	5.788	0.173	2.9E-05	2.2E-05	0.74	1.19	0.76	1.00
51	22798	12807078	42795	2368254	5.588	0.184	4.3E-04	7.8E-04	0.74	1.19	0.76	1.00
52	13094	14219189	16097	3006519	5.752	0.195	2.0E-04	2.4E-04	0.74	1.19	0.76	1.00
53	8450	12376286	6458	2515890	5.429	0.217	1.8E-04	1.3E-04	0.74	1.19	0.76	1.00
54	12681	14921952	8818	3061239	5.838	0.18	1.7E-04	1.2E-04	0.74	1.19	0.76	1.00
55	9364	13743798	6235	4074240	5.345	0.274	1.6E-04	1.0E-04	0.74	1.19	0.76	1.00
56	4500	15010873	1123	4270232	5.708	0.268	6.7E-05	1.6E-05	0.74	1.19	0.76	1.00
57	1710	12989933	1061	2844175	5.749	0.247	3.5E-05	2.1E-05	0.74	1.19	0.76	1.00
58	1219	13512637	591	2961636	5.842	0.228	2.2E-05	1.0E-05	0.74	1.19	0.76	1.00
59	990	13035152	489	2677563	5.907	0.222	1.9E-05	9.0E-06	0.74	1.19	0.76	1.00
60	1013	13214267	160	3439276	5.571	0.258	1.8E-05	2.8E-06	0.74	1.19	0.76	1.00

	%	mass fraction	ppm
F1	7.4499	0.07450	74499
	7.488	0.07488	74880
	7.46895	0.07469	74690
F2	5.2264	0.05226	52264
	5.2923	0.05292	52923
F3	8.3975	0.08398	83975
	8.3906	0.08391	83906
1	0.1029	0.00103	1029
	0.1033	0.00103	1033
5	0.1399	0.00140	1399
	0.1401	0.00140	1401
10	0.078	0.00078	780
12	0.0291	0.00029	291
15	0.0742	0.00074	742
20	0.029	0.00029	290
25	0.0484	0.00048	484

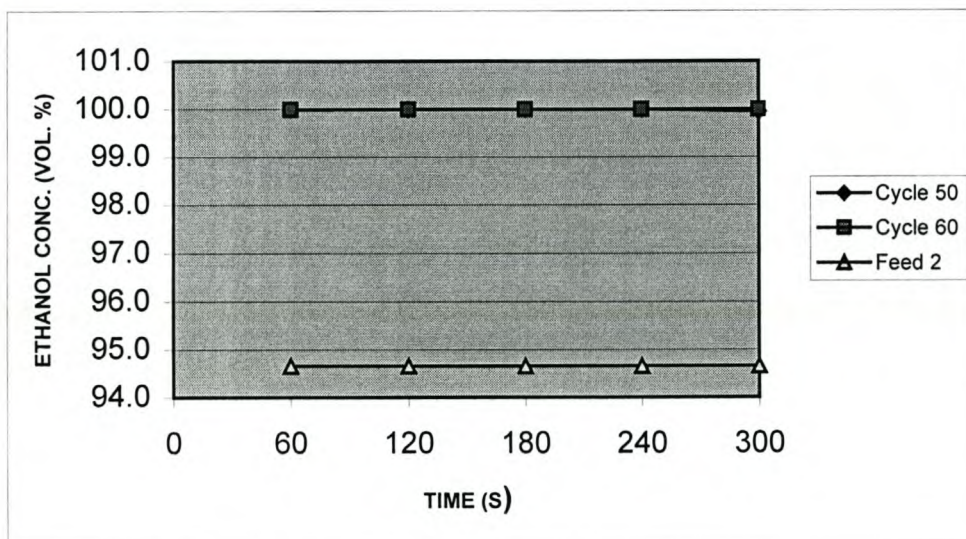
Appendix H3. Additional Results (Group I)

Additional ethanol adsorption curves (not shown in chapter 5):

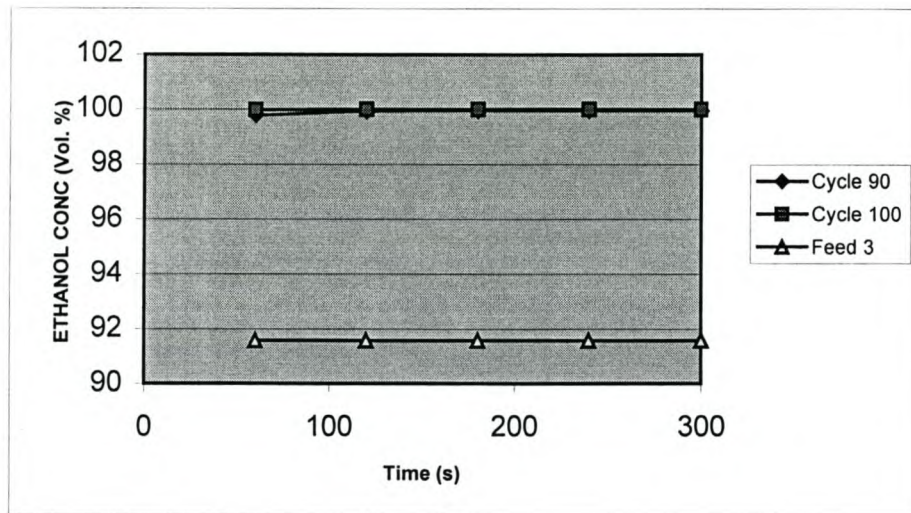
Cycles 10 and 20



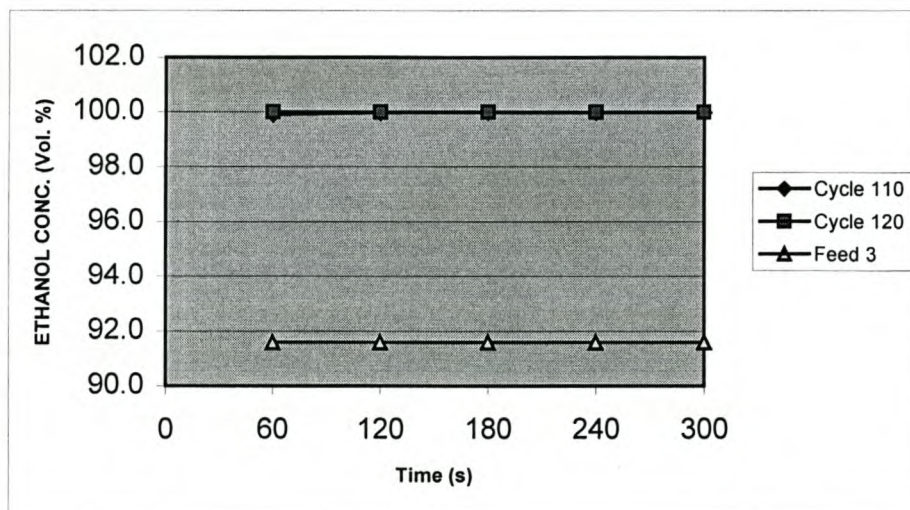
Cycles 50 and 60



Cycles 90 and 100

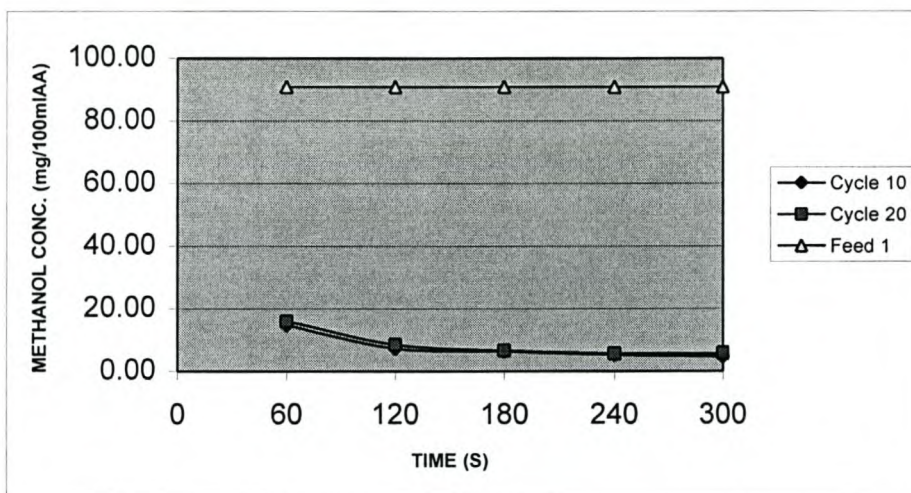


Cycles 110 and 120

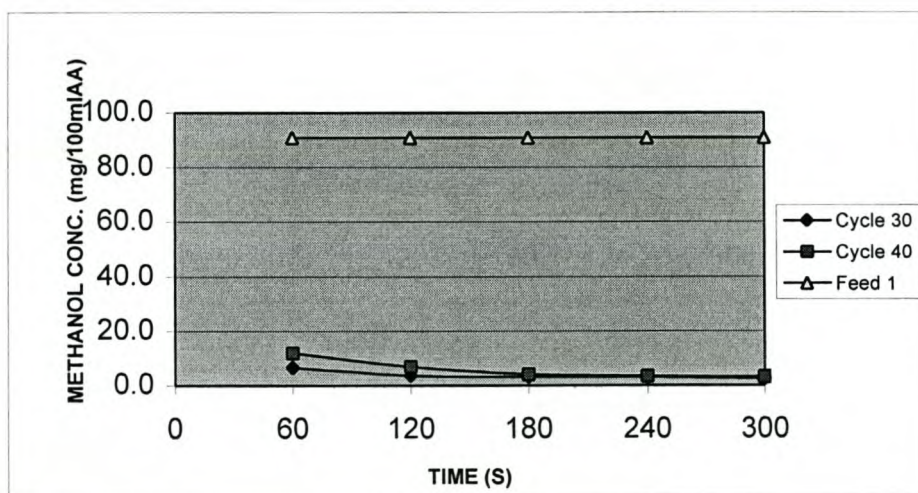


Additional methanol adsorption curves (not shown in chapter 5):

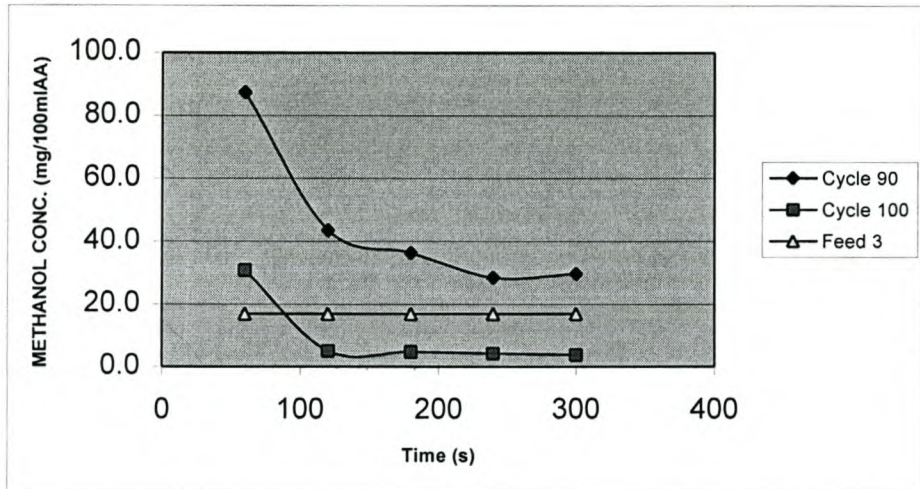
Cycles 10 and 20



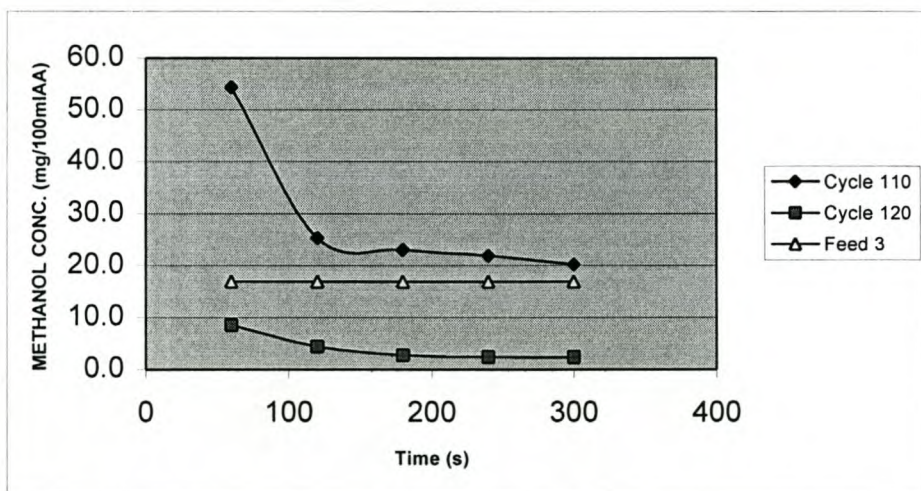
Cycles 30 and 40



Cycles 90 and 100



Cycles 110 and 120



**Appendix H4. Experimental Layout and Analytical
Results (Group II)**

SAMPLE #	DESCRIPTION	TIME s	DENSITY kg/l	METHANOL ppm wt	METHANOL mg/100g	METHANOL mg/100mlAA	STRENGTH vol %
1	Feed C1		0.8112	470.0	47.0	57.9	95.1
2	Feed C3		0.8058	653.0	65.3	81.0	96.4
3	Feed C2		0.8141	111.0	11.1	13.6	94.3
Feed concentration							
Batch 1							
4	C1	360	0.7898	50.0	5.0	6.3	99.9
5	C1	720	0.7894	45.0	4.5	5.7	100.0
6	C1	1080	0.7894	36.0	3.6	4.6	100.0
7	C1	1440	0.789	50.0	5.0	6.3	100.0
8	C1	1800	0.7896	75.0	7.5	9.5	100.0
Batch 2							
9	C2	360	0.7899	161.0	16.1	20.4	99.9
10	C2	720	0.7894	165.0	16.5	20.9	100.0
11	C2	1080	0.7893	164.0	16.4	20.8	100.0
12	C2	1440	0.7897	186.0	18.6	23.6	99.9
13	C2	1800	0.7894	253.0	25.3	32.0	100.0
Batch 3							
14	C3	360	0.7893	244.0	24.4	30.9	100.0
15	C3	720	0.7894	64.0	6.4	8.1	100.0
16	C3	1080	0.7893	69.0	6.9	8.7	100.0
17	C3	1440	0.7895	100.0	10.0	12.7	100.0
18	C3	1800	0.7893	141.0	14.1	17.9	100.0
Feed flowrate							
Batch 4							
19	F1	360	0.7893	130.0	13.0	16.5	100.0
20	F1	720	0.7894	133.0	13.3	16.8	100.0
21	F1	1080	0.7893	147.0	14.7	18.6	100.0
22	F1	1440	0.7893	139.0	13.9	17.6	100.0
23	F1	1800	0.7906	127.0	12.7	16.1	99.7
Batch 5							
	F2	360	0.7893	244.0	24.4	30.9	100.0
	F2	720	0.7894	64.0	6.4	8.1	100.0
	F2	1080	0.7893	69.0	6.9	8.7	100.0
	F2	1440	0.7895	100.0	10.0	12.7	100.0
	F2	1800	0.7893	141.0	14.1	17.9	100.0
Batch 6							
24	F3	360	0.7893	93.0	9.3	11.8	100.0
25	F3	720	0.7895	119.0	11.9	15.1	100.0
26	F3	1080	0.7893	187.0	18.7	23.7	100.0
27	F3	1440	0.7893	233.0	23.3	29.5	100.0
28	F3	1800	0.7893	338.0	33.8	42.8	100.0
Regeneration pressure							
Batch 7							
29	P1	360	0.7895	94.0	9.4	11.9	100.0
30	P1	720	0.7895	115.0	11.5	14.6	100.0
31	P1	1080	0.7893	180.0	18.0	22.8	100.0
32	P1	1440	0.7893	261.0	26.1	33.1	100.0
33	P1	1800	0.7895	418.0	41.8	52.9	100.0
Batch 8							
34	P2	360	0.7893	232.0	23.2	29.4	100.0
35	P2	720	0.7893	183.0	18.3	23.2	100.0
36	P2	1080	0.7893	198.0	19.8	25.1	100.0
37	P2	1440	0.7893	210.0	21.0	26.6	100.0
38	P2	1800	0.7893	284.0	28.4	36.0	100.0
Batch 9							
39	P3	360	0.7893	190.0	19.0	24.1	100.0
40	P3	720	0.7896	163.0	16.3	20.6	100.0
41	P3	1080	0.7898	195.0	19.5	24.7	99.9
42	P3	1440	0.7899	295.0	29.5	37.3	99.9
43	P3	1800	0.7896	381.0	38.1	48.3	100.0

SAMPLE #	DESCRIPTION	TIME s	DENSITY kg/l	METHANOL ppm wt	METHANOL mg/100g	METHANOL mg/100mlAA	STRENGTH vol %
Purge flowrate							
Batch 10							
44	m1	360	0.79	216.0	21.6	27.3	99.9
45	m1	720	0.7894	179.0	17.9	22.7	100.0
46	m1	1080	0.7899	166.0	16.6	21.0	99.9
47	m1	1440	0.7903	240.0	24.0	30.4	99.8
48	m1	1800	0.7896	295.0	29.5	37.4	100.0
Batch 11							
49	m2	360	0.7894	226.0	22.6	28.6	100.0
50	m2	720	0.7894	172.0	17.2	21.8	100.0
51	m2	1080	0.7896	268.0	26.8	33.9	100.0
52	m2	1440	0.7895	312.0	31.2	39.5	100.0
53	m2	1800	0.7896	389.0	38.9	49.3	100.0
Batch 12							
54	m3	360	0.7894	202.0	20.2	25.6	100.0
55	m3	720	0.7896	184.0	18.4	23.3	100.0
56	m3	1080	0.7893	154.0	15.4	19.5	100.0
57	m3	1440	0.7893	202.0	20.2	25.6	100.0
58	m3	1800	0.7893	274.0	27.4	34.7	100.0
Synthetic methanol							
Batch 13							
59	CS1	360	0.7894	147.0	14.7	18.6	100.0
60	CS1	720	0.7894	155.0	15.5	19.6	100.0
61	CS1	1080	0.7895	233.0	23.3	29.5	100.0
62	CS1	1440	0.7895	425.0	42.5	53.8	100.0
63	CS1	1800	0.7897	599.0	59.9	75.9	100.0
Batch 14							
64	CS2	360	0.7893	172.0	17.2	21.8	100.0
65	CS2	720	0.7893	213.0	21.3	27.0	100.0
66	CS2	1080	0.7894	294.0	29.4	37.2	100.0
67	CS2	1440	0.7893	554.0	55.4	70.2	100.0
68	CS2	1800	0.7894	975.0	97.5	123.5	100.0
Batch 15							
69	CS3	360	0.7895	404.0	40.4	51.2	100.0
70	CS3	720	0.7895	378.0	37.8	47.9	100.0
71	CS3	1080	0.7895	555.0	55.5	70.3	100.0
72	CS3	1440	0.7893	1075.0	107.5	136.2	100.0
73	CS3	1800	0.7893	1509.0	150.9	191.2	100.0
Initial bed temperature							
Batch 16							
74	T1	360	0.7894	840.0	84.0	106.4	100.0
75	T1	720	0.7893	1223.0	122.3	154.9	100.0
76	T1	1080	0.7894	1705.0	170.5	216.0	100.0
77	T1	1440	0.7893	2228.0	222.8	282.3	100.0
78	T1	1800	0.7894	2172.0	217.2	275.1	100.0
Batch 17							
	T2	360	0.7893	244.0	24.4	30.9	100.0
	T2	720	0.7894	64.0	6.4	8.1	100.0
	T2	1080	0.7893	69.0	6.9	8.7	100.0
	T2	1440	0.7895	100.0	10.0	12.7	100.0
	T2	1800	0.7893	141.0	14.1	17.9	100.0
Batch 18							
79	T3	360	0.7897	1003.0	100.3	127.0	99.9
80	T3	720	0.7895	900.0	90.0	114.0	100.0
81	T3	1080	0.7895	1169.0	116.9	148.1	100.0
82	T3	1440	0.7895	1535.0	153.5	194.4	100.0
83	T3	1800	0.7895	1982.0	198.2	251.0	100.0
84*	Feed CS1		0.7895	3946.0	394.6	499.8	100.0
85*	Feed CS2		0.7896	6394.0	639.4	809.8	100.0
86*	Feed CS3		0.7897	8826.0	882.6	1117.6	99.9

* Samples 84, 85 and 86 are the synthetic methanol feed concentrations.

Appendix H5. Synthetic Methanol Specifications

The methanol used to create a synthetic methanol condition in the adsorbers were of the type used for HPLC purposes. The methanol had the following specification,

BDH Methanol for HPLC

EC-Label 200-659-6

Maximum limits of impurities

Water	0.05%
(HCOOH) Acidity	0.0003 %
(NH ₃) Alkalinity	0.0002 %
Non volatile matter	0.0005 %

Appendix H6. La Grange Interpolation Function

La Grange interpolation was used to create a mathematical function that could integrate the methanol bed exit concentration as a function of time. The interpolation was done over the following 5 points which corresponded with the 5 samples drawn during each adsorption cycle:

$$(t_1, c_1) ; (t_2, c_2) ; (t_3, c_3) ; (t_4, c_4) ; (t_5, c_5)$$

The function took the following form:

$$c = \frac{(t-t_2)(t-t_3)(t-t_4)(t-t_5)}{(t_1-t_2)(t_1-t_3)(t_1-t_4)(t_1-t_5)} \cdot c_1 + \frac{(t-t_1)(t-t_3)(t-t_4)(t-t_5)}{(t_2-t_1)(t_2-t_3)(t_2-t_4)(t_2-t_5)} \cdot c_2$$

$$+ \frac{(t-t_1)(t-t_2)(t-t_4)(t-t_5)}{(t_3-t_1)(t_3-t_2)(t_3-t_4)(t_3-t_5)} \cdot c_3 + \frac{(t-t_1)(t-t_2)(t-t_3)(t-t_5)}{(t_4-t_1)(t_4-t_2)(t_4-t_3)(t_4-t_5)} \cdot c_4$$

$$+ \frac{(t-t_1)(t-t_2)(t-t_3)(t-t_4)}{(t_5-t_1)(t_5-t_2)(t_5-t_3)(t_5-t_4)} \cdot c_5$$

To determine the area for calculation of the methanol bed loading, the following integral was applied:

$$\text{Area under breakthrough curve} = \int_{t_1}^{t_5} f(t) \cdot dt$$

Calculated areas are given in Table 5.5.

**Appendix I. Methanol/Ethanol Vapour / Liquid
Equilibrium Data**

To determine the ease/difficulty of separation by distillation, the relative volatility (α) for the ethanol (A) / methanol (B) system needs to be determined.

From Perry^[50], pure component vapour pressure data are given in the following table:

Vapour pressure (mm Hg)	200	400	760	1520
Temperature for ethanol (°C)	48.4	62.5	78.4	97.5
Temperature for methanol (°C)	34.8	49.9	64.7	84

The boiling point ranges will be between the pure boiling points^[50] of the low boiling component (64.7 °C) to the high boiling component (78.4°C). From the Clausius-Clapeyron equation, $\ln P$ vs. $1/T$ (T in Kelvin) is a linear relationship. By utilising this linear relationship, we can determine vapour pressures for various temperatures.

The interpolating equation for methanol becomes(data for T 64.7 and 84 °C):

$$\frac{\ln 760 - \ln P_A}{\ln 760 - \ln 1520} = \frac{\frac{1}{337.7} - \frac{1}{T}}{\frac{1}{337.7} - \frac{1}{357}}$$

The interpolating equation for ethanol becomes(data for T 62.5 and 78.4 °C):

$$\frac{\ln 400 - \ln P_B}{\ln 400 - \ln 760} = \frac{\frac{1}{335.5} - \frac{1}{T}}{\frac{1}{335.5} - \frac{1}{351.4}}$$

Vapour pressure data can now be calculated as follows:

T (°C)	T (°K)	$\ln P_A$	P_A	$\ln P_B$	P_B
64.7	337.7	6.633	760	6.084	439
68	341	6.757	860	6.220	503
71	344	6.868	961	6.342	568
74	347	6.977	1072	6.462	640
75.5	348.5	7.031	1131	6.521	679
78.4	351.4	7.133	1253	6.633	760

With the following relationships:

$$x_A = \frac{P_i - P_B}{P_A - P_B} \quad ; \quad y_A = \frac{P_A x_A}{P_i} \quad ; \quad \alpha = \frac{P_A}{P_B}$$

α can be determined as well as x-y and T-x-y plots.

T (°C)	P _A (mm Hg)	P _B (mm Hg)	x _A	y _A	α
64.7	760	439	1	1	1.731
68	860	503	0.7199	0.8146	1.710
71	961	568	0.4885	0.6178	1.692
74	1072	640	0.2778	0.3918	1.675
75.5	1131	679	0.1792	0.2667	1.666
78.4	1253	760	0	0	1.649

Avg = 1.69

T-x-y diagram

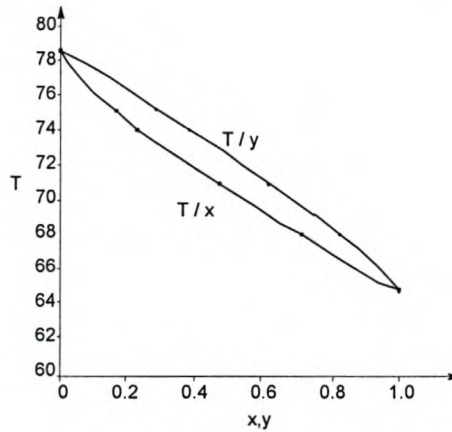


Figure 2.2(a) was derived from the following figure:

x-y diagram

